INTERNATIONAL DOCTORAL
SCHOOL OF THE USC

Patricia
Mondelo Macía

PhD Thesis

Liquid Biopsy and Precision Medicine: Characterization of Circulating Biomarkers in Patients with Advanced Lung Cancer

Santiago de Compostela, 2023

Doctoral Programme in Molecular Medicine

DOCTORAL THESIS

LIQUID BIOPSY AND PRECISION MEDICINE: CHARACTERIZATION OF CIRCULATING BIOMARKERS IN PATIENTS WITH ADVANCED LUNG CANCER

Patricia Mondelo Macía

INTERNATIONAL DOCTORAL SCHOOL OF THEUNIVERSITY OF SANTIAGO DE COMPOSTELA

DOCTORAL PROGRAMME IN MOLECULAR MEDICINE

SANTIAGO DE COMPOSTELA

2023

DECLARACIÓN DA AUTORA DA TESE

Dna. **Patricia Mondelo Macía**

Título da tese: **"Liquid biopsy and precision medicine: Characterization of circulating biomarkers in patients with advanced lung cancer"**

Presento a miña tese, seguindo o procedemento axeitado ao Regulamento, e declaro que:

1) A tese abarca os resultados da elaboración do meu traballo.
2) De ser o caso, na tese faise referencia ás colaboracións que tivo este traballo.
3) Confirmo que a tese non incorre en ningún tipo de plaxio doutros autores nin de traballos presentados por min para a obtención doutros títulos.
4) A tese é a versión definitiva presentada para a súa defensa e coincide a versión impresa coa presentada en formato electrónico.

E comprométome a presentar o Compromiso Documental de Supervisión no caso de que o orixinal non estea na Escola.

En **Santiago de Compostela**, **12 de Abril de 2023**.

Fdo. **Patricia Mondelo Macía**

AUTORIZACIÓN DO DIRECTOR / TITOR DA TESE

“Liquid biopsy and precision medicine: Characterization of circulating biomarkers in patients with advanced lung cancer”

Dna. Laura Muinelo Romay

D. Roberto Díaz Peña

D. Rafael López López

INFORMAN:

Que a presente tese, correspóndese co traballo realizado por Dna. **Patricia Mondelo Macía**, baixo a miña dirección/titorización, e autorizo a súa presentación, considerando que reúne os requisitos esixidos no Regulamento de Estudos de Doutoramento da USC, e que como director desta non incorre nas causas de abstención establecidas na Lei 40/2015.

De acordo co indicado no Regulamento de Estudos de Doutoramento, declara tamén que a presente tese de doutoramento é idónea para ser defendida en base á modalidade de **Monográfica con reprodución de publicacións**, nos que a participación do/a doutorando/a foi decisiva para a súa elaboración e as publicacións se axustan ao Plan de Investigación.

En Santiago de Compostela, 12 de Abril de 2023

Fdo. Laura Muinelo Romay	Fdo. Roberto Díaz Peña	Fdo. Rafael López López
(Directora)	(Director)	(Titor)

I, Patricia Mondelo Macía, author of this thesis, declare that I am the author of one patent developed in the context of the present thesis: *MAPRI: In vitro method for predicting cancer patient response to PD-1 and/or PD-L1 inhibitors; EP No. 23 382 377.2.*

I, Patricia Mondelo Macía, author of this thesis, have no other conflicts of interest to declare.

I, Patricia Mondelo Macía, author of this thesis, declare that, unless clarified, all the images presented in this thesis have been produced by the author. In the case of images reused or adapted from other manuscripts, permission has been granted by the publishers, and the mode of legal use has been clarified at the bottom of the corresponding figures.

The studies described in this thesis were performed withing the framework of the Liquid Biopsy Analyses Unit, Translational Medical Oncology (Oncomet) at the Health Research Institute of Santiago (IDIS) - University Hospital Complex of Santiago de Compostela, Spain.

The work presented in this thesis was financed by all the donors who participated in the Liquid Biopsy Crowdfunding campaign in 2017 and also supported by the Galician Agency of Innovation (GAIN IN607D2021/05), Consellería de Economía Empleo e Industria (IN606A-2018/026) and by the Translational Medical Oncology (ONCOMET) group.

Aos meus avós, A Inés, O Vilachá, A Lena e O Xaxá.

A mis padres y a mi hermana.

"La tierra (y la ciencia) para que produzca, hay que mulirla."

Baltasar Mondelo.

"So a lembranza de onde veño me axuda a saber cara onde vou."

Rosalía de Castro.

AGRADECIMIENTOS

AGRADECIMIENTOS

¡¡¡Finito!!! Después de casi 6 años, ha llegado el día. El día con el que se cierra esta gran etapa, la cual no habría sido posible ni tan increíble de no ser por todos vosotros.

En primer lugar, quiero agradecer a los pacientes y a sus familias, los que luchan cada día contra esta enfermedad y a pesar de sus circunstancias, apuestan por la investigación, haciendo posible nuestro trabajo. Esto va por vosotros. Gracias también a todas y cada una de las personas que participaron en la Campaña de Biopsia Líquida, por creer que el progreso y la investigación son herramientas clave para luchar contra esta patología.

Gracias al **Dr. López**, jefe de Servicio de Oncología. Rafa, en primer lugar, gracias por la oportunidad de dejarme formar parte de ONCOMET. Gracias por ser el motor de este grupo, apostando por la investigación, convirtiéndonos así en un centro de referencia.
A **Laura** y a **Roberto**, mis directores y los guías en este proceso de aprendizaje. Laura, gracias por estar siempre, por ver siempre el lado bueno de las cosas y por preocuparte por mi presente y mi futuro. Roberto, gracias por enseñarme desde el minuto uno y contar siempre conmigo, por esas reuniones en las que entro con mil dudas y salgo con cero. Infinitas gracias.
Gracias también a los miembros de la Unidad Mixta, en especial a **Gloria** y a **Ana Dávila**, por la ayuda recibida estos últimos meses, junto con **Susana Bravo,** responsable de la unidad de proteómica del IDIS. A **Mercedes**, nuestra odontóloga de excelencia. Gracias por tu actitud positiva y tener siempre tiempo para recibirnos.
Gracias al grupo de ONCOMET en general, pero especialmente a **Luis León** y a **Jorge García**, por ayudarme en cualquier duda clínica y echar una mano siempre que es posible. Gracias a enfermer@s, auxiliares y oncólog@s, que hacen posible este trabajo.
Gracias al grupo de ensayos clínicos, en primer lugar, por estar siempre dispuestos a sacarnos sangre, y segundo, por haberme acogido tan bien en estos últimos meses.

Volevo ringraziare anche i colleghi con cui ho lavorato a Milano. Grazie a **Daidone** e **Vera** per avermi aperto le porte del loro laboratorio. A **Marta**, **Rosita**, **Patrizia**, **Silvia**, **Elisa**, eccetera per avermi aiutato e fatto sentire a casa. In particolare, ringrazio **Carolina** per avermi ospitato il primo mese e per avermi aperto le porte della sua casa e del suo mondo.

Gracias también a los colaboradores externos, por su ayuda tanto de recursos como de conocimientos.

Al laboratorio 17, mi labo.
Gracias a Nasas group **Alba**, **Lore** y **Jorge** por estar dispuestos siempre a ayudar, y a enseñarnos lo que haga falta. En especial, gracias a Jorge por haber sacado tiempo para mostrarnos a los *predocs* todas las posibles vidas que existen después de la tesis.
Gracias a Alicia y a Ramón, mis primeritos profesores junto con **Manuel Abreu,** por acompañarme en mis primeros días de incertidumbre y torpeza. **Ali**, aunque los inicios sean duros (jeje), gracias por enseñarme una y mil cosas, por conseguir lo que sea cuando sea y por ser una fuente inagotable de caramelos. **Ramón**, gracias por todo el aprendizaje como profesional pero también como persona, eres grande (y no solo literalmente). Gracias incluso por tus chistes malos que alegran días *regulinchis*.
Andrea, **Aroa**, **Yoel**, **Ana Torres**, los recién llegados, gracias por vuestras sonrisas constantes y a por todas. **Mimí**, el último gran descubrimiento, no cambies y ¡a tope con el código! Rachel, Anita gracias por ese aire fresco que aportáis. **Anita**, sigue con esa fuerza y energía que tú tienes, llegarás a todo lo que te propongas. **Rachel**, mi chula. Te has convertido en una gran compañera y amiga a pesar de tenerte desde hace poquito tiempo. Eternamente agradecida de haber coincidido contigo. Gracias por acompañarme en estos últimos meses a planes tan de jóvenes como gimnasio, biblioteca y música del 2000. A tope con la tesis, no dudes que estaré ahí para verla, tú puedes.
Carlos, Aida, Aitor, Óscar, para vosotros no tengo las suficientes palabras para agradeceros lo vivido en esta etapa. **Carlos**, gracias por tu ayuda constante, por Grecia, Barcelona, por no dejarte pegar la COVID, esos viajes de post trabajo a la playa, cafés,

cenas, etc. Gracia por ser apoyo, compañero y sobre todo, amigo. **Aida**, mi coruñesa *fav*. Gracias por ayudarme siempre, por los desahogos, por los cotilleos, por Sanxenxo, Málaga o Santiago. Estoy segura de que este camino continuará contigo cerca. **Aitor**, gracias por tu buen humor constante, por tu ayuda en cualquier momento, y estar siempre dispuesto a una buena caña after-*work*. Gracias también a **Manuel**, un Epi más. Y no me olvido de **Nico**, el tercer integrante de Epi, dispuesto siempre a una buena orquesta (si no hay fútbol). Gracias al **doctor Rapado**, Oscarín por ser siempre lugar de paz y tranquilidad. Gracias por ser como eres Óscar. Nos vemos en Oporto!!

Quiero agradecer también a los pedazos de doctores con los que empezó esta aventura. **Thais, Nuria, Inés,** Pablo, Carol. Gracias a todos. **Pablo**, nuestro murciano favorito, gracias por todo lo que nos diste y por seguir escapándote cuando es posible. **Carol**, mi Caroline. Gracias por todos esos años de compi de mesa, de escritura de inicio de tesis, de bodorrio y por convertirte en una amiga. Se te echa de menos.

Saínza, la nano doctora. Gracias por tus consejos de diseño profesional y ser la persona más organizada del mundo. Estoy segura de que llegarás lejos. Gracias a **Sandra Alijas,** por esos primeros años. Gracias a las mini nanos, **María C, Soraya, Emma, Laura, Jen,** por vuestra sonrisa permanente.

Sandra Díez, a ti, gracias por demasiado. Por ser una amiga fuera y dentro, por tu ayuda tanto profesional como personal. Por todos esos "si" ante cualquier plan. Por más surf de desconexión, más furgonetas, y más ver mundo. Gracias por aparecer y seguir.

Tengo claro que no podría haberme tropezado con unos compañeros mejores, "El club de Wendoline", "El club de Oncoline". Sois la magia y la fuerza que tanto se necesita en días grises. Gracias por hacerme formar una segunda familia con la que compartir esta experiencia, con todo lo bueno que hemos vivido y esas cosas malas que al final no lo son tanto. Por responder a todos los "qué preferirías" y hacer que estar 24/7 con la tesis en la mente se lleve mejor. Se cierra una etapa chicos. Eternamente agradecida de encontraros en ella. Os llevo conmigo.

No puedo terminar sin darle las gracias a mis amigos de siempre, a mi grupo “Topo the coldmind”, por ser únicos, escuchar mis discursos, aportar otras visiones y ayudarme a desconectar en nuestro querido valle. **Dani, Óscar, Vasco, Xabi, Ine, Vero,** gracias. Especialmente, agradecer a **Noe, Yaiza, Nani y Judi**, las de siempre, por estar y ser como siempre. Por muchos kilómetros que nos separen, siempre llevo un pedacito de vosotras conmigo.

Gracias también a mis compañeros de piso. Desde los inicios hasta ahora. **Sergio, Nani, Maye, Lucas** y **Patri** “la nueva”. Gracias, por compartir las diferentes etapas conmigo, siempre escuchando y haciendo de Santiago Chile un dulce hogar. A **Peter**, por estar, pero sobre todo por escuchar y apaciguar mis momentos de crisis.

A mi familia, en especial a mis padrinos, **Merce** y **Moncho** por interesarse por cada *paper*. A mi abuelo **Baltasar**, gracias por alegrarte de cada paso que doy, escucharme y ser mi confidente y amigo. Eres mi alegría, avó. A mis abuelos, **Elena**, **Inés** y **Manolo**. Aunque no hayáis podido ver este final de camino, gracias por alegraros más que yo cuando empecé esta etapa, por interesaros cuando no entendíais ni lo que hacía. Gracias por todo lo que me disteis.

A mis padres. **Papá**, **mamá**, gracias por todo lo que me habéis dado para poder llegar hasta aquí. Gracias por apoyarme en todo, animarme y hacerme saber que pasara lo que pasara vosotros estaríais ahí. Esto es solo gracias a vosotros. A mi hermana, **Paula** y a **Carlos**, el otro ya casi integrante de la familia. Pauli, mi otra mitad con la que no podría vivir. Gracias por estar a mi lado siempre. Por tu ayuda en lo que sea, cuando sea y cómo sea.

En definitiva, gracias a todos y cada una de las personas que se han cruzado en este camino. Esta tesis no podría haber sido posible sin todos vosotros.

Nos vemos en los bares y, como diría mi abuelo:

¡Sigan bien!

Xuntos avanzamos.

INDEX

INDEX

ABBREVIATIONS AND ACRONYMS

ABBREVIATIONS AND ACRONYMS

A

AA: Amino acid

ADC: Adenocarcinoma

AF: Alexa fluor

AIC: Akaike information criterion

AJCC: American Joint Committee on Cancer

APC: Allophycocyanin

APC: Antigen presenting cell

ATCC: American Type Culture Collection

AUC: Area under the curve

B

BEAMing: Beads, emulsions, amplification, and magnetics method

C

CAV: Doxorubicin and vincristine

CCLE: Cancer Cell Line Encyclopedia

CEA: Carcinoembryonic antigen

cfDNA: Circulating free DNA

CH: Chemotherapy

CH-IM: CH plus immunotherapy

CI: Confidence interval

CKs: Cytokeratins

CMCs: Circulating melanoma cells

CN: Copy number

CNAs: Copy number alterations

Cq: Cycle of quantification

CR: Complete response

CSF: Cerebrospinal fluid

CT: Computerized tomography

CTCs: Circulating tumour cells

ctDNA: Circulating tumour DNA

CTL-4: Cytotoxic T lymphocyte antigen-4

D

DAPI: Nuclear dye 4',6-diamidino-2-phenylindole

DDA: Data-dependent acquisition (DDA)

ddPCR: Droplet digital PCR

DEP: Dielectrophoresis

DEPs: Differentially expressed proteins

DIA: data-independent acquisition

DLA: Diagnostic leukapheresis

dPCR: Digital PCR

DTT: Dithiothreitol

E

EBUS: Endobronchial ultrasound

ECOG-PS: Eastern Cooperative Oncology Group Performance Status

ED-SCLC: Extensive disease SCLC

EGFR: Epidermal growth factor receptor

EMA: European Medicines Agency

EMT: Epithelial-to-mesenchymal transition

EpCAM: Epithelial cell adhesion molecule

EVs: Extracellular vesicles

F

FDA: Food and Drug Administration

FDR: False discovery rate

FFPE: Formalin-fixed paraffin-embedded

FISH: Fluorescence in situ hybridization

FITC: Fluorescein

FLU: Fluorescein

G

GE: Genomic equivalents

gDNA: genomic DNA

H

HGF: Hepatocyte growth factor

HMW-MAA: Anti-high molecular weight melanoma-associated antigen

HR: Hazard ratio

hTERT: Human telomerase reverse transcriptase

I

ICIs: Immune checkpoint inhibitors

IF: Immunofluorescence

IFN-γ: Interferon-gamma

IgG4: Human immunoglobulin G4

IHC: Immunohistochemistry

K

KEGG: The Kyoto Encyclopedia of Genes and Genomes

L

LCC: Large cell carcinoma

LDH: Lactate dehydrogenase

LD-SCLC: Limited disease SCLC

LOD: Limit of detection

M

mAb: Monoclonal antibody

MAPK: Mitogen-activated protein kinase

MDSCs: Myeloid-derived suppressor cells

MET or c-MET: Hepatocyte growth factor receptor

MHC: Major histocompatibility complex

miRNA: MicroRNA

MMRD: Mismatch repair deficiency

MS: Mass spectrometry

MSI: Microsatellite instability

N

NGS: Next-generation sequencing

NK: Natural killers

NLR: Neutrophil-to-lymphocyte ratio

NR: Non-responder

NSCLC: Non-small cell lung cancer

NSCLC-NOS: NSCLC-not otherwise specified

NT: Not tested

O

ORR: Objective response rate

OS: Overall survival

P

PCI: Prophylactic cranial irradiation

PD: Progression disease

PD-1: Programmed cell death protein 1

PD-L1: Programmed cell death ligand 1

PE: Phycoerythrin

PFS: Progression-free survival

PI3K-AKT: Phosphatidylinositol 3-kinase pathway

PR: Partial response

Q

qPCR: Quantitative polymerase chain reaction

R

RECIST: Response Evaluation Criteria in Solid Tumours

R: Responder

ROC: Receiver operating characteristic

Rova-T: Rovalpituzumab tesirine

RT: Retention time

RTK: Receptor tyrosine kinase

S

SCC: Squamous cell carcinoma

SCLC: Small cell lung cancer

SD: Standard deviation

SDi: Stable disease

SNP: Single-nucleotide polymorphism

SNV: Single nucleotide variant

SPC: Sample processing control

SWATH-MS: Sequential Window Acquisition of All Theoretical Mass Spectra

STAT: Signal transducer and activator of transcription

T

TCR: T-cell receptor

TFF1: Thyroid transcription factor 1

TILs: Tumour-infiltrating lymphocytes

TKIs: Tyrosine kinase inhibitors

TMB: Tumour mutational burden

TNM: Tumour, node and metastasis staging system

TPS: Tumour proportion score

U

UICC: Union for International Cancer Control

V

VAF: Variant allele frequency

VALG: Veterans Administration of Lung Study Group

W

WES: Whole-exome sequencing

WGS: Whole-genome sequencing

WHO: World Health Organization

WT: Wild type

RESUMEN *in extenso*

RESUMEN *in extenso*

El cáncer se define como un conjunto de enfermedades en las que las células crecen de manera descontrolada, provocando fallos en los tejidos a los que afecta. Estas células de crecimiento descontrolado pueden crecer y propagarse a otros tejidos y órganos a través del sistema circulatorio o linfático, y pueden interferir con el funcionamiento normal del cuerpo. Hoy en día, el cáncer es una de las principales causas de muerte a nivel mundial, superado sólo por las enfermedades cardiovasculares. El cáncer de pulmón es el tipo de cáncer que más muertes provoca al año en todo el mundo, con más de 1.8 millones de muertes en 2020. En el 57% de los casos, su diagnóstico se produce en etapas avanzadas en el que el pronóstico de los pacientes es malo, ya que menos del 5.3% sobrevive 5 años. Histológicamente, el cáncer de pulmón se puede dividir en dos tipos: el cáncer de pulmón de células no pequeñas (NSCLC, del inglés *non-small cell lung cancer*) que constituye el 85% de los casos, y el cáncer de pulmón de células pequeñas (SCLC, del inglés *small cell lung cancer*), que constituye un 15% de los casos. Este último tipo se caracteriza por su mayor agresividad, siendo su tasa de supervivencia a 5 años de solo el 2.8%.

Durante muchos años, la estrategia terapéutica más frecuente para hacer frente al cáncer de pulmón se basaba en el uso de la quimioterapia, la cual bloquea la división celular de las células tumorales. Sin embargo, la quimioterapia también afecta negativamente a células sanas, produciendo efectos secundarios no deseados que disminuyen la calidad de vida de los pacientes. Además, la resistencia al tratamiento con este tipo de fármacos

puede ocurrir con frecuencia. En las últimas décadas, un mayor conocimiento de los mecanismos moleculares del cáncer de pulmón ha permitido el desarrollo y la aprobación de nuevos fármacos específicos contra el cáncer, mejorando éstos la supervivencia y la calidad de vida de los pacientes. En concreto, en el NSCLC el descubrimiento de alteraciones en genes *drivers* ha permitido el uso de terapias dirigidas donde el fármaco se dirige solamente hacia las células tumorales que presentan diferentes alteraciones. Recientemente la inmunoterapia ha emergido como una terapia alternativa cuando no hay mutaciones en genes *drivers*. Por otro lado, en el SCLC actualmente no existen terapias dirigidas hacia genes *drivers* mientras que la inmunoterapia ha sido incorporada al manejo clínico de los pacientes hace relativamente pocos años. En ambos tipos de cáncer, seleccionar el tratamiento adecuado e identificar a aquellos pacientes que se beneficiarán de las diferentes terapias que existen en la actualidad para mejorar las tasas de supervivencia, es esencial. Sin embargo, los actuales biomarcadores no siempre son suficientemente eficaces para seleccionar a aquellos pacientes que responderán a estos tratamientos.

Actualmente, la identificación de las alteraciones tumorales en la práctica clínica para seleccionar el mejor tratamiento debe realizarse en el tejido tumoral. Sin embargo, esta aproximación no está exenta de desventajas. En primer lugar, las biopsias sólidas pueden ser invasivas y dolorosas, lo que puede causar malestar y complicaciones en algunos pacientes. En segundo lugar, la accesibilidad al tumor no siempre está disponible en los casos de cáncer de pulmón o la cantidad de muestra obtenida no es suficiente para realizar un análisis molecular extenso. Por último, estas biopsias pueden no ser representativas de todo el tumor, ya que solo se toma una pequeña muestra

del tejido, lo que puede conducir a errores de diagnóstico y/o una selección de un tratamiento inadecuado. Además, la heterogeneidad tumoral es un factor clave en los pacientes con cáncer avanzado donde el tumor primario no siempre es representativo de la imagen total de la enfermedad. Por último, la monitorización de la enfermedad en tiempo real durante el tratamiento es fundamental para determinar la eficacia de éste y prevenir o adelantarse a la aparición de resistencias que produzcan el avance de la enfermedad. Dado el carácter invasivo de las biopsias sólidas, realizar éstas a diferentes puntos del tratamiento, con el fin de monitorizar la respuesta, no es adecuado. Por todo ello, la necesidad de utilizar alternativas no invasivas y repetitivas para mejorar el diagnóstico y permitir la monitorización de la enfermedad durante el tratamiento del cáncer de pulmón, destaca la importancia de desarrollar técnicas que puedan complementar o reemplazar a las biopsias sólidas.

Dentro de este contexto, hace aproximadamente 20 años nace la biopsia líquida, una herramienta alternativa para el manejo de varias enfermedades, entre ellas, el cáncer. La biopsia líquida es una técnica no invasiva que permite detectar y analizar células tumorales y material genético del tumor en muestras de sangre u otros fluidos corporales. Esta técnica revolucionaria ofrece ventajas en comparación con las desventajas previamente mencionadas de las biopsias sólidas: no requiere procedimientos invasivos, se puede realizar con mayor frecuencia durante el tratamiento para monitorizar la progresión del cáncer y detectar posibles resistencias y, además, ofrece información más precisa y completa sobre la heterogeneidad molecular que caracteriza a muchos tumores.

El ADN libre circulante (cfDNA, del inglés *circulating free DNA*), las células tumorales circulantes (CTCs, del inglés *circulating tumour cells*) y

otros componentes de la biopsia líquida han demostrado su utilidad como biomarcadores predictivos y pronósticos en el campo de la oncología (Figura 1). Sin embargo, no está claro cuál es el mejor abordaje para analizar las alteraciones tumorales utilizando muestras de sangre, cómo se deben cuantificar los diferentes biomarcadores y qué técnicas son las más apropiadas en cada caso.

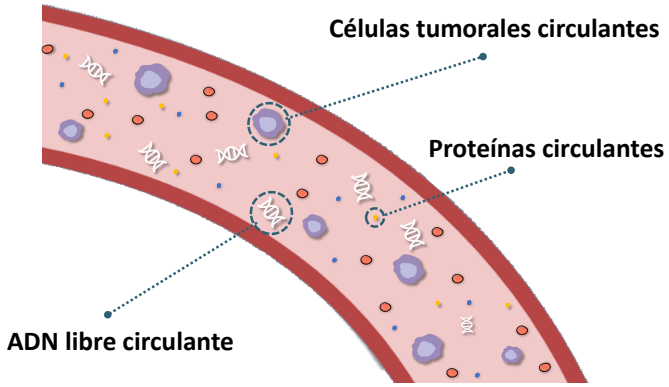

Figura 1. Principales componentes de la biopsia líquida estudiados a lo largo de la presente tesis.

En vista de los antecedentes mencionados previamente, las necesidades actuales, y el potencial de la biopsia líquida para el abordaje clínico del cáncer de pulmón, el principal objetivo de esta tesis se centra en el desarrollo y validación de estrategias que nos permitan realizar la caracterización de biomarcadores circulantes de forma eficaz con el fin de mejorar el manejo de pacientes con cáncer de pulmón avanzado en distintos contextos de tratamiento.

Para ello, el primer capítulo de esta tesis se centra en el estudio y desarrollo de diferentes metodologías para el análisis del ADN tumoral circulante (ctDNA, del inglés *circulating tumour cell*) y las CTCs para

seleccionar y monitorizar diferentes terapias dirigidas en pacientes con NSCLC avanzado. Durante los últimos años, la detección de alteraciones en diferentes receptores tirosina quinasa (RTKs, del inglés *receptors tyrosine kinase*) como el receptor del factor de crecimiento epidérmico (*EGFR*) y el receptor del factor de crecimiento hepático (*MET* o c-MET*)* en los pacientes con NSCLC se ha convertido en una parte habitual de la práctica clínica. La detección de estas alteraciones permite seleccionar a aquellos pacientes que se beneficiarán de tratamientos dirigidos contra estos genes y las vías que regulan, permitiendo un aumento en la supervivencia de los pacientes.

Con este fin, en primer lugar (**CHAPTER IA;** Figura 2), se han analizado las ventajas que tendría la implementación en la práctica clínica de un ensayo simple y rápido de PCR cuantitativa (qPCR, del inglés *quantitative PCR*) para detectar alteraciones en el gen *EGFR* a partir de muestras de sangre. Para ello, 40 pacientes con NSCLC fueron incluidos en el estudio, en los cuales se recogieron muestras de sangre antes de iniciar el tratamiento y durante diferentes puntos de este. En total, 53 muestras de plasma fueron analizadas mediante el ensayo de qPCR "ctEGFR de Idylla™ mutational assay" y los datos obtenidos mediante este sistema fueron comparados con los datos obtenidos en las muestras de biopsia sólida, actualmente el *gold* estándar en la práctica clínica. La concordancia entre ambas muestras fue del 71.8%. Respecto a los casos discordantes entre ambas muestras, es importante resaltas que en más de la mitad de los casos (6/11) la diferencia de tiempo entre la muestra sólida y la muestra de sangre era superior a 3 meses. Seguidamente, con el fin de determinar cuán sensible era el sistema a estudio, se compararon los resultados obtenidos de la técnica Idylla™ con otras dos técnicas de análisis de alteraciones a partir de muestras de plasma: la tecnología

BEAMing (una técnica basada en PCR digital (ddPCR, del inglés *digital droplet PCR*)) y técnicas de secuenciación masiva (NGS, del inglés *next-generation sequencing)* empleando un panel dirigido (AVENIO ctDNA Expanded panel). Los resultados obtenidos mostraron una gran concordancia de la estrategia de qPCR con la tecnología BEAMing y el panel de secuenciación AVENIO (88.9% y 93.3%, respectivamente). Sin embargo, a pesar de la buena concordancia obtenida, aquellas alteraciones que se encontraban con una frecuencia alélica igual o menor del 0.13% no fueron detectables mediante la tecnología Idylla™. Por otro lado, muestras procedentes de 10 pacientes con NSCLC se analizaron antes y durante el tratamiento con el sistema Idylla™ con el fin de monitorizar la respuesta al tratamiento y detectar de forma temprana la aparición de posibles resistencias. A pesar de que en nuestra cohorte no se detectó la aparición de resistencias al tratamiento, cambios en los niveles de cfDNA y variaciones en las mutaciones sugieren que el sistema Idylla™ constituye un buen enfoque para monitorizar la respuesta a la terapia en pacientes bajo terapias con inhibidores de tirosina quinasa (TKIs, del inglés *tyrosine kinase inhibitors)*.

En general, los resultados obtenidos en este estudio piloto permiten concluir que el ensayo de "Idylla™ ctEGFR mutational assay" es una herramienta rápida y sencilla que podría emplearse como una primera prueba para detectar mutaciones de *EGFR* en la rutina clínica habitual, obteniendo el resultado el mismo día de consulta del paciente, evitando así largos tiempos de espera. Sin embargo, es importante destacar que en aquellos casos que no se detecte ninguna mutación debido al bajo contenido de ctDNA en plasma, se debe emplear otra técnica más sensible como una estrategia basada en ddPCR o NGS para confirmar el resultado negativo. En relación con esto,

algunos aspectos deben tenerse en cuenta para la selección de los pacientes que se beneficiarán de esta plataforma. Por ejemplo, los tumores con múltiples ubicaciones metastásicas y altamente vascularizados tendrán niveles más altos de ctDNA y, por lo tanto, el genotipado de mutaciones clínicamente relevantes será más fácil de detectar mediante la técnica Idylla™.

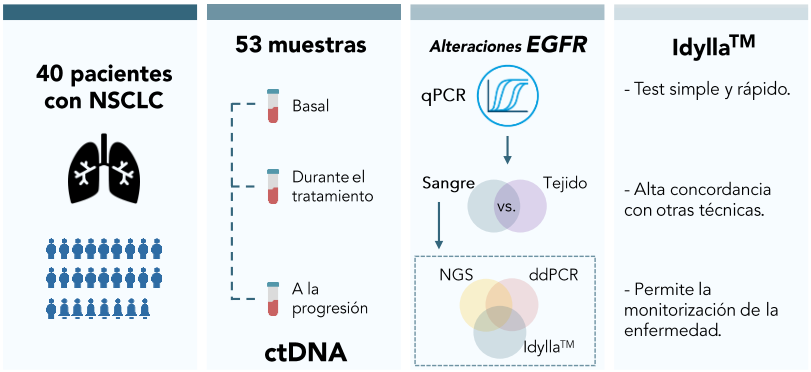

Figura 2. Resumen gráfico del trabajo realizado en el CHAPTER IA. Abreviaturas: NSCLC, del inglés *non-small cell lung cancer*, cáncer de pulmón no microcítico; ctDNA, del inglés *circulating tumour DNA,* DNA tumoral circulante*;* qPCR, PCR cuantitativa.

Siguiendo con las diversas mutaciones que se pueden encontrar en el cáncer de pulmón, es ampliamente reconocido que distintas mutaciones en el gen *MET* pueden causar resistencia a ciertas terapias, especialmente a TKIs. En la actualidad, las terapias con inhibidores de MET permiten aumentar el pronóstico de los pacientes con alteraciones en este gen, sin embargo, no hay métodos estandarizados para confirmar dichas alteraciones moleculares. Por ello, otro de los objetivos de la presente tesis se centró en desarrollar herramientas basadas en biopsia líquida para evaluar las alteraciones de *MET* en pacientes con cáncer y determinar su utilidad, centrándonos particularmente en pacientes con NSCLC (**CHAPTER IB**; Figura 3). Para alcanzar este objetivo, se reclutaron un total de 174 pacientes con diferentes

tipos de cáncer y 49 controles sanos. En esta cohorte de pacientes, se aplicó un ensayo basado en ddPCR para analizar el número de copias de *MET* en muestras de cfDNA en pacientes con tumores refractarios. Tras validar técnicamente el ensayo, se analizaron 77 pacientes con NSCLC y un 12.99% de los pacientes presentó amplificación de *MET*, siendo posibles candidatos a fármacos inhibidores de MET. Por otro lado, complementando nuestra estrategia no invasiva para caracterizar el estado de MET, estudiamos la población de CTCs aplicando dos enfoques diferentes (sistemas CellSearch® y Parsortix) para determinar su número y el nivel de expresión de la proteína c-MET en 16 pacientes con NSCLC metastásico. Los resultados obtenidos en ambos sistemas mostraron una concordancia del 62.5% a la hora de detectar la presencia de CTCs, sin embargo, el sistema Parsortix mostró una mayor eficiencia ya que permitió la detección de un mayor número de CTCs (en el 56.2% de los pacientes se detectaron CTCs frente al 31.25% usando el sistema CellSearch®). Respecto a la detección de la sobreexpresión de c-MET, los datos obtenidos sugieren que el sistema Parsortix es capaz de aislar más CTCs con sobreexpresión de c-MET (un 37.1% de las CTCs detectadas mostraron sobreexpresión) que el sistema CellSearch® (10.9%), resultados que concuerdan con el fenotipo mesenquimal propio de estas CTCs. Estos resultados preliminares indican que el sistema Parsortix sería más eficaz a la hora de detectar la sobreexpresión de c-MET en CTCs de pacientes con NSCLC tras varias líneas de tratamiento, sin embargo, estudios con una cohorte mayor de pacientes son necesarios para obtener resultados más robustos. Finalmente, dos casos de pacientes con NSCLC evidenciaron cómo la detección de las alteraciones de *MET* (amplificación de *MET* y/o sobreexpresión de c-MET mediante el sistema CellSearch® o Parsortix) puede ser informativa para la selección de tratamiento, así como en la monitorización

de la aparición de mecanismos de resistencia en respuesta al tratamiento anti-EGFR.

En conclusión, en el capítulo IB mostramos los resultados del desarrollo de ensayos específicos y no invasivos para monitorizar la expresión de c-MET en CTCs y la detección de la amplificación de *MET* en cfDNA a partir de muestras de sangre de pacientes con cáncer avanzado refractario. Ambas alteraciones moleculares se detectaron en la cohorte de pacientes con NSCLC por lo que demostramos su potencial para caracterizarlas de manera no invasiva y dinámica, siendo estas un biomarcador con relevancia terapéutica que juega un papel importante en el desarrollo de resistencias. Ambas estrategias tienen interés para seleccionar a los pacientes que se beneficiarán de los inhibidores de MET así como para monitorizar el seguimiento de los pacientes bajo terapias con TKIs.

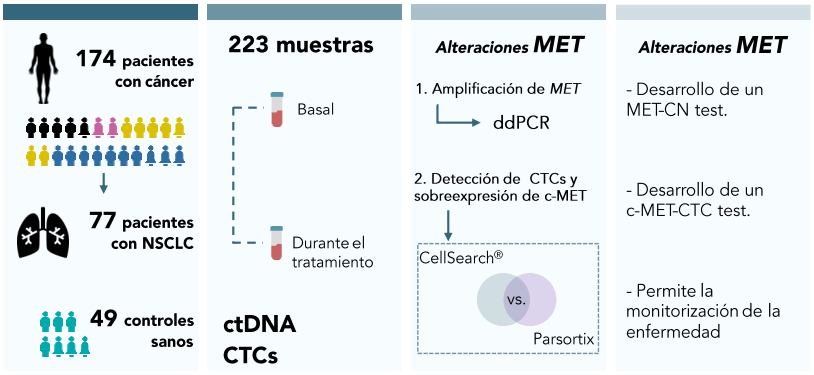

Figura 3. Resumen gráfico del trabajo realizado en el CHAPTER IB. Abreviaturas: ddPCR, del inglés *digital droplet PCR,* PCR digital; NSCLC, del inglés *non-small cell lung cancer*, cáncer de pulmón no microcítico; ctDNA, del inglés *circulating tumour DNA,* ADN tumoral circulante*;* CTCs, del inglés *circulating tumour cells,* células tumorales circulantes; CN, del inglés *copy number,* número de copias.

Tras el estudio de diferentes tecnologías para detectar alteraciones en cfDNA o CTCs para seleccionar y monitorizar terapias dirigidas a genes RTKs, otro de los objetivos de la presente tesis se centró en el estudio del cfDNA y de las CTCs como herramienta pronóstica o predictiva para guiar el tratamiento con inmunoterapia en pacientes con NSCLC. Los inhibidores de puntos de control inmunológico, como pembrolizumab, han revolucionado la terapia oncológica en diferentes tipos de cáncer, incluyendo el NSCLC. Sin embargo, solo un subconjunto de pacientes se beneficia de esta terapia, y actualmente no existe un biomarcador claro para seleccionar a estos pacientes. Por ello, existe una clara necesidad de nuevos biomarcadores que permitan una mejor selección de los pacientes, punto que abordamos en dos de los capítulos de esta tesis **(CHAPTER II y CHAPTER IV).**

Con este objetivo, en el capítulo II de la presente tesis (**CHAPTER II**; Figura 4), se diseñó un estudio en el que se reclutaron 50 pacientes con NSCLC avanzado tratados con inmunoterapia en los cuales se exploró el posible valor pronóstico y predictivo de respuesta que presenta el análisis del cfDNA y las CTCs presentes en la sangre de los pacientes. Además, con el fin de evaluar si el cfDNA puede ser utilizado como herramienta de monitorización de la enfermedad y/o respuesta al tratamiento, se recogieron un total de 109 muestras de sangre a diferentes puntos del tratamiento: antes del inicio y a las 6 y 12 semanas post-inicio de tratamiento. En primer lugar, los niveles de cfDNA se midieron mediante un ensayo de qPCR cuantificando el número de copias de una secuencia del gen *hTERT*. Tras analizar los resultados de dicha cuantificación en relación con la supervivencia de los pacientes, se determinó que aquellos con niveles altos de cfDNA antes de iniciar el tratamiento, tuvieron unas supervivencias libres de progresión (PFS,

del inglés *progression-free survival*) y global (OS, del inglés *overall survival*) significativamente peores que aquellos con niveles bajos. Además, los pacientes con cambios desfavorables en los niveles de cfDNA desde el momento basal hasta las 12 semanas mostraron un mayor riesgo de progresión de la enfermedad. En segundo lugar, se analizó la presencia de CTCs en muestras de sangre antes del inicio del tratamiento en estos pacientes, utilizando dos tecnologías de enriquecimiento (sistemas CellSearch® y Parsortix) diferentes para evaluar la eficacia de ambos enfoques en cuanto a la cuantificación del número de CTCs y analizar la expresión de la proteína de ligando de muerte celular programada 1 (PD-L1, del inglés, *programmed death-ligand 1*) en esta población circulante. El sistema con el que se detectaron más CTCs PD-L1 positivas fue el sistema Parsortix. Sin embargo, la expresión de PD-L1 en CTCs no presentó ninguna asociación con la supervivencia de los pacientes, en ninguna de las dos técnicas empleadas. Sin embargo, los resultados obtenidos indicaron que los pacientes en los que se detectaron CTCs utilizando el sistema CellSearch® tuvieron una PFS y una OS significativamente más cortas que los pacientes que no tenían CTCs, independientemente del estado de PD-L1. Finalmente, análisis de regresión multivariante mostraron que si se combinaba la presencia de CTCs detectadas mediante sistema CellSearch® con los niveles de cfDNA antes de iniciar el tratamiento en los pacientes con NSCLC avanzado, la combinación de ambos muestra valor como biomarcador pronóstico independiente de la progresión de la enfermedad. Así, el segundo capítulo de la presente tesis demostró que la combinación de los niveles basales de CTCs y cfDNA aporta información relevante sobre el pronóstico y la evolución de la respuesta a la terapia con pembrolizumab en pacientes con NSCLC metastásico. Utilizando dicho enfoque, es posible identificar un subgrupo de pacientes negativos para CTCs

y que presentan niveles bajos de cfDNA, que se benefician particularmente del tratamiento con inmunoterapia. Por otro lado, nuestros resultados indican que evaluar los niveles de cfDNA a las 12 semanas de iniciar el tratamiento, podría permitir a los médicos decidir si el beneficio clínico que experimenta el paciente es suficiente para continuar el tratamiento, evitando toxicidades y costes económicos innecesarios en aquellos casos en los que los niveles de cfDNA han sufrido cambios desfavorables.

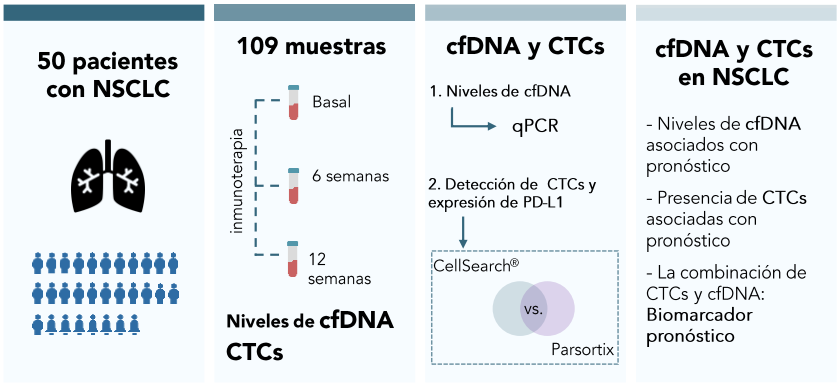

Figura 4. Resumen gráfico del trabajo realizado en el CHAPTER II. Abreviaturas: NSCLC, del inglés *non-small cell lung cancer*, cáncer de pulmón no microcítico; cfDNA, del inglés *circulanting free DNA,* ADN libre circulante*;* CTCs, del inglés *circulating tumour cells,* células tumorales circulantes; qPCR, PCR cuantitativa.

Basándonos en estos resultados, posteriormente quisimos investigar si el estudio del cfDNA y las CTCs podría proporcionarnos información sobre la evolución clínica en pacientes con SCLC. En este tipo de cáncer de pulmón menos frecuente, la falta de biomarcadores para la selección y la monitorización del tratamiento junto con las limitadas opciones terapéuticas que existen actualmente se asocia con un pronóstico muy pobre en estos pacientes. Por ello es importante explorar el valor de nuevos marcadores para mejorar el manejo de estos pacientes. Con estas premisas, en el capítulo III de

la presente tesis (**CHAPTER III**; Figura 5) se realizó un estudio con un enfoque similar al realizado en el capítulo II pero en pacientes con SCLC. Se reclutaron para ello 46 pacientes con SCLC avanzado y 20 controles sanos, recogiendo un total de 131 muestras de sangre. Los niveles de cfDNA se cuantificaron longitudinalmente en diferentes puntos durante la primera línea de terapia (quimioterapia o inmunoterapia en combinación con quimioterapia) mediante un ensayo de qPCR. De manera similar a los resultados obtenidos en los pacientes con NSCLC, los niveles elevados de cfDNA antes del inicio de la terapia mostraron asociación con una PFS y una OS más corta en la cohorte de SCLC. Además, niveles altos de cfDNA a las 3 semanas y en el momento de la progresión de la enfermedad, se asociaron con un peor pronóstico, mostrando independencia respecto a otras variables clínicas. Por otro lado, en una cohorte de 21 pacientes se analizó la presencia de CTCs antes del inicio del tratamiento, empleando la tecnología CellSearch®. Mientras en NSCLC la presencia de CTCs mostró valor pronóstico para predecir PFS y OS, en la cohorte de SCLC solo la presencia de un número elevado de CTCs (>150 CTCs) mostró una asociación discreta con menores tasas de PFS, pero sin mostrar valor pronostico independiente. Finalmente, se exploró el valor pronóstico del análisis del cfDNA junto con otras variables clínicas, como el estado del paciente según la escala ECOG PS (del inglés, *eastern cooperative oncology group performance status*) y el sexo. Este modelo permitió estratificar a los pacientes en diferentes grupos de riesgo identificando aquellos que podían beneficiarse más del tratamiento con quimioterapia o inmunoterapia.

En resumen, el capítulo III, se describen resultados que avalan el interés del análisis de los niveles de cfDNA para ayudar a los oncólogos a hacer un

pronóstico más certero sobre la evolución de la enfermedad y la respuesta al tratamiento en pacientes recién diagnosticados con SCLC. En particular, con este estudio demostramos que la combinación del análisis del cfDNA y características clínicas estándar (ECOG PS y sexo) puede ayudar a estratificar mejor a los pacientes y detectar aquellos que podrían beneficiarse especialmente del tratamiento.

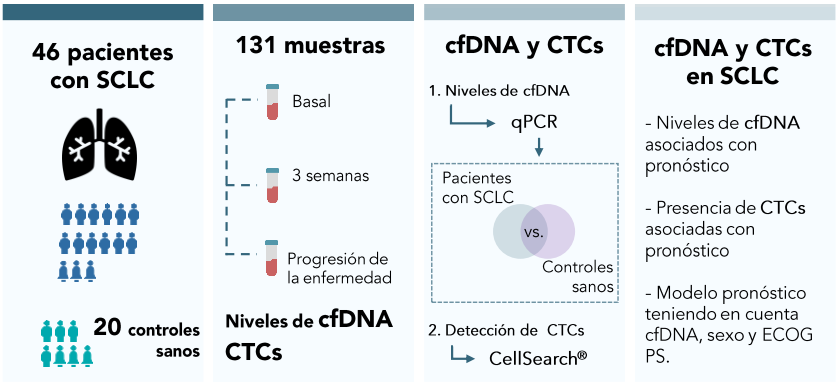

Figura 5. Resumen gráfico del trabajo realizado en el CHAPTER III. Abreviaturas: SCLC, del inglés *small cell lung cancer*, cáncer de pulmón microcítico; cfDNA, del inglés *circulanting free DNA,* ADN libre circulante*;* CTCs, del inglés *circulating tumour cells,* células tumorales circulantes; qPCR, PCR cuantitativa; ECOG PS, del inglés *Eastern Cooperative Oncology Group Performance Status.*

Por último, en el cuarto capítulo de esta tesis (**CHAPTER IV**; Figura 6) se centró en la identificación de marcadores proteicos presentes en plasma con potenciales biomarcadores predictivos de respuesta a inmunoterapia en pacientes con NSCLC. Respecto al cfDNA y a las CTCs, las proteínas circulantes son típicamente más fáciles de medir, lo que las convierte en un biomarcador accesible y rentable para el uso en un contexto clínico. Además de proporcionar información sobre las células tumorales, el proteoma plasmático puede proporcionar información sobre el microambiente que rodea

al tumor, incluyendo su composición inmune o el estado inflamatorio del mismo. Con el objetivo de identificar proteínas plasmáticas con interés para guiar el tratamiento con inmunoterapia en pacientes con NSCLC avanzado, se diseñó un estudio en el que se incluyeron 64 pacientes tratados con pembrolizumab. Las muestras de sangre fueron recogidas en diferentes puntos del tratamiento: antes de iniciar el tratamiento, a las 6 y 12 semanas tras el inicio de la terapia y en el momento de la progresión de la enfermedad. En total se recogieron 171 muestras en las cuales se analizaron las proteínas presentes en el plasma mediante la tecnología SWATH-MS (del inglés, *sequential window acquisition of all theoretical fragment ion mass spectra*), un método de adquisición independiente de datos que permite cuantificar cientos de proteínas en un solo ensayo. Un análisis comparativo entre muestras de pacientes respondedores y no respondedores permitió identificar 324 proteínas diferencialmente expresadas entre ambos grupos. De ellas, 172 proteínas presentaban niveles más altos en los pacientes respondedores mientras que 152 proteínas, presentaban niveles más altos en los no respondedores. A partir del global de proteínas diferencialmente expresadas, se identificó una firma proteómica de 7 proteínas (ATG9A, HPS5, DCDC2, PGTA, FIL1L, LZTL1 y SPTN2) que permite discriminar a los pacientes que responden al tratamiento con inmunoterapia. Individualmente las proteínas mostraban un poder de discriminación alto, con áreas bajo la curva (AUC, del inglés *área under the curve*) entre 0.72 y 0.78, mejorando así el poder predictivo de la expresión de PD-L1 en tejido (AUC= 0.638). El uso combinado de las 7 proteínas mejoró estos valores, obteniendo una AUC=1. Por otro lado, análisis de supervivencia revelaron que niveles bajos de ATG9A se asociaron de manera significativa con una mejor PFS, mientras que los valores altos de SPTN2 mostraron valor pronóstico positivo para PFS. Así

mismo, niveles bajos de HPS5 y DCDC2 se asociaron de manera significativa con una mayor OS. Finalmente, la cuantificación de estas 7 proteínas a diferentes puntos del tratamiento reveló que el modelo propuesto permite predecir la respuesta tanto a las 6 semanas como a las 12 semanas tras el inicio del tratamiento con pembrolizumab. En resumen, los resultados derivados del capítulo IV de esta tesis, nos permitieron identificar una firma proteómica de 7 proteínas plasmáticas con potencial para seleccionar aquellos pacientes que se beneficiarán de inmunoterapia basada en anti-PD1.

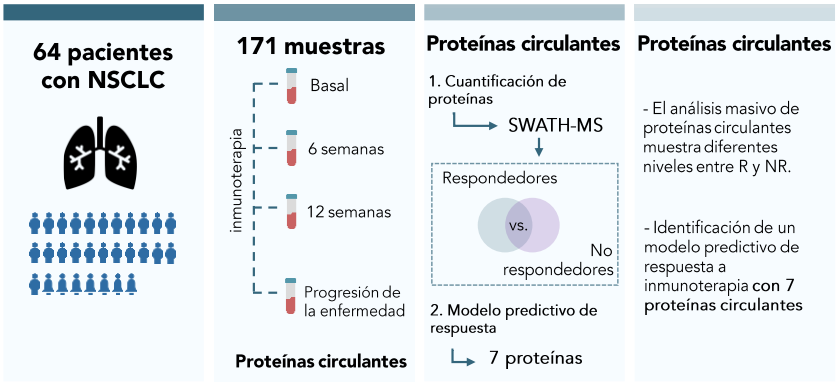

Figura 6. Resumen gráfico del trabajo realizado en el CHAPTER IV. Abreviaturas: NSCLC, del inglés *non-small cell lung cancer*, cáncer de pulmón no microcítico.

En resumen, el cáncer de pulmón metastásico es una enfermedad compleja y heterogénea que requiere un enfoque multidisciplinario para su diagnóstico y tratamiento. Las "ómicas", incluyendo la genómica y proteómica, son herramientas esenciales para identificar biomarcadores y dianas terapéuticas para abordar el tratamiento del cáncer. Además, el estudio de biopsias líquidas, incluyendo el análisis de CTCs, cfDNA y otras moléculas presentes en la sangre, ha surgido como una herramienta no invasiva y altamente sensible para la detección del cáncer y el seguimiento de la

respuesta al tratamiento, donde cada componente proporciona información única sobre el tumor y su microambiente. La combinación de estos marcadores circulantes con las diferentes "ómicas" y datos clínicos como el evolutivo de los pacientes o las imágenes radiológicas de seguimiento, ofrece un enfoque poderoso para comprender la complejidad del cáncer de pulmón metastásico y desarrollar estrategias de tratamiento personalizadas.

Dadas las diferencias individuales y la heterogeneidad molecular del cáncer de pulmón, las distintas estrategias de análisis de biopsia líquida aplicadas en la presente tesis nos aportan una visión más integral de la enfermedad. Centrando nuestros estudios en una muestra no invasiva de sangre hemos podido comprender mejor la biología del cáncer de pulmón y sobre todo, desarrollar herramientas moleculares con potencial para guiar el tratamiento y mejorar la esperanza y calidad de vida en pacientes con cáncer de pulmón metastásico. En concreto, hemos demostrado que: a) podemos genotipar el estado de *EGFR* y *MET* en cfDNA mediante una técnica de qPCR y ddPCR de forma robusta en tumores con alta carga tumoral, b) el análisis del cfDNA representa una técnica efectiva para pronosticar la evolución de los pacientes con NSCLC o SCLC avanzado y monitorizar la respuesta a inmunoterapia en los primeros, c) podemos caracterizar la expresión de proteínas clínicamente relevantes como MET o PD-L1 en la población de CTCs de pacientes con cáncer de pulmón, d) el número de CTCs combinado con los niveles de cfDNA aporta información pronóstica en pacientes con NSCLC y, e) la caracterización del proteoma plasmático nos puede proporcionar biomarcadores con valor para identificar a los pacientes que van a presentar una mejor respuesta al tratamiento con inmunoterapia.

Finalmente, es importante destacar que nuestros resultados han permitido estandarizar y validar estrategias de análisis que representan actualmente una herramienta diagnóstica de utilidad real en la práctica clínica de nuestro hospital, pero también identificar nuevos biomarcadores cuyo valor clínico deberá ser determinado en futuros estudios prospectivos.

RESUMO *in extenso*

RESUMO *in extenso*

O cancro defínese como un conxunto de enfermidades nas que as células crecen de maneira descontrolada, provocando fallos nos tecidos aos que afecta. Estas células de crecemento descontrolado poden medrar e propagarse a outros tecidos e órganos a través do sistema circulatorio ou linfático, e poden interferir co funcionamento normal do corpo. Hoxe en día, o cancro é unha das principais causas de morte a nivel mundial, superado só polas enfermidades cardiovasculares. O cancro de pulmón é o tipo de cancro que máis mortes provoca ao ano en todo o mundo, con máis de 1.8 millóns de mortes en 2020. No 57% dos casos, o seu diagnóstico prodúcese en etapas avanzadas, no cal o prognostico dos pacientes é moi baixo, onde menos do 5.3% sobrevive 5 anos. Histolóxicamente, o cancro de pulmón pode dividirse en dous tipos: o cancro de pulmón de células non pequenas (NSCLC, do inglés *non-small cell lung cancer*) que constitúe o 85% dos casos, e o cancro de pulmón de células pequenas (SCLC, do inglés *small cell lung cancer*), que constitúe o 15% dos casos. Este último tipo caracterízase pola súa maior agresividade sendo a súa taxa de supervivencia a 5 anos de so o 2.8%.

Durante moitos anos, a estratexia terapéutica máis frecuente para facer fronte ao cancro de pulmón baseábase no uso da quimioterapia, a cal bloquea a división celular das células cancerosas. Sen embargo, a quimioterapia tamén afecta negativamente as células sas, producindo efectos secundarios non desexados que diminúen a calidade de vida dos pacientes. Por outro lado, a resistencia a este tipo de fármacos pode ocorrer con frecuencia. Nas últimas décadas, un maior coñecemento dos mecanismos moleculares do cancro de pulmón permitiu o desenvolvemento e a aprobación de novos fármacos máis

específicos contra o cancro, mellorando a supervivencia e a calidade de vida dos pacientes. En concreto, no NSCLC o descubrimento de alteracións en xenes *drivers* permitiu o uso de terapias dirixidas onde o fármaco diríxese só cara as células cancerígenas que presentan ditas alteracións. Recentemente a inmunoterapia emerxeu como unha terapia alternativa cando as mutacións nos xenes *drivers* non están presentes. Doutra banda, no SCLC actualmente non existen terapias dirixidas cara xenes *drivers* mentres que a inmunoterapia foi incorporada ao manexo clínico dos pacientes fai relativamente poucos anos. En ambos tipos de cancro, seleccionar o tratamento adecuado e identificar a aqueles pacientes que se beneficiarán das diferentes terapias que existen na actualidade para mellorar as taxas de supervivencia é esencial. Non obstante, os actuais biomarcadores non sempre son o suficientemente eficaces para seleccionar aqueles pacientes que responderán a eles.

Actualmente, a identificación das alteracións tumorais na práctica clínica para seleccionar o mellor tratamento debe realizarse no tecido tumoral. Non obstante, esta aproximación non está exenta de desvantaxes. En primeiro lugar, as biopsias sólidas poden ser invasivas e dolorosas, o que pode causar malestar e complicacións en algúns pacientes. En segundo lugar, a accesibilidade ao tumor non sempre está dispoñible nos casos de cancros de pulmón ou a cantidade de mostra obtida non é suficiente para realizar un análise molecular extenso. Por último, estas biopsias poden non ser representativas de todo o tumor, xa que só se toma unha pequena mostra do tecido, o que pode conducir a erros de diagnóstico e/ou tratamento inadecuado. Ademais, a heteroxeneidade tumoral é un factor clave nos pacientes con cancros avanzados onde o tumor primario non sempre é representativo da imaxe total da enfermidade. Por outra banda, a vixilancia da

enfermidade en tempo real durante o tratamento é fundamental para determinar a eficacia da terapia e previr ou anticiparse á aparición de resistencias que produzan o avance da enfermidade. Dado o carácter invasivo das biopsias sólidas, realizar estas de maneira repetitiva en diferentes puntos do tratamento non é adecuado. Por todo isto, a necesidade de utilizar alternativas non invasivas e repetitivas para mellorar o diagnóstico e permitir a vixilancia en tempo real da enfermidade, destaca a importancia de desenvolver técnicas que poidan complementar ou substituír as biopsias sólidas. Dentro deste contexto, fai aproximadamente 20 anos nace a biopsia líquida, unha ferramenta alternativa para o manexo de varias enfermidades, entre elas, o cancro.

A biopsia líquida é unha técnica non invasiva que permite detectar e analizar células tumorais e material xenético do tumor en mostras de sangue ou outros fluídos corporais. Esta técnica revolucionaria ofrece vantaxes en comparación coas desvantaxes previamente mencionadas das biopsias sólidas: non require procedementos invasivos, pódese realizar con maior frecuencia durante o tratamento do cancro e permite a detección de posibles resistencias. Ademais, ofrece información máis precisa e completa sobre a heteroxeneidade da enfermidade molecular que caracteriza a maioría dos tumores.

O ADN libre circulante (cfDNA, do inglés *circulating free DNA*), as células tumorais circulantes (CTCs, do inglés *circulating tumour cells*) e outros compoñentes da biopsia líquida demostraron a súa utilidade como biomarcadores preditivos e prognósticos no campo da oncoloxía (Figura 7). Non obstante, non está claro cal é o mellor abordaxe para analizar as alteracións tumorais utilizando mostras de sangue, como se deben cuantificar

os diferentes biomarcadores e que técnicas son as máis apropiadas en cada caso.

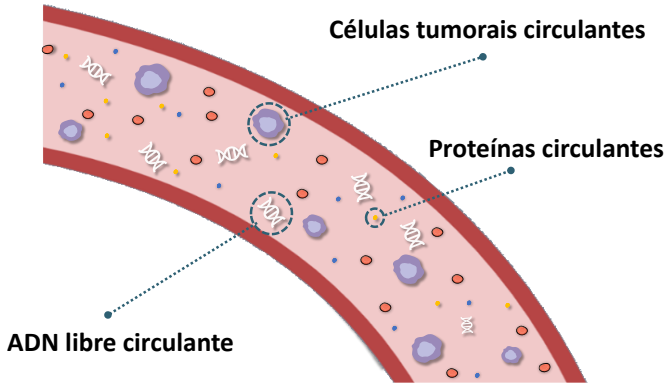

Figura 7. Principais compoñentes da biopsia líquida estudados ao longo da presente tese.

Dado os antecedentes mencionados previamente, as necesidades actuais e o potencial da biopsia líquida para o abordaxe clínico do cancro de pulmón, o principal obxectivo desta tese céntrase no desenrolo e validación de estratexias que nos permitan realizar a caracterización de biomarcadores circulantes de forma eficaz co fin de mellorar o manexo de pacientes con cancro de pulmón avanzado en distintos contextos de tratamento.

Para isto, o primeiro capítulo desta tese centrase no estudo e desenvolvemento de diferentes metodoloxías para o análise do ADN tumoral circulante (ctDNA, do inglés *circulating tumour cell*) e as CTCs para seleccionar e monitorizar diferentes terapias dirixidas utilizadas en pacientes con NSCLC avanzado. Durante os últimos anos, a detección de alteracións en diferentes receptores tirosina quinasa (RTKs, do inglés *receptor tyrosine kinases*) como o receptor do factor de crecemento epidérmico (*EGFR*) e o receptor do factor de crecemento hepático (*MET* ou c-MET) nos pacientes con NSCLC, converteuse nunha parte habitual da práctica clínica. A detección

destas alteracións permite seleccionar aqueles pacientes que se beneficiarán de tratamentos dirixidos contra estes xenes e as vías que regulan, permitindo un aumento na supervivencia dos pacientes.

Con este fin, en primeiro lugar (CHAPTER I.A; Figura 8), analizáronse as vantaxes que tería a implementación na práctica clínica dun ensaio simple e rápido de PCR cuantitativa (qPCR, do inglés *quantitative PCR*) para detectar alteracións no xene *EGFR* a partir de mostras de sangue. Para isto, 40 pacientes con NSCLC foron incluídos no estudo, nos cales se recolleron mostras de sangue antes de iniciar o tratamento e durante diferentes puntos deste. En total, 53 mostras de plasma foron analizadas mediante o ensaio de qPCR "ctEGFR de Idylla™ mutational assay" e os datos obtidos mediante este sistema foron comparados cos datos obtidos nas mostras de biopsia sólida, actualmente o *gold* estándar na práctica clínica. A concordancia entre ambas mostras foi do 71.8%. Respecto aos casos discordantes entre ambas mostras, é importante sinalas que en máis da metade dos casos (6/11), a diferenza de tempo entre a mostra sólida e a mostra de sangue foi superior a 3 meses. Ademais, co fin de determinar a sensibilidade do sistema a estudio, compararónse os resultados obtidos da técnica Idylla™ con outras dúas técnicas de análise de alteracións a partir de mostras de plasma: a tecnoloxía BEAMing (unha técnica baseada en PCR dixital (ddPCR, do inglés *digital droplet PCR*)) e técnicas de secuenciación masiva (NGS, do inglés *next generation sequencing*) empregando un panel dirixido (AVENIO ctDNA Expanded panel). Os resultados obtidos mostraron unha gran concordancia entre a estratexia de qPCR coa tecnoloxía BEAMing e o panel de secuenciación AVENIO (88.9% e 93.3%, respectivamente). Con todo, a pesar da boa concordancia obtida, aquelas alteracións que se encontran por debaixo

(ou igual) do 0.13% de frecuencia alélica non foron detectables mediante a tecnoloxía Idylla™. Por outra banda, mostras procedentes de 10 pacientes con NSCLC foron analizadas antes e despois da terapia co sistema Idylla™ con fin de monitorizar a resposta á terapia e detectar de forma temperá a aparición de posibles resistencias. A pesar de que na nosa cohorte non se detectaron mutacións asociadas a resistencia ao tratamento, os resultados preliminares mostraron que os cambios no perfil mutacional poderían proporcionar información valiosa para monitorizar a resposta terapéutica en pacientes baixo terapias con inhibidores de tirosina quinasa (TKIs, do inglés en inglés *tyrosin kinase inhibitors*).

En xeral, os resultados deste estudo piloto permiten concluír que o ensaio de "Idylla™ ctEGFR mutational assay" é unha ferramenta rápida e sinxela que podería empregarse como unha primeira proba para detectar mutacións de *EGFR* na rutina clínica habitual, obtendo o resultado o mesmo día de consulta do paciente e evitando así longos tempos de espera. Con todo, é importante destacar que nos casos en que non se detecte ningunha mutación debido ao baixo contido de ctDNA no plasma, debe empregarse outra técnica máis sensible, como unha estratexia baseada en ddPCR ou NGS para confirmar o resultado negativo. En relación con isto, algúns aspectos deben terse en conta para a selección dos pacientes que se beneficiarán desta plataforma. Por exemplo, os tumores con múltiples localizacións metastáticas e altamente vascularizados terán niveis máis altos de ctDNA e, por tanto, o xenotipado de mutacións clinicamente relevantes será máis fácil de detectar mediante a técnica Idylla™.

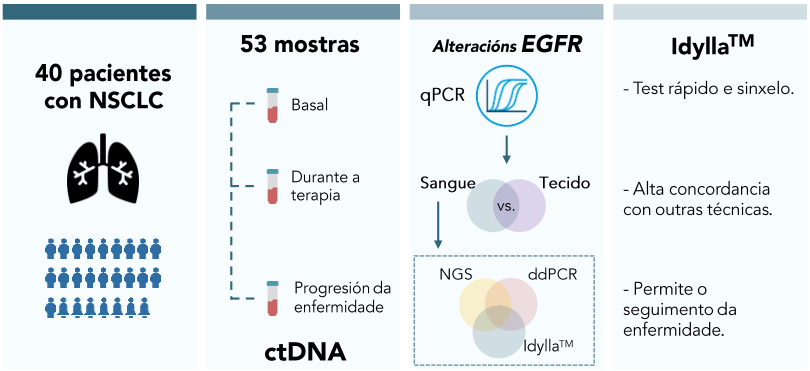

Figura 8. Resumo gráfico do traballo realizado no **CHAPTER IA**. Abreviaturas: NSCLC, do inglés *non-small cell lung cancer*, cancro de pulmón non microcítico; ctDNA, do inglés *circulating tumour DNA*, ADN tumoral circulante; qPCR, do inglés *quantitative PCR*, PCR cuantitativa.

Doutra banda, diferentes alteracións no xene *MET* poden provocar resistencia a certas terapias, en concreto resistencia a TKIs. Na actualidade, as terapias con inhibidores de MET permiten aumentar o prognostico dos pacientes con alteracións do xene, sen embargo, non hai métodos estandarizados para confirmar estas alteracións moleculares. Por iso, outro dos obxectivos da presente tese centrouse en desenrolar ferramentas baseadas en biopsia líquida para avaliar as alteracións de *MET* en pacientes con cancro e determinar a súa utilidade, centrándonos particularmente, en pacientes con NSCLC (CHAPTER I.B; Figura 9). Para acadar este obxectivo, recrutáronse un total de 174 pacientes con diferentes tipos de cancros e 49 controles. Nesta cohorte de pacientes, aplicouse un ensaio baseado en ddPCR para analizar o número de *MET* en mostras de cfDNA en pacientes con tumores refractarios. Tras validar técnicamente o ensaio, analizáronse 77 pacientes con NSCLC, dos cales o 12.99% dos pacientes presentou amplificación de *MET*, sendo posibles candidatos a fármacos inhibidores de MET. Doutra banda, complementando a nosa estratexia non invasiva para caracterizar o estado de

MET, estudouse a poboación de CTCS aplicando dous enfoques diferentes (sistemas CellSearch® e Parsortix) para determinar o seu número e o nivel de expresión da proteína c-MET en 16 pacientes con NSCLC metastático. Os resultados obtidos en ambos sistemas mostraron unha concordancia do 62.5% á hora de detectar a presencia de CTCs, sen embargo, o sistema Parsortix mostrou unha maior eficiencia permitindo a detección dun maior número de CTCs (no 56.2% de los pacientes detectáronse CTCs fronte ao 31.25% usando o sistema CellSearch®). Respeto á deteción da sobreexpresión de c-MET, os datos obtenidos suxiren que o sistema Parsortix é capaz de illar máis CTCs con sobreexpresión de c-MET (o 37.1% das CTCs detectadas mostraron sobreexpresión) que o sistema CellSearch® (10.9%), resultados asociados co fenotipo mesenquimal propio destas CTCs. Ditos resultados preliminares indican que o sistema Parsortix sería máis eficaz á hora de detectar a sobreexpresión de c-MET en CTCs de pacientes con NSCLC tras varias líneas de tratamento, sen embargo, estudios cunha cohorte máis ampla de pacientes son necesarios para obter resultados máis robustos. Finalmente, dous casos de pacientes con NSCLC evidenciaron como a detección das alteracións de *MET* (amplificación de *MET* e/ou sobreexpresión de c-MET mediante el sistema CellSearch® o Parsortix) pode ser informativa para a selección de tratamento así coma para a identificación da aparición de mecanismos de resistencia en resposta ao tratamento anti-EGFR.

En conclusión, no capítulo IB mostramos os resultados de desenrolo de ensaios específicos e non invasivos para monitorizar a expresión de c-MET en CTCs e a detección da amplificación do xene *MET* en cfDNA a partir de mostras de sangue de pacientes con cancro avanzado refractario. Ambas alteracións moleculares detectáronse na cohorte de pacientes con NSCLC,

demostrando o seu potencial para caracterizalas de maneira non invasiva e dinámica, sendo un biomarcador con relevancia terapéutica que xoga un papel importante na adquisición de resistencias. Ambas estratexias teñen interese para seleccionar ós pacientes que se beneficiarán dos inhibidores de MET, así como para monitorizar o seguimento dos pacientes baixo terapias con TKIs.

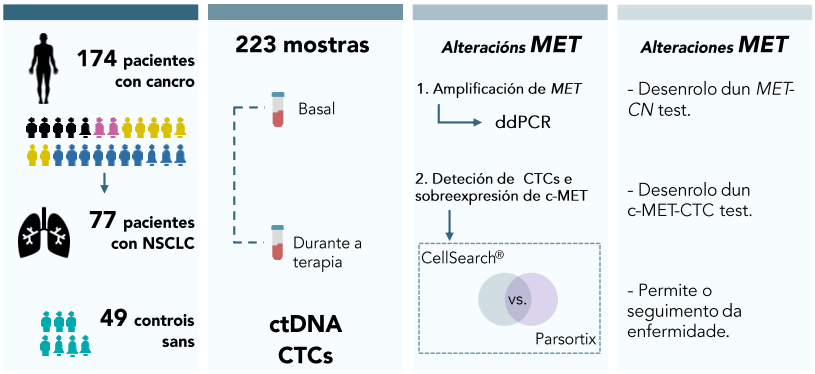

Figura 9. Resumo gráfico do traballo realizado no CHAPTER IB. Abreviaturas: ddPCR, do inglés *dixital droplet PCR,* PCR dixital; NSCLC, do inglés *non-small cell lung cancer*, cancro de pulmón non microcítico; ctDNA, do inglés *circulating tumour DNA*, ADN tumoral circulante; CTCs, do inglés *circulating tumour cells*, células tumorales circulantes; CN, do inglés *copy number*, número de copias.

Tras o estudo de diferentes tecnoloxías para detectar alteracións en cfDNA ou CTCs para seleccionar e monitorizar terapias dirixidas a xenes RTKs, outro dos obxectivos da presente tese centrouse no estudo do cfDNA e das CTCs como ferramenta prognostica ou preditiva para guiar o tratamento con inmunoterapia en pacientes con NSCLC. Os inhibidores de puntos de control inmunolóxico, como pembrolizumab, revolucionaron a terapia oncolóxica en diferentes tipos de cancro, incluíndo o NSCLC. Con todo, só un subconxunto de pacientes benefícianse desta terapia, e actualmente onde non existe un biomarcador claro para seleccionar a estes pacientes. Debido a

isto, existe unha clara necesidade de atopar novos biomarcadores que permitan unha mellor selección dos pacientes, punto que abordamos en dous dos capítulos desta tese (CHAPTER II e CHAPTER IV).

Con este obxectivo, no capítulo II da presente tese (CHAPTER II; Figura 10), deseñouse un estudo no que se recrutaron 50 pacientes con NSCLC avanzado tratados con inmunoterapia nos que se explorou o posible valor prognóstico e preditivo de reposta que presentan o análise de cfDNA e as CTCs presentes no sangue dos pacientes. Ademais, co fin de avaliar se o cfDNA pode ser utilizado como ferramenta de seguimento da enfermidade e/ou resposta ao tratamento, recolléronse un total de 109 mostras de sangue en diferentes puntos do tratamento: antes do inicio deste e ás 6 e 12 semanas post-inicio do tratamento. En primeiro lugar, os niveis de cfDNA foron medidos mediante un ensaio de qPCR cuantificando o número de copias dunha secuencia do xene *hTERT*. Tras analizar os resultados de dita cuantificación en relación á supervivencia dos pacientes, determinouse que aqueles con niveis altos de cfDNA antes de iniciar o tratamento, tiveron unhas supervivencias libre de progresión (PFS, do inglés *progresion-free survival*) e global (OS, do inglés *overall survival*) significativamente peores que aqueles con niveis baixos. Ademais, os pacientes con cambios desfavorables nos niveis de cfDNA desde o momento basal ata as 12 semanas mostraron un maior risco de progresión da enfermidade. En segundo lugar, analizouse a presenza de CTCs en mostras de sangue antes do inicio do tratamento nestes pacientes, utilizando dúas tecnoloxías de enriquecemento (sistemas CellSearch® e Parsortix) diferentes co fin de avaliar a eficacia de ambos enfoques para cuantificar o número de CTCs e analizar a expresión da proteína de ligando de morte celular programada 1 (PD-L1, do inglés, *programmed*

death-ligand 1) nesta poboación circulante. O sistema que presentou unha maior taxa de detección de CTCs PD-L1 positivas foi o sistema Parsortix. Sen embargo, a expresión de PD-L1 en CTCs non mostrou ningunha asociación coa supervivencia dos pacientes, con ningunha das dúas técnicas empregadas. En contraste, os resultados obtidos indicaron que os pacientes nos que se detectaron CTCs utilizando o sistema CellSearch® tiveron unha PFS e unha OS significativamente máis curtas que os pacientes que non tiñan CTCs, independentemente do estado de PD-L1. Finalmente, análises de regresión multivariante mostraron que a combinación da presenza de CTCs detectadas mediante o sistema CellSearch® cos niveis de cfDNA antes de iniciar o tratamento nos pacientes con NSCLC avanzado, mostrou un valor como biomarcador prognostico independente da progresión da enfermidade. Así, o segundo capítulo da presente tese revelou que a combinación dos niveis basais de CTCs e cfDNA aporta información relevante sobre o prognóstico e a evolución da resposta á terapia con pembrolizumab en pacientes con NSCLC metastático. Utilizando dito enfoque, é posible identificar un subgrupo de pacientes negativos para CTCs e que presentan niveis baixos de cfDNA, os cales se benefician particularmente do tratamento con inmunoterapia. Por outro lado, os resultados obtidos indican que avaliar os niveis de cfDNA ás 12 semanas de iniciar o tratamento podería permitir aos médicos decidir se o beneficio clínico que experimenta o paciente é suficiente para continuar o tratamento, evitando toxicidades e custos económicos innecesarios nos casos nos que os niveis de cfDNA tiveran sufrido cambios desfavorables.

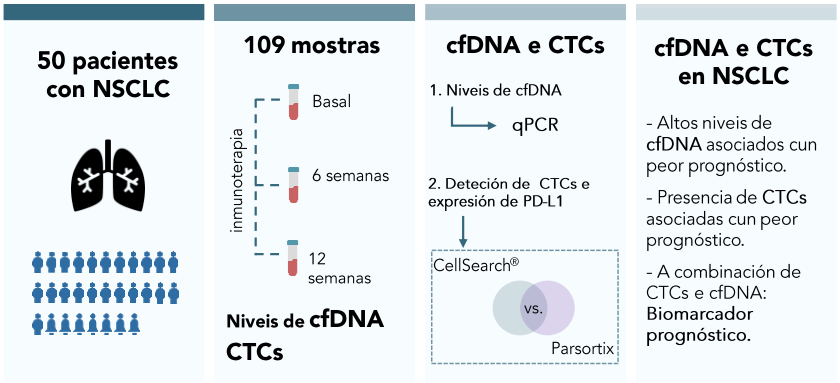

Figura 10. Resumo gráfico do traballo realizado no CHAPTER II. Abreviaturas: NSCLC, do inglés *non-small cell lung cancer*, cancro de pulmón non microcítico; cfDNA, do inglés *circulanting free DNA*, ADN libre circulante; CTCs, do inglés *circulating tumour cells*, células tumorais circulantes; qPCR, do inglés *quantitative PCR,* PCR cuantitativa.

Baseándonos nestes resultados, o seguinte paso centrouse en investigar se estudios de cfDNA e CTCs poderían proporcionarnos información sobre a evolución clínica de pacientes con SCLC. Neste tipo de cancro de pulmón menos frecuente, a falta de biomarcadores para a selección e o seguimento do tratamento xunto coas limitadas opcións terapéuticas que existen hoxe en día, asociase co mal prognóstico nestes pacientes. Por elo, é importante explorar o valor de novos marcadores para mellorar o manexo dos pacientes con SCLC. Con estas premisas, no capitulo terceiro da presente tese (CHAPTER III; Figura 11), realizouse un estudo cun enfoque similar ao realizado no capítulo II pero en pacientes con SCLC. Así, recrutáronse 46 pacientes con SCLC e 20 controles sans. recollendo un total de 131 mostras de sangue. Os niveis de cfDNA se cuantificaron lonxitudinalmente a diferentes puntos durante a primeira liña de terapia (quimioterapia ou inmunoterapia en combinación con quimioterapia) mediante un ensaio de qPCR. De maneira similar aos resultados obtidos nos pacientes con NSCLC, os niveis elevados de cfDNA antes do inicio da terapia mostraron asociación cunha PFS e unha OS máis

curta na cohorte de SCLC. Ademais, niveis altos de cfDNA ás 3 semanas e no momento da progresión da enfermidade se asociaron cun peor prognóstico, mostrando independencia respecto a outras variables clínicas. Doutra banda, nunha cohorte de 21 pacientes analizouse a presenza de CTCs antes do inicio do tratamento, empregando a tecnoloxía CellSearch®. Mentres en NSCLC a presenza de CTCs mostrou o seu valor prognóstico para predicir PFS e OS, na cohorte de SCLC só a presenza dun número elevado de CTCs (>150 CTCs) mostrou unha asociación discreta con menores taxas de PFS, pero sen mostrar o seu valor independente. Finalmente, e dados estes resultados, explorouse o valor prognóstico do análises do cfDNA xunto con outras variables clínicas como o estado do paciente segundo a escala ECOG PS (del inglés, *eastern cooperative oncology group performance status*) e o sexo. Este modelo permitiu estratificar a los pacientes en diferentes grupos de risco identificando aqueles que poderían beneficiarse más del tratamento con quimioterapia o inmunoterapia

En resumo, no capítulo III descríbese resultados que avalan o interese do análises dos niveis de cfDNA como axuda aos oncólogos a realizar un prognóstico máis certeiro sobre a evolución da enfermidade e a resposta ao tratamento en pacientes recen diagnosticados con SCLC. En particular, con este estudio, demóstrase que a combinación do análises do cfDNA e características clínicas estándar (ECOG PS e sexo) poden axudar a estratificar mellor aos pacientes e detectar aqueles que poderían beneficiarse especialmente do tratamento.

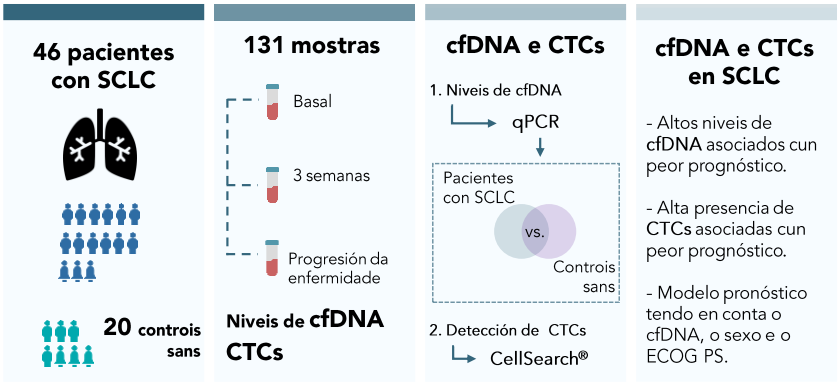

Figura 11. Resumo gráfico do traballo realizado no CHAPTER III. Abreviaturas: SCLC, do inglés *small cell lung cancer*, cancro de pulmón microcítico; cfDNA, do inglés *circulanting free DNA*, ADN libre circulante; CTCs, do inglés *circulating tumour cells*, células tumorales circulantes; qPCR, do inglés *quantitative PCR*, PCR cuantitativa; ECOG PS, do inglés *Eastern Cooperative Oncology Group Performance Status.*

Por último, no cuarto capítulo desta tese (CHAPTER IV; Figura 12), centrouse na identificación de marcadores proteicos presentes en plasma como potenciais biomarcadores preditivos de resposta a inmunoterapia en pacientes con NSCLC. Respecto ao cfDNA e ás CTCs, as proteínas circulante son tipicamente máis fáciles de medir, o que as converte nun biomarcador accesible e rendible para o uso nun contexto clínico. Ademais de proporcionar información sobre as células tumorais, o proteoma plasmático pode proporcionar información sobre o microambiente que rodea ao tumor, incluíndo a súa composición inmune e o estado inflamatorio do mesmo. Co obxectivo de identificar proteínas plasmáticas con interese para guiar o tratamento con inmunoterapia en pacientes con NSCLC avanzado, deseñouse un estudo no que se incluíron 64 pacientes tratados con pembrolizumab. As mostras de sangue foron recollidas en diferentes puntos do tratamento: antes de iniciar o tratamento, ás 6 e 12 semanas tras o inicio da terapia e no momento da progresión da enfermidade. En total, foron recollidas 171 mostras. O perfil

das proteínas presentes no plasma dos pacientes analizáronse empleando unha novedosa tecnoloxía baseada na adquisición independente de datos de numerosas proteínas: a tecnoloxía SWATH-MS (do inglés, *sequential window acquisition of all theoretical fragment ion mass spectra*). Un análises comparativo entre mostras de pacientes respondedores e non-respondedores mostraron permitiu identificar 324 proteínas diferencialmente expresadas entre ambos grupos. Destas, 172 proteínas presentaban niveis máis altos nos pacientes respondedores mentres que 152 proteínas presentaban niveis máis altos en non-respondedores. A partir do global de proteínas diferencialmente expresadas, identificouse unha firma proteómica de 7 proteínas (ATG9A, HPS5, DCDC2, PGTA, FIL1L, LZTL1 e SPTN2) con valor para discriminar aos pacientes que responderon ao tratamento con inmunoterapia. Individualmente, as proteínas identificadas mostraban un poder discriminatorio alto, con areas baixo a curva (AUC, do inglés *area under the curve)* entre 072 e 0.78, mellorando así o poder preditivo da expresión de PD-L1 en tecido (AUC= 0.638). O uso combinado das 7 proteínas mellorou estes valores, obtendo una AUC=1. Por outro lado, análises de supervivencia revelaron que niveis baixos de ATG9A asociáronse de maneira significativa cunha mellor PFS, mentres que valores altos de SPTN2 mostraron valor prognóstico positivo para PFS. Así mesmo, niveles baixos de HPS5 e DCDC2 asociáronse de maneira significativa cunha maior OS. Finalmente, a cuantificación destas 7 proteínas a diferentes puntos do tratamento, revelaron que o modelo proposto permite predicir a resposta á inmunoterapia tanto as 6 semanas coma as 12 semanas tras o inicio do tratamento con pembrolizumab. En resumo, os resultados derivados do capítulo IV desta tese, permitíronnos identificar unha firma proteica de 7 proteínas plasmáticas con potencial para

seleccionar aqueles pacientes que se beneficiarán da inmunoterapia baseada en anti-PD1.

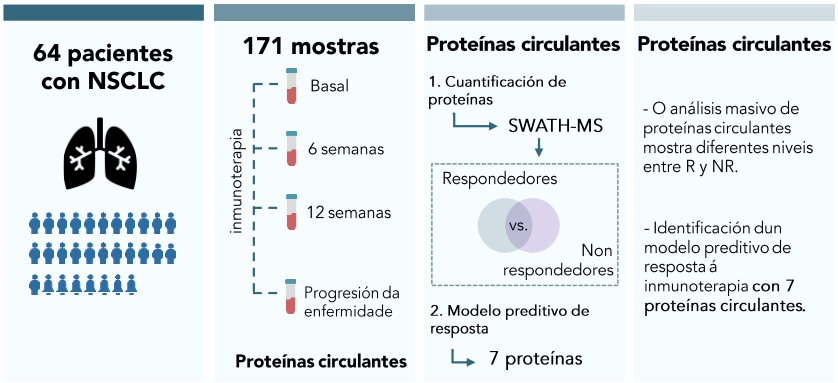

Figura 12. Resumo gráfico do traballo realizado no CHAPTER IV. Abreviaturas: NSCLC, do inglés *non-small cell lung cancer*, cancro de pulmón non microcítico.

En resumo, o cancro de pulmón metastático é unha enfermidade complexa e heteroxénea que require dun enfoque multidisciplinario para o seu diagnóstico e tratamento. As "ómicas", incluíndo a xenómica e a proteómica, son ferramentas esenciais para identificar biomarcadores e dianas terapéuticas para abordar o tratamento do cancro. Ademais, o estudio de biopsias líquidas, incluíndo a análise de CTCs, cfDNA e outras moléculas presentes na sangue, xurdiu como unha ferramenta non invasiva e altamente sensíbel para a detección do cancro e o seguimento da resposta ao tratamento, onde cada compoñente proporciona información única sobre o tumor e o seu microambiente. A combinación destes marcadores circulantes coas diferentes "ómicas" e datos clínicos, como o evolutivo dos pacientes e as imaxes radiolóxicas de seguimento, ofrece un enfoque poderoso para comprender a complexidade do cancro de pulmón metastático e desenvolver estratexias de tratamento personalizadas.

Dadas as diferencias individuais e a heteroxeneidade molecular que caracteriza ao cancro de pulmón, as distintas estratexias de análise de biopsia líquida, aplicadas na presente tese, apórtannos unha visión máis integral da enfermidade. Centrando os nosos estudios nunha mostra non invasiva de sangue pódese comprender mellor a bioloxía do cancro de pulmón e sobre todo, deseñar ferramentas moleculares con potencial para guiar o tratamento e mellorar a esperanzado e a calidade de vida dos pacientes con cancro de pulmón avanzado. En concreto púidose demostrar que: a) Podemos xenotipar o estado de *EGFR* e *MET* en cfDNA mediante técnicas de qPCR e ddPCR de maneira robusta en tumores con alta carga tumoral; b) o análise do cfDNA representa unha técnica efectiva para prognosticar a evolución dos pacientes con NSCLC o SCLC avanzado e monitorizar a resposta a inmunoterapia nos primeiros.; c) pódemos caracterizar a expresión de proteínas clinicamente relevantes como c-MET ou PD-L1 en poboación de CTCs de pacientes con cancro de pulmón; d) o número de CTCS combinado cos niveis de cfDNA arroxa información prognóstica en pacientes con NSCLC; e) a caracterización do proteoma plasmático pódenos proporcionar biomarcadores con valor para identificar aos pacientes que van a presentar unha mellor resposta ao tratamento con inmunoterapia.

Finalmente, é importante destacar que os nosos resultados permitiron estandarizar e validar estratexias de análises que representan actualmente unha ferramenta diagnóstica de utilidade real na práctica clínica do noso centro hospitalario pero tamén, identificar novos biomarcadores cuxo valor clínico deberá ser determinado en futuros estudios prospectivos.

SUMMARY

SUMMARY

Lung cancer is the leading cause of death globally, resulting in over 1.8 million deaths in 2020. Diagnosis often happens in advanced stages, making surgery impossible and prognosis poor. Histologically, there are two types of lung cancer: Non-small cell lung cancer (NSCLC) and small cell lung cancer (SCLC), with the latter being more aggressive. New therapies such as targeted and immunotherapy have been approved for these patients in recent years. However, selecting the right treatment is crucial for improving survival rates. Despite of tumour tissue is the gold standard for identifying tumour alterations, liquid biopsy, which includes components such as circulating free DNA (cfDNA) and circulating tumour cells (CTCs), has potential as a predictive and prognostic biomarker in oncology, but the appropriate techniques for analysing tumour alterations and quantifying different liquid biopsy biomarkers are unclear. Therefore, thesis's primary objective was to investigate the importance of liquid biopsy components in managing metastatic lung cancer patients.

First, the potential value of two PCR-based technologies (a qPCR technology and a digital droplet PCR technology) to detect specific mutations in circulating tumour DNA (ctDNA) in NSCLC patients, and therefore select specific therapies, was investigated. In addition, a technology to detect c-MET overexpression in CTCs from NSCLC patients was developed. Besides, cfDNA and CTCs showed potential utility to detect *EGFR* alterations and *MET* alterations in blood samples that will improve the clinical management of NSCLC patients.

Second, the potential utility of liquid biopsy components to select and monitor immunotherapy regimen was evaluated. Hence, high cfDNA levels (quantified through an easy and simple qPCR assay) before and during immunotherapy treatment showed a negative predictive and prognostic factor in NSCLC patients. Moreover, CTCs number was associated with survival rates in this cohort of patients, however the expression of PD-L1 on CTCs was not associated with PD-L1 expression in tumour tissue and nor with survival rates. Importantly, the combined analysis of cfDNA and CTC levels at diagnosis showed an improvement to select NSCLC patients who will benefit from this therapy.

Third, a similar approach was performed in the other lung cancer type, SCLC. Similarly, a negative, robust and independent prognostic value of cfDNA levels at diagnosis, during therapy and at progression disease was found in SCLC patients treated with chemotherapy or immunochemotherapy regimens. In contrast with NSCLC disease, high CTCs showed a discrete association with shorter progression free survival (PFS), but did not show their independent value. In this context, a prognostic model which included the cfDNA levels, ECOG PS and sex of patients, was proposed to stratify patients and detect those who could particularly benefit from the treatment.

Finally, the fourth chapter of the present thesis focuses on the search for new predictive protein biomarkers to select patients who will benefit from immunotherapy regimens to solve the current lack of accurate predictive tools. For this objective, circulating proteins present in plasma samples from NSCLC patients were analysed using a novel proteomic technology, SWATH-MS. With the results obtained, we identified a signature of 7

circulating proteins with value to determine therapy response in new diagnosed NSCLC patients.

Overall, we evidenced that different liquid biopsy components are useful to improve therapy selection and the disease monitoring in advanced lung cancer patients. The analysis of ctDNA present in cfDNA, allows us to determine the status of clinically relevant alterations in blood samples to select the best therapy in lung cancer patients. Moreover, high cfDNA levels were associated with worse survival rates in lung cancer patients, and importantly, showed their potential utility to guide and monitor therapy response. In contrast, CTCs value was reported as an independent factor in terms of survival rates only in NSCLC patients. Besides, a novel proteomic signature to predict immunotherapy response was developed as result of the present thesis. Finally, it is important to mention that part of the protocols developed in the present work have been incorporated into the practical routine in our hospital or are being used in clinical studies and also resulted in a patent, evidencing the important translational spirit of the thesis.

INTRODUCTION

INTRODUCTION

Section 2.1 has been adapted/extracted from a published review entitled "Circulating Free DNA and Its Emerging Role in Autoimmune Diseases" (1)**.**

Section 2.1.1 has been adapted/extracted from a published book chapter entitled "Methods for the Detection of Circulating Biomarkers in Cancer Patients" (2).

Section 2.2 has been adapted/extracted from a published book chapter entitled "Current status and future perspectives of liquid biopsy in small cell lung cancer. Biomedicines" (3).

INTRODUCTION

1. LUNG CANCER

1.1 Epidemiology and aetiology

Lung cancer, with an estimated 1.8 million deaths per year worldwide, is the leading cancer-related cause of death among malignant solid tumours and the second most diagnosed cancer, behind female breast cancer, with more than 2.2 million new cases per year (4) (Figure 13). Incidence and mortality rates are around 2 times higher in men than in women and 3 to 4 times higher in industrialized countries than in transitioning countries (4).

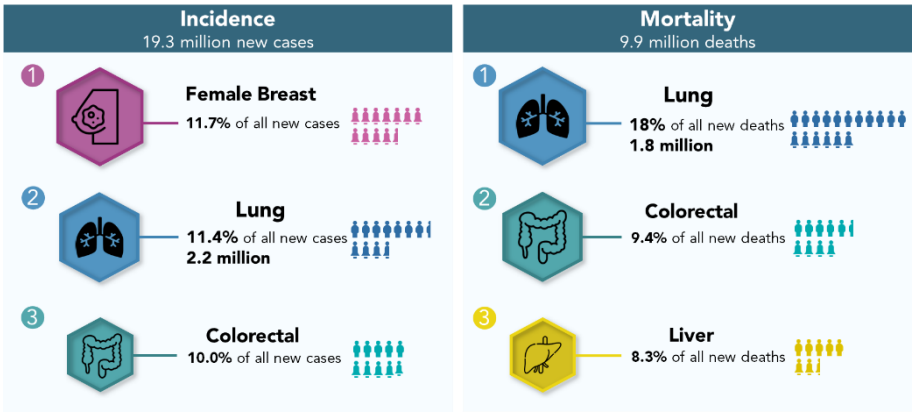

Figure 13. Distribution of cases and deaths for the top 3 most common cancers in 2020. Source: GLOBOCAN 2020.

Cough, seen in 50-75% of patients, is the most common symptom, followed by haemoptysis, chest pain, and dyspnea (5). The main aetiological factor in all lung cancer types is tobacco consumption. Indeed, its carcinogenic effect on the lung has been described from 1950 to the 1960s (6,7). The World Health Organization (WHO) estimated that 71% of deaths by lung cancer are

caused by smoking. Although in the last years the reduction of smoking rates at global level has contributed to the reduced incidence of lung cancer and improved survival, in transitioning countries prevalence of tobacco consumption is increasing followed by an increase in new lung cancer deaths and diagnoses (8,9). Hence, the most effective intervention for reducing lung cancer mortality remains smoking cessation. However, tobacco is not the unique aetiological factor in lung cancer. One quarter of lung cancer cases worldwide occur in people who have never smoked (10–12) and they are associated with air pollution, poor diet and occupational exposures (13,14). Regarding the familial risk of lung cancer, it has been estimated the heritability at 18% (15), however many of the genetic component remains unidentified.

1.2 Lung cancer classification

1.2.1 Histological classification

Histologically, lung cancer is a heterogeneous disease with wide-ranging clinicopathological features (16). Commonly, lung cancer can be divided into two major subtypes: Non-small cell lung cancer (NSCLC) and small cell lung cancer (SCLC), which accounts for 85% and 15% of total diagnoses, respectively (17). Both subtypes may share a similar cell of origin, the alveolar type II cell. NSCLC can be subdivided into four major subgroups: adenocarcinoma (ADC), squamous cell carcinoma (SCC), large cell carcinomas (LCC) and others. Oncogenic driver alterations are well reported in NSCLC and targeted therapies have allowed to reach better patients' outcomes (17). In all subtypes, tobacco consumption remains to be the main cause, however, the association is stronger with SCC than with ADC, being

ADC the most common histology in never smokers (10), associated with environmental exposures that include second-hand smoking, pollution and inherited genetic susceptibility among others (12).

In another hand, SCLC is a neuroendocrine tumour highly associated with tobacco consumption (18) and characterised by its rapid growth and aggressiveness. In contrast with NSCLC, the lack of specific somatic mutations and the poor progress of targeted therapies in SCLC makes the management of SCLC patients a real clinical challenge (19).

1.2.2 Clinical classification

In both cases, the classification of lung tumours through optimal staging is essential for selecting the most appropriate treatment and management. Thus, stage refers to the extent of the cancer, and indicates how large the tumour is, and if it has spread at the moment of diagnosis. Nowadays, there are many staging systems, however the most clinically useful is the tumour, node and metastasis staging system (TNM), developed by the American Joint Committee on Cancer (AJCC) in collaboration with the Union for International Cancer Control (UICC) (20). The AJCC-TNM staging system has three principal components (Figure 14):

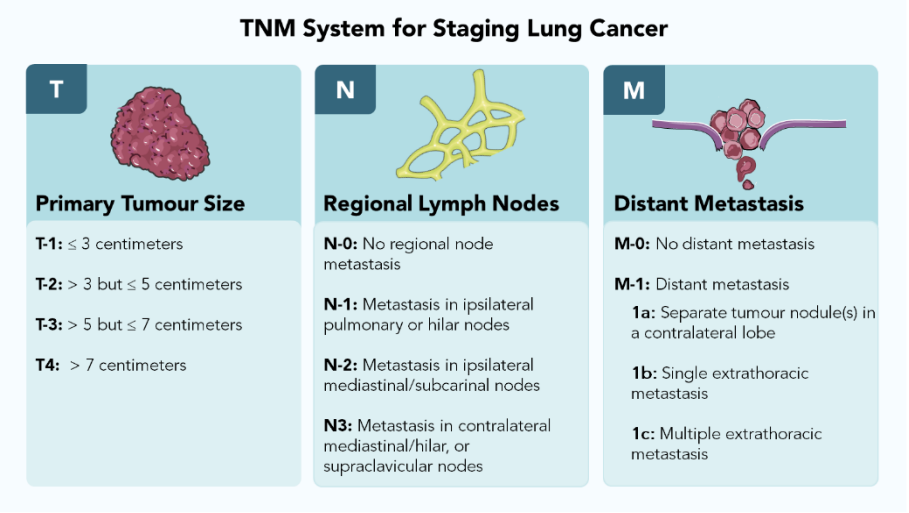

Figure 14. Definitions for T, N and M components in lung cancer tumours.

- The T refers to the size and extent of the primary tumour.
- The N refers to the number of nearby lymph nodes that present cancer cells.
- The M refers to whether the cancer has metastasized and spread from the primary tumour to other parts of the body.

Depending on the above terms defined, lung cancer patients can be classified into 4 principal stages: stage I, stage II, stage III and stage IV (Table 1) (21). In SCLC staging with the conventional TNM criteria is recommended, but according to the Veterans Administration of Lung Study Group (VALG) staging, SCLC is commonly classified into two stages: limited disease (LD-SCLC), when it is confined to a hemithorax, where curative treatment with radio-chemotherapy is feasible (TNM stages I-III) and extensive disease (ED-SCLC), defined as the presence of metastatic disease outside the hemithorax at first diagnosis (TNM stage IV) (22,23).

Table 1. Eight Edition of lung cancer stage grouping according the AJCC-TNM staging system (21) and the correspondence VALG staging for SCLC (23).

T/M	Label	N0	N1	N2	N3	According VALG in SCLC
T1	**T1**	IA	IIB	IIIA	IIIB	
T2	**T2a** >3-4 cm	IB	IIB	IIIA	IIIB	**SCLC** Limited Disease
	T2b >4-5 cm	IIA	IIB	IIIA	IIIB	
T3	**T3**	IIB	IIIA	IIIB	IIIC	
T4	**T4**	IIIA	IIIA	IIIB	IIIC	
M1	**M1a-b**	**IVA**	**IVA**	**IVA**	**IVA**	**SCLC** Extensive Disease
	M1c	**IVB**	**IVB**	**IVB**	**IVB**	

Abbreviations: VALG, Veterans Administration of Lung Study Group.

Unfortunately, most lung cancer patients are diagnosed at an advanced stage (stage IV; 57%), when surgery is not possible. Advanced lung cancer patients present a poor prognosis, when only 5.2% of patients survive 5 years after diagnosis (24). These data show the need for finding new strategies and biomarkers to improve the management of advanced lung cancer patients, in both subtypes, although the differences between them should be considered.

1.3 Advanced non-small cell lung cancer

NSCLC represents 85% of total lung cancer diagnoses overworld. Approximately 55% of them are diagnosed at an advanced stages, with a 5-year survival of 6.1% (24). Its diagnosis requires a tissue biopsy for histological confirmation. Bronchoscopy or bronchoscopy combined with endobronchial ultrasound (EBUS) are the recommended techniques to obtain this tissue biopsy. In the case of peripheral lesions, transthoracic percutaneous fine needle aspiration and/or *core* biopsy, under imaging guidance is

proposed, however, there is a high risk of pneumothorax complication (17-50%) (25).

Histological diagnosis of NSCLC, as well as the molecular and genomic profile of the tumour, is crucial to make treatment decisions. Histologically, as described above, NSCLC can be divided into four major groups: ADC, SCC, LCC and others**.** ADC is the most common subtype, with about 50-60% of all NSCLC cases, followed by SCC (20-30%), both arising from alveolar cells located in the smaller airway epithelium. LCC and other types such as transitional cell carcinoma, sarcomatous carcinoma and other unclassified cancers, represent 10-20% of cases (26) (Figure 15).

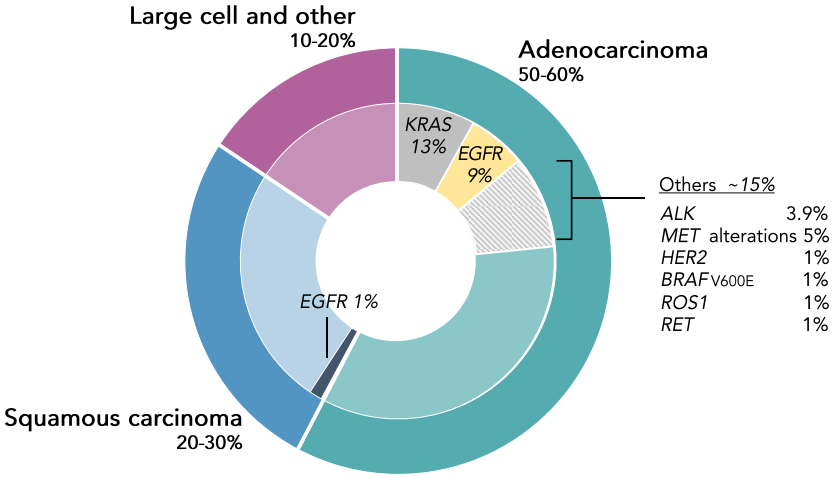

Figure 15. Molecular landscape of NSCLC. ADC is the most common subtype, with about 50-60% of all NSCLC cases, followed by SCC (20-30%). Most prevalent targetable mutations in ADC includes mutations in *EGFR*, *ALK*, *RET*, *ROS1* and *MET* among others. Adapted from Wang et al. (26).

Immunohistochemistry (IHC) is recommended to obtain a correct histological diagnosis of lung cancer. In addition to morphology,

characterization with specific antibodies is employed to confirm the different subtypes. Thus, ADC subtype is associated with thyroid transcription factor 1 (TTF1) positivity and napsin A, while p40 positivity with probable SCC. If neither are positive, the diagnosis remains NSCLC-not otherwise specified (NSCLC-NOS) (25). LCC are typically poorly differentiated and characterized by large cells with abundant cytoplasm and large nucleoli.

Molecularly, NSCLC is a heterogeneous disease composed of sub-populations of cells or clones with distinct molecular features. Several alterations in targetable oncogenic pathways in this subtype have been reported in the last decades, allowing a better treatment selection. The common alterations found in NSCLC are also dependent on the histology. Thus, the most frequently mutated genes in ADC include *KRAS* and *EGFR*, and the tumour suppressor genes *TP53, KEAP1,* and *NF1*, among others. Contrary, common mutated genes in SCC include the tumour suppressor *TP53* (90% of cases) and *CDKN2A*. Unlike ADC, actionable mutations in receptor tyrosine kinase (RTKs) are rarely detected in SCC. For example, only a small subset of SCC cases present mutations in *EGFR* (27) (Figure 15).

1.3.1 Current therapies applied in advanced NSCLC

Over the past decade, treatment options for NSCLC have changed dramatically (27). Importantly, these advances in lung cancer treatment and improvements in understanding the disease in the last years allowed a reduction in its incidence and mortality (28). However, the survival of patients with this type of tumour remains the poorest of all tumour types (29). Briefly, the different approaches for NSCLC management include targeted therapies,

immune checkpoint inhibitors (ICIs), chemotherapy and radiotherapy (Figure 16).

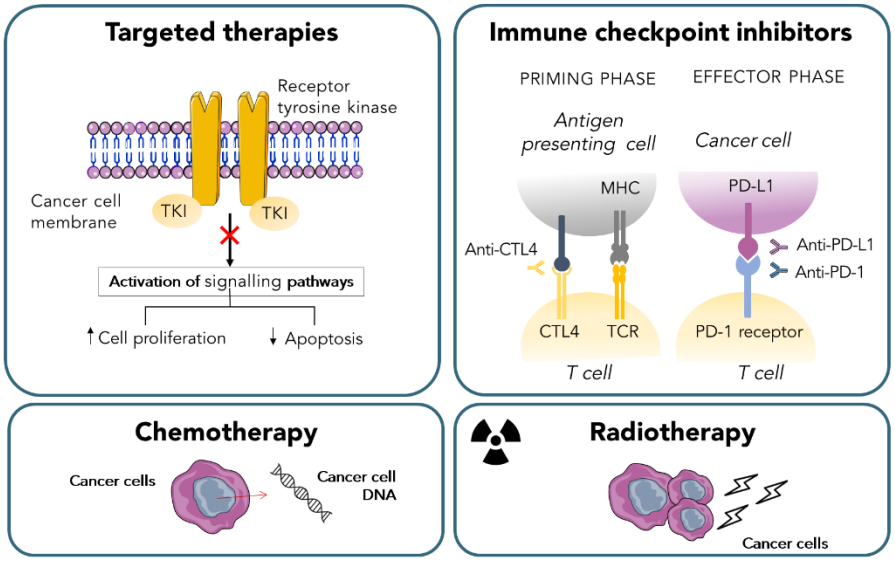

Figure 16. Different mechanisms of anticancer therapies, including targeted therapies, ICIs, chemotherapy, and radiotherapy**.** Abbreviations: MHC, major histocompatibility complex; TKI, tyrosine kinase inhibitor; TCR: T-cell receptor.

Targeted therapies

The molecular testing of *EGFR*, *BRAF*, *ALK* and *ROS1* genes in all NSCLC patients at diagnosis is mandatory. If these genes present any alteration, targeted therapy with tyrosine kinase inhibitors (TKIs) in the first line is recommended (25). TKIs inhibit the activation of kinase signalling pathways in cancer cells, and therefore, induce apoptosis. *EGFR* mutations are the most common targetable driver mutations in lung cancer. Thus, first and second-generation EGFR-TKIs have significantly improved progression-free survival (PFS) compared with platinum-doublet chemotherapy in patients

with sensitising *EGFR* mutations (30–35). In the same line, it has been reported that inhibitors of ALK, RET, BRAF, ROS1, MET and NTRK (26) activity have also improved the prognosis of advanced NSCLC patients (17). Nowadays several TKIs drugs are approved by the Food and Drug Administration (FDA) for the treatment of metastatic NSCLC with the most common driver mutations (Figure 17).

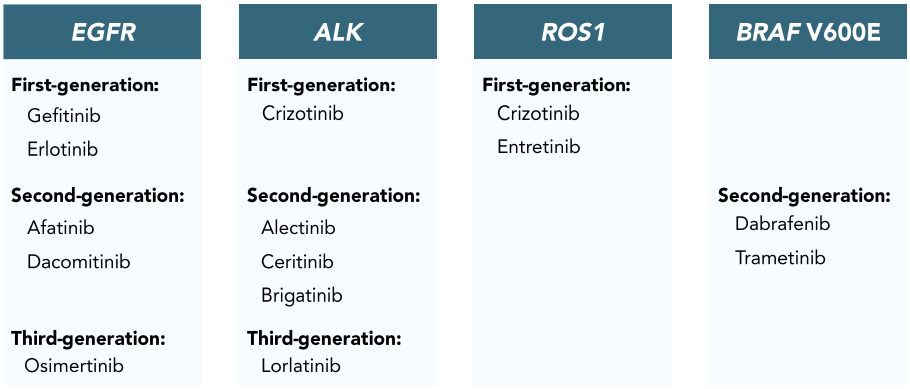

Figure 17. FDA-approved targeted therapies for the treatment of metastatic NSCLC with alterations in *EGFR*, *ALK*, *ROS1* and *BRAF* genes.

Despite the improvement in survival rates, less than 25% of patients can benefit from a targeted therapy and the majority of NSCLC patients finally develop resistance to TKIs based therapies through several molecular mechanisms (36). One of the common mechanisms of acquired resistance to first-generation and second-generation EGFR TKIs occurs with the appearance of a second mutation in the same gene: the substitution of threonine 790 with methionine (T790M) (37). The T790M mutation accounts for about half of all resistance to first line of different TKIs (38), so third-generation TKIs with activity against T790M mutant cells, such as osimertinib, have been approved for clinical use (25). In another hand, different MET alterations such as *MET* amplification or c-MET

overexpression also seems to be related to mechanism of evasion in the tumour after several TKIs therapies. Importantly, *MET* amplification is the most frequent off-target mechanism of resistance to osimertinib treatment (39).

Unusually, transformation of NSCLC ADC to SCLC can occur in 3-5% of patients as a resistance mechanism in *EGFR*-mutated adenocarcinomas after receiving therapy with EGFR-TKIs, associated with loss of *RB1* and *TP53* (40–42) (Figure 18).

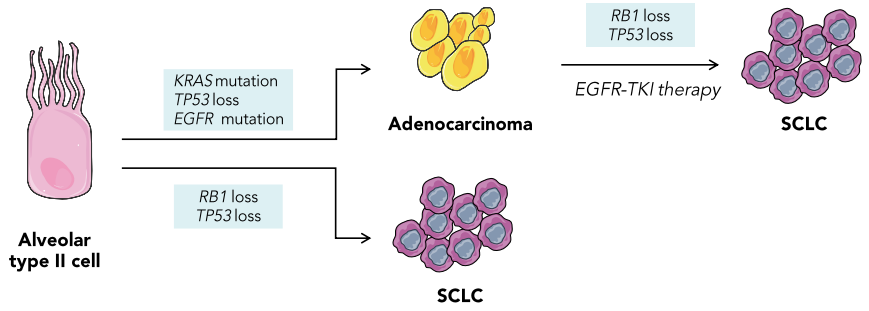

Figure 18. Possible origin of both lung cancer subtypes and transformation of NSCLC adenocarcinoma to SCLC. Adapted from Boumahdi et al. (43).

Other mechanisms of resistance associated with ALK inhibitors have also been reported in advanced NSCLC patients (36), showing the importance to monitor the disease not only through imaging techniques.

Immune checkpoint inhibitors

Immunotherapy, and ICIs have emerged as a new therapeutic strategy with an important impact on the treatment of advanced NSCLC patients. Due to cancer cells present multiple immunosuppressive mechanisms to escape from the normal immunological response and survive (44), immunotherapy aims to activate or regulate the immune system to detect and kill cancer cells.

Essentially, ICIs are monoclonal antibodies that target molecules used by cancer cells to escape the immune system: cytotoxic T lymphocyte antigen-4 (CTL-4), programmed death receptor (PD-1) and PD-ligand 1 (PD-L1). Briefly, the immune evasion has two mechanisms. First, T-cell activation requires antigen presentation by major histocompatibility complex (MHC) class II molecules on antigen presenting-cell (APC) (Figure 16). Then, a second activation signal that occurs with the binding between MHC and T-cell through CTL-4 is required to inhibit T cell activation. Anti-CTLA-4 antibodies can inhibit the CTLA-4 binding negative regulatory signal. Another immune checkpoint occurs when PD-1 receptors, expressed on activated T cells, bind to its ligand, PD-L1, expressed on tumour cells, which promote T-cell apoptosis. Of note, both anti-PD-1 and anti-PD-L1 antibodies inhibit this immune evasion strategy (45). In the last years it has been reported that this scenario is more complex where more regulatory molecules including natural killer cells (NK), macrophages, and myeloid-derived suppressor cells (MDSCs) plays an important role (46).

In advanced NSCLC, immunotherapy is recommended in patients without the presence of the above molecular alterations described (25). Currently, 6 ICIs are approved by the FDA for the treatment of advanced NSCLC, being pembrolizumab the standard first-line option (Figure 19).

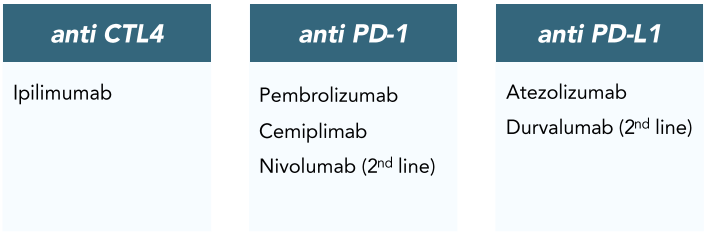

Figure 19. FDA-approved immunotherapy drugs for the treatment of metastatic NSCLC without alterations in *EGFR*, *ALK*, *ROS1* or *BRAF* genes.

Generally, the use of immunotherapy in advanced NSCLC showed superior survival rates compared with chemotherapy (47–49). Pembrolizumab, the mentioned humanized IgG4 mAb directed against PD-1, led to significant improvements in overall survival (OS), PFS, and objective response rate (ORR) in comparison with platinum-based chemotherapy (50,51). On the other hand, nivolumab, a human immunoglobulin G4 (IgG4) monoclonal antibody (mAb) that targets PD-1, has also improved OS, PFS and ORR in advanced NSCLC patients in comparison with docetaxel (52,53). However, not all patients respond and only a subset of them benefits from immunotherapy (54). Importantly, to improve ICIs efficiency, the combination of immunotherapy with chemotherapy is nowadays employed. Thus, the addition of pembrolizumab to platinum-based chemotherapy in previously untreated metastatic NSCLC has demonstrated a significant improvement in survival rates (55,56). Combined immunotherapy with chemotherapy is now suggested for those patients presenting with advanced or metastatic NSCLC without an *EGFR*, *ALK* or other driver alteration (25) and with good performance status.

Chemotherapy

Cytotoxic agents could inhibit enzymes required for the synthesis of DNA bases or bind to purine DNA bases, preventing its replication and transcription, and therefore, promoting cell death. For the majority of NSCLCs without an identifiable targeted therapy option, combination chemotherapy regimens have been the main option for over four decades obtaining poor OS rates (less than 15 months) (57–59). Currently, chemotherapy without combination of ICIs or TKIs is limited to a small subset

of patients who do not have actionable oncogenic drivers or present clinical contraindications for the use of immunotherapy (25).

Radiotherapy

Radiotherapy delivers ionizing radiation to the affected tissue, resulting in cellular death and ultimately curbing the progression of the malignancy. The application of this modality is often determined by various factors, such as the overall health and age of the patient, as well as the size and location of the metastasis. The utilization of radiotherapy in patients with metastatic NSCLC is currently being employed as a palliative measure to alleviate symptoms and manage localized tumour growth (25). In conjunction with chemotherapy or target therapies, radiotherapy forms an integral component of a multi-disciplinary approach in managing advanced NSCLC. Further studies are underway to optimize the use of radiotherapy in conjunction with other treatment modalities for an improved clinical outcome (60).

1.3.2 Current biomarkers to guide therapies in advanced NSCLC

To select the best therapy for each patient and to monitor disease evolution, several biomarkers and techniques are currently employed in the context of NSCLC. In advanced NSCLC patients, clinical factors such as age, Eastern Cooperative Oncology Group Performance Status (ECOG-PS) and sex, together the histology and molecular pathology described above should be considered. In addition, imaging tools to determine the disease evolution and treatment response are also employed. The most relevant molecular factors and techniques to select and guide the therapy are detailed below.

The tumour molecular profile of advanced NSCLC is a key element to choose the therapy for each patient. Although the presence of mutations in

oncogenic drivers is more associated with patients with adenocarcinoma histology and a never or light smoking history, driver mutations can be found across all histologies, ages, and smoking histories. Hence, *BRAF* mutations (61,62) and MET alterations (63) are found in a higher proportion in smokers than in non-smokers. Therefore, current guidelines recommend the testing for *EGFR* mutations; *ALK* and *ROS1* rearrangements; *BRAF* mutations (specially V600E); *RET* rearrangements; and *MET* exon 14 skipping mutations in all newly diagnosed advanced NSCLC (64,65). Regarding the technique and the sample of reference for the molecular characterization, multiplex gene testing with next-generation sequencing (NGS) in tissue samples is recommended, however the tissue availability is sometimes a limitation (65).

In contrast to targeted therapy, developing biomarkers to assess the efficacy of immunotherapy is considerably more complex, as it requires taking into account a wide range of dynamic factors such as the tumour microenvironment and host immune response, in addition to changes occurring in the tumour cells themselves (46). Nowadays, the expression of PD-L1 on the surface of tumour cells is the predictive biomarker employed to guide and select ICIs regimen in advanced NSCLC patients. Indeed, to select patients who will be treated with immunotherapy in monotherapy, PD-L1 expression in tumour tissue is mandatory, showing PD-L1 expression in more than 50% of tumour cells. The unique validated companion diagnostic test is based on immunohistochemistry characterization in tumour tissues, and its analysis is recommended in all patients with newly diagnosed advanced NSCLC (25). Despite some studies indicating that PD-L1 expression in tumour tissue could predict response to ICI (66), this association was not always observed (52,54), perhaps due to the intratumoral and intertumoral

heterogeneity of PD-L1 expression (67). In addition, there are several challenges associated with the technique itself, such as the selection of the correct antibody, among others (68). Recently, microsatellite instability (MSI) has been associated with a higher likelihood of response to immunotherapy in cancer patients (69). Nevertheless, due to the small subset of NSCLC patients who present a MSI-high status (70), MSI testing is not routinely performed in clinical practice, and the value of MSI as an immunotherapy biomarker in lung cancer is unclear. Thus, a significant gap remains in the identification of reliable and predictive response biomarkers that can be utilized in a clinical setting to effectively stratify patients for immunotherapy.

In another hand, routine laboratory test including haematology, renal and hepatic function and blood biochemistry are required into the management of NSCLC patients under therapy, however the use of serum markers, such as carcinoembryonic antigen (CEA) is not recommended (71).

Finally, to guide therapy and evaluate treatment response, clinical guidelines recommended the use of imaging tools, such as computerized tomography (CT) scan. Thus, first response evaluation is recommended after two to three cycles of therapy and performed every 6-9 weeks during course of disease. Measurement of lesions should follow Response Evaluation Criteria in Solid Tumours (RECIST) v1.1 (25,72).

1.3.3 Challenges and potential biomarkers in advanced NSCLC

Above, the different biomarkers employed into clinic routine to select the best therapy and monitor advanced NSCLC patients' evolution were summarized. Nevertheless, they are limited and, in some cases (for example, the use of PD-L1 determination to select immunotherapy candidates), their

efficacy is low. Therefore, in the last years and with the purpose to find new and better biomarkers into the management of advanced NSCLC, potential biomarkers are being under investigation.

Actually, several studies have reported the analysis of the tumour mutational burden (TMB) (73) as useful biomarkers to select patients who benefit from immunotherapy. Indeed, several clinical trials have shown a high TMB associated with an improved ORR and PFS in NSCLC treated with ICIs (74). However, more research is needed to confirm its utility as a reliable biomarker. The tumour-infiltrating lymphocytes (TILs) (75), the neutrophil-to-lymphocyte ratio (NLR) (76) and lactate dehydrogenase (LDH) also could be employed as useful biomarkers to select patients who will benefit from immunotherapy (66,77). Particularly, pre-treatment NLR together LDH has been reported as a potential prognostic marker, but prospective validations are needed (78).

In this context, liquid biopsy emerges as a potential tool to search new biomarkers, both at diagnosis and during the disease evolution (see expanded information in **section 2**).

1.4 Advanced small cell lung cancer

SCLC is a high-grade neuroendocrine carcinoma and the most aggressive form of lung cancer. SCLC accounts for approximately 15% of total lung cancer diagnoses worldwide and up to 25% of lung cancer deaths (79). This subtype is highly related to tobacco smoking and approximately, 75% of patients are diagnosed at advanced stages, with a 5-year survival of 2.8% (24).

For pathological diagnosis, histology is preferred over cytology. IHC for analysing neuroendocrine markers, such as synaptophysin, chromogranin or CD56 is commonly used, however, SCLC can be negative or focally positive for only one of these markers. TTF1 is expressed in 90% of cases and 50% of nuclei are positive for Ki-67. Negativity for p40 characterizes this tumour subtype, in contrast with p40 positivity in SCC (80).

Regarding their molecular features, large studies of genome-wide analyses have confirmed loss-of-functions mutations of *TP53* and *RB1* genes in almost all SCLC cases (81–84). Moreover, frequent inactivation of *Notch* family members was also observed (81). Due to all these alterations are loss-of-function, the ability to target oncogenic mutations therapeutically is limited in SCLC, in contrast with NSCLC.

Importantly, recent advances have made it possible to deepen the molecular knowledge of SCLC, which has allowed to distinguish between four different subtypes characterized by distinct gene expression profiles. These subtypes are the neuroendocrine subtypes SCLC-A (ASCL1-positive) and SCLC-N (NEUROD1-positive), and the non-neuroendocrine subtypes SCLC-P (POU2F3-positive) and SCLC-Y (YAP1-positive) (85), that could offer new therapeutic options in the close future.

1.4.1 Current therapies applied in advanced SCLC

This section has been adapted/extracted from a published review (3).

Systemic treatment of advanced SCLC patients in first line is based on the combination of platinum and etoposide-based chemotherapy, with median survival ranging from 6 to 12 months (86). Commonly, chemotherapy regimens are administered together radiotherapy, in curative as well as in

palliative therapy. The use of prophylactic cranial irradiation (PCI) and thoracic radiotherapy has improved outcomes in patients who have responded to first-line treatment (87), being their use incorporated into SCLC treatment guidelines (80).

Recently, the use of immunotherapy has been also incorporated in patients with metastatic disease (88–91). In first-line, the blockade of the PD-1 receptor or its ligand PD-L1 has been shown to improve the prognosis of patients with ED-SCLC (92,93). The Impower 133 (NCT02763579) and CASPIAN phase III trials (NCT03043872) demonstrated that adding atezolizumab or durvalumab to platinum plus etoposide chemotherapy improves OS and PFS compared to chemotherapy alone (94,95). More recently, the KEYNOTE-604 (NCT03066778) study reported that combining pembrolizumab with platinum and etoposide improves PFS but does not significantly improve OS in patients with ED-SCLC (96) (Figure 20).

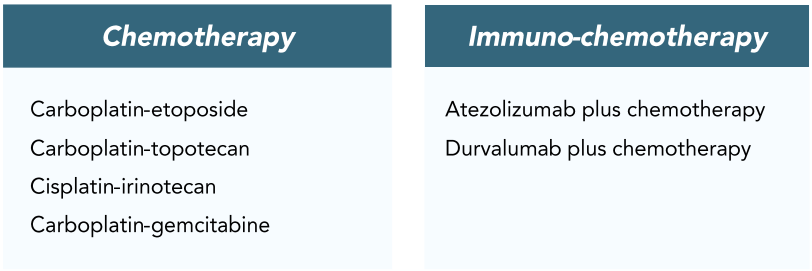

Figure 20. FDA-approved therapies for the treatment of ED-SCLC in 1st line.

Despite the therapeutic efforts and a good initial therapy response, unfortunately the majority of SCLC patients progress within the first 6 months of first line therapy completion (80). Until now, the choice of the second-line treatment is limited to topotecan or cyclophosphamide, doxorubicin and

vincristine (CAV), with poor response rates, typically less than 10% (97). Nowadays, more options can be considered, such as Lurbinectedin, which has been approved by the FDA for salvage treatment of SCLC that has relapsed from first-line chemotherapy (98). On the other hand, nivolumab and pembrolizumab have also been approved by the FDA for refractory SCLC based on the results of the CheckMate-032 (NCT01928394) and Keynote-158 (NCT02628067) clinical trials, respectively (99,100). However, in the Checkmate-331 trial (NCT02481830), nivolumab failed to demonstrate an improvement in OS versus standard treatment in patients with relapsed or refractory SCLC treated with a platinum-based line of chemotherapy (101).

Regarding other options and in contrast with NSCLC, in SCLC there are no clear driver genes or kinase targets and, consequently, no approved targeted therapies are being employed to treat these patients (102). Existing drugs have failed to demonstrate an improvement in patients' outcomes (103) and the identification of new therapeutic targets in SCLC has been challenging, partly because driver mutations are primarily loss-of-function (genes *RB1* and *TP53*) or currently difficult to target (104,105). Nevertheless, new therapies such as abemaciclib (a CDK4/6 inhibitor), veliparib (an oral PARP inhibitor) (106), SLFN11 (107,108), Rovalpituzumab tesirine (Rova-T) (109) and alisertinib (106,110) are being under investigation.

1.4.2 Current biomarkers in advanced SCLC and future challenges

Nowadays, there are still no validated biomarkers that can be used for treatment decisions in the context of SCLC. Besides, in contrast with NSCLC, PD-L1 expression and testing is not recommended in routine clinical practice in this tumour (80). Regarding disease monitorization, the actual therapeutic

approach is similar than in NSCLC. Therapy response is evaluated using imaging tools such as CT scan every 2-3 months (80).

Like in NSCLC field, some biomarkers are being under investigation to improve SCLC management in advanced patients and new therapeutic approaches have opened new horizons and hopes for improving SCLC outcomes. Indeed, NLR have shown its potential utility as predictive biomarker in advanced SCLC patients (111), however, more research is still required to reach a better understanding of the molecular mechanisms behind SCLC biology and its response to the different therapies to advance in the identification of new predictive biomarkers to apply the most convenient therapeutic strategy for each patient. Notably, the information obtained from the analysis of liquid biopsy components would be crucial for this objective.

2. LIQUID BIOPSY

The term liquid biopsy was born in the past years as a new strategy to improve the management of different pathologies or physiologic states such as cancer (112–114), liver diseases (115) and prenatal analyses (116), among others. The analysis of liquid biopsy allows to evaluate different molecules obtained from body fluids and to monitor their changes over the time, which enable to follow the disease evolution (113). Nowadays, blood is the most common fluid employed, although, in the last years, other fluids such as saliva (117) or urine (118) are being employed.

In the oncology field, the interest in liquid biopsy has increased in the last decades, providing new opportunities in the management of different stages of the disease: early detection of the disease or tumour recurrence,

individual risk assessment and the treatment monitoring (119). Also, cancer screening is considered another potential application (120).

Hence, liquid biopsy has emerged as an alternative to the tumour tissue-based analysis, the current gold standard for the management of patients with cancer. Nowadays, the genetic profile of tumours is obtained from surgical or biopsies specimens, but this procedure cannot be always successfully performed. Indeed, in lung cancer, biopsy samples are often of poor quality or quantity, justifying the need to explore new tools for the molecular characterization (121,122). A tissue biopsy involves several undesirable effects such as potential surgical complications and clinical risk to the patient. Besides, the solid biopsy cannot be obtained repeatedly during the therapy. Of note, the non-invasive nature of liquid biopsy offers the opportunity to obtain samples in a non-invasive way at any moment and, therefore, enables to track the genomic evolution of the tumour in real-time. Other advantage of liquid biopsy is that it can offer a complete image of the tumour biology of different lesions, while the solid biopsies only capture a part of them (113). In addition, metastases remain the principal cause of cancer-related deaths (123) and they can develop different genomic characteristics absent or poorly represented in the biopsy of the primary tumour. Large studies of primary and metastatic tumours (124,125) have shown the relevance of intra-tumoral and inter-tumoral heterogeneity and how this characteristic contributes to treatment failure in patients with cancer (126,127). Thus, liquid biopsy can capture the genetic landscape of both lesions (primary and metastatic) since the tumoral material present in body-fluids can come from the different tumoral lesions (Figure 21).

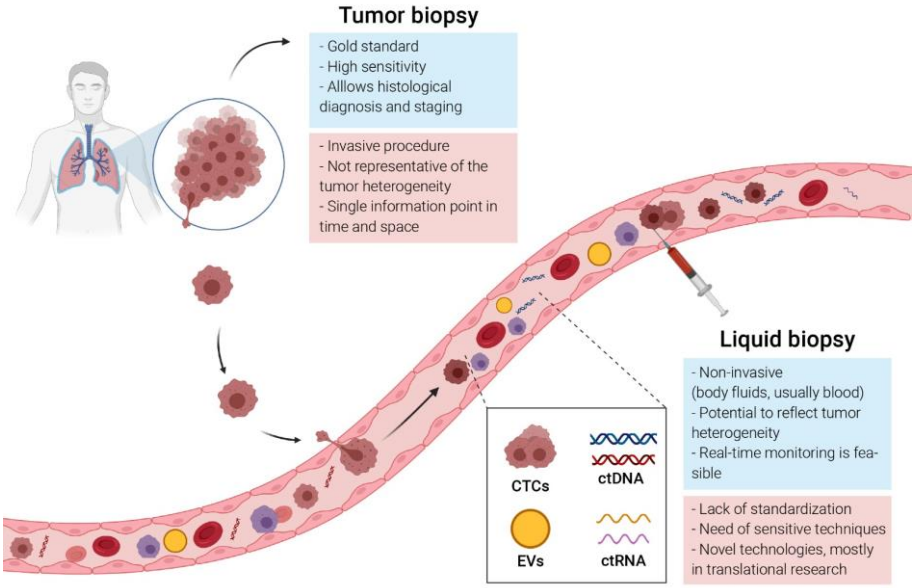

Figure 21. Tissue biopsy versus liquid biopsy: comparison of the advantages and limitations (Mondelo-Macía et al., 2021. Biomedicines).

The most common circulating elements present in liquid biopsies are circulating free DNA (cfDNA) and circulating tumour cells (CTCs). cfDNA can be released into the blood by normal and tumour cells. The fraction released from tumour cells constitutes the circulating tumour DNA (ctDNA). Similarly, CTCs can be released to the blood from the primary or metastatic tumour locations. In the past years, the clinical interest of both liquid biopsy components is reflected by an increase in their analysis in several clinical trials. Currently, the database ClinicalTrials.gov (www.clinicaltrials.gov: accessed on 20th February 2023) lists more than 300 active clinical trials that analyse CTCs and more than 100 trials interrogating cfDNA/ctDNA levels in different cancer diseases. In addition, technological advances in the detection and characterization of liquid biopsy components have enable the introduction

of liquid biopsy into the clinic routine to manage some tumour types. Thus, the FDA has already approved several liquid biopsy assays (based on blood or on urine analyses) for their use to help oncologists in the patients' managing (1,128).

Due to their clinical interest the characteristics of CTCs and cfDNA are explained in more detail within the next sections.

2.1 Circulating free DNA

The next section has been adapted/extracted from a recently published review (1).

CfDNA was first reported in healthy individuals by Mandel and Métais in 1948 (129). However, it was not until 1966 when the discovery of high values of cfDNA in patients with systemic lupus erythaematosus (130) showed the potential of cfDNA as a biomarker for autoimmune diseases. Ten years later, Leon et al. characterized cfDNA for the first time in the field of oncology and reported higher levels in cancer patients than in healthy individuals, suggesting its potential as a diagnostic marker and to characterize tumours in a non-invasive and dynamic way (131). In 1994, cfDNA was recognized as an important tool to detect several mutations in the blood of patients with myeloid disorders (132) and pancreatic adenocarcinomas (133) and currently represents a key element for precision oncology (134).

CfDNA consists of a heterogeneous and complex DNA fraction present in free body fluids associated with extracellular vesicles (EVs) or as part of macromolecular complexes such as nucleosomes (135). The size of cfDNA is highly variable depending on the mechanisms involved in its fragmentation, with a normal peak of 166 bp fragments, which corresponds to the length of the DNA bound to a nucleosome (136). Due to this high fragmentation,

cfDNA origin is mainly associated with cell death mechanisms; however, to date, the origin of cfDNA remains partially unclear, and different mechanisms have been suggested in several studies (137–139). Here, we summarize the principal origins and sources of cfDNA described until now (Figure 22):

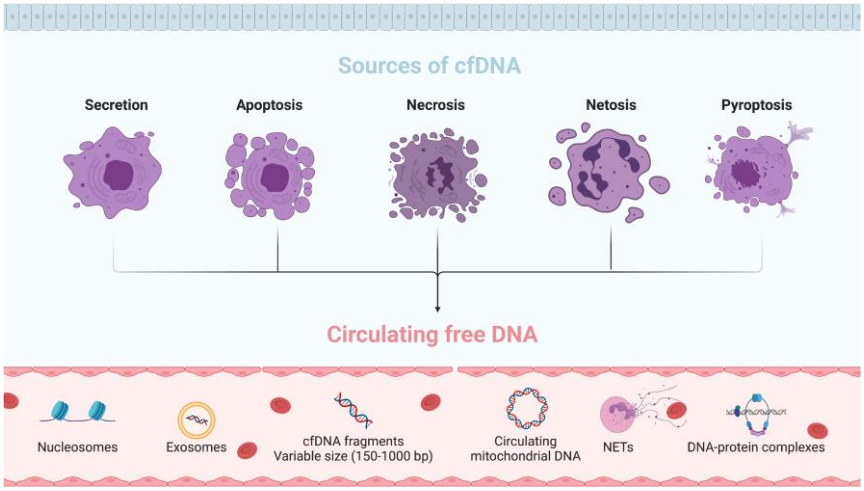

Figure 22. Mechanisms involved in the release of circulating free DNA. (Mondelo-Macía et al., 2021. JPM).

Secretion. Most cfDNA release into the circulation is associated with active secretion in EVs, such as exosomes, microparticles, or apoptotic bodies. This cfDNA is protected from nucleases and can be released into circulation through the breakdown of EVs. Some studies have reported that over 90% of cfDNA is associated with this type of release (140).

Apoptosis. Apoptosis, also known as programmed cell death, is an essential process to maintain cellular homeostasis. This process allows the removal of damaged cells by caspase activation. When the caspase pathway is activated, the cell starts to suffer morphological and biochemical changes that will result in cell and nuclear retraction, lipid redistribution, and DNA

fragmentation. The cfDNA released by apoptosis is highly fragmented, double stranded, of low molecular weight, and approximately 150–200 bp in size (141).

Necrosis. Necrosis is an accidental cell death in response to physical or chemical injury characterized by cell swelling followed by loss of membrane integrity, with the consequent release of intracellular content. This process is more rapid than apoptosis, and there is no specific digestion of chromatin; therefore, the cfDNA obtained is larger, approximately 1000 bp (138).

NETosis. NETosis is a form of programmed cell death that neutrophils can undergo in response to microbes and sterile inflammation. The cfDNA fragments obtained via NETosis are similar to those obtained via necrosis (138).

Pyroptosis. Pyroptosis is an inflammatory process that induces the activation of inflammatory cytokines, interleukins and rapid cell death in response to diverse infections (142). It has been reported to be closely associated with some diseases, such as atherosclerosis and diabetic nephropathy, and with cancer (143).

Recently, Aucamps et al., after an extensive bibliography review, concluded that cfDNA can arise from a single source but also from combinations of various sources and causes (138). The sex of individuals as well physiological processes, such as obesity (144), age (145), stress (146), and exercise (147) can induce the release of cfDNA into the circulation.

Once in circulation, the cfDNA half-life varies from several minutes to 1–2 hours (137,144,148) and it has been reported that their clearance is due to their degradation by some enzymes, such as deoxyribonuclease II and

phosphodiesterase I. Additionally, cfDNA is eliminated from the circulation by organs such as the liver, spleen and kidney (137,141). The liver was reported to play a major role in the clearance of cfDNA, while the kidney did not seem to be so involved in this process (144). Therefore, the cfDNA level in blood is a result of a balance between cfDNA release and cfDNA clearance processes. In healthy individuals, cfDNA appears at low levels due to cells undergoing apoptosis and is rapidly removed. However, in malignancies, clearance of cfDNA is insufficient, and cfDNA levels increase (131).

Levels of cfDNA originating from tumour cells is denominated ctDNA and vary widely among individuals and tumour types (149). In cancer patients, ctDNA is found in a variable but normally very low percentage (0.01-1%) in relation to all cfDNA. This fraction varies depending on the stage, location or degree of vascularization of the tumour. Thus, tumours with multiple metastatic locations and highly vascularized will have higher levels of ctDNA (149,150). A good correlation between ctDNA levels and tumour burden has been well reported (151), while many other studies have demonstrated the value of ctDNA to monitor driver mutations and guide therapy (134,152).

2.1.1 Technologies to analyse cfDNA

The present section has been adapted/extracted from a recently published chapter (2).

In the past years, several technologies have been developed to analyse and characterize the cfDNA from blood samples. Firstly, four main strategies are commonly used to characterize the concentration and size of isolated cfDNA: spectrometry, fluorometry, electrophoresis, and PCR-based techniques. The most specific and sensitive of the four options is the assessment of cfDNA quantity by PCR-based strategies to detect conserved

sequences in the genome (153). Next, specific cfDNA analyses allow to identify rearrangements, methylation changes, point mutations and copy number alterations (CNA), among others, which are present in the ctDNA fraction (153). These alterations can be associated with therapy resistance and serve to guide the treatment selection (153) (Figure 23).

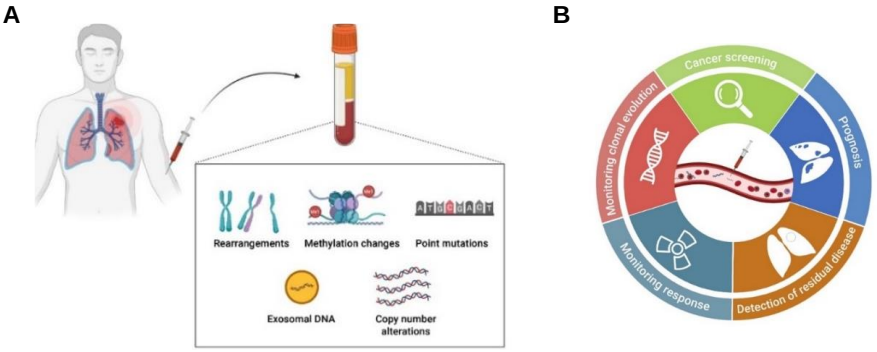

Figure 23. Potential clinical applications of ctDNA in lung cancer patients. (A) Range of alterations in circulating free DNA. (B) Applications of ctDNA analysis during the disease management. (Mondelo-Macía et al., 2021. Biomedicines).

Nevertheless, the low concentration of ctDNA in total cfDNA involves a challenge for detecting genetic alterations. Thus, two principal approaches have been developed to solve this challenge: single-gene analysis (PCR-based methods) or genome-wide analysis (through NGS strategies) (Table 2).

PCR-based techniques were the first assays that allowed to detect single or a low number of point mutations using highly sensitive and specific techniques with a rather fast and cost-effective rate. Quantitative PCR (qPCR) was the first assay employed, reporting specific known mutations, but with a limited sensitivity (0.1-1%) (154). These strategy include assays such as the Cobas EGFR mutations Test v2, which was approved in 2016 by the FDA and

the European Medicines Agency (EMA) in NSCLC patients (155), and the Idylla platform, which combines the cfDNA isolation and the qPCR thanks to microfluidic technology. In the last years, new approaches such as digital PCR (dPCR) methods, that include droplet digital PCR (ddPCR) and BEAMing (beads, emulsions, amplification and magnetics), provided high concordance with results obtained in tumour tissue (156–158) analysing small panels of variants and showed improved sensitivity (0.01–0.1%) and specificity (100%) (159). The main limitation of ctDNA analyses using PCR-based techniques is the requirement of previous information about the mutations characterizing this tumour. For this reason, PCR-based techniques are commonly employed to select targeted therapies, monitor the patients' evolution or detect resistance associated mutations during the treatment.

The second approach is focused on a genome-wide analysis of CNAs or point mutations through NGS strategies. Based on the assay panel size, there are single-locus/multiplexed assays, targeted sequencing, and genome-wide sequencing (160). Genome-wide characterization allows a more complete and patient-specific genotyping to assess tumour heterogeneity and to follow the clonal evolution across the treatment. Among these approaches, ctDNA can be analysed by specific panels covering a high number of targeted genes (by NGS panels) or analysing the total genome by whole-genome sequencing (WGS) or whole-exome sequencing (WES). The main limitation of NGS-based strategies is the high cfDNA input requirement and their low specificity (80–99%) (150,154).

Table 2. Summary of the most common strategies for ctDNA analysis.

Method	Platform	Sensitivity	Specificity	Limitations
PCR-based	qPCR	1-0.1%	99%	Detects only known mutations; medium sensitivity
	ddPCR	0.01 - 0.1%	100%	Detects only known mutations; limited in multiplexing
	BEAMing	0.01%	100%	Detects only known mutations
Genome wide analyses	NGS panels	> 0.4	> 99%	High ctDNA input; bioinformatic interpretation
	WGS/WES	0.02%	80-90 %	High ctDNA input; bioinformatic interpretation; higher risk of false positives

WES and WGS based methods allow the detection of all possible aberrations in DNA, although it has limited analytical sensitivity in cfDNA applications due to the efficiency by which the genetic regions of interest can be captured/enriched from cfDNA and the higher error rate of sequencing reactions (135).

2.1.2 Clinical relevance

Due to the great development of technology focused on circulating biomarkers characterization, cfDNA testing is nowadays implemented for the therapy selection in some advanced tumours. NSCLC was the first tumour in which the analysis of ctDNA for tumour phenotyping was included in the guidelines. Thus, in 2016 the FDA approved the first diagnostic test based on liquid biopsy: the Cobas® EGFR Mutation Test v2 (Roche Molecular Systems, Inc., Pleasanton, CA, USA) thanks to the good results obtained in the clinical trial NCT01342965. The test allows the detection of *EGFR* mutations using cfDNA from plasma samples in NSCLC patients for guiding the selection of

patients who could benefit from anti-EGFR therapies (161). In the same year, the Epi proColon® test was the first FDA-approved blood-based colorectal cancer screening test, through the detection of methylated Septin9 DNA (162). Therascreen PIK3CA RGQ PCR kit has also been approved by the FDA as a companion diagnostic for the detection of *PIK3CA* mutations in plasma samples from patients with advanced-stage breast cancer (163). Recently, two cfDNA-tests based on NGS technology have been also approved for a clinical application: the Guardant360 CDx (Guardant Health, Inc., Redwood City, CA, USA) in the context of NSCLC (164) and FoundationOne Liquid CDx test (Foundation Medicine, Inc., Cambridge, MA, USA) for patients with different solid tumours (165). Both panels allow the identification of patients who may benefit most from treatments based on targeted therapies. In the context of immunotherapy, the determination of MSI and mismatch repair deficiency (MMRD) by FoundationOne Liquid CDx test allows to select candidates for fist-line immunotherapy, in patients with unresectable or metastatic solid tumours with MSI-high or MMRD, independent of the tumour histology (69,166).

2.2 Circulating tumour cells

The next section has been adapted/extracted from a recently published review (3)

CTCs are another principal liquid biopsy biomarker in use. CTCs were first observed in the blood of a metastatic cancer patient by Thomas Ashworth in 1869 (167). He described the microscopic observation of cells with similar characteristics to the tumour cells in the blood of a patient and he concluded that are tumour cells released from the tumour to the bloodstream. Next, during the decades 1950-1960, the interest of these cells increased and several works were published (168–170).

Nowadays, as it is well known, CTCs are tumour cells originating from the primary or metastatic sites that can enter the circulation and disseminate to distant sites. Peripheral blood offers the possibility to analyse the presence of this circulating tumour population for cancer diagnosis and disease monitoring. The importance of CTCs for diagnostic and prognostic purposes has been well reported in different cancer types, such as metastatic breast (171,172), prostate (173), NSCLC (174) and colorectal cancer (175). Interestingly, in SCLC several studies have described higher CTC levels in comparison to other cancer types (176), supporting the interest of this circulating population as an accessible tumour biopsy. However, the proportion of CTCs in the bloodstream is very low, with approximately 1 CTC per 10^6–10^7 leukocytes (177), being a challenge their detection and isolation.

CTCs have a very short half-life (1–2.4 hours) (112), and the majority of them are rapidly cleared; however, some of them evade recognition by immune cells, survive into the bloodstream and can reach distant locations to generate metastasis (178–180) into secondary organs. These cells are characterized by a hybrid phenotype in terms of epithelial and mesenchymal markers that favour their survival in circulation (179–182).

2.2.1 Technologies for CTCs analyses

The low proportion of CTCs in the bloodstream together with the molecular heterogeneity that characterizes these cells is the principal challenge for CTCs isolation and detection. Several CTCs detection platforms have been developed in the past decades to obtain an enriched sample of CTCs. All technologies isolate these cells focusing on differential features between CTCs and blood cells, such as protein expression, morphology,

volume and biophysical properties, presenting different advantages and limitations. These technologies can be categorized based on the method of isolation as antigen-dependent (affinity-based) or antigen-independent (183) (Figure 24).

Antigen-dependent

Antigen-dependent isolation approaches are the most common methods employed and they are based on the presence of specific surface markers in CTCs (called positive enrichment) or by blood cells (negative enrichment).

A. Positive enrichment, the most employed strategy is usually carried out using antibodies that recognize epithelial cell adhesion molecule (EpCAM) (184) conjugated with magnetic nanoparticles**.** Among the current EpCAM-based technologies, CellSearch® system (Menarini, Silicon Biosystem, Bologna, Italy) (185) has become the "gold standard" for the CTC-detection methods. CellSearch® system employs anti-EpCAM-coated ferrofluid nanoparticles for the selection of EpCAM positive cells. Next, an immunostaining step discriminates CTCs from leukocytes based on the positive expression of cytokeratins and the absence of CD45 staining together with morphologic criteria. A high number of alternatives that employ magnetic nanoparticles conjugated with anti-EpCAM antibodies are available (186).

Recently, new positive enrichment methods are being developed, in which the specific surface markers are immobilized on the surface of microfluidic chips (186) to increase the contact between the cells and, therefore, to enhance capture efficiency. However, the isolation in all these approaches is based on the EpCAM expression, therefore, they are not able to

detect CTCs without EpCAM expression, for example, CTCs of non-epithelial tumours such as sarcomas or CTCs that have undergone epithelial-to-mesenchymal transition (EMT) (187,188).

B. Negative enrichment methods employ magnetic nanoparticles conjugated with antibodies against the well-established leukocyte antigen CD45 (189) or other antigens expressed in blood cells and represent a good alternative to avoid the limitations of the EpCAM-dependent isolation. They allow isolating CTCs independently of any membrane marker expression, however due to the low proportion of CTCs and the recent observation that they travel into the bloodstream coated with blood cells (190), the resulting recovery rate is often relatively low (191).

Antigen-independent

Antigen-independent methods are based on the physical properties of CTCs such as density, electric charges (DEP, dielectrophoresis), size and deformability, among others. The principal advantage and difference with the antigen-dependent methods are that they do not require specific surface markers on CTCs, so they also allow the isolation of CTCs with a low epithelial phenotype. Density-based methods were the first techniques developed. These methods allow the processing of high volumes of blood (about 25 mL) in a short time, however, they generally show a low efficiency and purity of the sample obtained (186). The size-based methods are the most common. They are based on the fact that tumour cells are larger than blood cells (191,192) and, therefore, they can be isolated using filter-based strategies (such as ISET assay (Rarecells Diagnostics, Paris, France) (193), microfluidic chips (such as Parsortix system (Angle, UK))(194) and methods based on

centrifugal forces (195). The different charges between blood cells and CTCs can also be employed in their isolation. DEP field forces are employed to move CTCs independently to other blood cells, and represent a highly specific approach for isolation (196).

Antigen-independent methods are generally easy to implement, however they depend on the availability of advanced materials or assistive engineering technologies for better clinical application (20). Interestingly, new methods combining antigen-based capture with the advantages of microfluidics strategies, such as CTC-iChip, are being developed for increasing the isolation efficacy (197). However, nowadays the development of a robust and standardized platform to capture CTCs for clinical application remains a challenge.

Finally, it's important to remark that small volumes processed with the methods here described may be a serious limitation for the detection of these rare events, especially in cancer patients without metastases, in which the number of CTCs is expected to be very low. To solve this problem, some "*in vivo*" approaches such as GILUPI Nanodetector® (198) or the Diagnostic leukapheresis (DLA) can be employed (199).

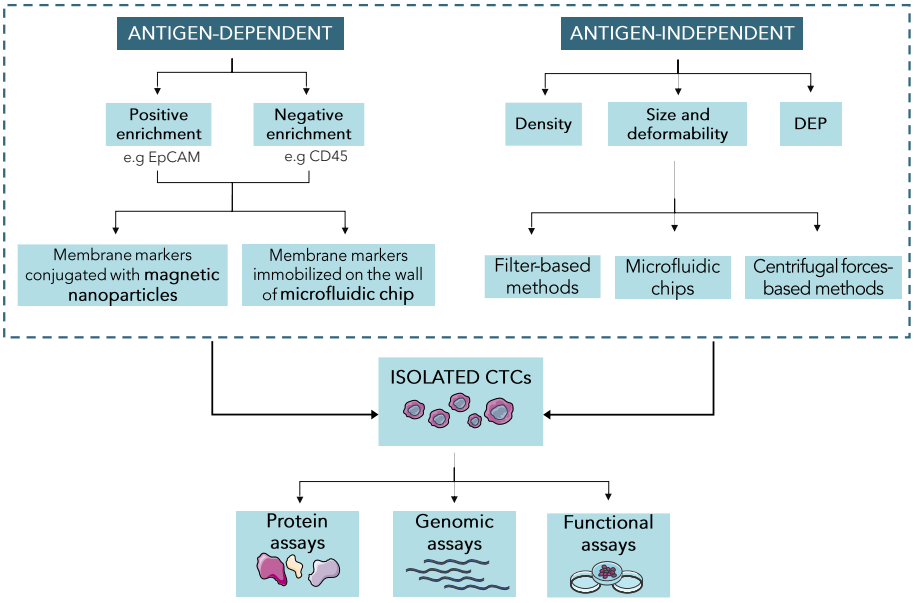

Figure 24. Different strategies for CTCs enrichment and detection. Abbreviations: DEP, dielectrophoresis.

After enrichment, the CTCs fraction usually still contains a substantial number of leukocytes (184). This background of leukocytes is seen in all CTCs enrichment platforms being the posterior molecular analyses of CTCs a challenge. Therefore, after the first enrichment of CTCs there are some platforms that allow the isolation of pure CTCs at the single level by the use of micromanipulation or via dielectron force manipulation, such as the DEPArray system (Menarini, Silicon Biosystem, Bologna, Italy), among other strategies (200). Analyses of individual CTCs/clusters at the DNA, RNA or protein level provide valuable information about the molecular heterogeneity of these cells and a more precise characterization of the disease (201). In addition, surface proteins, which can be key targets for personalized therapies, can be analyzed by immunofluorescence (IF). Thus, certain protein expression

in CTCs has been studied, such as ER and HER2 in breast cancer, among others (202).

2.2.2 Clinical relevance

During the last decades, several platforms have reported the feasibility to detect CTCs and monitor changes during the course of treatment in patients with several metastatic carcinomas (197,203,204). Moreover, the presence of CTCs before the treatment in the blood of patients with cancer has shown prognostic significance and their levels after the treatment can be predictive of response to the therapy. Nowadays, the clinical value of CTC presence remains controversial because CTCs number is very variable between different tumour types (205), and only 2 platforms were approved by the FDA.. CellSearch® system was the first FDA-approved platform for CTCs isolation and enumeration for clinical use in metastatic breast, prostate, and colorectal cancer. First, it was approved in 2004 for use in a clinical setting to predict outcomes for metastatic breast cancer patients (206). Although in the posterior years, CellSearch® system was also granted FDA approval to aid in monitoring metastatic colorectal (175) and prostate cancer patients (207), its real use in clinical routine is scarce. Recently, in May 2022, Parsortix system was approved for clinical use in metastatic breast cancer patients (208).

2.3 Other circulating biomarkers

CTCs and cfDNA are not the unique biomarkers employed to improvement the management of cancer patients. Thus, there are other markers in the field of liquid biopsy with great potential for future clinical applications. One example are EVs which are nanosized particles with membranes released by any cell type, including cancer cells. The most

common subtypes of EVs are exosomes, with a size between 50 and 150 nm. Exosomes are very abundant, express membrane proteins on their surface and contain several particles, such as proteins, nucleic acids, and lipids (209). Thus, exosomes offer the possibility to analyse the expression of proteins of interest on their surface, such as PD-L1. Actually, EVs have shown to be valuable tools as biomarkers for longitudinal monitoring, defining tumour type, stage, progression and treatment response (210,211). Other elements, such as circulating microRNA (miRNA), circulating RNA, platelets, and circulating proteins, are at the early stages of investigation (212). In recent years the potential of tumour-educated blood platelets as a non-invasive tumour biomarker has been demonstrated (213,214). Platelets are involved in the progression and spread of various solid cancers, and their RNA molecular signatures can provide specific information about the presence, location, and molecular characteristics of the tumours (215).

Regarding circulating proteins, few studies have investigated their possible value as prognostic or predictive biomarker in lung cancer, however, global protein changes may provide an independent biomarker that reflects the tumour evolution (216).

OBJECTIVES

OBJECTIVES

The general goal of this thesis is to explore the clinical utility of different circulating biomarkers, such as cfDNA, CTCs, or plasma proteins, to improve both therapy selection and monitoring of advanced lung cancer patients. Specifically, the secondary objectives of the thesis are:

CHAPTER I. Blood-based technologies to select non-small cell lung cancer (NSCLC) patients who will benefit from targeted therapies.

1.1. To evaluate the efficacy of a qPCR technology (Idylla™ test) to determine *EGFR* status in blood samples of advanced NSCLC patients and monitor the response to EGFR inhibitors.

1.2. To develop a blood-based test to identify both *MET* amplification and c-MET overexpression in cancer patients for monitoring the appearance of resistance to several lines of TKIs in NSCLC patients.

CHAPTER II. Circulating free DNA and circulating tumour cells as prognostic and predictive biomarkers in non-small cell lung cancer (NSCLC) patients treated with immunotherapy.

2.1. To develop an efficient approach to detect and analyse PD-L1 expression in CTCs and investigate the predictive value of this tumour circulating population in advanced NSCLC patients.

2.2. To determine the value of CTCs and total cfDNA levels as a prognostic, predictive, and monitoring tool in advanced NSCLC patients under first-line of pembrolizumab therapy.

CHAPTER III. Plasma circulating free DNA and circulating tumour cells as prognostic biomarkers in small cell lung cancer (SCLC) patients.

3.1. To investigate the prognostic and predictive value of CTCs and cfDNA levels in newly diagnosed advanced SCLC patients receiving first-line standard therapy.

3.2. To develop a predictive model to identify SCLC patients who will benefit from first-line therapy.

CHAPTER IV. Circulating proteins as predictive biomarkers for immunotherapy in metastatic non-small cell lung cancer (NSCLC) patients.

4.1. To identify a proteomic signature with value in predicting the response to immunotherapy in advanced NSCLC patients.

CHAPTER I

Blood-based technologies to select non-small cell lung cancer patients who will benefit from targeted therapies.

I.A *EGFR* mutations: Simple and rapid blood-based qPCR test to select and guide treatment of advanced NSCLC patients.

I.B Development of a blood-assay to detect *MET* alterations using circulating free DNA and circulating tumour cells in NSCLC patients.

CHAPTER I.A

EGFR mutations: Simple and rapid blood-based qPCR test to select and guide treatment of advanced NSCLC patients.

EGFR mutations: simple and rapid blood-based qPCR test to select and guide treatment of advanced NSCLC patients.

"Rapid Idylla™ mutational testing to detect EGFR mutations in plasma samples and to monitor therapy in advanced NSCLC patients (217)**"**

Patricia Mondelo-Macía[1,2,3], Ramón Manuel Lago-Lestón[1], Aitor Rodríguez-Casanova[2,3,4,5], Alicia Abalo[1], Ángel Díaz-Lagares[3,4,8], Jorge García-González[6,7,8], Luis León-Mateos[2,3,6,7,8], Roberto Díaz-Peña[3,9]*, Laura Muinelo-Romay[1,3,8]*.

[1] *Liquid Biopsy Analysis Unit, Translational Medical Oncology (Oncomet), Health Research Institute of Santiago (IDIS), Santiago de Compostela, Spain.*

[2] *Universidade de Santiago de Compostela (USC), Santiago de Compostela, Spain.*

[3] *Galician Precision Oncology Research Group (ONCOGAL), Medicine and Dentistry School, Universidade de Santiago de Compostela (USC), Santiago de Compostela, Spain.*

[4] *Epigenomics Unit, Cancer Epigenomics, Translational Medical Oncology (Oncomet), Health Research Institute of Santiago (IDIS), Santiago de Compostela, Spain.*

[5] *Roche-CHUS Joint Unit, Translational Medical Oncology Group (Oncomet), Health Research Institute of Santiago (IDIS), 15706 Santiago de Compostela, Spain.*

[6] *Department of Medical Oncology, Complexo Hospitalario Universitario de Santiago de Compostela (SERGAS), Santiago de Compostela, Spain.*

[7] *Translational Medical Oncology (Oncomet), Health Research Institute of Santiago (IDIS), Santiago de Compostela, Spain.*

[8] *Centro de Investigación Biomédica en Red de Cáncer (CIBERONC), Madrid, Santiago de Compostela, Spain.*

[9] *Fundación Pública Galega de Medicina Xenómica, SERGAS; Grupo de Medicina Xenómica-USC, Health Research Institute of Santiago (IDIS), Santiago de Compostela, Spain.*

** Corresponding.*

EGFR mutations: Simple and rapid blood-based qPCR test to select and guide treatment of advanced NSCLC patients.

ABSTRACT

During the last few years, detection of *EGFR*-activating mutations has become a routine part of clinical practice for NSCLC in order to select the optimal treatment strategy. The use of complemental techniques that allow to analyse *EGFR*-activating mutations in blood samples, would help improve the management of NSCLC patients.

In this study, we investigated the feasibility to use Idylla™ ctEGFR mutation assay to detect *EGFR* alterations in 40 NSCLC patients before and during the treatment. The concordance between the blood-based test and tissue-based test was investigated. Furthermore, comparison with different liquid biopsy-based approaches (BEAMing technology and NGS method) was performed. Our results suggest that Idylla™ ctEGFR mutation assay is a fast and optimal tool for therapy selection in advanced NSCLC and also a good approach to monitor the therapy response in patients under TKIs therapies.

Keywords: Idylla™, NSCLC, liquid biopsy, *EGFR* mutations.

1. INTRODUCTION

NSCLC represents 85% of total lung cancers, with about 2 million new cases per year (4). Target therapies are the first choice in NSCLC patients with specific mutations profile, such as *EGFR* mutations, present in 17% of metastatic NSCLC patients (218). Thus, *EGFR* TKIs have become the standard therapy for patients with *EGFR* activating mutations, leading to a longer survival (17). To select patients who present *EGFR* mutations, and offer appropriate *EGFR* TKI treatment, mutation testing of solid tumour samples is required. However, tissue/cytologic samples are not always available or evaluable. CfDNA analyses represent a good alternative strategy to assess the *EGFR* status though the use of like NGS or digital PCR based technologies. Nevertheless, these methods require technical expertise and long turn-around time. Idylla™ ctEGFR mutation assay (Biocartis NV, Mechelen, Belgium) is a fully integrated real-time PCR-based test with a rapid and easy protocol that allow an easy implementation of liquid biopsy analyses into the clinical routine.

The aim of the present study was to interrogate the accuracy and performance of the Idylla™ solution as a non-invasive test to detect *EGFR* mutations in plasma samples of advanced NSCLC patients.

In this context, we think that the Idylla™ ctEGFR mutation assay could be a good alternative tool to analyse the molecular characteristics of NSCLC patients. With this purpose we evaluated the concordance of *EGFR* status between cfDNA using Idylla™ and tissue samples. In addition, the concordance among different liquid biopsy-based approaches BEAMing (Sysmex Inostics), AVENIO (Roche Diagnostics) and Idylla™ was investigated to evaluate the performance of Idylla™ solution versus the other

approaches. In addition, we determine the feasibility to use the ctEGFR assay to monitor NSCLC patients during the treatment.

2. MATERIAL AND METHODS

2.1 Synthetic DNAs

We calculated the limit of detection (LOD) of Idylla™ solution using four different commercial cfDNA standards that covers 10 *EGFR* variants with specific variant allele frequencies (VAF) of 5%, 1%, 0.1% and 0% (*EGFR* wild type) (Cat nº. HD825, Horizon Discovery Ltd., Cambridge, United Kingdom). The commercial cfDNA standards were obtained from human cell lines with *EGFR* mutations fragmented to 160 bp to mimics cfDNA extracted from human plasma. All standards were quantified using the Qubit dsDNA HS assay kit and Qubit 3.0 Fluorometer instrument (Thermo Fisher Scientific, Waltham, USA). Seven of the total 10 *EGFR* alterations presents in the reference cfDNA are included in the panel analysed by the Idylla™ ctEGFR Mutation Assay (5 single nucleotide variants (SNVs) including L861Q, L858R, S768I, T790M and G719S; one exon 20 insertion (V769-D770insASV) and one exon 19 deletion (Del15)). The LOD was defined for each of these seven alterations as the lowest mutant allele frequency yielding a positive result.

2.2 Study design

Fifty-three blood samples from 40 advanced NSCLC patients treated between January 2018 and March 2022 at the Medical Oncology Service of Complexo Hospitalario Universitario de Santiago de Compostela were retrospectively included in the study. The study was performed in accordance

with the Declaration of Helsinki (as revised in 2013) and all individuals signed informed consent forms approved by Santiago de Compostela and Lugo Ethics Committee (Ref: 2017/538) prior to enrolling in the study.

2.3 Blood collection and sample processing

Peripheral blood was obtained by direct venepuncture using CellSave (Menarini, Silicon Biosystems, Bologna, Italy), Streck Cell-Free DNA BCT (Streck Inc, Omaha, NE, USA) or EDTA tubes (219). Plasma and cellular components were separated by two centrifugation steps: one centrifugation at 1,600 g for 10 minutes at room temperature and a second time at 5,500 g for 10 minutes at room temperature to remove any remaining cellular debris. Plasma samples were aliquoted and storage at -80 ºC until posterior analyses. In addition, when high volume of plasma was available, cfDNA was isolated using the QIAamp Circulating Nucleic Acid Kit (Qiagen, Hilden, Germany) according to the manufacturer's instructions and quantified by the fluorometric instrument Qubit 4 using the Qubit dsDNA HS Assay Kit (Thermo Fisher Scientific, Waltham, USA).

2.4 Idylla™ ctEGFR mutation assay

Idylla™ ctEGFR mutation assay (Biocartis NV, Mechelen, Belgium) is a real-time PCR assay that allows the qualitative detection of 49 mutations of the *EGFR* gene using plasma samples: Detects 4 SNVs of exon 18 (G719A/C/S), 2 SNVs of exon 20 (T790M and S768I) and 4 SNVs of exon 21 (L858R and L861Q); 34 different exon 19 deletions: and 5 exon 20 insertions. Commercial cfDNA standards and a total of 53 samples from patients with NSCLC were analysed using the Idylla™ assay. For the analyses, 2 ml of plasma together with 200 µl of proteinase K (20 mg/ml,

Qiagen, Hilden, Germany) were directly pipetted in the cartridge. The Idylla™ system performs the cfDNA extraction, a real time PCR amplification and detection of *EGFR* mutations. Finally, Idylla™ console software analyses PCR amplification curves determining the cycle of quantification (Cq) in each sample. To know that sample is suitable in terms of quality and quantity, the assay used a Sample Processing Control (SPC) signal, that corresponded to the amplification of an *EGFR* wild-type control. Based on the difference between the *EGFR*-mutant Cq and the SPC (denominated ΔCq), an automatic report with the result is obtained. The total time to obtain a result using Idylla™ ctEGFR mutation assay is less than 3 hours.

2.5 Cobas® *EGFR* Mutation Test

Tissue *EGFR* status was determined in the primary tumour obtained at diagnosis using Cobas® EGFR Mutation Test v2 (Roche, Basel, CH) in 25 patients, as manufacturer's guidelines. The test is a real-time PCR-based test that identifies 42 mutations in exons 19, 19, 20 and 21 of the *EGFR* gene using a tissue biopsy sample. Briefly, formalin-fixed, paraffin-embedded tissue (FFPE) specimens are processed using the Cobas® DNA Sample Preparation Kit (Roche, Basel, CH). After preparation, amplification and detection of *EGFR* mutations are carried out using real-time PCR test. The total time to obtain a result using Cobas® *EGFR* mutation test in tumour sample is approximately 8 hours.

2.6 BEAMing technology

In parallel, BEAMing method was performed with the OncoBEAM EGFR kit (Sysmex Inostics, Hamburg, Germany) using 2 mL of plasma in 17 samples. cfDNA used for the analyses was isolated employing the QIAamp

Circulating Nucleic Acid Kit (Qiagen, Hilden, Germany) according to the manufacturer's instructions. Once cfDNA was extracted, the assay performs a hybridization step between DNA-coated beads and a sequence specific fluorescein-labelled probe. Then, amplificated samples are analysed by flow cytometry. Finally, results are reported as "no mutation detected" or "mutation detected" (220). The total time to obtain a result using BEAMing technology is approximately 72 hours.

2.7 Next-generation sequencing analyses

Next-generation sequencing (NGS) analyses was performed in 15 samples with the AVENIO ctDNA Expanded panel (221) (Roche, Basel, CH), which covers alterations in 77 genes including all coding regions of *EGFR*. cfDNA used for the analyses was isolated from 4 mL of plasma, following the AVENIO ctDNA Expanded panel (Roche, Basel, CH) protocol. Libraries were sequenced on a NextSeq 500 (Illumina, San Diego, CA) which provided high-depth sequencing with a mean coverage of ~9000x (range: 7621x - 10402x).

2.8 Statistical analyses

Statistical analyses were performed using R version 4.1.1. The Kappa test was used to determine the concordance between *EGFR* mutations based on tissue and plasma analyses and among the three different based-blood platforms (Idylla™, BEAMing and AVENIO panel). GraphPad Prism 8 and Venny 2.1.0 (https://bioinfogp.cnb.csic.es/tools/venny/) (222) were employed for the graphical representations.

3. RESULTS

3.1 LOD determination using commercial standards

To explore in house the performance of the assay we first explored the technique sensitivity. With this aim, we calculated the LOD of Idylla™ ctEGFR mutation test using commercial cfDNA standards with different VAFs that covers different *EGFR* variants. Thus, LOD was determined as 5% VAF for L861Q and G719S; 1% for L858R, the insertion of exon 20 and T790M; and 0.1% VAF for Del15 of exon 19 and the point mutation S768I using a total of 160 ng of commercial cfDNA (Table 1.1).

Table 1.1. Sensitivity of Idylla™ system using commercial cfDNA (160 ng).

***EGFR* exon**	**Variant**	**AA mutation**	**LOD (%)**
Exon 18	G719S	p.Gly719Ser	5
Exon 19	Deletion 15	p.Glu746_Ala750del	0.1
Exon 20	Insertion exon20	p.Val769_Asp770insAlaSerVal	1
	S768I	p.Ser768Ile	0.1
	T790M	p.Thr790Met	1
Exon 21	L858R	p.Leu858Arg	1
	L861Q	p.Leu861Gln	5

Abbreviations: LOD, limit of detection; AA: amino acid.

3.2 Patients' characteristics

Forty NSCLC patients were included in the study. Their clinical and pathological characteristics are presented in detail in Table 1.2. The median age was 63.5 (range 40-81) with 52.5% females and 37.5% of patients were never smokers. Most patients had tumours with adenocarcinoma histology

(80.0%) and presented at least one alteration in *EGFR* gene (67.5%) in tumour sample. Only one patient analysed presented stage III disease.

Table 1.2. Demographics and clinical characteristics of the patients.

Baseline Characteristics	Patients n* (%)
Mean age (years) ± SD, range	64.8 ± 8.9, 40-81
Sex	
Female	21 (52.5%)
Male	19 (47.5%)
Smoking	
Smoker	19 (47.5%)
Former smoker	4 (10.0%)
Never	15 (37.5%)
Unknow	2 (5.0%)
Histology	
Adenocarcinoma	32 (80.0%)
Squamous cell carcinoma	8 (20.0%)
Stage	
III	1 (2.5%)
IV	38 (95.0%)
Unknow	1 (2.5%)
***EGFR* status in tissue**	
Mutated	27 (67.5%)
No mutated	12 (30.0%)
Unknown	1 (2.5%)

*n=40; SD: standard deviation.

3.3 Analyses of blood samples from NSCLC patients using Idylla™ solution

Once established the experimental LOD with the commercial cfDNA standards, a total of 53 samples from 40 patients with NSCLC were analysed using the Idylla™ assay (Figure 1.1A).

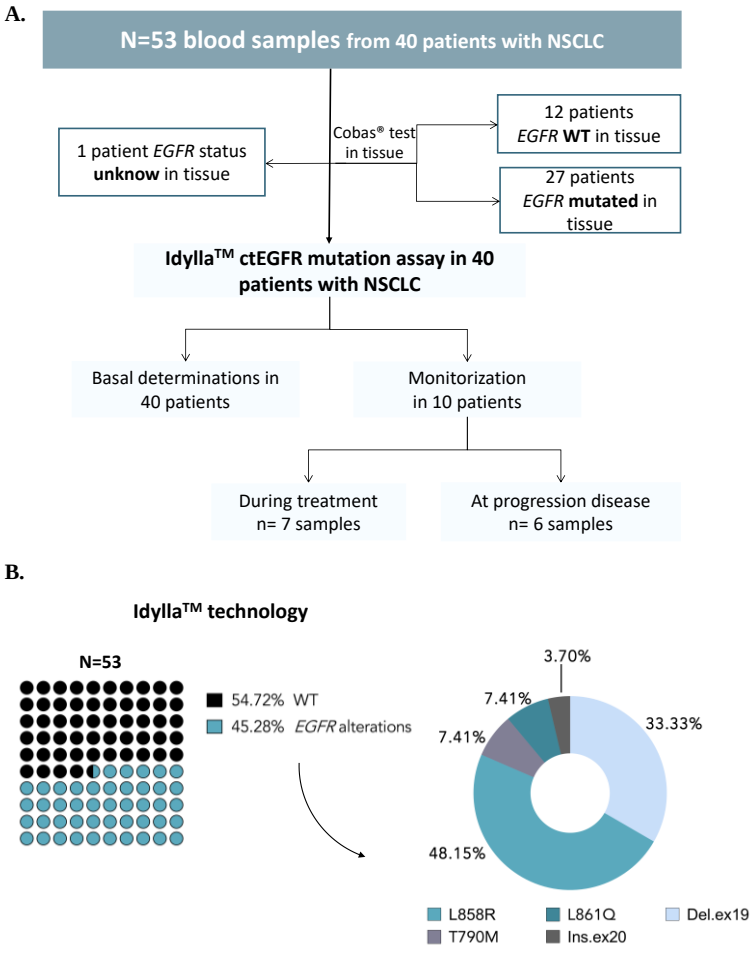

Figure 1.1. *EGFR* status in NSCLC patients using the Idylla™ EGFR Mutation Assay. (A) Study scheme. (B) Proportion of patients with *EGFR* alterations or WT in total 53 plasma samples. Abbreviations: WT: wild type.

Of the total samples analysed with the Idylla™ assay, 45.3% (24/53) presented at least one *EGFR* mutation. Among the 24 positive samples, 2 had more than one mutation, (harboured both L858R mutation and the T790M resistance mutation) and one presented 2 different exon 19 deletions, detecting

27 alterations in total. L858R mutation (48.1%) and Del.ex19 (33.3%) were the most frequent alterations detected (Figure 1.1B).

In addition, in 39 patients *EGFR* tissue status was determined using Cobas® *EGFR* Mutation Test v2. Overall concordance between Cobas® assay applied in tissue samples and Idylla™ assay on plasma samples was 71.8% (n=28/39) (Cohen's Kappa=0.472) reporting a moderate agreement (Figure 1.2). In 6/11 discordant patients the time between plasma sample collection and tissue biopsy was higher than 3 months (Table 1.3). In addition, no clear association between discordant samples and clinical characteristics, such as metastatic localizations, was found. However, it is important to note that two discordant cases with a short time between liquid and solid biopsy (≤21 days) presented only brain metastasis. Of note, we observed a low concordance rate in cases with Del.ex19 (concordance rate=0.42), while a high concordance rate was found in the case of L858R mutation (rate=0.8) (Figure 1.2).

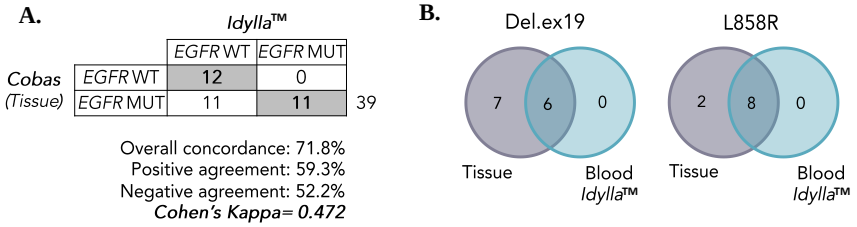

Figure 1.2. Comparison between tissue samples and blood samples analyzed by Idylla™. (A) Concordance between ctEGFR Idylla™ mutation assay in cfDNA and Cobas® test in tissue in 39 patients. (B) Venn diagrams show the number of samples that present Del.ex19 or L858R mutation in tissue sample and blood sample using Idylla™ solution. Abbreviations: MUT: mutated; WT: wild type.

3.4 Comparison among Idylla™ Platform, digital PCR based method (BEAMing) and NGS (AVENIO)

Seventeen paired plasma samples (before treatment or during therapy) were also analysed using OncoBEAM *EGFR* V2, reporting an overall concordance with Idylla™ assay of 88.9% with a substantial agreement (n=16/18 samples) (Cohen's Kappa=0.78) (Figure 1.3A) in all samples. Nevertheless, 3 samples that showed VAFs equal or below 0.06% by OncoBEAM were undetectable on Idylla™ solution (Figure 1.3C), in concordance with the results obtained with commercial cfDNA standards and the LOD observed.

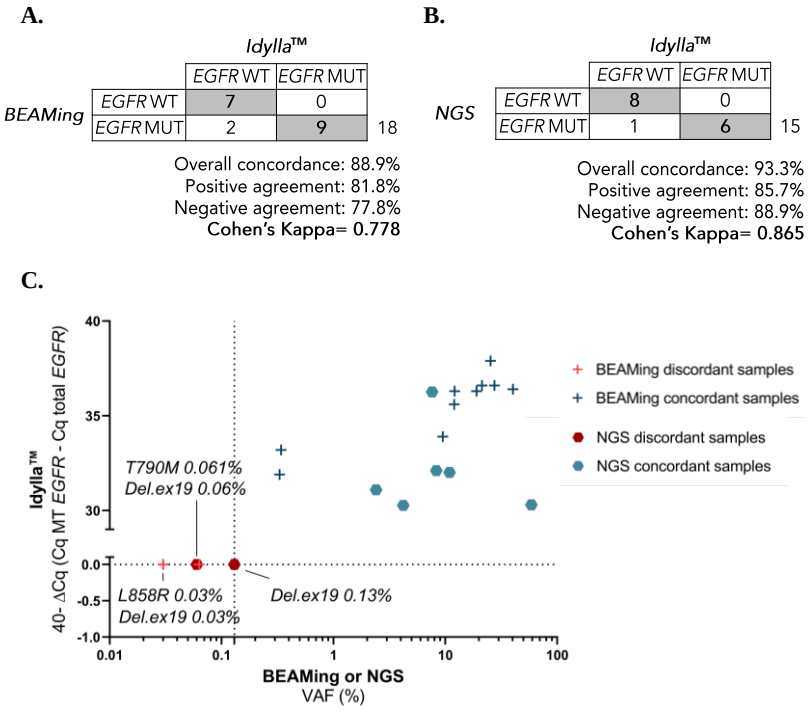

Figure 1.3 Comparison among BEAMing, *AVENIO* and Idylla™ technologies. (A) Concordance between BEAMing and Idylla™ assay in cfDNA samples (n=18). (B)

Concordance between NGS and Idylla™ assay in cfDNA samples (n=15). (C) VAF detected by BEAMIng or NGS panel versus Idylla™ ΔCq. Red symbols represent discordant samples detected by BEAMing or NGS (n=3), green symbols represent concordant samples detected by both technologies. Abbreviations: MUT: mutated; WT: wild type; VAF, variant allele frequency.

In another hand, 15 paired samples were analysed with both NGS and Idylla™ assay, reporting a concordance with Idylla™ assay of 93.3% (n=14/15 samples) (Cohen's Kappa=0.865) (Figure 1.3B) in all samples. Similar to results above reported using BEAMing, determinations with low VAFs (below 0.13% in this case, n=2) were undetectable on Idylla™ solution (Figure 1.3C).

Overall, considering both technologies (NGS and BEAMing), Idylla™ solution presented a high concordance rate (90.9% of concordance, Cohen's Kappa= 0.820). Detailed results of all samples analysed with Idylla™ system and other liquid biopsy approaches are showed in Table 1.3.

Table 1.3. Sample determinations included in the study.

Sample id.	*EGFR* tissue status	*EGFR* Idylla™ status	Time blood-tissue (days)	*EGFR* BEAMing status	*EGFR* NGS status
01	Del.ex19	Del.ex19	21	Del.ex19	NT
02	Ins.ex20	WT	24	WT	NT
03	L858R	L858R	23	L858R	NT
04	Del.ex19	Del.ex19	975	Del.ex19/T790M	NT
05	NT	WT	NA	WT	NT
06	WT	WT	-4	WT	NT
07	WT	WT	-5	WT	NT
08	L858R/ S768I	L858R	706	L858R	NT
09	L858R	WT	332	NT	NT
10	Del.ex19	WT	744	NT	NT
12	L858R	L858R	41	NT	NT
14	WT	WT	107	WT	NT
15	L861Q	WT	567	WT	NT
20	WT	WT	48	NT	NT
21	Del.ex19	WT	162	NT	NT
23	L858R	L858R	20	NT	NT
25	Del.ex19	WT	21	NT	NT

Sample id.	*EGFR* tissue status	*EGFR* Idylla™ status	Time blood-tissue (days)	*EGFR* BEAMing status	*EGFR* NGS status
26	L858R	WT	14	L858R	NT
27	L858R	L858R	7	NT	NT
29	Del.ex19	WT	804	NT	NT
30	Del.ex19	WT	1089	Del.ex19/T790M	NT
31	Del.ex19	2 Del.ex19	629	Del.ex19	NT
33	L858R/ T790M	L858R/T790M	753	L858R/T790M	NT
35	L858R	L858R	1028	NT	NT
36	L858R	L858R	472	L858R	NT
38	Del.ex19	WT	21	Del.ex19	NT
39	Ins.ex20	Ins.ex20	8	NT	Ins.ex20
40	Del.ex19	Del.ex19	3122	NT	Del.ex19
41	Del.ex19	Del.ex19	14	NT	Del.ex19
43	L861Q	L861Q	1644	NT	L861Q
44	Del.ex19	WT	112	NT	Del.ex19
45	Del.ex19	Del.ex19	45	NT	Del.ex19/T790M
46	WT	WT	15	NT	WT
47	WT	WT	37	NT	WT
48	WT	WT	624	NT	WT
49	WT	WT	20	NT	WT
50	WT	WT	689	NT	WT
51	WT	WT	35	NT	WT
52	WT	WT	18	NT	WT
53	WT	WT	45	NT	WT

Abbreviations: NT: Not tested; WT: wild type.

3.5 Monitoring patients using Idylla™ solution

We also analysed the feasibility of using the Idylla™ ctEGFR Mutation Assay to monitor NSCLC patients during the treatment. Twenty-three samples from 10 NSCLC patients were analysed at different time points during therapy and at progression disease (Figure 1.4).

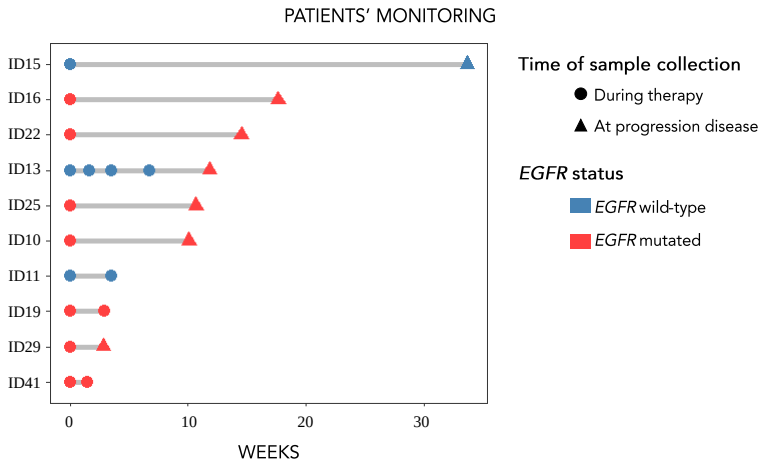

Figure 1.4. Monitoring *EGFR* status in NSCLC patients using the ctEGFR Idylla™ mutation assay. Swimmer' plot on monitored patients (n=10).

Specially in one case (ID13), we observed that analysis using Idylla™ solution allows to detect the progression disease (Figure 1.5). A 62-year-old male was diagnosed in March of 2017 with NSCLC adenocarcinoma stage IIIA. Tissue sample analyses revealed the presence of L861Q mutation in *EGFR* gene. In May, image analyses reported lesions into the SNC. The patient started chemotherapy and radiotherapy and showed a good response. In March of 2018, the patient had a progression and he started gefitinib treatment (day 0). Before the treatment onset, a blood sample was collected and cfDNA analyses were performed by BEAMing technology and Idylla™ solution. Both results reported a negative result for the mutation *EGFR* L861Q, probably due to location of the metastatic lesions and the consequent circulating tumour DNA (ctDNA) low levels. Longitudinal analyses during gefitinib treatment (day 49, 103 and day 201) in cfDNA reported the absence of L861Q mutation in plasma samples until day 355, when the patient presented progression disease at different levels by image analyses. At

progression, an increase in cfDNA levels and the presence of the mutation L861Q using Idylla™ solution were determined, in accordance with the disease evolution.

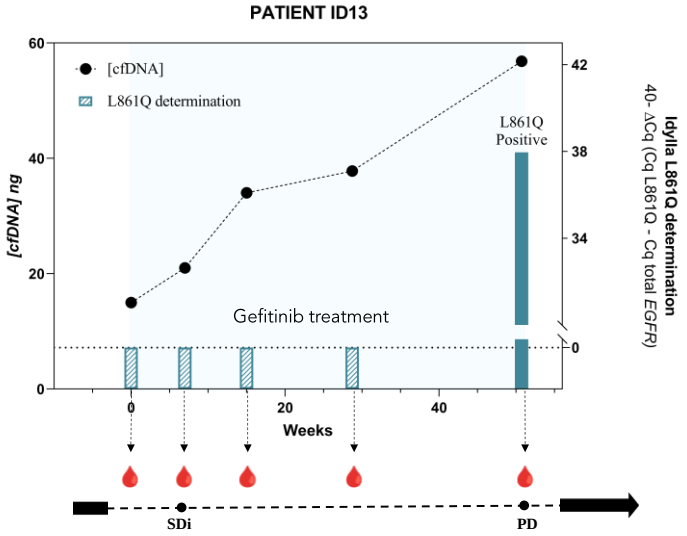

Figure 1.5. Evolution of cfDNA levels and *EGFR* L861Q mutations in patient ID13 during Gefitinib treatment. The L86Q1 mutation appeared at progression disease, which confirmed by image analyses. Abbreviations: SDi: stable disease; PD: progression disease.

Other cases maintained the mutation positivity at baseline and progression disease and/or showed increased ctDNA levels such as happened in patients ID19 and ID11 (Figure 1.6A). Patient ID19 and ID11 were followed up during different TKIs treatment and in both cases all determinations were positive for the mutation L858R. Patient ID19 progressed at 12 weeks and an increase in L858R mutation and cfDNA levels was found at this time, supporting the interest of using Idylla™ solution to detect progression disease. Patient ID11 showed stable disease at 10 weeks by image analyses and a VAF reduction of L858R mutation was found using Idylla™ solution despite of an increase in cfDNA levels, suggesting an active response

to gefitinib but probably a progression due to a different tumour clone. One month later, patient showed a clinical deterioration and died. In this type of cases, imaging tests may be of limited value, while liquid biopsy could provide useful information on the disease evolution.

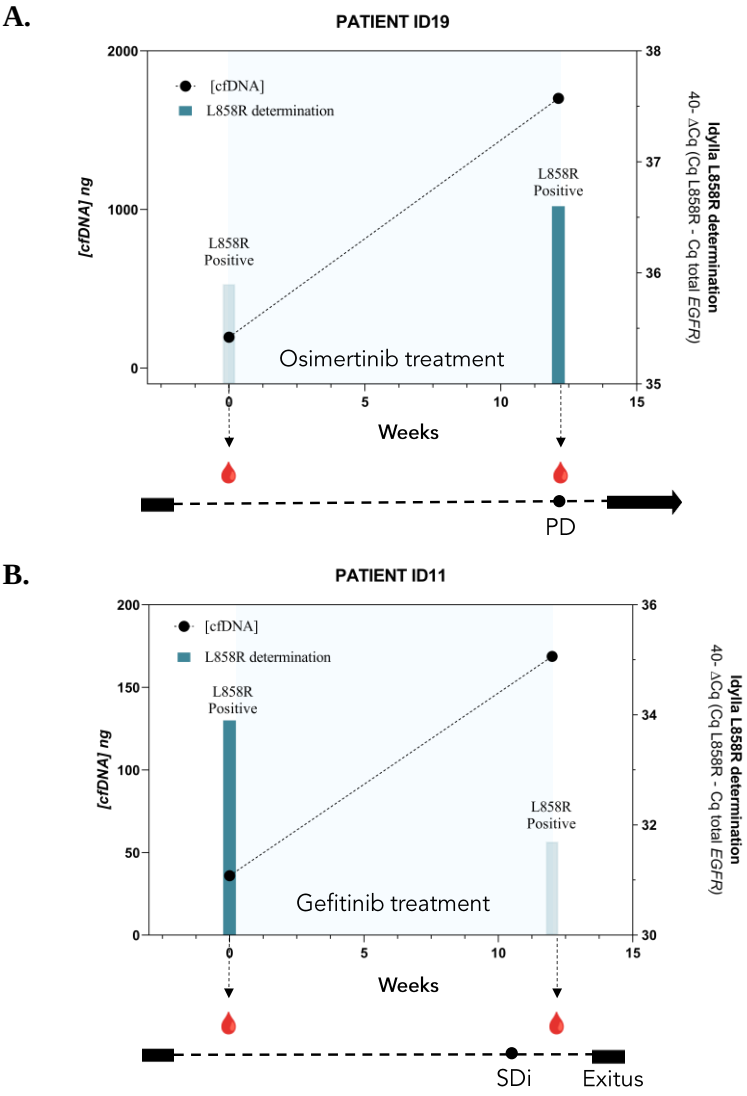

Figure 1.6. Evolution of cfDNA levels and *EGFR* L858R mutation in patient ID19 (A) and patient ID11 (B) during different TKIs treatment. Abbreviations: PD: progression disease; SDi: stable disease.

4. DISCUSSION

Regarding the interest of improving the options to interrogate *EGFR* status in cfDNA, it is important to have in mind that tumour analyses have several limitations in NSCLC patients such as access difficulty (mainly to biopsy metastasis), the impossibility to characterize the disease at real time and the lack of representativity of the tumour heterogeneity. To solve these limitations, in the last years, liquid biopsy has emerged as a clear alternative and one of the main pillars for personalized oncology, reporting promising results mainly focused on the cfDNA analyses (205). In the present study we explored the feasibility of determine *EGFR* status in cfDNA by Idylla™ solution in NSCLC patients, previously reported in tissue (223,224) and plasma samples (225) and its potential value to monitor the therapy response in NSCLC patients looking for a fast technique not make the tumour genotyping . Of note, a good concordance rate between analyses in tissue and plasma cfDNA with the Idylla™ *BRAF* Mutation Test has been previously described (226). In our study, a moderate agreement between tissue and plasma results was found. This result can be partially explained due to the time between blood and tissue samples collection in the discordant patients. As higher time between samples collection as bigger probability to find a molecular evolution of the tumour. In another hand, although we reported a low concordance rate of exon 19 deletions in contrast with the high concordance of the point mutation L858R, the small size of our cohort could not allow us to arise solid conclusions regarding this aspect. However, it's

important to highlight that 2/7 discordant samples presented a VAF lower than 0.13% by NGS or BEAMing assay and in 5/7 discordant samples, the time between plasma sample collection and tissue biopsy was higher than 5 months. Therefore, the lower ctDNA content and the tumour evolution could explain this lower concordance.

Furthermore, we investigated the concordance rates among Idylla™ solution and other reference technologies, BEAMing and NGS, and found a good overall agreement determining *EGFR* status. In line with our study in lung cancer, the automatized system demonstrated a good diagnostic performance for *KRAS* analyses in patients with colorectal cancer , reaching a high concordance with BEAMing (227). Besides, studies in tissue samples reported the good concordance between Idylla™ assay and NGS panels (224). Of note, we also reported a good correlation of Idylla™ solution and AVENIO panel employing plasma samples but with a lower time-to-result with Idylla that can be crucial for metastatic patients (228).

In another hand, it's important to remark that Idylla™ solution allowed us to analyse the mutational profile of NSCLC patients in longitudinal plasma samples during treatment without the need to perform further tissue biopsies. This advantage is important in whose patients that undergone treatment resistance. For example, the mutation T790M appears as a mechanism of resistance during TKIs therapy. Its detection is crucial to select whose patients that should be treated with a third generation of TKIs (17). In our study, although we only detected the T790M mutation in two plasma samples, our analysis with commercial cfDNA showed that Idylla™ system allows to detect the TKIs resistance mutation with a LOD of 1%. Preliminary studies have reported a moderate T790M detection rate of 66.6-80.0% in plasma samples using Idylla™ solution (225,229), according to our study. In addition,

in our work paired plasma samples analysis showed that T790M mutations with a variant allele frequency lower than 0.06% using BEAMing/NGS cannot be detected by Idylla™ system. However, analyses with a larger cohort of patients harbouring the resistance mutation T790M are needed to validate the clinical value of the kit for specifically detect T790M mutations.

Overall, the results obtained in the in this pilot study with a real-world cohort of patients allow us to conclude that Idylla™ ctEGFR Mutation Assay could be employed as a first screen to detect *EGFR* mutations fast and on demand. If no *EGFR* mutation is detected due to the low ctDNA content in plasma, another sensitive technique such as a ddPCR-based strategy should be employed to confirm the negative result. To this regard, some aspects should be considered for the selection of an optimal platform or analytic circuit to analyse *EGFR* alterations in ctDNA. For example, tumours with multiple metastatic locations and highly vascularized will have higher levels of ctDNA and therefore the genotyping of clinically relevant mutation will be easier to detect (150). Regarding the value as a monitoring tool, our preliminary results showed that changes in the mutational profile of *EGFR* samples using Idylla™ solution, could provide valuable information to monitor the therapy response in patients under TKIs therapies.

CHAPTER I.B

Development of a blood-assay to detect *MET* alterations using circulating free DNA and circulating tumour cells in NSCLC patients.

Development of a blood assay to detect *MET* alterations using circulating DNA and circulating tumour cells in NSCLC patients.

This chapter has been adapted from a recently published article entitled "**Detection of *MET* Alterations Using Cell Free DNA and Circulating Tumor Cells from Cancer Patients**" (230).

Patricia Mondelo-Macía[1#], Carmela Rodríguez-López[2,3#], Laura Valiña[4,5], Santiago Aguín[2,3], Luis León-Mateos[2,3], Jorge García-González[2,3,6], Alicia Abalo[1], Óscar Rapado-González[1,7], Mercedes Suárez-Cunqueiro[3,6,7], Angel Díaz-Lagares[6,8], Teresa Curiel[3], Silvia Calabuig-Fariñas[6,9,10,11], Aitor Azkárate[5,12], Antònia Obrador-Hevia[5,13], Ihab Abdulkader[14], Laura Muinelo-Romay[1,6*], Roberto Diaz-Peña[1,15*] and Rafael López-López[1,2,6].

[1] *Liquid Biopsy Analysis Unit, Translational Medical Oncology (Oncomet), Health Research Institute of Santiago (IDIS), 15706 Santiago de Compostela, Spain.*
[2] *Department of Medical Oncology, Complexo Hospitalario Universitario de Santiago de Compostela (SERGAS), 15706 Santiago de Compostela, Spain.*
[3] *Translational Medical Oncology (Oncomet), Health Research Institute of Santiago (IDIS), 15706 Santiago de Compostela, Spain.*
[4] *Department of Laboratory Medicine, Hospital Universitari Son Espases, 07120 Palma, Balearic Islands, Spain.*
[5] *Group of Advanced Therapies and Biomarkers in Clinical Oncology, Institut d'Investigació Sanitària de les Illes Balears (IdISBa), 07120 Palma, Balearic Islands, Spain.*
[6] *Centro de Investigación Biomédica en Red de Cáncer (CIBERONC), 28029 Madrid, Spain.*
[7] *Department of Surgery and Medical Surgical Specialties, Medicine and Dentistry School, Universidade de Santiago de Compostela, 15705 Santiago de Compostela, Spain.*
8 Cancer Epigenomics, Oncomet, Health Research Institute of Santiago (IDIS), Complexo Hospital Univeritario de Santiago de Compostela (SERGAS), 15706 Santiago de Compostela, Spain.
[9] *Molecular Oncology Laboratory, Fundación Hospital General Universitario de Valencia, 46014 Valencia, Spain.*
[10] *Department of Pathology, Universitat de València, 46010 València, Spain.*
[11] *TRIAL Mixed Unit, Centro de Investigación Príncipe Felipe-Fundación para la Investigación del Hospital General Universitario de València, 46012 València, Spain.*
[12] *Medical Oncology Department, Hospital Universitari Son Espases, 07120 Palma, Balearic Islands, Spain.*
[13] *Molecular Diagnosis Unit, Hospital Universitari Son Espases, 07120 Palma, Balearic Islands, Spain*
[14] *Department of Pathology, Complexo Hospital Universitario de Santiago de Compostela (SERGAS), Universidade de Santiago de Compostela, 15706 Santiago de Compostela, Spain.*
[15] *Faculty of Health Sciences, Universidad Autónoma de Chile, Talca 3460000, Chile*

* *Corresponding.*
[#] *These authors have contributed equally to this work.*

Development of a blood-assay to detect *MET* alterations using circulating free DNA and circulating tumour cells in NSCLC patients.

ABSTRACT

MET alterations are present in several cancer types and sometimes they are associated with resistance at certain therapies in metastatic patients. Nowadays, therapies with MET inhibitors allow to increase the prognosis of patients with *MET* alterations, however there are no standardized methods to confirm these molecular alterations. *MET* alteration may be a potential biomarker for the evaluation of patients who will benefit from treatment with MET inhibitors, especially in NSCLC patients, where about 4% of patients present these alterations. Therefore, the purpose of the present study was to develop and investigate the utility of a liquid biopsy-based strategy to assess *MET* alterations in cancer patients, and particularly in NSCLC patients. Thus, in one hand, we analysed *MET* amplification in cfDNA from 174 patients with different cancer types and 49 healthy controls to demonstrate the validity and accuracy of the analysis to detect this alteration in patients with cancer. In this analysis we established the cut-off to determine the amplification status. Importantly, a significant correlation between cfDNA concentration and *MET* copy number (CN) in cancer patients (r= 0.57, p-value $<10^{-10}$) was determined probably associated with a higher ctDNA content. In NSCLC subgroup, we detected *MET* amplification in 12.99% of patients. In another hand, we evaluated two different approaches (CellSearch® and Parsortix systems) to detect the level of expression of c-MET protein on CTCs in 16

metastatic NSCLC patients. Finally, we reported two cases that evidenced how the detection of *MET* alterations may be informative in monitoring the appearance of resistance mechanism in response to anti-EGFR treatment. In conclusion, we developed specific and non-invasive assays to monitor *MET* status in cfDNA/CTCs and demonstrated its utility as a biomarker for monitoring the appearance of resistance to anti-EGFR therapy in NSCLC patients.

Keywords: *MET* amplification; *MET* copy number; c-MET protein expression; circulating free DNA (cfDNA); circulating tumour cells (CTCs); targeted therapy.

1. INTRODUCTION

RTKs are crucial regulators of key cellular processes such as cell growth, differentiation, neovascularization, and tissue repair. Hepatocyte growth factor receptor (MET or c-MET) is an RTK produced predominantly in cells of epithelial origin (231). Its only known high-affinity ligand is the hepatocyte growth factor (HGF) (232) and both are essential to embryonic development and organ regeneration. The binding of c-MET and HGF activates the kinase activity of MET and several pathways, such as the MAPK cascade, the PI3K-AKT pathway, the STAT pathway, and the IκBα–NF-κB complex (233). These pathways can activate cell proliferation, survival, migration, motility, invasion, angiogenesis, apoptosis, and epithelial-to-mesenchymal transition (233,234). In addition, c-MET can interact with other cell membrane receptors, such as integrins, CD44, class B Plexins, and other tyrosine kinase receptors (e.g., HER2, AXL, EGFR, and VEGF) (Figure 1.7) (231,232).

Deregulation of the c-MET pathway has been associated with cancer growth and metastasis in several tumours types (lung, head and neck, gastric, and colorectal, among others) (231,233), taking place through several mechanisms including overexpression, amplification, autocrine signalling, and mutational activation (235). In fact, *MET* amplification has been also described in diverse tumour types, such as NSCLC, gastric cancer, oesophageal cancer, colorectal cancer, medulloblastoma, and glioblastoma, and has been associated with bad prognosis and poor survival (231,236–239).

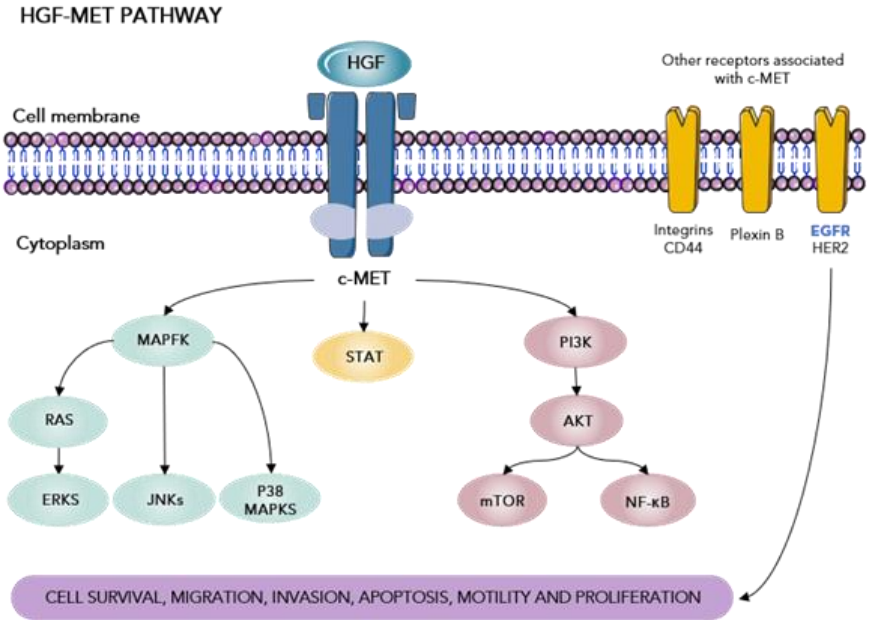

Figure 1.7. Signalling pathway of c-MET and HGF.

On the other hand, c-MET overexpression is known to activate the c-MET signalling pathway, promoting tumour cell growth, survival, migration, and invasion. This alteration has been associated with bad prognosis and the generation of metastasis in different tumour types, such as NSCLC, hepatocellular carcinoma, kidney cancer, head and neck cancer, colorectal cancer, gastric cancer, nasopharyngeal carcinoma, and glioblastomas (232,233,238–242).

In addition to its role as an oncogenic driver, *MET* alterations have been described as a mechanism of resistance to different therapies (231,240,243). Thus, *MET* amplification has been specifically associated with the development of resistance to anti-EGFR TKIs and is more frequent in metastatic patients (231,236).

In NSCLC, acquired secondary *MET* amplification has emerged as one of the most common resistance mechanisms in TKI-therapies. Around 5–20% of patients treated with first generation EGFR TKIs (for example, gefitinib and erlotinib) and 25% of patients who progress on a third generation EGFR TKI (for example, osimertinib) presented *MET* amplification (244). All these data indicate that *MET* amplification and/or c-MET overexpression, are strongly associated with cancer development. *MET* alterations may be a potential biomarker for the evaluation of patients who will benefit from treatment with MET inhibitors, especially in NSCLC patients.

Several clinical trials have assessed the efficacy of selective and broad-spectrum MET inhibitors in an extensive panel of cancers (245). Nevertheless, nowadays there are no standardized methods to confirm these molecular alterations. In fact, variable *MET* amplification rates can be detected, depending on the detection techniques (242), for example, fluorescence in situ hybridization (FISH), single-nucleotide polymorphism (SNP) genotyping, or qPCR, in which different scoring criteria may define high amplification. In the same line, c-MET protein levels can be dependent on the antibodies employed, which can recognize different c-MET epitopes and domains, showing different membrane and/or cytoplasmic staining intensities by IHC (242). Furthermore, *MET* genomic changes have mostly been associated with metastatic patients and normally appear with the progression of disease (235). Tissue re-biopsy constitutes the best alternative for such molecular analysis in tissue samples; however, re-biopsy is often not possible, making the validation of liquid biopsy strategies to address *MET* status essential.

CTCs and cfDNA represent an accessible and non-invasive alternative for detecting alterations in patient's blood, particularly in patients for whom tissue

biopsies are inaccessible or problematic to carry out or repeat (246). Thus, the purpose of the present study was to investigate the utility of a liquid biopsy-based strategy to assess *MET* alterations in cancer patients. For this aim, we developed a cfDNA-assay, to evaluate the *MET* CN status in cfDNA from a cohort of cancer patients with different tumour types. Also, we developed a CTC-assay to analyse c-MET expression in CTCs from NSCLC patients. Finally, two cases in which the clinical potential to detect the appearance of resistances and to guide the treatment in NSCLC patients in a non-invasive manner are showed.

2. MATERIAL AND METHODS

2.1 Cell lines

The *MET* Genetic Alteration Cell Panel was purchased from the American Type Culture Collection (ATCC, TCP-1036). The panel was composed of five human tumour cell lines (SNU-5, Hs746T, C32, AU565, and NCI-N87) showing various degrees of *MET* gene CN and expression levels. We also included the MET-negative prostate cancer cell line LNCaP and the cancer cell lines A549 (lung, NSCLC) and PC3 (prostate), purchased from the ATCC, in the study. The cell lines were routinely cultured in ATCC's recommended growth medium at 37 °C, 5% CO_2, and 95% humidity.

MET CN data of the eight cell lines were obtained from the Cancer Cell Line Encyclopedia (CCLE) database (http://www.broadinstitute.org/ccle), determined using the Affymetrix Genome-Wide Human SNP Array 6.0 platform. In addition, genomic DNA (gDNA) was extracted from the same cancer cell lines with QIAamp DNA Blood Mini Kit (Qiagen, Hilden, Germany), according to the manufacturer's suggested protocol. DNA quantity

and quality was assessed using a NanoDrop spectrophotometer (Thermo Fisher Scientific, Waltham, MA, USA) and *MET* CN was determined by ddPCR.

c-MET expression of the eight cell lines was determined by immunofluorescence. Cell lines were staining with Alexa Fluor (AF)546-conjugated pan-Cytokeratin (CKs) (C11, sc-8018, Santa Cruz, CA, USA), AF647-conjugated CD45 (35-Z6, sc-1178, Santa Cruz, CA, USA), anti-MET fluorescein (FITC)-conjugated (D-4, sc-514148, Santa Cruz, CA, USA), and nuclear dye 4′,6-diamidino-2-phenylindole (DAPI) to fluorescently label the cells. Results were captured and analysed by a fluorescence microscope (Leica DMI8, Leica Microsystems, Germany).

2.2 Study design and sample collection

In total, 174 cancer patients and 49 healthy controls were enrolled in the present study. One-hundred and forty-six patients and 49 healthy controls were recruited between August 2017 and October 2019 at the Medical Oncology Service of Complexo Hospitalario Universitario and Hospital HM La Rosaleda of Santiago de Compostela (Santiago de Compostela, Spain). Twenty-eight patients were collected between September 2016 and November 2019 at the Medical Oncology Service of Hospital Universitario Son Espases (Mallorca, Spain).

All individuals gave written informed consent approved by Santiago de Compostela and Lugo and Islas Baleares Ethics Committees (Ref: 2017/538 and IB2584/15; respectively) prior to enrolling in the study. The protocol approved by the Ethics Committee was conducted according to the Declaration of Helsinki.

2.3 Circulating free DNA isolation from plasma samples

Ten mL of peripheral whole blood from controls and patients were obtained by direct venepuncture in Streck Cell-Free DNA blood collection tubes (Streck, NE, USA). Plasma was separated within 96 hours after blood collection as a result of two sequential centrifugation steps (10 minutes at 1,600 g and 10 minutes at 6,000 g; both at room temperature), and then stored at -80 ºC for further processing. cfDNA was extracted from 3 mL of plasma using a QIAmp Circulating Nucleic Acid Kit (Qiagen, Hilden, Germany), according to the manufacturer's instructions. cfDNA yields were assessed using a Qubit 1X dsDNA Hs Assay Kit, according to the manufacturer's instructions (Thermo Fisher Scientific, Waltham, MA, USA).

2.4 Droplet digital PCR to detect *MET* CN

Genomic DNA extracted from the cancer cell lines (n=8) and cfDNA isolated from plasma (n=140 metastatic patients, n=34 non-metastatic patients, and n=49 healthy controls) was amplified using ddPCR to analyze *MET* CN. The ddPCR experiments were performed according to the manufacturer's protocol (Bio-Rad, CA, USA). Each assay contained 20 µL reaction mixture of 10 µL ddPCR Supermix for Probes (Bio-Rad, CA, USA), 1 µL PrimePCR ddPCR CN assay for *MET* with a FAM fluorophore (dHsaCP2500321, Bio-Rad, CA, USA), 1 µL PrimePCR ddPCR CN assay for the reference gene with a HEX fluorophore (*EIF2C1*, dHsaCPE2500349, Bio-Rad, CA, USA), and 8 µL DNA template and nuclease-free water. In the case of gDNA from cancer cell lines, we added the HaeIII enzyme (Takara Bio, USA) to the mix, according to the manufacturer's instructions. Droplets were generated using a QX200 AutoDG Droplet Digital PCR System (Bio-Rad, CA, USA) with Droplet Generation Oil for Probes (Bio-Rad, CA, USA) and

transferred to a 96-well plate. PCR amplification was performed with the following conditions: 95 °C for 10 minutes, followed by 40 cycles of 94 °C for 30 seconds, 60 °C for 60 seconds, and 10 minutes incubation at 98 °C. The plates were read on a Bio-Rad QX200 droplet reader (Bio-Rad, CA, USA) and we calculated *MET* CN using the QuantaSoft Pro software (Bio-Rad, CA, USA).

2.5 Fluorescent in situ hybridization (FISH) analysis

FISH analysis was conducted on FFPE tissues in a subgroup of patients who had a blood sample taken within 2 months after tissue biopsy (n=12). The tissue sections were hybridized with *MET* (SpectrumRed)/*CEN7* (SpectrumGreen) Dual Color FISH Probe (Vysis, Abbott Molecular) following the manufacturer's protocol. In each case, 60 non-overlapping nuclei were examined by a fluorescence microscope (BX51, Olympus Corporation, Barcelona, Spain). FISH positivity was estimated using the standard Colorado criteria (gene amplification; 2> *MET* gene (red)/*CEP7q* (green) per cell plus high polysomy; 5 copies> mean *MET* per cell) (247).

2.6 Spiked experiments

The assays to evaluate c-MET expression on CTCs were tested using cancer cell lines spiked in whole blood from the healthy volunteers recruited. A total of 7.5 mL of blood from healthy donors was collected in CellSave tubes (Menarini, Silicon Biosystems, Bologna, Italy). Cells were spiked at a final concentration of 30 cells per mL of blood. Concurrently, we employed samples from three healthy donors per each cell line. These samples were analyzed using the CellSearch® and Parsortix Systems, running identical

blood samples with both technologies. All spiked samples were enriched within 96 h of collection.

2.7 Analysis of c-MET expression on CTCs isolated using CellSearch®

A total of 7.5 mL of peripheral whole blood samples were collected in CellSave tubes (Menarini, Silicon Biosystems, Bologna, Italy) for CTCs enumeration using the CellSearch® system (Menarini, Silicon Biosystems, Bologna, Italy). CellSearch® Circulating Tumor Cell Kit (Menarini, Silicon Biosystems, Bologna, Italy) was used for these specific experiments, including ferrofluids coated with epithelial cell-specific anti- EpCAM antibodies to immunomagnetically enrich epithelial cells; a mixture of antibodies directed to CKs 8, 18, and 19 conjugated to phycoerythrin (PE); anti-CD45 mAb conjugated to allophycocyanin (APC); and DAPI to fluorescently label the cells. The C32 cells and human melanoma samples were analyzed using a CellSearch® Circulating Melanoma Cell Kit (Menarini, Silicon Biosystems, Bologna, Italy), which included ferrofluid coated with antibodies targeting the CD146 antigen to capture circulating melanoma cells (CMCs) and fluorescent reagents against anti-high molecular weight melanoma-associated antigen (HMW-MAA-PE (MEL-PE)), anti-CD34-APC for endothelial cells, anti-CD45-APC for leukocytes, and DAPI for staining cell nuclei. The open 4th antibody position of the CellSearch® system was used to evaluate c-MET expression. We employed the anti-MET FITC-conjugated monoclonal antibody (D-4, sc-514148, Santa Cruz, CA, USA) at a final concentration of 20 μg/mL. CTCs were identified as $EpCAM^+$, CK^+, $CD45^-$, and $DAPI^+$, and the level of c-MET expression was recorded for each

CTC, on a 0–3 scale, by comparison to the c-MET expression levels of the different reference cell lines.

2.8 Analysis of c-MET expression on CTCs isolated using Parsortix system

A total of 7.5 mL of peripheral whole blood was collected in CellSave tubes (Menarini, Silicon Biosystems, Bologna, Italy) and loaded into the Parsortix microfluidic device (Angle Inc, Guildford, UK). CTCs were then enriched from blood samples in disposable Parsortix cassettes (GEN3D6.5, Angle Inc, Guildford, UK), according to the manufacturer's guidelines. CTCs were trapped in the Parsortix cassette due to their large size and lower compressibility than the remaining blood cells. After separation, we fixed the sample and carried out immunofluorescence staining. CTCs were subjected to on-cassette-staining with selected antibodies, according to the manufacturer's guidelines, followed by fluorescence microscopy detection (Leica DMI8, Leica Microsystems, Germany). The selected antibodies included AF546-conjugated pan-CK (C11, sc-8018, Santa Cruz, CA, USA), AF647-conjugated CD45 (35-Z6, sc-1178, Santa Cruz, CA, USA), anti-MET FITC-conjugated (D-4, sc-514148, Santa Cruz, CA, USA), and DAPI to fluorescently label the cells. CTCs were identified as CK^+, $CD45^-$, and $DAPI^+$, and the level of c-MET expression on CTCs was determined, on a scale of 0–3 scale, depending on the c-MET antibody intensity, according to the results obtained in cell lines controls.

2.9 Statistical analysis

Statistical analyses were performed using R version 3.4.0 and GraphPad Prism 8. Pearson's correlation and linear regression were used to evaluate the

relationship between ddPCR and SNP6.0 or FISH results. The Mann–Whitney–Wilcoxon U-Test was used to compare the *MET* CN between cancer patients and healthy controls. Two-tailed *p*-values of 0.05 or less were considered significant. The cut-off value for the *MET* CN test to define the presence of *MET* amplification was determined using the mean plus 3 standard deviations of healthy controls. The Kappa test was used to determine the concordance between *MET* amplification based on FISH and ddPCR analyses. Paired Student t tests were used to compare the CTCs enrichment potential between the Parsortix and the CellSearch® systems.

3. RESULTS

3.1 Clinical characteristics and sample collection

In total, 174 cancer patients were enrolled in the study. Their clinicopathological characteristics are presented in Table 1.4. One-hundred and forty patients were diagnosed with diverse metastatic cancers (such as NSCLC, colorectal cancer, head and neck, or melanoma, among others) and all patients had progressed to at least one line of therapy. Of these patients, 77 patients presented NSCLC, and 28 of them presented any *EGFR* mutation. These 28 NSCLC patients had a progression to first-line TKIs and some of them even to osimertinib (third TKIs generation) in second-line. In another hand, 34 non-metastatic cancer patients were included. Finally, 49 healthy controls were enrolled in the present study. Sample collection was performed before therapy onset (baseline) in all patients.

Table 1.4. Demographics and clinical characteristics of the patients at baseline.

Baseline Characteristics	Metastatic patients N* (%)	Non-metastatic patients N+ (%)
Mean age (years) ± SD, range	63.9 ± 8.5, 35-83	61.8 ± 9.2, 45-79
Sex		
Female	55 (39.3)	10 (29.4%)
Male	85 (60.7)	23 (67.7%)
Unknown	-	1 (2.9%)
Tumor type		
NSCLC	77 (55.0)	19 (55.9%)
Head and neck	30 (21.4)	4 (11.8%)
Colon	8 (5.7)	6 (17.6%)
Melanoma	6 (4.3)	1 (2.9%)
Pancreas	3 (2.2)	4 (11.8%)
Others**	16 (11.4)	0 (0.0%)
Number of lines of treatment		
≤1	75 (53.6)	-
>1	59 (42.1)	-
Unknown	6 (4.3)	-
Number of metastatic sites		
≤2	54 (38.6)	-
>2	73 (52.1)	-
Unknown	13 (9.3)	-

*N=140 at baseline. +N=34 at baseline. **Biliary (4), gastric (4), ovarian (3), renal (3), retrocural (1) and skin (1) cancers. Abbreviations: SD: standard deviation.

The study design for testing the utility of blood samples to assess the *MET* status in cancer patients is shown in Figure 1.8.

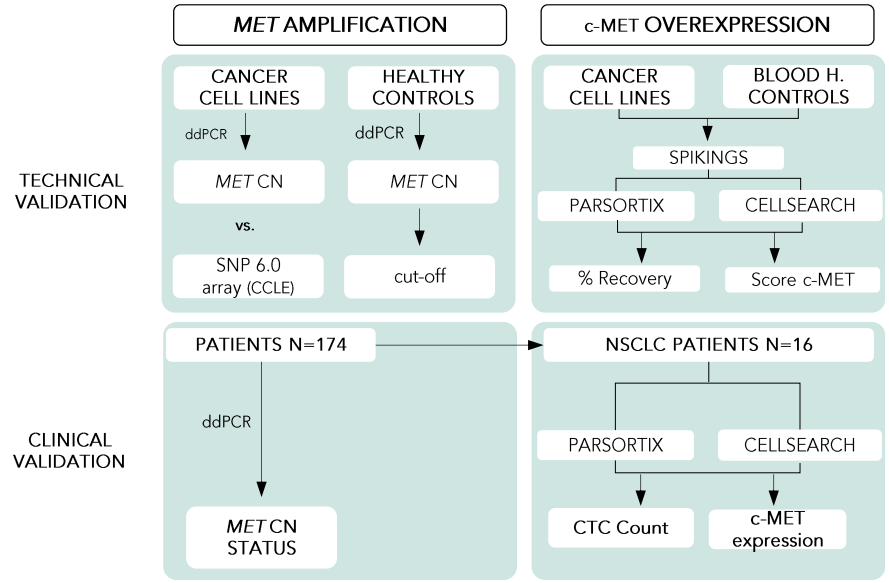

Figure 1.8. Study design for *MET* status assessment in cancer patients. CN: copy number; CCLE: cancer cell line encyclopedia.

3.2 *MET* amplification: Accuracy of ddPCR to detect *MET* CNA

We designed a prospective study to analyze *MET* amplification in different cancer types.

First, we optimized the ddPCR assay using DNA isolated from a panel of cell lines representative of different levels of *MET* amplification and different cancer tumour types (lung, colon, prostate, skin, breast, and gastric). We obtained *MET* CN data as determined by microarray (Affimetrix SNP6.0 Array) from the publicly available CCLE database. Then, we compared the data with our ddPCR results in the same cancer cell lines. After the comparative analysis, a strong linear association of *MET* CN measurements based on Pearson's correlation (r= 0.98; p-value $<10^{-4}$) was observed,

validating the accuracy of our analytic approach (Figure 1.9A). We also used serial dilutions of genomic DNA from the cancer cell lines representing different CN values (Figure 1.9B). Therefore, we set up that the minimum amount of DNA to detect *MET* CN was 2.3 ng total in each ddPCR reaction. Below of these values, there was no reproducibility of the results. All cfDNA samples used in the present study were above of this value in the ddPCR analysis.

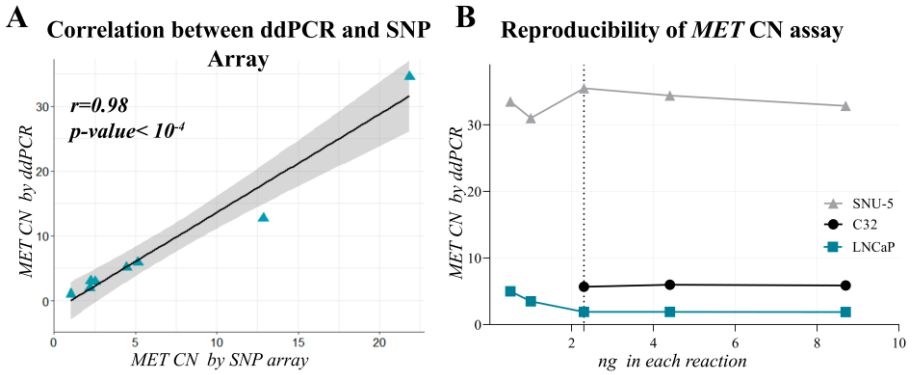

Figure 1.9. *MET* CN analysis. (A) Scatterplot representing correlation between *MET* CN in cancer cell lines determined by ddPCR versus SNP array (n = 8) using Pearson's correlation. (B) Reproducibility of the *MET* CN determination by ddPCR. We represented some examples of the determination in 3 cancer cell lines in different assays with increasing DNA concentration. Abbreviations: CN, copy number.

3.3 *MET* CN assessment in cfDNA from cancer patients and healthy controls

Next, we evaluated *MET* CN in cfDNA from the plasma of 140 patients with metastatic cancer progressing to at least one treatment and 34 non-metastatic patients. To test the specificity of the *MET* CN analyses, 49 healthy volunteers were recruited as controls. The control group was employed to set the normal values associated with a non-amplified *MET* status. Therefore,

based on the CN values in the control population (*MET* CN between 1.9 and 2.66), a threshold of 2.8 was established to define the presence of *MET* amplification (Figure 1.10A).

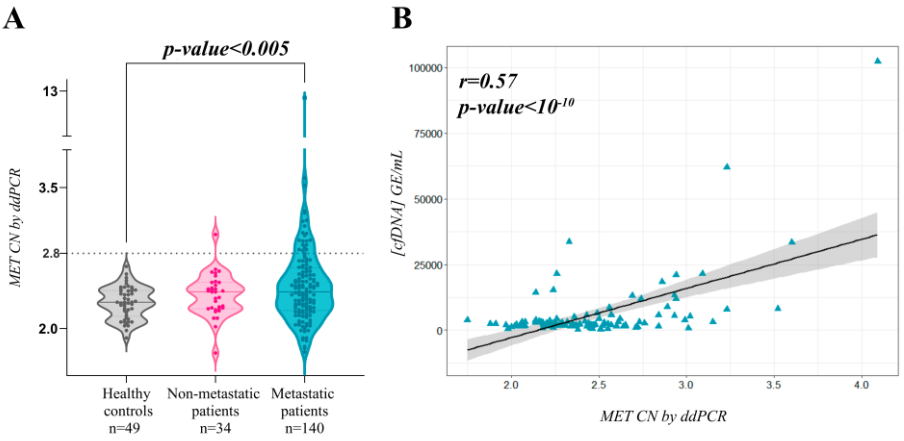

Figure 1.10. *MET* CN analysis. (A) Plasma *MET* CN detected in healthy controls (n= 49), non-metastatic patients (n=34) and metastatic patients (n= 140). Differences were analysed using the Mann-Whitney-Wilcoxon U-Test. (B) Correlation between cfDNA levels and plasma *MET* CN in metastatic cancer patients (n= 140) using Pearson's correlation. Abbreviations: CN, copy number.

Importantly, *MET* CN values in patients were found between 1.75 and 12.7 and the comparison of the *MET* CN values between metastatic patients and healthy controls showed a statistically significant difference between the two populations (*p*-value =0.003; Mann–Whitney-Wilcoxon U-Test test; Figure 1.10A), reinforcing the accuracy of our analytical strategy. In fact, 23 values from the metastatic patients were higher than 2.8, being considered as positive for *MET* amplification. The CN range in the non-metastatic cohort was similar to the healthy controls, and only one patient showed *MET* amplification. Of note, a significative correlation between cfDNA concentration and *MET* CN was observed (r= 0.57, p-value $<10^{-10}$) (Figure

1.10B) in metastatic patients evidencing the higher capacity to detect *MET* amplification in patients with high cfDNA levels. On the other side, no association was found between *MET* CN values from metastatic cancer patients and clinical characteristics, such as the number of metastatic sites or the treatment lines received prior to sample collection (Table 1.5).

Table 1.5. Baseline demographics and clinical characteristics of the metastatic cancer patient population analysed for *MET* amplification.

Features	All	Number of lines of treatment			Number of metastatic sites		
		≤1	>1	Unknown	≤2	>2	Unknown
	N* (%) *MET* CN (Mean±SD)	N (%) *MET* CN (Mean±SD)			N (%) *MET* CN (Mean±SD)		
Sex							
Male	85 (60.7%) 2.5 ± 0.4	48 (34.3) 2.4 ± 0.4	33 (23.6) 2.5 ± 0.5	4 (2.3) 2.3 ± 0.4	31 (22.1) 2.5 ± 0.5	46 (32.9) 2.5 ± 0.4	8 (5.7) 2.2 ± 0.2
Female	55 (39.3%) 2.6 ± 1.4	27 (19.3) 2.4 ± 0.3	26 (18.6) 2.8 ± 2.0	2 (1.4) 2.2 ± 0.1	23 (16.4) 2.4 ± 0.4	27 (19.3) 2.9 ± 2.0	5 (3.6) 2.2 ± 0.1
Tumour type							
NSCLC	77 (55.0%) 2.5 ± 1.2	36 (25.7) 2.4 ± 0.3	38 (27.1) 2.6 ± 1.7	3 (2.1) 2.3 ± 0.2	22 (15.7) 2.4 ± 0.3	45 (32.1) 2.6 ± 1.6	10 (7.1) 2.2 ± 0.1
Head and neck	30 (21.4%) 2.4 ± 0.4	29 (20.7) 2.4 ± 0.4	1 (0.7) 2.5	-	24 (17.1) 2.4 ± 0.4	6 (4.3%) 2.5 ± 0.3	-
Colon	8 (5.7%) 2.6 ± 0.8	1 (0.7) 2.5	6 (4.3) 2.8 ± 0.9	1 (0.7) 1.8	1 (0.7) 4.1	6 (4.3) 2.6 ± 0.6	1 (0.7) 1.8
Melanoma	6 (4.3%) 2.4 ± 0.5	4 (2.9) 2.4 ± 0.5	2 (1.4) 2.4 ± 0.7	-	3 (2.1) 2.2 ± 0.1	3 (2.1) 2.6 ± 0.7	-
Others **	19 (13.4%) 2.6 ± 0.3	5 (4.3) 2.6 ± 0.3	12 (8.6) 2.7 ± 0.3	2 (1.4) 2.6 ± 0.2	4 (2.9) 2.8 ± 0.2	13 (9.3) 2.6 ± 0.3	2 (1.4) 2.4 ± 0.0

*N=140 at baseline. ** Biliary (4), gastric (4), ovarian (3), renal (3), pancreas (3), retrocural (1) and skin (1) cancers. Abbreviations: CN: copy number; SD: standard deviation.

We also found a high variability of the *MET* CN status between the different tumour types, which was not significantly different among groups. However, it is remarkable that all patients with renal cancer (n=3) showed *MET* CN values over the threshold (2.89, 2.92, and 3.09 values) (Figure 1.11; Table 1.5).

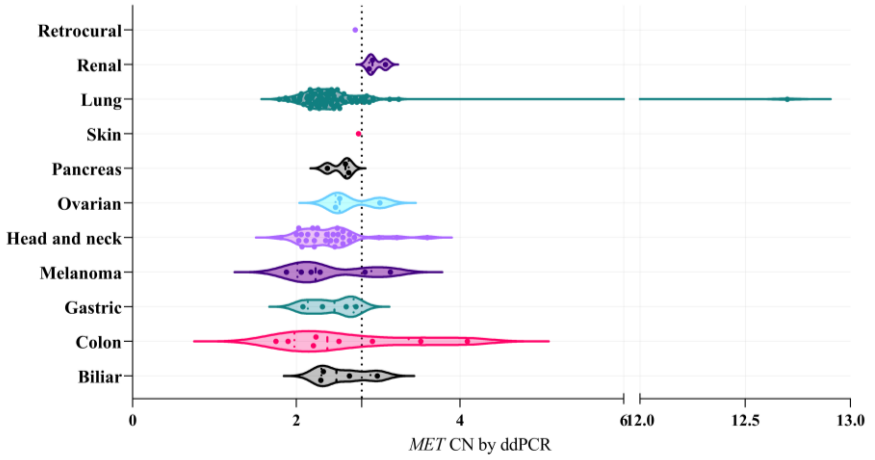

Figure 1.11. Plasma *MET* CN values in the different metastatic cancers included in the study. Abbreviations: CN, copy number.

In NSCLC, we determined *MET* CN in 77 NSCLC patients by our ddPCR assay and *MET* amplification (*MET* CN >2.8) was detected in 10/77 NSCLC patients (12.99%; median CN, 2.5; range, 1.8-12.7).

3.4 *MET* amplification: Concordance between cfDNA and tissue samples

Currently, in routine studies, FISH is the standard method used to evaluate the *MET* CN (247,248). We evaluated the sensitivity and specificity of our *MET* CN assay compared to the FISH ratio *MET/CEN*-7 > 4 (based on standard Colorado criteria). For this purpose, we tested the concordance of *MET* amplification between cfDNA and tissue samples in 12 patients with

melanoma (n = 4), NSCLC (n = 3), ovarian (n = 2), head and neck (n = 2), and skin cancers (n = 1) by ddPCR and FISH, respectively (Figure 1.12).

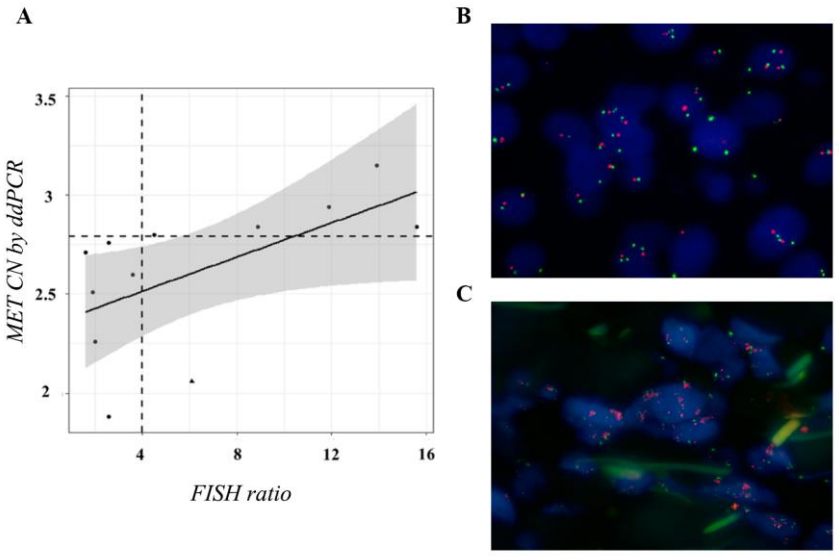

Figure 1.12. Comparison of *MET* CN status in tissue and cfDNA. (A) Distribution of *MET* CN measured by ddPCR and FISH (the point larger indicates the discordant value, whereas the horizontal and vertical dotted lines indicate cut-off points of ddPCR and FISH, respectively). (B) Representative example of a negative case for *MET* amplification obtained in a NSCLC patient by FISH. (C) Representative example of a positive case for *MET* amplification obtained in a NSCLC patient by FISH. Abbreviations: CN, copy number.

It is important to remark that, in these patients, the date of tissue and plasma sampling collection was less than 2 months. The linear association between *MET* CN analysed by ddPCR and the *MET/CEN*-7 ratio analysed by FISH was relatively moderate (r= 0.58; p-value <0.05; Figure 1.12A), while the concordance rate was 91.67% with Cohen's kappa of 0.833 (95% CI: 0.615–0.998, p-value <0.005). Sensitivity and specificity to detect the *MET* amplification present in tissue by means of plasma ddPCR were 85.7% and 100%, respectively, demonstrating a good performance of the technique.

3.5 c-MET expression: Accuracy of detect c-MET expression on CTCs

To complement our approach in characterizing *MET* status by means of liquid biopsy, we developed a strategy to assess c-MET expression in the CTCs population. First, we evaluated the enrichment potential of the CellSearch® and Parsortix systems, using preserved blood samples from healthy controls spiked with six human tumour cells (LNCaP, NCI-N87, Hs746T, AU565, SNU-5 and C32), representative of the variability of c-MET expression. The average percentage of spiked cells captured by the Parsortix system was 73.04 ± 19.23% (range 54–99.01%), while, for the CellSearch® system, the average recovery was 71.60 ± 22.58% (range 32.65–91.32%). Importantly, we observed a different isolation efficacy with CellSearch® and Parsortix platforms to isolate the cell lines as result of the differential strategy for the CTCs enrichment applied by both platforms (p-value <0.005, in all comparisons; Figure 1.13A).

The Parsortix system that isolates CTCs based on their size and deformability showed higher isolation efficiency compared to the EpCAM-dependent enrichment method of CellSearch® in the case of Hs746T and C32 cancer cell lines (p-value =2.63×10^{-5} and 2.90×10^{-7}, respectively). These cell lines are characterized by a low EpCAM expression explaining the low recovery with an EpCAM-dependent strategy (Figure 1.13B-C). Once the performance of both technologies was assessed, we established immunoscores for c-MET expression on single CTCs for both systems to grade this expression (Figure 1.14).

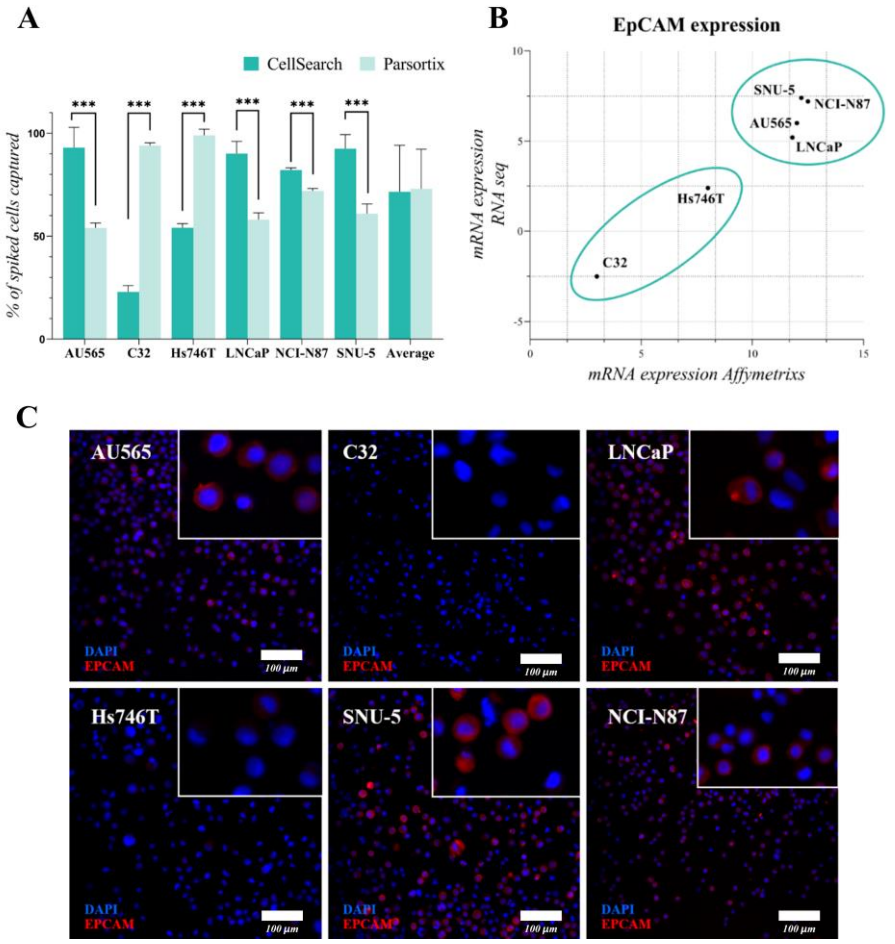

Figure 1.13. Evaluation of the enrichment capacity of CellSearch® and Parsortix systems, using healthy blood spiked with cancer cell lines. (A) Percentage of spiked tumor cancer cells captured using CellSearch® and Parsortix systems. p-value <5x10-3, in all comparisons between CellSearch® and Parsortix System in each cell line using paired student t test. (B) Correlation between EpCAM mRNA expression levels measured by Affymetrix microarrays and RNA seq. (C) Immunofluorescence characterization of EpCAM in our cancer cell lines. Scale bar represents 100 µm.

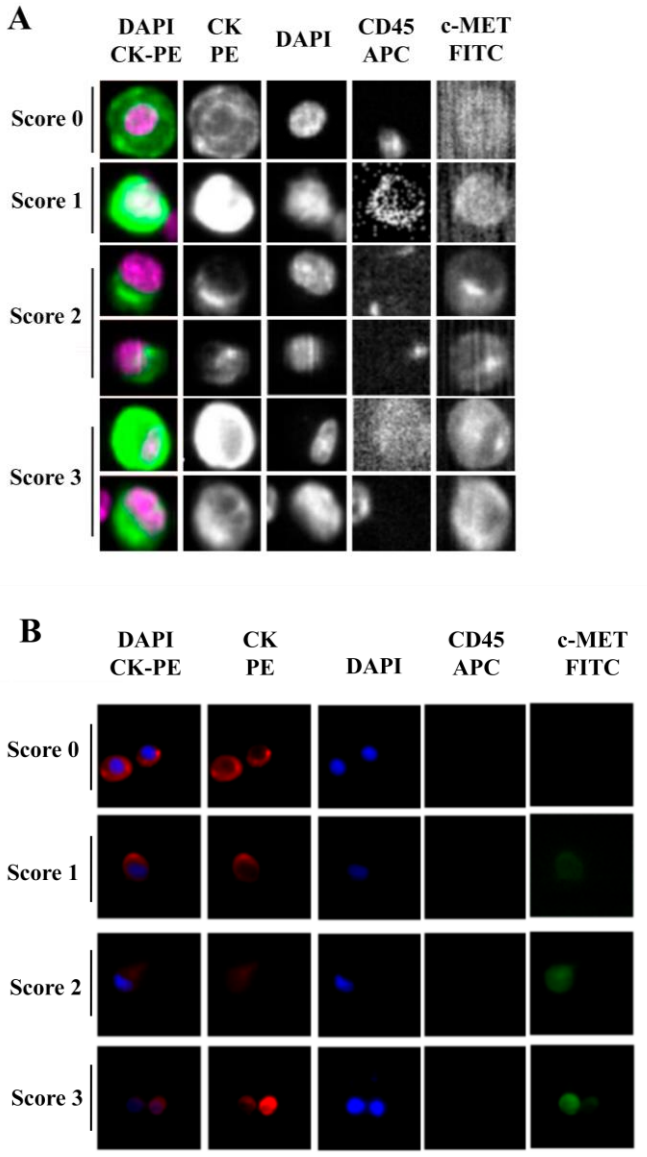

Figure 1.14. Detection of c-MET expression using tumour cancer cells with the CellSearch® and Parsortix systems (Figure A and B, respectively). Representative images of c-MET expression scored on score 0 (cell line LNCaP), 1 (cell line AU565), 2 (cell line Hs746T) and 3 (cell line SNU-5).

We defined four different levels for the intensity of c-MET presence: score 0 (negative), 1+ (weak), 2+ (moderate), or 3+ (strong) based on the signal obtained in cells with 0 (LNCaP), 1+ (AU565), 2+ (Hs746T), or 3+ (SNU-5).

3.6 *c*-MET expression on CTCs from NSCLC patients

Thus, we analysed the c-MET expression in CTCs using the optimized conditions described above. We found that at baseline, using the CellSearch® system, at least one CTC was detected in 5 patients (31.25%), ranging from 1 to 77 CTCs in 7.5 mL of blood (mean= 4.83 CTCs). From these 5 patients, only 2 showed c-MET overexpression (score 2 or 3), representing 13.33% of all patients analysed. Using the Parsortix system, at least one CTC was detected in 9 patients (56.2%) at baseline, ranging from 1 to 83 CTCs in 7.5 mL of blood (mean= 8.8 CTCs), being c-MET overexpression found in 4 NSCLC patients out of 16 (25.0%) (Figure 1.15; Table 1.6).

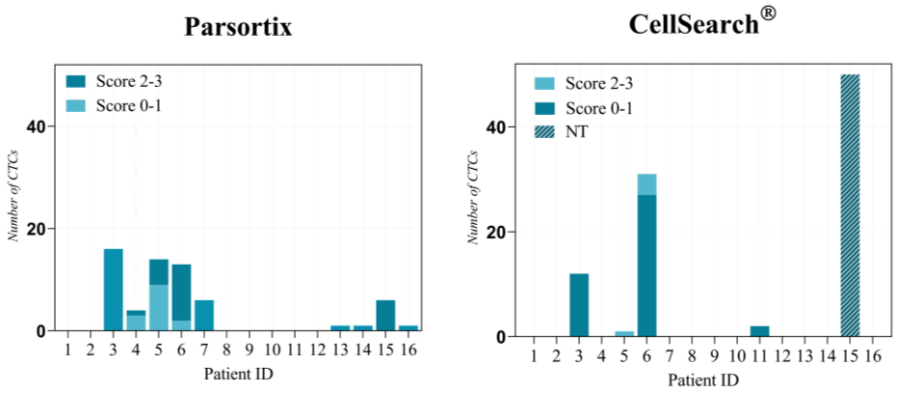

Figure 1.15. CTCs enumeration and c-MET expression in blood samples evaluated by the CellSearch® (right panel) and Parsortix (left panel) systems. Distribution of c-MET scores in CTCs from patients with NSCLC. Abbreviations: NT, not tested.

Table 1.6. CTC detection and c-MET expression on CTCs using CellSearch® and Parsortix systems in patients with NSCLC.

NSCLC Patient ID	CELLSEARCH®			PARSORTIX		
	CTC Total number	MET CTC Score		CTC Total number	MET CTC Score	
		0-1	2-3		0-1	2-3
5	0	0	0	0	0	0
9	0	0	0	0	0	0
11	12	12	0	16	16	0
14	0	0	0	4	3	1
18	1	0	1	14	9	5
26	31	27	4	13	2	11
28	0	0	0	6	6	0
67	0	0	0	0	0	0
72	0	0	0	0	0	0
75	0	0	0	0	0	0
80	2	2	0	0	0	0
81	0	0	0	0	0	0
82	0	0	0	1	1	0
90	0	0	0	1	1	0
91	77	NT	NT	6	0	6
92	0	0	0	1	1	0

NT: not tested.

These results evidence a higher efficiency of Parsortix system in comparison to CellSearch® in our cohort of patients with NSCLC. In fact, 5 patients with NSCLC were positive for CTCs using Parsortix system but negative using CellSearch® while the inverse situation was observed only in 1 patient. The overall positive concordance of both strategies was 62.5% (Table 1.6).

3.7 *MET* status in NSCLC patients under anti-EGFR therapy

Finally, we investigated the utility of *MET* status monitoring in NSCLC patients under anti-EGFR therapy and focus our attention in two cases receiving this treatment.

A 72-year-old female was diagnosed with a stage IV NSCLC adenocarcinoma *L858R* carrier with bone lesions compatible with bone metastases (patient id26). She was recruited at the start of erlotinib therapy and *MET* CN status in cfDNA and c-MET expression in CTCs were evaluated. She had 31 CTCs in the CellSearch® system, 4 of them showing c-MET overexpression (12.9%); whereas 13 CTCs were detected with Parsortix system (11 c-MET-positive, 84.62%). In addition, *MET* amplification was detected in plasma sample. Despite she did not show radiological progression, there was a serious clinical deterioration and the patient died within two months.

Another case of the retrospective study evidenced how *MET* CN detection may be informative in monitoring the appearance of resistance mechanisms in response to anti-*EGFR* treatment (Figure 1.16). An 84-year-old female was diagnosed with stage IV NSCLC adenocarcinoma (patient id60) with metastases in bone and liver. An *EGFR* mutation (L858R) was detected at the disease diagnosis and erlotinib, a first-generation *EGFR* tyrosine kinase inhibitor (TKI), was started. Longitudinal plasma samples were collected during the course of the disease. She progressed at day 145 (T790M-positive) and, 8 days after, the first plasma sample was collected (day 153). *MET* CN analyses showed the presence of *MET* amplification. At day 180 she started osimertinib therapy, a third-generation TKI. Two months after the start of osimertinib therapy (day 234) a plasma sample was again collected, showing a decrease in *MET* CN and allelic frequency of *EGFR* mutations. She continued osimertinib until progression (day 265). At day 261, plasma analyses showed an increase in *MET* CN and L858R allelic frequency. She died on day 281.

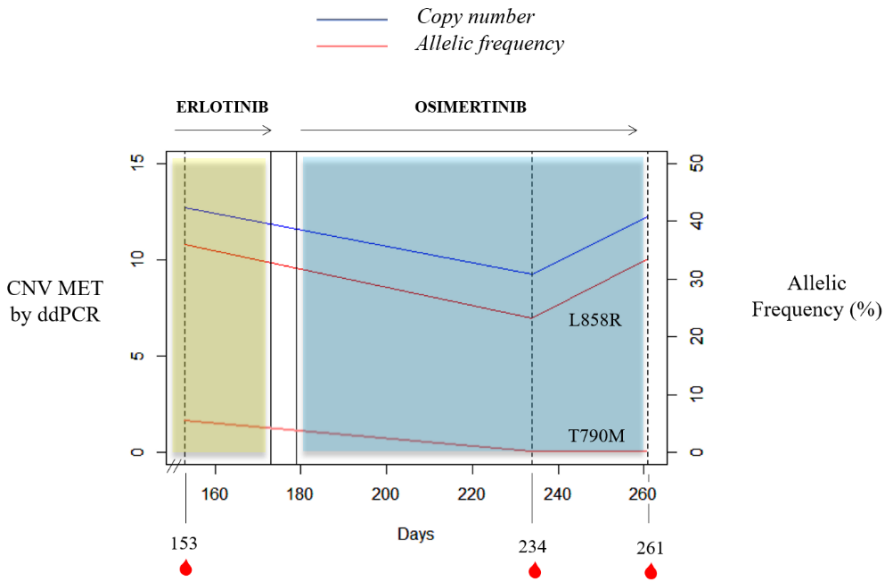

Figure 1.16. Timeline for the clinical course of patient id60. The blue and yellow bars represent the treatments time frame, and the red drops indicate blood collection time points. Percent mutant allelic frequency (L858R and T790M) and *MET* CN for patient id60 are shown. Abbreviations: CN, copy number.

4. DISCUSSION

This study was designed to investigate the utility of liquid biopsy in assessing c-MET protein expression and *MET* CN, defined as *MET* status, in NSCLC cancer patients. We used ddPCR to quantify *MET* CN in cfDNA and in a complementary way, we evaluated two approaches to detect c-MET presence on CTCs to overcome the complexity of isolating different phenotypes of CTCs (CellSearch® and Parsortix systems).

For CTCs analysis, we implemented the c-MET expression detection using the CellSearch® and the Parsortix platforms routine. Due to the ultra-rare nature of CTCs, with numbers as low as 1 CTC per 10^6-10^7 leukocytes,

most assays for CTCs analyses use a combination of enrichment and detection/characterization techniques (249). It is important to remark that the most widely used CTCs enrichment technique is the immunomagnetic-based selection of CTCs, being CellSearch® system the first FDA approved device for CTCs enumeration, although there are others based on this strategy (e.g., IsoFlux™, AdnaTest, and MACS®). The main limitation of this approach is the lack of a "universal marker" that can be used independently of both the tumour type and the stage of disease progression (250). To solve this problem, new CTCs isolation strategies have been developed such as size-based enrichment (e.g., Parsortix, ScreenCell®, and ISET®) and microfluidic-based enrichment (e.g., Parsortix, CTC-Chip/iChip, IsoFlux™, and GILUPI CellCollector™). The Parsortix system uses a combination of microfluidic and size/deformability-based approaches to separate CTCs from blood samples. Its main advantage over CellSearch® is the ability to enumerate CTCs independently of their epithelial or mesenchymal status. However, cell size-based systems have difficulty to completely separate cancer cells and leukocyte by their size since patient's CTCs exhibit a high degree of pleomorphism, where the size of the captured tumour cells can vary from 4-30 μm (251). Therefore, size overlapping between CTCs and leukocytes will result in the loss of small CTCs. Besides, although CTCs can be detected in non-metastatic patients using both approaches, their low levels of non-advanced disease limit the application of these technologies as diagnostic tools (205).

In our cohort of patients with NSCLC, we found that the Parsortix approach identified a higher proportion of CTC-positive patients than the CellSearch® system, indicating that an antigen CTCs independent isolation

approach can overcome the EpCAM expression heterogeneity that characterizes these tumours. Therefore, some non-epithelial or mesenchymal CTCs from cancer patients would be detected on the Parsortix platform but could escape the antigen-dependent enrichment method of the CellSearch® EpCAM assay, and *vice versa* with epithelial CTCs, such as reflected our spiking experiments with different cell lines expressing different levels of EpCAM. Therefore, although the good results obtained using Parsortix system, a larger cohort of patients would be necessary to clearly determine which technology should be used to characterize CTCs in this population.

Independently to the CTCs enumeration rate showed by both technologies, our study provides a proof-of-concept for the analysis of c-MET expression in CTCs to determine *MET* status in patients that might be eligible in clinical trial testing MET inhibitors and could be useful to monitor the appearance of therapy resistance. Previously, Zhang et al. developed a non-invasive assay for c-MET$^+$ CTCs capture and characterization from multiple patients with metastatic carcinomas using the CellSearch® system (252). Due to the strategy used, they identified a high prevalence of CD45-positive leukocytes expressing c-MET in patients with metastatic solid tumours, although the clinical relevance of this cell population is unknown. Ilie et al. also evaluated the prevalence of c-MET expression in CTCs from NSCLC patients (253), using a combined strategy similar to the one employed in the present work. In their study, c-MET expression was assessed using a CellSearch® system and by immunocytochemistry on ISET-enriched CTCs from advanced-stage NSCLC patients. They found that c-MET expression was lower in CTCs analyzed by CellSearch® than using ISET. In fact, only 3.52% patients showed CTCs with high c-MET expression (scores of 2^+ or 3^+) in CellSearch®, whereas c-MET-

positive CTCs from advanced-stage NSCLC patients were successfully detected using the ISET platform, being 54 of the 75 (72%) patients' blood samples defined as c-MET positive. Our data showed that the prevalence of c-MET expression in CTCs isolated by CellSearch® is greater than previously reported data (12.5% c-MET-positive patients with scores of 2^+ or 3^+). Importantly, using Parsortix system, we found 25% of patients with c-MET-positive scores of 2^+ or 3^+, being the concordance to detect the presence of CTCs overexpressing c-MET between both technologies, of 50%. These results showed that c-MET is expressed on CTCs with a considerable patient dependent and technology variability. Obviously, these results reflect the distinct CTCs enrichment methodologies of the two platforms.

In addition to the CTCs analysis, we demonstrated the ddPCR approach to be a useful tool for detecting *MET* amplification in plasma samples from cancer patients. Zhang et al. had already shown this capacity, detecting *MET* CN in genomic DNA from cancer cell lines and tumour samples (254). Recently, a study in cfDNA obtained from plasma of different tumour types showed that detection of *MET* alterations (amplification and point mutations) by liquid biopsy was feasible using the Guardant360 NGS panel (255). In this study, they found 7% of patients with *MET* amplification in plasma, most of them with metastatic disease. Although NGS panels can provide more complete information regarding the status of other driver genes, our goal was the validation of a more sensitive and easier to implement test to monitor *MET* CN in plasma using ddPCR. For this aim, a cohort of healthy controls and cancer patients with different tumour types and metastatic stages were analysed to detect *MET* CN by ddPCR. In our study, 12.99% of NSCLC patients (and 16.4% of all metastatic patients) and 3% of the non-metastatic

were defined as positive for *MET* amplification, being higher rates than the previously described using an NGS approach and higher than in tissues (1.14%) (255). Besides, we evaluated the concordance of the *MET* CN detection between plasma and tumour samples obtained at the same time as the disease evolution. Importantly, *MET* amplification positivity detected by ddPCR was comparable to that detected by FISH. Only one melanoma patient with *MET* amplification determined by FISH (*MET*/*CEN-7* ratio= 6.1) did not show *MET* amplification in plasma using ddPCR (CN> 2.8). These results reinforced the value of the *MET* analysis in plasma samples as a more accessible monitoring tool to guide anti-MET therapies.

Actually, *MET* amplification is a relevant resistance mechanism to first-generation EGFR-TKIs (gefitinib and erlotinib), being detectable in approximately 5%-22% of NSCLC patients with acquired resistance to these drugs (256). Osimertinib, a third generation EGFR-TKIS, inhibits the *EGFR* variants Del19 and L858R, as well as the resistant T790M mutation. About 20% of such patients do not respond well to osimertinib, and almost all patients have eventually relapsed and developed resistance to the treatment. These resistance mechanisms are largely unknown, except for the C797S mutation and *MET* amplification (256). There have been preclinical studies suggesting that monotherapy with osimertinib is not effective for the treatment of *EGFR* mutant NSCLC with acquired resistance to first-, second, or third-generation EGFR-TKIs, due to *MET* amplification, or even *MET* hyperactivation (257). Targeting *EGFR* and *MET* simultaneously may be required to overcome resistance to EGFR-TKIs by *MET* alteration, making it necessary to assess MET status before osimertinib treatment. Thus, some studies have reported the successful administration of dual EGFR and MET therapies (258–260). The combination

of osimertinib and MET inhibitors can be safe and effective in NSCLC patients with *MET* amplification detected by ddPCR as an acquired resistance mechanism. In this context, our results demonstrated the utility of plasma *MET* determination as a valuable biomarker for monitoring the appearance of resistance to anti-EGFR therapy. In fact, we reported a case of *MET* amplification detected in plasma from a NSCLC patient harbouring *EGFR* L858R mutation after disease progression to erlotinib and before osimertinib therapy,

Regardless of the value of our findings, some limitations to our study should be kept in mind. The small number of tissue samples (obtained close to plasma collection) that were available did not allow us to carry out a robust comparative study between *MET* CN obtained from plasma and tissue. Despite this limitation, we showed that plasma may be a good option for monitoring the molecular evolution of the disease, which is even more relevant in patients for which a tissue-rebiopsy is not feasible. In addition, we implemented the detection of c-MET expression in CTCs from cancer patients using two complementary technologies and obtaining promising results. Nevertheless, considering the limited cohort size, the real clinical value of the assessment of c-MET expression in CTCs must be evaluated also in a larger cohort of patients.

In conclusion, we developed specific and non-invasive assays to monitor c-MET expression on CTCs and *MET* CN on cfDNA using blood from cancer patients. Both molecular alterations were detected in patients with NSCLC and represent a good opportunity to characterize them in a non-invasive and dynamic way, as well as monitoring patients who will benefit of MET inhibitors.

CHAPTER II

Clinical potential of circulating free DNA and circulating tumour cells in patients with metastatic NSCLC treated with pembrolizumab.

Clinical potential of circulating free DNA and circulating tumour cells in patients with metastatic non-small cell lung cancer treated with pembrolizumab.

This chapter has been adapted/extracted from a recently published article entitled "Clinical Potential of Circulating Free DNA and Circulating Tumour Cells in Patients with Metastatic Non-Small-Cell Lung Cancer treated with Pembrolizumab" (261).

Patricia Mondelo-Macía[1,2], Jorge García-González[3,4,5], Luis León-Mateos[3,4,5], Urbano Anido[3,4], Santiago Aguín[3,4], Ihab Abdulkader[6], María Sánchez-Ares[6], Alicia Abalo[1], Aitor Rodríguez-Casanova[7,8], Ángel Díaz-Lagares[5,7], Ramón Manuel Lago-Lestón[1], Laura Muinelo-Romay[1,5], Rafael López-López[3,4,5] and Roberto Díaz-Peña[1,5*].

1 Liquid Biopsy Analysis Unit, Translational Medical Oncology (Oncomet), Health Research Institute of Santiago (IDIS), Santiago de Compostela, Spain.
2 Universidade de Santiago de Compostela (USC), Santiago de Compostela, Spain
3 Department of Medical Oncology, Complexo Hospitalario Universitario de Santiago de Compostela (SERGAS), Santiago de Compostela, Spain.
4 Translational Medical Oncology (Oncomet), Health Research Institute of Santiago (IDIS), Santiago de Compostela, Spain.
5 Centro de Investigación Biomédica en Red de Cáncer (CIBERONC), Madrid, Santiago de Compostela, Spain.
6 Department of Pathology, Complexo Hospital Universitario de Santiago de Compostela (SERGAS), Universidade de Santiago de Compostela, Santiago de Compostela, Spain.
7 Cancer Epigenomics, Translational Medical Oncology (Oncomet), Health Research Institute of Santiago (IDIS), Santiago de Compostela, Spain.
8 Roche-CHUS Joint Unit, Translational Medical Oncology (Oncomet), Health Research Institute of Santiago (IDIS), Santiago de Compostela, Spain.

** Corresponding.*

Clinical potential of circulating free DNA and circulating tumour cells in patients with metastatic non-small cell lung cancer treated with pembrolizumab.

ABSTRACT

Immune checkpoint inhibitors, such as pembrolizumab, are revolutionizing therapeutic strategies for different cancer types, including NSCLC. However, only a subset of patients benefits from this therapy, and new biomarkers are needed to select better candidates. In this study, we explored the value of liquid biopsy analyses, including cfDNA and CTCs, as a prognostic or predictive tool to guide pembrolizumab therapy. For this purpose, a total of 109 blood samples were collected from 50 patients with advanced NSCLC prior to treatment onset and at 6 and 12 weeks after the initiation of pembrolizumab. Plasma cfDNA was measured using *hTERT* quantitative PCR assay. CTC levels at baseline were also analysed using two enrichment technologies (CellSearch® and Parsortix systems) to evaluate the efficacy of both approaches at detecting the presence of PD-L1 on CTCs. Notably, patients with high baseline *hTERT* cfDNA levels had significantly shorter PFS and OS than those with low baseline levels. Moreover, patients with unfavourable changes in the *hTERT* cfDNA levels from baseline to 12 weeks showed a higher risk of disease progression. Additionally, patients in whom CTCs were detected using the CellSearch® system had significantly shorter PFS and OS than patients who had no CTCs. Finally, multivariate regression analyses confirmed the value of the combination of CTCs and cfDNA levels as an early independent predictor of disease progression,

identifying a subgroup of patients who were negative for CTCs, who presented low levels of cfDNA and who particularly benefited from the treatment.

Keywords: biomarkers, cfDNA, CTCs, immunotherapy, NSCLC, PD-L1.

1. INTRODUCTION

Lung cancer ranks first in morbidity and mortality rates among malignant tumours worldwide (262). Under normal physiological conditions, immune checkpoint proteins are crucial for the maintenance of self-tolerance, protecting tissues from damage when the immune system responds to infections. However, the expression of immune checkpoint proteins is dysregulated by tumours as an immune resistance mechanism (263). Over the past decade, immunotherapy has become a milestone in the treatment of NSCLC. Currently, ICIs can target both PD-1 and PD-L1. Specifically, pembrolizumab is a humanized IgG4 monoclonal antibody that binds to the PD-1 receptor of T cells and inhibits its binding with the PD-L1 of tumour cells. When used as a monotherapy, it is the standard first-line treatment for selected patients with metastatic NSCLC presenting high PD-L1 tissue expression (≥50%) (51). The standard method to determine the levels of PD-L1 is IHC of tumour tissues, which is recommended for all patients with newly diagnosed advanced NSCLC in routine clinical practice (25). However, PD-L1 expression does not seem to be an optimal predictive biomarker since not all patients experience an effective response to ICIs based on the established selection criteria (264). Thus, the addition of pembrolizumab to platinum-based chemotherapy in patients with previously untreated advanced NSCLC has recently produced a significant improvement in survival outcomes, independent of PD-L1 expression (55,56).

The determination of PD-L1 expression in tissues is highly variable according to the time and site of biopsy, and sometimes PD-L1 expression is not detected due to the limited tissue sample. Moreover, a unique tissue biopsy may not be representative of the entire molecular landscape of the tumour, and

therefore some PD-L1-positive patients do not receive immunotherapy. The management of NSCLC with ICIs requires identification of new and reliable biomarkers to select patients who will benefit from immunotherapy while limiting ineffective therapy that may produce adverse reactions in patients (265). Liquid biopsy is a rapid and non-invasive alternative tool to obtain new biomarkers of several cancers and to monitor its evolution over time (230,266,267). CfDNA and CTCs, the most common and standardized liquid biopsy biomarkers, representing promising tools for the diagnosis, selection of ICI treatment and monitoring of patients with NSCLC receiving immunotherapy (268). Moreover, analyses using combinations of multiple liquid biopsy biomarkers are being conducted to improve the accuracy of detection (269,270). Some studies have suggested that monitoring cfDNA dynamics might help clinicians select patients with NSCLC who will benefit most from immunotherapy (270–272).

In this study, we explored the value of the cfDNA determination to anticipate the evolution of metastatic NSCLC in patients receiving first-line pembrolizumab as a monotherapy or combination therapy. In addition, we also focused our attention on CTC levels, including an analysis of the PD-L1-positive subpopulation, to complete our liquid biopsy approach. For this aim, we compared CTC enrichment technologies, such as an epitope-dependent, EpCAM-based system (CellSearch®), with an epitope-independent, microfluidic system (Parsortix). Overall, cfDNA and CTCs monitoring provides clinically relevant information to select patients who will benefit most from immunotherapy. To our knowledge, this study is the first to examine the association of combined levels of both circulating biomarkers with survival and the response to first-line pembrolizumab therapy in patients with metastatic NSCLC.

2. MATERIALS AND METHODS

2.1 Cell lines and culture

The lung cancer cell lines A549, NCI-H322 and NCI-H460 were purchased from the ATCC (ATCC® CCL-185™; Manassas, VA) and routinely cultured in the ATCC-recommended growth medium at 37 °C, 5% CO_2, and 95% humidity. Cancer cell lines were treated with 100 ng/mL interferon-gamma (IFN-γ) (Merck KGaA, Darmstadt, Germany) for 48 hours to obtain different levels of PD-L1 expression.

2.2 Patients and blood sample collection

We designed a prospective study including patients with advanced NSCLC treated with pembrolizumab as first-line therapy between June 2017 and January 2021 at the Department of Medical Oncology of Complexo Hospitalario Universitario de Santiago de Compostela. Fifty consecutive patients were recruited. Samples were collected from each patient at different time points: prior to the start of treatment (baseline) and 6 and 12 weeks after the first pembrolizumab dose (Figure 2.1). One hundred nine peripheral blood samples were obtained from patients. All individuals provided written informed consent prior to enrolling in the study, and the procedure was approved by Santiago de Compostela and Lugo Ethics Committee (Ref: 2017/538). The approved protocol was conducted according to the Declaration of Helsinki.

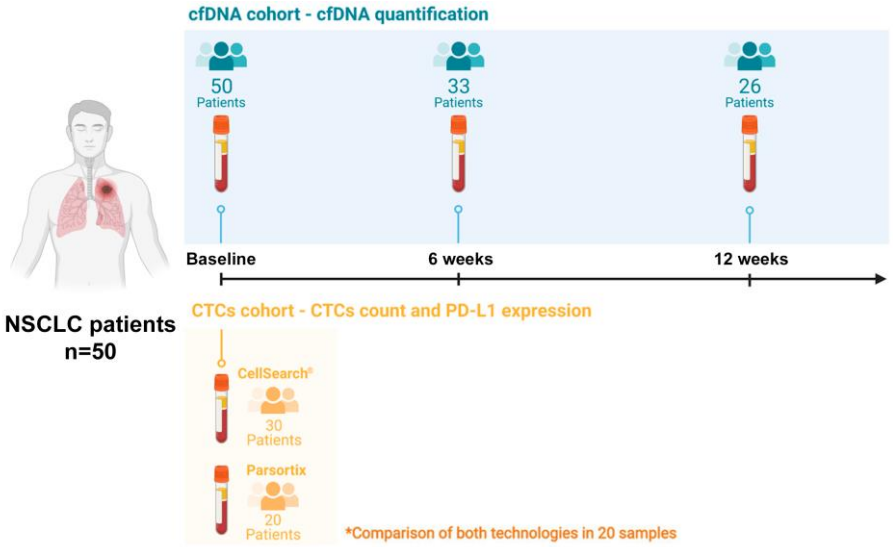

Figure 2.1. Study schema and monitoring of the patient cohort, including patient enrolment and sample collection.

The efficacy of the treatment was evaluated based on RECIST1.1 criteria as follows: complete response (CR), partial response (PR), stable disease (SDi) or progressive disease (PD). PFS was defined as the time from the date of initial treatment until the date of disease progression, death or the last follow-up if progression or death had not occurred. OS was defined as the time from the date of initial treatments until death or the last follow-up.

2.3 CfDNA isolation from plasma samples

Twenty millilitres of peripheral whole blood from patients with cancer were obtained by direct venipuncture and collected using CellSave tubes (Menarini, Silicon Biosystems, Bologna, Italy). Plasma was separated within 96 hours after blood collection through two sequential centrifugation steps (10 minutes at 1,600 g and 10 minutes at 6,000 g; both at room temperature) and then stored at -80 °C until further processing. CfDNA was extracted from 3

mL of plasma using a QIAmp Circulating Nucleic Acid Kit (Qiagen, Hilden, Germany) and a vacuum pump, according to the manufacturer's instructions.

2.4 CfDNA quantification

CfDNA yields were determined using the quantitative PCR (qPCR) method by analysing the human telomerase reverse transcriptase (*hTERT)* single copy gene (Thermo Fisher Scientific, Waltham, MA, USA), as previously reported (273). The hydrolysis probe is located on chr. 5:1253373 with an 88 bp amplicon that maps within exon 16 of the *TERT* gene. qPCR was carried out in a final volume of 20 µL consisting of 10 µL of TaqMan Universal Mastermix (Thermo Fisher Scientific, Waltham, MA, USA), 1 µL of *hTERT* hydrolysis probe and 2 µL of sample. Amplification was performed under the following cycling conditions using a QuantStudio™ 3 real-time PCR system (Thermo Fisher Scientific, Waltham, MA, USA): 50°C for 2 minutes; 95°C for 10 minutes; 40 cycles of 95°C 15 seconds and 60°C for 1 minute. Data were analysed with Quantstudio™ Design & Analysis software, version 2.5.1 (Thermo Fisher Scientific, Waltham, MA, USA).

Each plate included a calibration curve and negative controls. The calibration curve was calculated based on a dilution series of standard human genomic DNA (Roche Diagnostics, Mannheim, Germany) fragmented into 184 bp fragments using a Covaris® E220 focused ultrasonicator (Covaris, Massachusetts, USA). gDNA was fragmented in a 6x16 mm microTUBE AFA Fibre Pre-Slit Snap-Cap (Covaris, Massachusetts, USA) using the following settings: 430 seconds duration, peak incident power of 175 Watts, duty factor of 10% and 200 cycles per burst. Fragment sizes were then determined using a TapeStation 4700 (Agilent, Santa Clara, CA, USA) and High Sensitivity DNA ScreenTape® (Agilent, Santa Clara, CA, USA). Each

sample was analysed in duplicate, and the final concentration was calculated by interpolation of the mean of the quantification cycle (Cq) with the calibration curve. Values with a Cq confidence interval less than 0.95 were discarded. Moreover, only assays with R^2 values greater than 0.98 for the standard curve and with an efficiency ≥88.8% were used.

In parallel, 2 µL of the sample were employed to quantify by the fluorometric instrument Qubit 4 using the Qubit dsDNA HS Assay Kit (Thermo Fisher Scientific, Waltham, MA, USA), to compare with the cfDNA levels obtained with the qPCR assay.

2.5 Spiked experiments

The assays to evaluate PD-L1 expression on CTCs were tested using the cancer cell lines A549, NCI-H322 and NCI-H460 spiked in whole blood from the healthy volunteers recruited for this study. The protocol employed was described previously (230). Briefly, cells were trypsinized to approximately 80% confluence, and then 200 cells were added manually (with a calculated pipetting error of 10%) to a total of 7.5 mL of blood from healthy donors collected in CellSave tubes (Menarini, Silicon Biosystems, Bologna, Italy). The samples were analysed using the CellSearch® and Parsortix systems, and two tubes of the same sample were analysed with both technologies. All spiked samples were enriched within 48 hours of collection.

2.6 Analysis of PD-L1 expression on CTCs isolated using CellSearch®

A total of 7.5 mL of peripheral whole blood samples was collected in CellSave tubes (Menarini, Silicon Biosystems, Bologna, Italy) for CTC enumeration using the CellSearch® system (Menarini, Silicon Biosystems, Bologna, Italy). A CellSearch® CXC Kit (Menarini, Silicon Biosystems,

Bologna, Italy) was used for these specific experiments, including ferrofluids coated with epithelial cell-specific anti-EpCAM antibodies to immunomagnetically enrich epithelial cells; a mixture of antibodies against CKs 8, 18, and 19 conjugated to fluorescein (FLU); an anti-CD45 mAb conjugated to APC; and DAPI to fluorescently label the cells. The open 4th antibody position of the CellSearch® system was used to evaluate PD-L1 expression according to the "Guideline for the Use and Optimization of User Defined Markers: CellSearch® Epithelial Cell Kit and CellSearch® CXC Kit, version 1.0" for its optimization. We employed the anti-human B7-H1/PD-L1 PE-conjugated antibody (Cat N° FAB1561P, R&D Systems, Minneapolis, MN) at a final concentration of 20 μg/mL, as described previously (274). CTCs were identified as EpCAM^{+}, CK^{+}, CD45^{-}, and DAPI^{+}, and PD-L1 expression was recorded for each CTC (presence or absence) by comparison to the PD-L1 expression levels in the cell lines. The specificity of the staining was confirmed by the lack of signals detected with our negative cell line, A549. As positive control we employed the cell line NCI-H460 stimulated with IFN-γ.

2.7 Analyses of PD-L1 expression on CTCs isolated using the Parsortix system

A total of 7.5 mL of peripheral whole blood was collected in CellSave tubes (Menarini, Silicon Biosystems, Bologna, Italy) and loaded into a Parsortix microfluidic device (Angle Inc., Guildford, UK), as described previously (230). Briefly, CTCs were then enriched from blood samples in disposable Parsortix cassettes with a size of 6.5 mm (GEN3D6.5, Angle Inc., Guildford, UK) and at 99 mbar of pressure, according to the manufacturer's guidelines. CTCs were trapped in the Parsortix cassette due to their large size and lower compressibility than the remaining blood cells. After separation, we

fixed the sample with 4% paraformaldehyde and carried out on-cassette staining with selected antibodies according to the manufacturer's guidelines, followed by fluorescence microscopy detection (Leica DMI8, Leica Microsystems, Germany). The selected antibodies included AF 647-conjugated CD45 (35-Z6, sc-1178, Santa Cruz, CA, USA) at a final concentration of 4 μg/mL to detect white blood cells; the same anti-human B7-H1/PD-L1 PE-conjugated antibody (R&D Systems, Minneapolis, MN) used in CellSearch® systems at a final concentration of 20 μg/mL to detect PD-L1 expression; AF 488-conjugated pan-CK (A4-108-C100, EXBIO Praha, Vestec, Czech Republic) at a concentration of 1.33 μg/mL; and DAPI to fluorescently label the cells. CTCs were identified as CK+, CD45-, and DAPI+, and PD-L1 expression on CTCs was determined (presence or absence) according to the results obtained from cell line-spiked samples. We employed Leica Application Suite X (Leica Microsystems, Germany) to identify the fluorescence intensity in each single cell, and PD-L1 expression on CTCs was determined (presence or absence) according to the results obtained from cell line-spiked samples. The specificity of the staining was confirmed by the lack of signals detected with our negative cell line, A549. As positive control we employed the cell line NCI-H460 stimulated with IFN-γ.

2.8 PD-L1 immunohistochemistry and scoring

PD-L1 IHC was carried out on 4 μm sections of FFPE tumour tissue samples using Dako PD-L1 IHC 28-8 pharmaDx (Agilent, Santa Clara, CA, USA). The test was performed using the EnVision FLEX visualization system on the Dako Autostainer Link 48 and Dako PT Ling Pretreatment Module (Agilent, Santa Clara, CA, USA). A minimum of 100 viable tumour cells must be present for evaluation. PD-L1 expression was evaluated only in tumour

cells. Scoring was determined according to the tumour proportion score (TPS), which is defined as the percentage of positive viable tumour cells among all viable tumour cells evaluated. A tumour cell was defined as positive for PD-L1 staining whenever any partial or complete membranous staining was detected. The percentage of PD-L1-positive tumour cells was assessed as previously described (275). Slides were assessed independently by two pathologists.

2.9 Statistical analyses

Statistical analyses were performed using R version 4.0.2. Pearson test was used to evaluate a pairwise correlation between the different strategies to quantify the cfDNA, by fluorometry and qPCR. Spearman correlation coefficients were calculated to assess the correlation between the PD-L1 TPS and PD-L1 status of CTCs. The kappa test was used to determine the concordance with a 95% confidence interval (CI). We dichotomized the CTC PD-L1 counts as positive and negative and categorized PD-L1 expression (PD-L1 tissue expression, 80-100% vs <80%) to calculate the kappa coefficients. Receiver operating characteristic (ROC) curves were constructed, and the area under the ROC curve (AUC) with 95% CIs was obtained to evaluate the thresholds of baseline *hTERT* cfDNA levels for OS and PFS analyses. The AUC and the 95% CIs for the sensitivity and specificity were estimated using the pROC package in R software (276). Univariate and multivariate Cox regression analyses were performed using the survival package in R (277), and a Kaplan-Meier analysis was then performed. The associations of CTCs and *hTERT* cfDNA with the best response were estimated using Fisher's exact test. We also used Fisher's exact test to compare the association between CTC counts and the response to therapy.

3. RESULTS

3.1 Study population

The characteristics of the patients enrolled in the study are summarized in Table 2.1. The median age was 63.3 years (range: 45–79), and most patients were males (74%), current or former smokers (86%) and had tumours with an adenocarcinoma histology (72%). Eighty percent of patients had an ECOG PS of 1–2, and 30% of patients had more than two metastases.

Table 2.1. Demographics and clinical characteristics of the patients at baseline.

Baseline Characteristics	Patients n* (%)
Mean age (years) ± SD, range	63.3 ± 8.3, 45-79
Sex	
Female	13 (26)
Male	37 (74)
Smoking	
Smoker	31 (62)
Former smoker	12 (24)
Never	7 (14)
Histology	
Adenocarcinoma	44 (88)
Squamous cell carcinoma	4 (8)
NSCLC-NOS	2 (4)
ECOG PS	
0	10 (20)
1	34 (68)
2	6 (12)
PD-L1 expression in the tissue	
<80%	33 (66)
≥80%	17 (34)
Number of metastatic sites	
≤2	35 (70)
>2	15 (30)
Pembrolizumab treatment	
Monotherapy	37 (74)
In combination with chemotherapy	13 (26)

*n=50; Abbreviations: SD: standard deviation; NSCLC-NOS: NSCLC-not otherwise specified.

Thirty four percent of patients exhibited PD-L1 expression in the tissue at a level ≥80%, and the median number of pembrolizumab treatment cycles was 6 (range 1–35 cycles). The median PFS and OS were 10.47 and 19.13 months, respectively, in the 50 patients with NSCLC. The ORR (CR or PR during ≥6 cycles) was 46.0%, with 1 complete and 22 partial responses.

3.2 Circulating free DNA analyses

3.2.1 Quantification of cfDNA levels in NSCLC patients

A good correlation between cfDNA levels obtained by *hTERT* qPCR assay and Qubit 4 Fluorometer (Thermo Fisher Scientific, Waltham, MA, USA) was reported in our patient's cohort (R^2= 0.79; Figure 2.2). Due to the qPCR assay is more sensible and specific to measure low DNA quantities, we focused our study on this quantitative method.

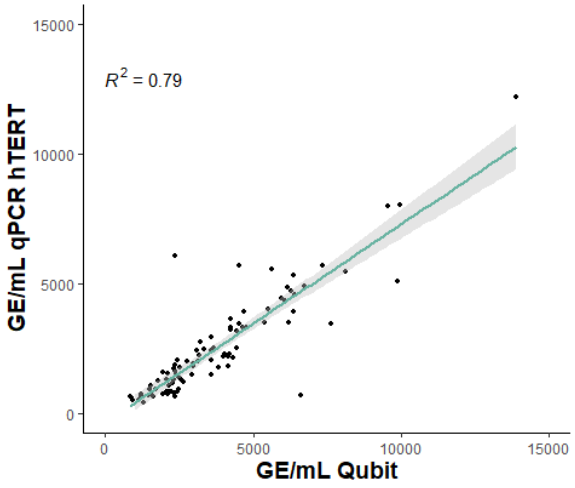

Figure 2.2. Correlation between cfDNA levels using Qubit method and qPCR assay (Pearson correlation, R^2= 0.79). Abbreviations: GE, genome equivalents.

3.2.2 Prognostic and predictive value of cfDNA levels at baseline

We next evaluated the role of cfDNA levels as a prognostic biomarker for pembrolizumab treatment outcomes in our cohort of patients with NSCLC. We employed the *hTERT* qPCR assay to determine the cfDNA levels. The cohort was dichotomized into two groups (high and low levels) according to a threshold calculated based on the baseline *hTERT* cfDNA levels observed in our cohort (Table 2.2). These levels were log10-transformed by choosing 7.665 (2132.39 genome equivalents/mL, (GE/mL) plasma) and 7.638 (2075.59 GE/mL plasma) for PFS and OS analyses, respectively, after considering sensitivity and specificity based on ROC curve analyses (Table 2.2).

Table 2.2. ROC analysis to determine the value of *hTERT* cfDNA levels to discriminate progression or death.

Parameters	AUC	Threshold	Sensitivity	Specificity
Progression free survival				
Log cfDNA at baseline	0.535	7.665	0.538	0.667
Log cfDNA at 6 weeks	0.600	7.336	0.722	0.533
Log cfDNA at 12 weeks	0.810	7.026	0.857	0.750
Overall survival				
Log cfDNA at baseline	0.650	7.638	0.640	0.720
Log cfDNA at 6 weeks	0.617	6.716	0.929	0.368
Log cfDNA at 12 weeks	0.746	7.026	0.818	0.600

Abbreviations: AUC, area under the curve.

Patients with high baseline *hTERT* cfDNA levels had a significantly shorter PFS (*p*-value <0.01; hazard ratio, 2.89; 95% CI, 1.30-6.45) and OS (*p*-value =0.005; hazard ratio, 3.26; 95% CI, 1.43-7.47) than those with low baseline levels (Figure 2.3A-B and Table 2.3). The median OS was 28.4

months in the low baseline *hTERT* cfDNA group and 4.9 months in the high baseline *hTERT* cfDNA group, whereas the median PFS was 14.6 and 5.1 months in the two cfDNA categories (low vs. high baseline levels, respectively) (Figure 2.3A-B).

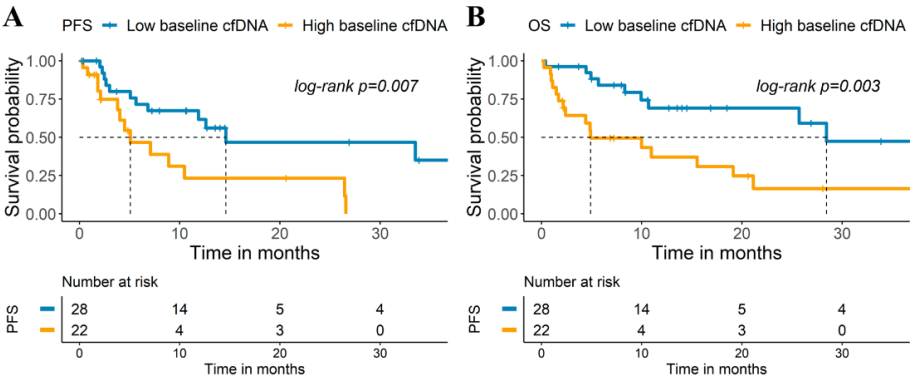

Figure 2.3. Kaplan-Meier survival analysis of *hTERT* cfDNA levels at baseline. Kaplan-Meier plots of PFS (A) and OS (B).

Considering various clinical and demographic variables (ECOG PS, sex, age, PD-L1 expression in the tissue, number of metastases and smoking status), univariate and multivariate Cox regression analyses of PFS and OS were performed (Table 2.3). In this analysis, *hTERT* cfDNA levels did not show value as an independent predictive biomarker of PFS and OS, with the number of metastases representing the main independent factor explaining the PFS rates.

Table 2.3. Univariate and multivariate Cox regression analyses of cfDNA levels, CTC counts and clinical parameters.

Variable	Univariate		Multivariate	
	***p*-value**	**HR (95% CI)**	***p*-value**	**HR (95% CI)**
Progression free survival				
Baseline log cfDNA (high vs., n=50)	0.009	2.89 (1.30-6.45)	0.80	1.18 (0.28-5.01)
Baseline CTC count, CellSearch® (≥1 vs. 0, n=30)	0.04	2.97 (1.04-8.45)	0.006	9.36 (1.88-46.6)
ECOG (≥1 vs. 0, n=50)	0.20	2.09 (0.72-6.08)		
PD-L1 expression in the tissue (≥80 vs. <80, n=50)	0.40	0.68 (0.27-1.76)		
Sex (male vs. female, n=50)	0.40	0.71 (0.32-1.57)		
Age (years, n=50)	0.60	0.99 (0.93-1.04)		
Number of metastasis (>2 vs. ≤2, n=50)	0.04	2.39 (1.03-5.55)	0.006	9.21 (1.87-45.3)
Smoking (yes vs. no, n=50)	0.40	0.68 (0.25-1.82)		
Overall survival				
Baseline log cfDNA (high vs. low, n=50)	0.005	3.26 (1.43-7.47)	0.90	1.13 (0.29-4.46)
Baseline CTC count, CellSearch® (≥1 vs. 0, n=30)	0.03	2.71 (1.11-6.64)	0.01	5.41(1.42-20.6)
ECOG (≥1 vs. 0, n=42)	0.06	4.05 (0.95-17.2)	0.70	1.51 (0.25-8.99)
PD-L1 expression in tissue (≥80 vs. <80, n=50)	0.50	1.36 (0.60-3.10)		
Sex (male vs. female, n=42)	0.70	1.18 (0.49-2.86)		
Age (years, n=42)	0.80	1.01 (0.95-1.07)		
Number of metastasis (>2 vs. ≤2, n=42)	0.005	3.12 (1.41-6.87)	0.001	9.08 (2.35-35.1)
Smoking (yes vs. no, n=42)	0.60	0.77 (0.29-2.05)		

Abbreviations: HR, hazard ratio. The levels of cfDNA were determined as low (<cut-off) or high (≥cut-off) based on the cut-off obtained from the ROC curve analyses.

3.2.3 Monitoring *hTERT* cfDNA levels and the response to therapy

We investigated the value of *hTERT* cfDNA kinetics as a prognostic biomarker during pembrolizumab treatment (Figures 2.4-2.5). cfDNA levels were quantified longitudinally, before the initiation of therapy, and at 6 and 12 weeks after the onset of pembrolizumab therapy. No significant differences were observed in the global cfDNA levels among any time point (Figure 2.4).

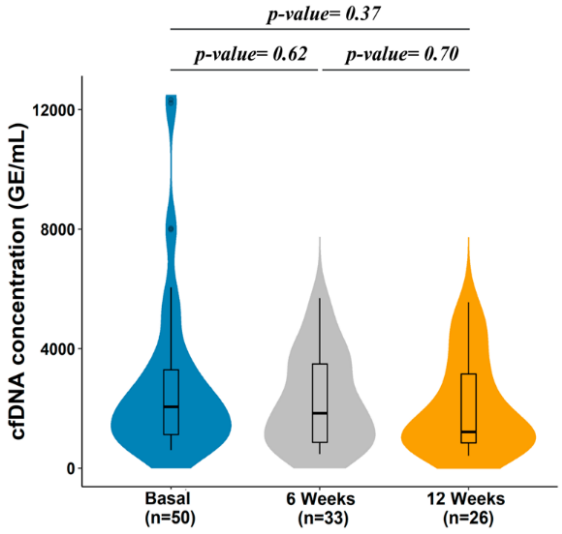

Figure 2.4. *hTERT* cfDNA levels at different time points (baseline, 6 and 12 weeks). No significant differences were found among any group (Wilcoxon test). Abbreviations: GE, genomic equivalents.

Next, we investigated the relationship between *hTERT* cfDNA levels at the different time points and the response to therapy in our patient cohort (Figure 2.5). We did not find any association between the cfDNA levels at baseline and the response to pembrolizumab therapy (Figure 2.5A).

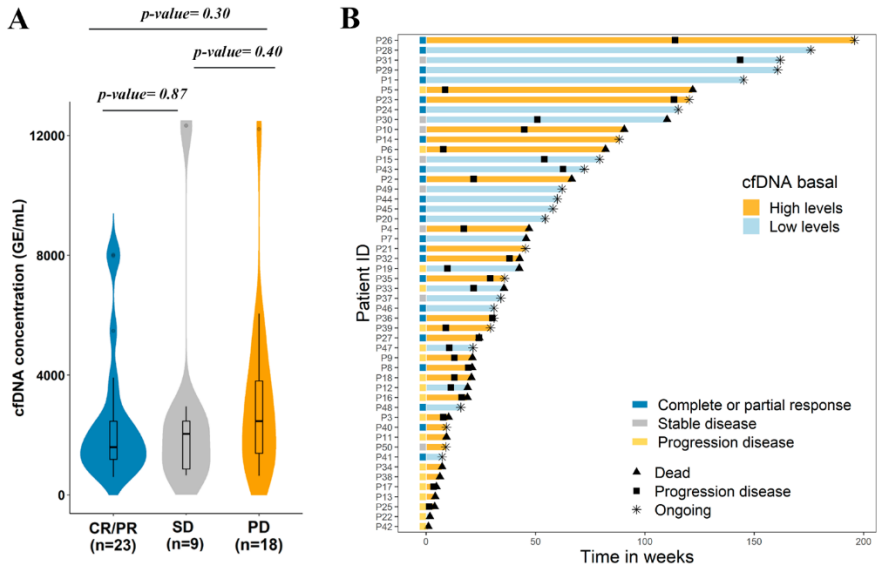

Figure 2.5. *hTERT* cfDNA levels during pembrolizumab therapy and their association with therapy response. (A) cfDNA levels at baseline according to the response to therapy. No significant associations were found (Wilcoxon test). (B) Clinical course for patients during pembrolizumab treatment. Swimmer plots for each patient (n=50) showing the levels of hTERT cfDNA at baseline (yellow colour indicates high *hTERT* cfDNA levels, and blue colour indicates low *hTERT* cfDNA levels). The total length of each bar indicates the duration of survival from start of pembrolizumab treatment. Left, squares are coloured according to the response based on RECIST1.1 criteria. Abbreviations: GE, genome equivalents; CR, complete response; PR, partial response; SDi, stable disease; PD, progression disease.

However, after considering the changes from baseline to 12 weeks, we found an association with treatment response (Figure 2.6A). We observed two patterns: an increase in *hTERT* cfDNA levels at 12 weeks (n=14) and a decrease in *hTERT* cfDNA levels at 12 weeks (n=12), with a median PFS of 6.8 months and 4.6 months, respectively (Figure 2.6B).

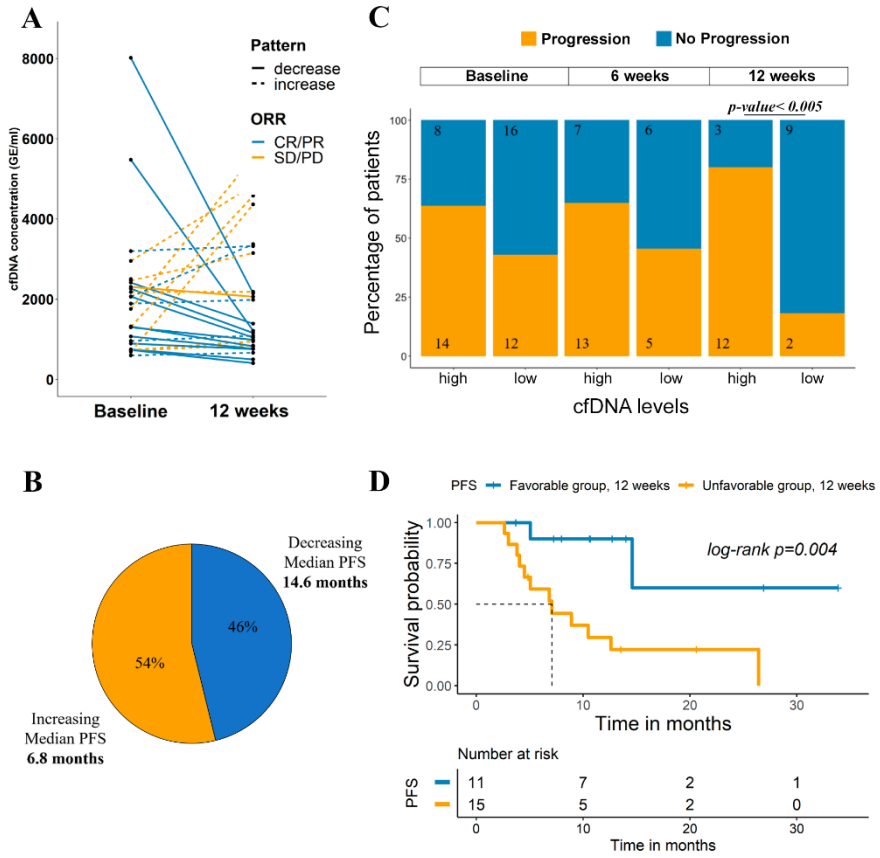

Figure 2.6. *hTERT* cfDNA changes from baseline to 12 weeks. (A) *hTERT* cfDNA concentrations for the two cfDNA patterns (increase/decrease at 12 weeks) and showing the response to therapy. (B) Percentage of patients and median PFS for each cfDNA pattern; (C) Proportion of patients with high and low levels baseline, 6 and 12 weeks. *p*-value was calculated by Fisher's exact test. (D) Kaplan-Meier plot of PFS of the favourable/unfavourable changes at 12 weeks. *Groups are composed of patients with unfavourable changes: both high hTERT cfDNA levels at baseline (cut-off ≥7.665) and at 12 weeks (cut-off ≥7.026), or low levels at baseline (cut-off <7.665) and high levels at 12 weeks (cut-off ≥7.026). The low-risk group (patients with favourable changes) is composed of patients with low hTERT cfDNA levels at baseline (cut-off <7.665) and low levels at 12 weeks (cut-off <7.026) or high levels at baseline (cut-off ≥7.665) and low levels at 12 weeks (cut-off <7.026) Abbreviations: CR/PR, complete response/partial response SDi/PD, stable disease/progression disease.

We also analysed the risk of disease progression at each time point. According to the ROC curve analysis, the thresholds of cfDNA levels at baseline, 6 weeks and at 12 weeks were chosen for the PFS analysis (Table 2.2). High levels of *hTERT* cfDNA at 12 weeks were a strong predictor of the risk of disease progression (*p*-value <0.005, odds ratio=18, 95% CI 2.5-131.3) (Figure 2.6C). Fifteen patients showed high levels at 12 weeks, and 12 of them (80%) developed progressive disease compared with 2 of the 11 patients (18.2%) with low levels. Moreover, at each time point, patients were divided into favourable and unfavourable risk groups after considering their changes in *hTERT* cfDNA levels. The median PFS was 7.07 months for the unfavourable risk group based on the changes between baseline and 12 weeks, whereas median PFS was not reached for the favourable risk group (*p*-value <0.01; hazard ratio, 6.8; 95% CI, 1.5-30.5) (Figure 2.6D).

3.3 Circulating tumour cell analyses

3.3.1 EpCAM-dependent versus antigen-independent CTC isolation to quantify CTCs and characterize the PD-L1 status

In addition to monitoring *hTERT* cfDNA levels, we analysed CTC levels, as they represent a more biological feature of the tumour. Therefore, we evaluated two different technologies, the EpCAM-based CellSearch® system and the label-independent microfluidic Parsortix system, to quantify CTCs and assess the expression of PD-L1 and to determine the advantages of non-EpCAM-dependent isolation method. First, we categorized the presence or absence of PD-L1 on single CTCs to grade its expression in each cell line (with known gradual increases in PD-L1 protein expression) using both approaches. To set up both approaches, we used preserved blood samples from healthy controls spiked with three lung cancer cell lines (A549, *no expression*;

NCI-H322, *low-medium expression*; and NCI-H460, *medium-high expression*) representative of the variability of PD-L1 expression (Figure 2.7 and Figure 2.8).

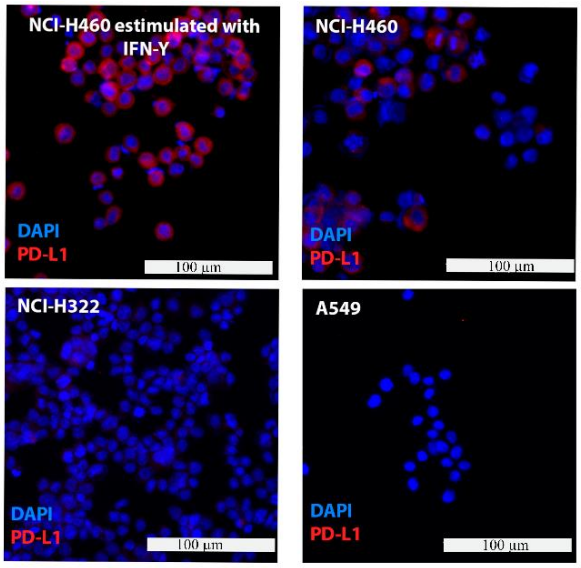

Figure 2.7. Immunofluorescence characterization of PD-L1 in cancer cell lines. We used three lung cancer cell lines with different grade of PD-L1 expression (NCI-H460, medium-high expression, NCI-H322, low-medium expression and A549, no expression). Scale bar represents 100 µm.

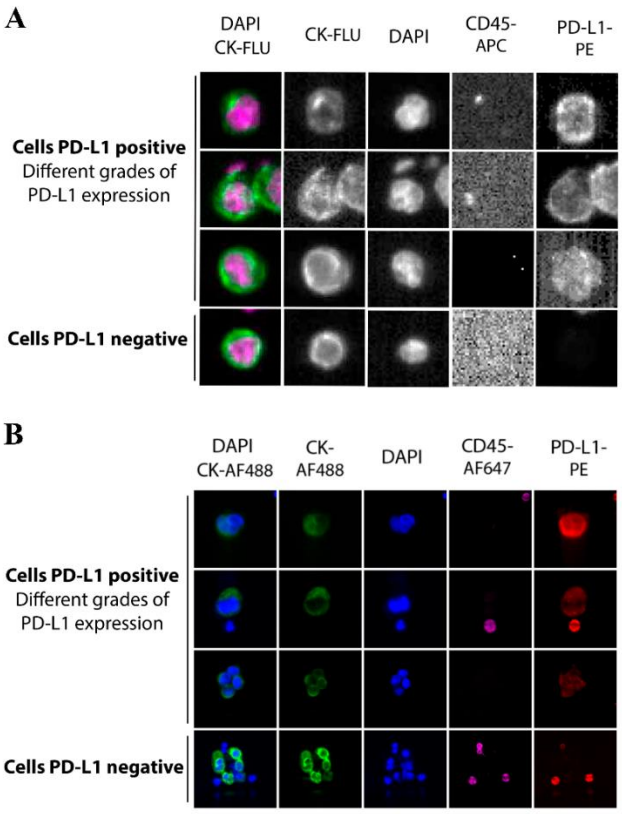

Figure 2.8. (A-B) Detection of PD-L1 expression after spiking cancer cells lines in healthy blood and analyse them with the CellSearch® and Parsortix systems, respectively and representative images of different grades of PD-L1 expression. NCI-H460 stimulated with IFN-γ shown high expression, NCI-H460 medium expression, NCI-H322, low-medium expression and A549, no expression.

Next, peripheral blood samples were collected from patients prior to treatment to analyse the presence of CTCs and their PD-L1 expression (Figure 2.9) as potentially valuable prognostic and predictive biomarkers.

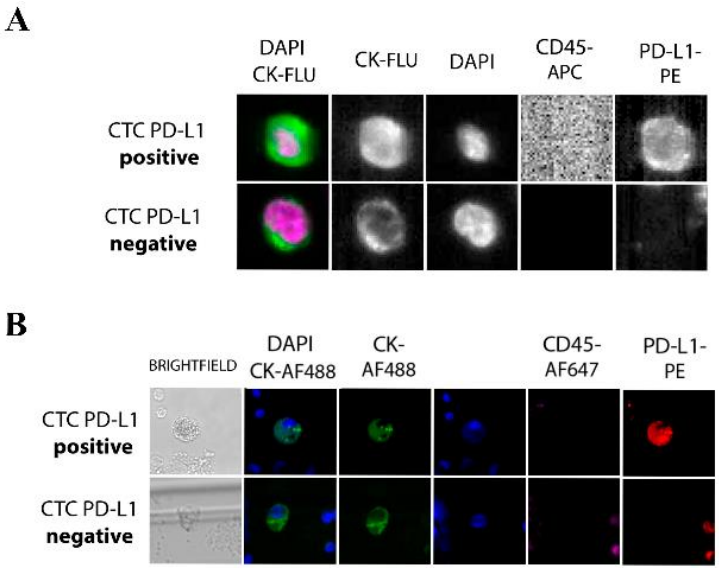

Figure 2.9. (A) Representative images of CTCs detected with the CellSearch® system in patients with NSCLC. Samples were subjected to immunostaining with DAPI, CD45 (APC), CKs (FLU) and PD-L1 (PE). (B) Representative images of CTCs detected with the Parsortix system in patients with NSCLC. Samples were subjected to immunostaining with DAPI, CD45 (AF647), CKs (AF488) and PD-L1 (PE).

In 20 patients' blood samples, we compared CTC enumeration using both strategies (CellSearch® and Parsortix systems) and evaluated the performance and concordance between them (Figure 2.10 and Table 2.4). Using the CellSearch® system, we detected ≥1 CTC in 50% (10/20) of samples (range 1-168; mean = 9.8), while using the Parsortix system, 35% (7/20) of samples had ≥1 CTC (range 1-56; mean = 4.7). Regarding the capacity to detect PD-L1 expression in CTCs, we detected PD-L1-positive CTCs in 2/17 samples (in 2/10 samples with CTCs) using the CellSearch® system. Compared to the label-independent system, we observed PD-L1-positive CTCs in 7/20 samples (in 7/7 samples with CTCs) using the Parsortix system. When we compared the concordance of both technologies, we found that kappa scores for the number of CTCs and PD-L1-positive CTCs presented negative values for both

technologies (-0.1 and 0.14, respectively), showing no correlation between them.

Table 2.4. Circulating tumour cells enumeration and PD-L1 analysed using CellSearch® and Parsortix systems.

Sample ID	Parsortix System		CellSearch® System	
	CTCs number*	PD-L1+ CTCs number* (%)	CTCs number*	PD-L1+ CTCs number* (%)
id1	9	5 (55.55)	0	0 (0.00)
id2	13	9 (69.23)	0	0 (0.00)
id3	8	6 (75.00)	0	0 (0.00)
id4	2	1 (50.00)	5	NT
id5	5	5 (100.00)	3	NT
id6	0	0 (0.00)	2	NT
id7	0	0 (0.00)	0	0 (0.00)
id8	0	0 (0.00)	4	0 (0.00)
id9	0	0 (0.00)	2	0 (0.00)
id10	0	0 (0.00)	0	0 (0.00)
id11	56	18 (32.14)	168	7 (4.16)
id12	0	0 (0.00)	1	0 (0.00)
id13	0	0 (0.00)	6	0 (0.00)
id14	0	0 (0.00)	1	1 (100.00)
id15	0	0 (0.00)	0	0 (0.00)
id16	1	1 (100.00)	0	0 (0.00)
id17	0	0 (0.00)	0	0 (0.00)
id18	0	0 (0.00)	3	0 (0.00)
id19	0	0 (0.00)	0	0 (0.00)
id20	0	0 (0.00)	0	0 (0.00)
id21	NT	NT	0	0 (0.00)
id22	NT	NT	0	0 (0.00)
id23	NT	NT	0	0 (0.00)
id24	NT	NT	0	0 (0.00)
id25	NT	NT	1	NT
id26	NT	NT	0	0 (0.00)
id27	NT	NT	0	0 (0.00)
id28	NT	NT	0	0 (0.00)
id29	NT	NT	0	0 (0.00)
id30	NT	NT	0	0 (0.00)

*Total CTCs count in 7.5mL of peripheral blood. Abbreviations: NT, not tested.

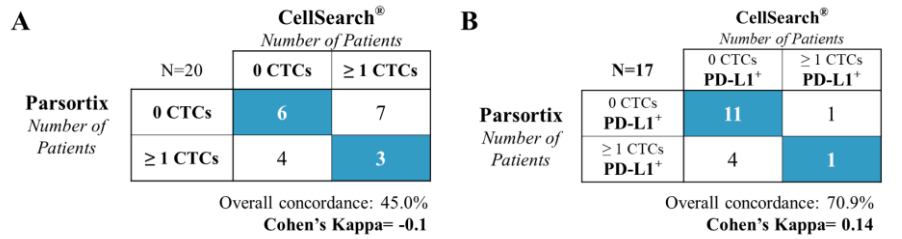

Figure 2.10. Correlation of PD-L1 positivity between tumour tissues (by tumour proportion scores) and CTCs with the CellSearch® (A) and Parsortix systems (B).

3.3.2 Correlation of the PD-L1 status in CTCs and tissue samples

We also compared the PD-L1 status of CTCs using CellSearch® and Parsortix systems with PD-L1 expression in the primary tumour biopsy obtained at the initial diagnosis (Figure 2.11). The mean time between tissue biopsy and liquid biopsy sample collection was 38.6 days (range 9-78). Nevertheless, the PD-L1 TPS in biopsies did not correlate with the percentage of PD-L1-positive CTCs at the initial diagnosis (*p*-value =0.476 and *p*-value =0.881 for the CellSearch® and Parsortix systems, respectively).

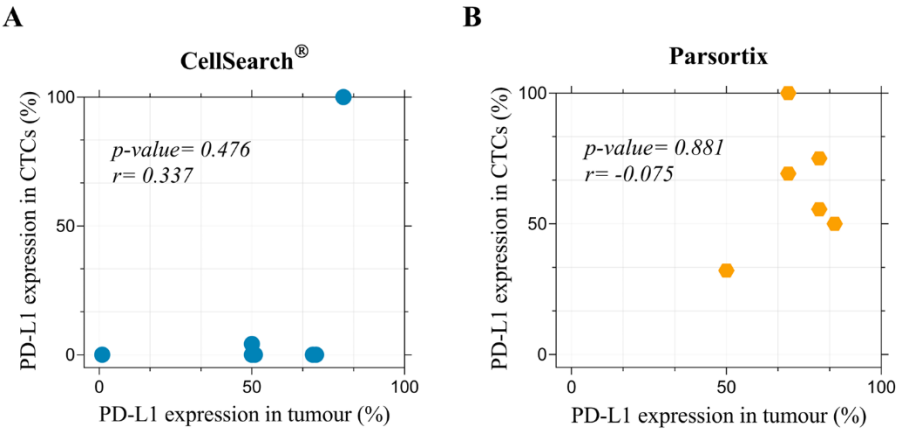

Figure 2.11. Correlation of PD-L1 positivity between tumour tissues (by tumour proportion scores) and CTCs with the CellSearch® (A) and Parsortix systems (B).

3.3.3 Prognostic and predictive values of CTC enumeration at baseline

We evaluated the role of CTC enumeration in prognosticating disease progression in response to pembrolizumab treatment in our cohort of patients with advanced NSCLC. For this purpose, we performed CTC enumeration at baseline in 30 patients using the CellSearch® system and 20 patients using Parsortix. Patients with CTCs identified using the CellSearch® system had significantly shorter PFS and OS than patients who had no CTCs (*p*-value <0.05) (Figure 2.12A-B). The median PFS was 12.6 and 3 months in the two groups (0 vs. ≥1 CTC, respectively). The median OS of the CTC-positive group was 4.9 months, whereas the median OS was 21.13 months for the CTC-negative group. In the multivariate regression analysis (Table 2.3), we confirmed that CTC positivity using the CellSearch® system was an independent predictive biomarker of PFS and OS (hazard ratio, 5.75; 95% CI, 1.35-24.5 *p*-value <0.05 and hazard ratio, 4.59; 95% CI, 1.32-16.0; *p*-value <0.05, respectively). We observed no significant results for PFS or OS when analysing CTC counts with the Parsortix system and evaluating PD-L1-positive CTCs, regardless of the technology employed (CellSearch® and Parsortix systems).

In addition, we also investigated the relationship between the CTC counts detected using both approaches and the response to pembrolizumab therapy in our patient cohort. Significant differences were observed between the CTC count detected with the CellSearch® system and the achievement of a complete or partial response and disease progression (*p*-value <0.05) (Figure 2.11C).

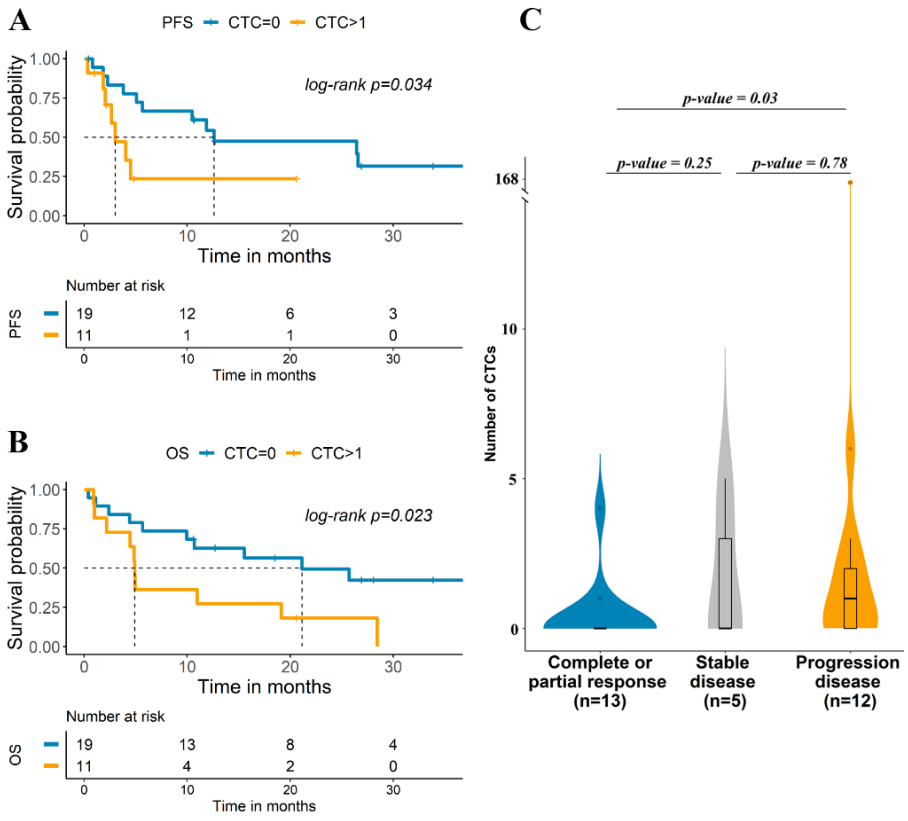

Figure 2.12. Kaplan–Meier survival analysis of CTCs at baseline. Kaplan–Meier plots of PFS (A) and OS (B). (C) Comparison of the response to pembrolizumab based on CTC detection using CellSearch®. *p*-value was calculated by Fisher's exact test.

The ORR was similar between patients with undetectable CTCs compared with patients with detectable PD-L1-positive or PD-L1-negative CTCs using CellSearch® and Parsortix technologies (Table 2.5).

Table 2.5. Comparison of the CTCs levels according to the response to therapy.

CTCs	CR *n (%)*	PR *n (%)*	SDi *n (%)*	PD *n (%)*	ORR *n (%)*
CellSearch® n=30					
Undetectable CTCs, n=19	1 (5.26)	10 (52.6)	3 (16.7)	5 (15.8)	11 (57.9)
Detectable CTCs n=11	0 (0.0)	2 (18.2)	2 (18.2)	7 (63.6)	2 (18.2)
*CTCs-PDL1-negative, n=6**	0 (0.0)	1 (16.7)	1 (16.7)	4 (66.7)	1 (16.7)
*CTCs-PDL1-positive, n=2**	0 (0.0)	1 (50.0)	0 (0.0)	1 (50.0)	1 (50.0)
Parsortix n=20					
Undetectable CTCs, n=13	0 (0.0)	4 (30.8)	2 (15.4)	7 (53.9)	4 (30.8)
Detectable CTCs n=7	0 (0.0)	2 (28.6)	1 (14.3)	4 (57.1)	2 (28.8)
CTCs-PDL1-negative, n=5	0 (0.0)	2 (40.0)	1 (20.0)	2 (40.0)	2 (40.0)
CTCs-PDL1-positive, n=7	0 (0.0)	2 (28.6)	1 (14.3)	4 (57.1)	2 (28.6)

Objective response ratio (ORR): complete response and partial response during ≥6 cycles. *The detection of PD-L1 expression on CTCs using CellSearch® system was unrealizable in 4 patients. Abbreviations: CR, complete response; PR, partial response; SDi, stable disease; PD, progression disease; ORR: objective response rate.

3.4 Clinical potential of combined CTC and cfDNA analyses

Finally, we evaluated the joint effect of baseline CTC counts using the CellSearch® system and *hTERT* cfDNA levels. First, we considered three risk subgroups: (1) CTCs <1 and low cfDNA baseline levels; (2) CTCs <1 and high cfDNA baseline levels or CTCs ≥1 and low cfDNA baseline levels; and (3) CTCs ≥1 and high cfDNA baseline levels. Multivariate Cox analyses confirmed that the combined analyses of CTCs using the CellSearch® system and *hTERT* cfDNA levels were independent predictive biomarkers of PFS (*p*-value <0.01; hazard ratio, 11.6; 95% CI, 2.04-66.1; *p*-value <0.05; hazard ratio, 14.3; 95% CI, 1.7-117) (Table 2.6).

Table 2.6. Univariate and multivariate Cox regression analyses of combined changes in CTCs and cfDNA levels.

Variable	Univariate		Multivariate	
	***p*-value**	**HR (95% CI)**	***p*-value**	**HR (95% CI)**
Progression free survival				
Group 1 (CTCs <1 and low cfDNA, n=12)	-	Reference	-	-
Group 2 (CTCs <1 and high cfDNA or CTCs ≥1 and low cfDNA, n=10)	0.005	5.37 (1.66-17.4)	0.009	13.1 (1.91-90.1)
Group 3 (CTCs ≥1 and high cfDNA, n=8)	0.05	4.12 (0.98-17.4)	0.01	14.5 (1.76-119)
Overall survival				
Group 1 (CTCs <1 and low cfDNA, n=12)	-	Reference		
Group 2 (CTCs <1 and high cfDNA or CTCs ≥1 and low cfDNA, n=10)	0.14	2.33 (0.76-7.15)	0.50	1.90 (0.33-11.0)
Group 3 (CTCs ≥1 and high cfDNA, n=8)	0.02	4.24 (1.29-14.0)	0.01	6.39 (1.37-29.8)

*Multivariate Cox regression model including sex, age, ECOG PS, PD-L1 expression in the tissue, number of metastases and smoking status. The levels of cfDNA were determined as low (<cut-off) or high (≥cut-off) based on the cut-off (7.665 for PFS and 7.638 for OS) obtained from the ROC curve analyses. Abbreviations: HR, hazard ratio.

Subsequently, we considered only two risk subgroups to simplify the analysis: (A) CTCs <1 and low cfDNA baseline levels; (B) CTCs <1 and high cfDNA baseline levels or CTCs ≥1 and low cfDNA baseline levels or CTCs ≥1 and high cfDNA baseline levels. Patients from subgroup A (undetectable CTCs using CellSearch® and low cfDNA levels) had significantly longer PFS (*p*-value <0.01; hazard ratio, 4.99; 95% CI, 1.6-15.6) and OS (*p*-value <0.05; hazard ratio, 2.9; 95% CI, 1.1-8.1) than patients from subgroup B (Table 2.7).

Table 2.7. Univariate and multivariate Cox regression analyses of combined changes in CTCs and cfDNA levels and clinical parameters.

Variable	Univariate		Multivariate	
	***p*-value**	**HR (95% CI)**	***p*-value**	**HR (95% CI)**
Progression free survival				
Group A (CTCs <1 and low cfDNA, n=12)	-	Reference	-	-
Group B (Other combinations, n=18)	0.006	4.99 (1.60-15.6)	0.005	13.6 (2.17-85.3)
Overall survival				
Group A (CTCs <1 and low cfDNA, n=12)	-	Reference	-	-
Group B (Other combinations, n=18)	0.04	2.91 (1.05-8.07)	0.05	4.02 (0.97-16.6)

*Multivariate Cox regression model including sex, age, Eastern Cooperative Oncology Group Performance Score, PD-L1 expression in the tissue, number of metastases and smoking status. Abbreviations: cfDNA, circulating free DNA; CTC, circulating tumour cell; ECOG, Eastern Cooperative Oncology Group Performance Score; HR, hazard ratio. The levels of cfDNA were determined as low (<cut-off) or high (≥cut-off) based on the cut-off (7.665 for PFS and 7.638 for OS) obtained from the ROC curve analyses.

The median PFS was not reached in group A (low cfDNA levels and undetectable CTCs at baseline), whereas the median PFS was 4.0 months in group B. Similarly, the median OS was not reached in group A, whereas the median OS was 4.9 months in group B (Figure 2.13A-B). Overall, the hazard ratios and *p*-values that emerged from the univariate and multivariate Cox analyses suggest a combinatory effect of both markers as early predictors of disease progression (Table 2.7).

Additionally, patients with CTCs identified using the CellSearch® system and high cfDNA levels at baseline showed a trend towards a poorer response to pembrolizumab therapy (Figure 2.13C).

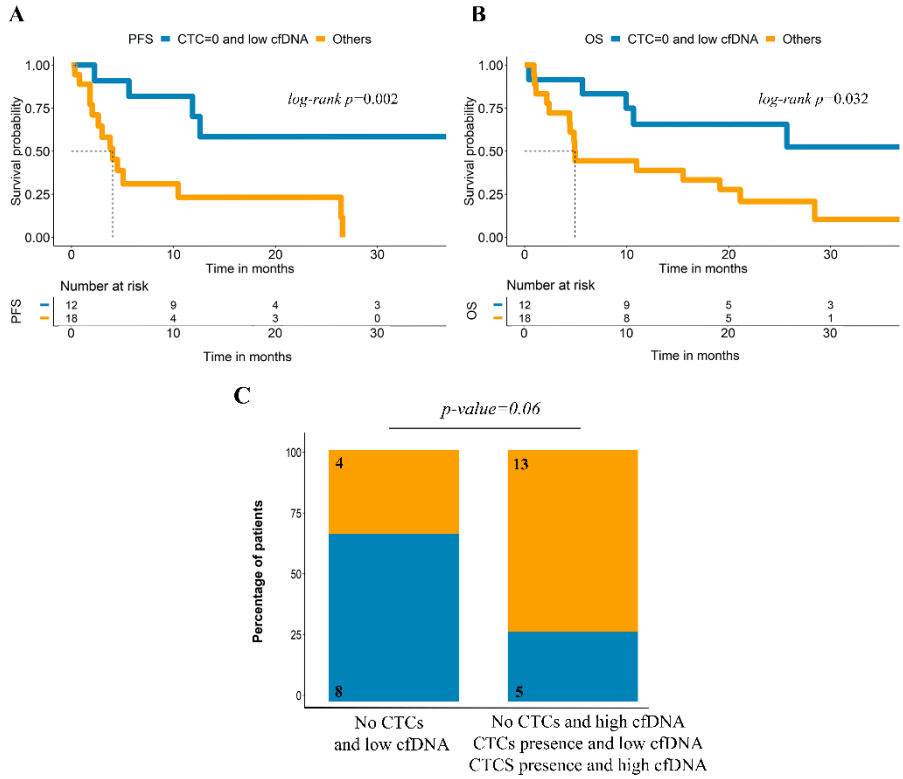

Figure 2.13. CTCs and hTERT cfDNA levels correlate with the prognosis of patients with NSCLC treated with pembrolizumab and the response of therapy. (A) Kaplan-Meier survival plot of PFS based on the combination of cfDNA and CTC levels at baseline. (B) Kaplan-Meier survival plot of OS based on the combination of cfDNA and CTC levels at baseline. (C) ORR in patients with low cfDNA levels and undetectable CTCs (n=12) versus patients with high cfDNA levels and undetectable CTCs or low cfDNA levels and detectable CTCs or high cfDNA levels and detectable CTCs (n=18).

4. DISCUSSION

Liquid biopsy represents a promising tool for the diagnosis, selection, and monitoring of response to ICI treatment in the context of NSCLC. Currently, PD-L1 is the best studied biomarker for ICI treatment selection, exhibiting a higher probability of response with higher expression of PD-L1

(268). In patients with advanced NSCLC and PD-L1 expression of at least 50% of tumour cells, pembrolizumab results in significantly longer PFS and OS (51), and thus, the determination of PD-L1 expression in tissue samples is the reference factor for the selection of ICI treatments. However, in clinical practice, patients with high levels of PD-L1 may not respond to ICI treatment; in contrast, in the absence of PD-L1, a clinical benefit may be obtained from the use of PD-1 or PD-L1 checkpoint inhibitors (268). A high TMB, which is associated with high levels of neoantigens, represent another potential candidate biomarker that would drive the choice of treatment (51), although this biomarker has not been translated into the clinic due to conflicting results among studies (278–283). Notably, these two markers have been mainly examined in tissue samples.

In the present study, we analysed the value of *hTERT* cfDNA and CTC analyses as potential prognostic and predictive non-invasive biomarkers to discriminate patients who will benefit from ICIs. We explored the clinical value of monitoring *hTERT* cfDNA levels and detected the presence of CTCs, including PD-L1 characterization, in a homogeneous cohort of patients with metastatic NSCLC receiving first-line treatment with pembrolizumab as a monotherapy or in combination with chemotherapy.

CfDNA has already been proposed as a prognostic and predictive biomarker in NSCLC (284–286), but few studies have reported the cfDNA concentration as a predictive marker of the immunotherapy response. Although cfDNA represents promising material, standardized protocols for the processing and total quantification are still missing (287). In our work, we propose the qPCR method for quantify *hTERT* cfDNA due to it is a sensitivity and cost-effective assay and based on previous results obtained in lung cancer patients (270,273,288). Alama et al. (270) reported that patients with NSCLC

who were treated with a 2nd or higher line of nivolumab and with cfDNA level below their cohort median values survived significantly longer than those with a cfDNA level above this threshold. In another study, patients with NSCLC treated mainly with second-line therapy with nivolumab and with low ctDNA concentrations at the first evaluation showed a long-term benefit (271). Notably, numerous studies have described the presence of somatic mutations in plasma cfDNA and their association with tumour response and survival (289–291). Recently, an early decrease or total clearance of ctDNA levels after pembrolizumab administration identified subsets of patients with advanced solid tumours who had a good prognosis (292,293), regardless of the tumour type, PD-L1 status or TMB. In a previous study, changes in the ctDNA concentration were reported as a predictor of a durable response in patients treated with anti-PD-1 drugs (294), where the persistence of ctDNA exerted a detrimental effect. Goldberg et al. also suggested that cfDNA levels may be an early marker of therapeutic efficacy (295), predicting prolonged survival in patients treated with immune checkpoint inhibitors for NSCLC. Based on these findings, serial ctDNA analyses could serve as a generalizable monitoring strategy for patients treated with ICIs, but researchers have not clearly determined whether this approach is transferable to cfDNA, which is clearly easier to analyse.

Regarding the on-treatment cfDNA levels, data are scarce, although cfDNA levels appear to be decreased in response to effective treatments (296–298). Our study prospectively evaluated the value of *hTERT* cfDNA kinetics as a prognostic biomarker during pembrolizumab treatment. Patients with NSCLC presenting high *hTERT* cfDNA levels at baseline or unfavourable changes from baseline to 12 weeks had a significantly greater risk of disease progression. Importantly, although the concentration of cfDNA can vary

among individuals, depending on physiological factors and tumour characteristics (299,300), the cfDNA analysis has clear advantages compared with the ctDNA determination, such as its feasibility, low detection cost and reproducibility. Therefore, our results reinforced the potential to monitor *hTERT* cfDNA dynamics in patients with NSCLC treated with ICIs, providing a simple tool to better anticipate the response to treatment.

We also investigated CTC levels using two CTCs enrichment technologies, the EpCAM-based CellSearch® system and the microfluidic epitope-independent-based method Parsortix system to complete our liquid biopsy approach. The Parsortix system uses a combination of size-based and microfluidic-based enrichment approaches to separate CTCs from blood samples and solve the dependence on a single biomarker, EpCAM, in this case, allowing the detection of CTCs with a more mesenchymal phenotype. In our study, the detection rate using the CellSearch® system (50%) was higher than that using the Parsortix system (35%), and many differences at the individual level were observed when comparing the results of both strategies for the same patient, reinforcing the isolation of different CTC types with both technologies.

In a previous comparative study of patients with NSCLC, Janning et al. reported a higher detection rate using the Parsortix than the CellSearch® system in patients with NSCLC receiving different therapy regimens (301), attributing the difference to the heterogeneity and low EpCAM expression of some CTCs and therefore to the inability of EpCAM-based CellSearch® to detect certain subpopulations. Our cohort was a more homogeneous cohort, with patients naive to previous treatments. This last factor can favour the epithelial characteristics of CTCs, since the EMT is induced as a result of drug resistance in NSCLC (302–305). However, we analysed only CK-positive

CTCs in combination with PD-L1; therefore, we were unable to make a firm statement in this regard. Despite previous works showed good recovery rates in cell lines and patients using Parsortix system (230,301,306), some methodological aspects can be impacting on the CTCs enumeration in our cohort. For instance, we used CellSave Preservative tubes which contain fixative reagents that can modify the deformability properties of the cells. Besides the staining protocol differs from previous publications (301), that described a higher detection rate using the Parsortix system in NSCLC.

Among the CTC population, we focused our attention on the PD-L1-positive subpopulation, which represents treatment targets. Although our data show that the determination of the PD-L1 status is feasible in CTCs from patients with NSCLC, we found that the PD-L1 status of CTCs does not correlate with the PD-L1 expression characterized in tissue samples or with the response to the treatment, regardless of the method employed. Despite of the lack of prognostic value of PD-L1 expression on CTCs obtained using both approaches, most of the CTCs isolated using the Parsortix system were PD-L1 positive (100% of patients with CTCs), while only 20% of samples with CTCs contained PD-L1-positive CTCs using the CellSearch® system. Thus, the epitope-independent-based Parsortix system showed a high recovery rate of PD-L1-positive CTCs, probably associated with a more mesenchymal phenotype of CTCs isolated with this EpCAM independent strategy. The use of CTCs and their potential to analyse PD-L1 expression has already been reported in patients with NSCLC (301,307–313), including the study by Janning, but their significance is not yet clear (314). The lack of concordance and contradictory results between the presence of PD-L1 in tissue and the percentage of PD-L1-positive CTCs have also been reported (301,307,308,311,313,315)(315). Importantly, in most studies assessing PD-

L1 expression in CTCs, different antibodies and CTC enrichment technologies have been used, which might partially explain the discrepancy.

Another important point is that CTCs originate from different tumour locations with different PD-L1 patterns (316), and tissue comparisons have been performed mainly with the primary tumour. Importantly, in our study, no association of PD-L1 expression on CTCs, such as prognostic or predictive biomarkers, was found. Despite the lack of clinical impact found for PD-L1-positive CTCs, the global CTC count at baseline determined using the CellSearch® system was significantly associated with PFS and OS, as previously described in patients treated with chemotherapy (174) and in patients receiving ICI treatment using the CellSearch® system or other technologies (268). Our results revealed a greater effect of the main epithelial circulating population in patients with NSCLC, since the CTC count determined using a non-EpCAM-dependent strategy failed to show any association with the patients' outcomes.

Finally, our study represents a pioneering approach combining CTC count and cfDNA levels to predict the response of patients with NSCLC to 1st line pembrolizumab treatment. We observed that patients with NSCLC presenting ≥1 CTC detected with the CellSearch® system and high levels of *hTERT* cfDNA at baseline had a significantly higher risk of disease progression during pembrolizumab treatment. Our results are consistent with a previous report focused on the prognostic role of these two easy-to-measure biomarkers in patients with metastatic NSCLC receiving nivolumab (270). These results confirmed the value of combining different circulating biomarkers to reach a higher prognostic and predictive accuracy and better discriminate the patients who will benefit most from ICI treatment, in addition to PD-L1 status.

On the other hand, several limitations in our design should be considered, which precludes us from drawing solid conclusions. First, we used different antibodies to analyse PD-L1 expression in CTCs and tumours, since the standard procedure was applied in tissue samples, while we used another antibody with CellSearch® and Parsortix. Second, we did not perform CTCs monitoring during therapy in our NSCLC cohort, which could provide more valuable information. Third, *hTERT* amplification has been reported in different cancer types, including lung cancer (317,318). Although the percentage of NSCLC patients with this alteration is very low (around 5-10% of lung cancer patients), we cannot exclude an over-estimation of the cfDNA content in a low percentage of the cases analysed due to a potential amplification. In addition, the sample size of the combined cohort was relatively small.

5. CONCLUSIONS

In summary, the study served to establish the best strategy to monitor PD-L1 expression on CTCs from patients with advanced NSCLC. In addition, our results revealed that the combination of baseline CTCs and *hTERT* cfDNA levels is significantly associated with PFS and the response to pembrolizumab therapy in patients with metastatic NSCLC. Notably, using our approach, we were able to identify a subgroup of patients who were negative for CTCs, presented low levels of *hTERT* cfDNA, who particularly benefited from the treatment. Early evaluation of the response to immunotherapy might enable clinicians to decide if the clinical benefit is sufficient to continue treatment, avoiding unnecessary toxicities and costs.

CHAPTER III

Plasma total circulating free DNA and circulating tumour cells as prognostic biomarkers in small cell lung cancer patients.

Plasma circulating free DNA and circulating tumour cells as prognostic biomarkers in small cell lung cancer patients.

This chapter has been adapted from a recently published article entitled "Plasma cell-free DNA and CTCs as prognostic biomarkers in small cell lung cancer patients" (319).

Patricia Mondelo-Macía[1,2], Jorge García-González[3,4,5], Alicia Abalo[1], Manuel Mosquera-Presedo[2], Santiago Aguín[3,4], María Mateos[3,4], Rafael López-López[3,4,5], Luis León-Mateos[*3,4,5], Laura Muinelo-Romay[*1,5], and Roberto Díaz-Peña[*1,6].

[1] *Liquid Biopsy Analysis Unit, Translational Medical Oncology (Oncomet), Health Research Institute of Santiago (IDIS), Santiago de Compostela, Spain.*
[2] *University of Santiago de Compostela (USC), Santiago de Compostela, Spain.*
[3] *Department of Medical Oncology, Complexo Hospitalario Universitario de Santiago de Compostela (SERGAS), Santiago de Compostela, Spain.*
[4] *Translational Medical Oncology (Oncomet), Health Research Institute of Santiago (IDIS), Santiago de Compostela, Spain.*
[5] *Centro de Investigación Biomédica en Red de Cáncer (CIBERONC), Madrid, Spain.*
[6] *Laboratory of Cellular and Molecular Pathology, Institute of Biomedical Sciences, Faculty of Health Sciences, Universidad Autónoma de Chile, Talca, Chile.*

[*] *Corresponding / These authors contributed equally to this work.*

Plasma circulating free DNA and circulating tumour cells as prognostic biomarkers in small cell lung cancer patients.

ABSTRACT

Background: Lack of biomarkers for treatment selection and monitoring in SCLC patients together with limited therapeutic options, result in poor outcomes. Therefore, new prognostic biomarkers are needed to improve their management. The prognostic value of cfDNA and CTCs have been less explored in SCLC.

Methods: We quantified cfDNA in 46 SCLC patients at different times during first-line of chemotherapy or chemo-immunotherapy. Moreover, CTCs were analysed in 21 patients before therapy onset using CellSearch® system. The possible association between both biomarkers and patients' outcomes was investigated to develop a prognostic model.

Results: High cfDNA levels before therapy were associated with shorter PFS and OS. Furthermore, cfDNA levels at 3 weeks and at progression disease were also associated with patients' outcomes. Multivariate analyses confirmed the independence of cfDNA levels as a prognostic biomarker. Finally, the three-risk category prognostic model developed included ECOG PS, sex and baseline cfDNA levels was associated with a higher risk of progression and death.

Conclusions: We confirmed the prognostic utility of cfDNA quantitative analysis in SCLC patients before and during therapy. Our novel risk

prognostic model in clinical practice will allow to identify patients who could benefit with actual therapies.

Keywords: Small cell lung cancer; liquid biopsy; circulating free DNA; circulating tumour cells; prognostic biomarkers.

1. INTRODUCTION

SCLC, which accounts for 15% of all lung cancer cases, is characterized by its aggressiveness, its strong association with tobacco and the poor outcome. About 70% of patients present extensive disease where only 2% survive 5 years after diagnosis (17,320,321). For many years, chemotherapy was the unique option to treat this tumour type. However, the scenario has changed in the last years (321). New therapies, such as immunotherapy, have been recently incorporated into the management of SCLC patients and, although some survival improvements have been reported in the patients with ED-SCLC (92–96), the majority of them do not benefit from this new treatment (322). The genomic profile of SCLC is characterized by extensive chromosomal rearrangements and a high mutational burden, including in nearly all, inactivation of the tumour suppressor genes *TP53* and *RB1* (81). However, nowadays the selection of treatment in SCLC patients is not dependent on the characteristics of the tumour (323), and the criteria to stratify patients is not clear, since no predictive biomarkers have been validated for the clinical practice (324). In this context, the use of liquid biopsies as a tool to guide treatment and/or for monitoring the patients' response represent a valuable alternative (325,326).

CtDNA, derived from tissue tumour cells, has demonstrated its clinical utility and represents a promising tool for guiding precision medicine in several cancer types (149,327). In SCLC, different studies have investigated the importance and the clinical value of analysing ctDNA levels. However, due to driver mutations known in SCLC are limited to *RB1* and *TP53* genes (3), arise conclusions are not easy. In contrast, total circulating free DNA (cfDNA) consists of a heterogeneous and complex DNA fraction released in

body fluids by any cell type through cell death mechanisms (138,150). The short half-life of cfDNA enables real-time monitoring for response or relapse, being an easy-to-implement biomarker to monitor cancer evolution and response to therapy (137). In fact, in lung cancer and other solid tumours, cfDNA analysis has been explored as a prognostic marker and surrogate for monitoring treatment response (328,329). High cfDNA level or positive ctDNA detection is clearly correlated tumour burden. Besides pre-treatment levels of cfDNA/ctDNA have value to predict long-term survival in locally advanced NSCLC (330). Early ctDNA changes can be detected at first follow-up to predict radiographic response, being their decreasing levels also associated with improved survival rates as our group previously described in NSCLC (261,331,332).

CTCs are tumour cells originated from the primary or metastatic sites that are able to enter the circulation and disseminate to distant sites, and constitute another frequent circulating biomarker investigated in cancer (326). As a high metastatic tumour type, SCLC is characterized by a strong release of CTCs, with detection rates of 60.2%-94% (3), suggesting that CTCs could be employed as a disease surrogate in SCLC. The analysis of CTCs originated from the primary or metastatic sites (179) as a prognostic biomarker has been reported in different cancer types (175,207,333) including SCLC. However, the prognostic threshold in SCLC has been not well established (334–338). The low proportion of CTCs in the bloodstream together with the molecular heterogeneity that characterizes these cells is the principal challenge for CTC isolation and detection. For this reason, several platforms have been developed in the last years (326,339). Despite their different nature, the combined

analysis of total cfDNA and CTCs in patients with SCLC could provide complementary information for improving SCLC patients' management.

In this study, we hypothesized that total cfDNA levels can serve as a useful biomarker for prognostic and follow-up of SCLC patients under first line of therapy. For this purpose, we analysed the total cfDNA levels in a cohort of 46 patients with SCLC prior to the start of therapy, at 3 weeks after the first dose, and at the time of progression of the disease. The additional value of CTCs was investigated in our cohort to provide a more complete view of the disease dynamics. Finally, we developed a simple model to segregate patients into three categories based on risk of progression and death (considering the cfDNA levels, ECOG PS and sex of patients). To our knowledge, this study is the first one to examine the possible role of total cfDNA levels as a prognostic and follow-up biomarker in SCLC patients.

2. MATERIALS AND METHODS

2.1 Patients and blood sample collection

We design a prospective study including newly diagnosed SCLC patients treated with first-line of standard chemotherapy or immunotherapy plus chemotherapy (chemo-immunotherapy). Inclusion criteria were newly diagnosed SCLC patients who received first-line treatment and adequate plasma collection, processing and storage. Forty-six patients treated between June 2017 and June 2021, at the Department of Medical Oncology of Complexo Hospitalario Universitario de Santiago de Compostela were enrolled in the study. In total 111 blood samples of NSCLC patients were collected at different time points: before therapy onset (baseline) (n=46), 3 weeks after therapy start (n=40) and at the progression of the disease (n=25).

A control cohort of 20 healthy individuals was also included to select the better assay to quantify total cfDNA. All individuals signed informed consent forms approved by Santiago de Compostela and Lugo Ethics Committee (Ref: 2017/538) prior to enrolling in the study and could withdraw their consent at any time. The study was performed in accordance with the Declaration of Helsinki (as revised in 2013).

Data of clinical characteristics such as age, sex, the ECOG PS, smoking status, stage, number of metastasis and liver metastasis were collected, to develop a prognostic model together the cfDNA levels and CTCs detected at baseline.

2.2 Clinical endpoints

PFS was defined as the time from the date of initial treatment until the date of progression disease, death or last follow-up, whichever occurred first. Progression date was defined as the date of disease progression based on RECIST (v.1.1), or the date of clinical progression if the patient discontinued the treatment due to clinical deterioration despite not meeting criteria for RECIST progression. OS was defined as the time from the date of initial treatment to the date of death or the last date of follow-up. For survival analyses about cfDNA levels at progression disease, OS was defined as the time from the date of sample obtained (at progression disease) to the date of death or the last date of follow-up.

2.3 Sample processing and circulating free DNA isolation

Peripheral blood was obtained by direct venepuncture in CellSave tubes (Menarini, Silicon Biosystems, Bologna, Italy) and processed within 96 hours after blood collection, since CellSave tubes allow to maintain blood samples

up to 96 hours without affect cfDNA levels (340). Plasma and cellular components were separated by centrifugation at 1,600 g for 10 minutes at room temperature. Plasma was centrifugated a second time at 5,500 g for 10 minutes at room temperature to remove any remaining cellular debris and aliquoted for storage at -80 ºC until the time of cfDNA extraction. cfDNA was isolated from 3 mL of plasma using the QIAamp Circulating Nucleic Acid Kit (Qiagen, Hilden, Germany) using a vacuum pump, according to the manufacturer's instructions and eluted in LoBind® tubes (Eppendorf AG, Hamburg, Germany).

2.4 Total circulating free DNA quantification

CfDNA levels were quantified using two different approaches: Qubit 4 Fluorometer (Thermo Fisher Scientific, Waltham, MA, USA) and quantitative PCR (qPCR) method by analysing *hTERT* single-copy gene (Thermo Fisher Scientific, Waltham, MA, USA). Two µL of the sample were employed to quantify by the fluorometric instrument Qubit 4 using the Qubit dsDNA HS Assay Kit (Thermo Fisher Scientific, Waltham, MA, USA).

In the other hand, samples were quantified by a qPCR assay, described previously (26). Briefly, each qPCR reaction was carried out in a final volume of 20 µL: 10 µL of TaqMan Universal Mastermix (Thermo Fisher Scientific, Waltham, MA, USA), 1 µL of hTERT hydrolysis probe and 2 µL of the sample. Each sample was analysed in duplicate. In addition, each plate included a calibration curve and negative controls. The calibration curve calculated based on a dilution series of a commercial standard human genomic DNA (Roche Diagnostics, Mannheim, Germany), was fragmented in 184 bp using Covaris® E220 Focused-ultrasonicator (Covaris, Massachusetts, USA)

using the following protocol: 430s duration, peak incident power of 175 Watts, duty factor of 10% and 200 cycles per burst. Fragments size was then determined using a TapeStation 4700 (Agilent, Santa Clara, CA, USA) and the High Sensitivity DNA ScreenTape® (Agilent, Santa Clara, CA, USA). Amplification was performed under the following cycling conditions using a QuantStudioTM 3 real-time PCR system (Thermo Fisher Scientific, Waltham, MA, USA): 50 °C for 2 min; 95 °C for 10 min; 40 cycles of 95 °C 15 s; and 60 °C for 1 min. Data were analysed with QuantStudioTM Design & Analysis software, version 2.5.1 (Thermo Fisher Scientific, Waltham, MA, USA).

The final concentration of each sample was calculated by interpolation of the mean of Cq values with the calibration curve. Values with a Cq confidence interval less than 0.95 were discarded. Moreover, only assays with R^2 values greater than 0.98 for the standard curve and with an efficiency ≥ 88.8% were used. Results obtained from both approaches (Qubit vs *hTERT* qPCR) were compared.

2.5 CTC detection and enumeration

CTCs analyses were performed using the CellSearch® system (Menarini, Silicon Biosystems, Bologna, Italy). Peripheral whole blood of each patient was collected in CellSave preservative tubes (Menarini, Silicon Biosystems, Bologna, Italy), stored at room temperature and processed within 96 hours after the blood was drawn.

Briefly, 7.5mL of whole blood were mixed with 6mL of buffer and centrifugated at 800 g for 10 minutes at room temperature. Next, samples were processed in the CellTracks Autoprep system using the Circulating Tumor Cell Kit (Menarini, Silicon Biosystems, Bologna, Italy). The kit consists of

ferrofluids coated with epithelial cell-specific anti-EpCAM antibodies to immunomagnetically enrich epithelial cells; a mixture of antibodies directed to CKs 8, 18, and 19 conjugated to phycoerythrin (PE); an antibody to CD45 conjugated to APC; DAPI to fluorescently label the cells as well as buffers to fix, permeabilize, wash and resuspend the cells. Finally, samples were analysed with the CellTracks Analyzer II according to the manufacturer's instructions. The CTCs were identified as round or oval cells with an intact nucleus (DAPI+), CK positive and CD45 negative.

2.6 Statistical analysis

Continuous data were summarized as mean, median and range whereas frequency and percentage were presented for categorical variables. Categorical variables were compared using the chi-square test or Fisher's exact test. Swimmer plot was provided to visualize the times of sample collection, every patient's therapy, and clinical outcomes. Pearson test was used to evaluate a pairwise correlation between the different strategies to quantify the cfDNA, by fluorometry and qPCR. The Mann–Whitney–Wilcoxon U-Test was used to compare continuous variables between groups. ROC curves were computed based on cfDNA levels of SCLC patients and healthy controls, representing the AUC values and computing the CI at 95% confidence levels. ROC curves were also constructed to evaluate the thresholds of cfDNA levels for PFS and OS analyses. To determine the CTCs cut-off, we analysed the prognostic value of different levels of CTCs to discriminate progression or death using the Evaluate Cutpoints tool (available in http://wnbikp.umed.lodz.pl/Evaluate-Cutpoints/). Kaplan-Meier method was used to plot the survival curves applying the log-rank test. Univariate and multivariate Cox regression analyses were used to evaluate factors

independently associated with PFS and OS. A final prognostic model for PFS and OS was developed. Comparisons of Cox proportional hazard regression models were made using the Akaike information criterion (AIC) technique (341), with a smaller AIC value indicating the better model. A stepwise backward elimination procedure was performed to minimize the AIC. All statistical analyses were performed using R version 4.1.1. The following R packages were used: survival (277), survminer, ggplot2 (342), pROC (276), gtsummary (343), swimplot, stats, rstatix.

3. RESULTS

3.1 Patient characteristics and sample collection

Forty-six SCLC patients were included in the study. Their clinicopathological characteristics are presented in Table 3.1. The median age was 67 (range 47-83) years, all the patients were current or former smokers, and most were males (84.78%) and stage IV tumours (89.13%). The ECOG PS <2 accounted for 67.39% of cases and 52.17% of patients had a number of metastases >2. The majority of patients included into the study were treated with chemotherapy (carboplatin and etoposide) (n=33; 71.74%), while 13 (28.26%) patients were treated with chemotherapy in combination with immunotherapy (n=9 carboplatin, etoposide and atezolizumab; n=4 carboplatin, etoposide and durvalumab). The median number of chemotherapy or chemotherapy/immunotherapy treatment cycles was 5 (range 1–11). At the time of analysis, 41 of the 46 (89.13%) evaluable patients had experienced disease progression and 38 of the 46 (82.6%) evaluable patients had died.

Table 3.1. Patients' demographics and clinical characteristics at baseline with cfDNA levels.

Characteristics	Baseline cfDNA, median (GE/ml)	*p*-value
Age (years) *(Median, Mean ± SD, range),*		
67, 66.83 ± 8.1, 47-83		
Below median, n=24 (52.17%)	6488.23	0.79
Above median, n=22 (47.82%)	8403.79	
Sex		
Male, n=39 (84.78%)	6130.59	0.61
Female, n=7 (15.22%)	15699.93	
Stage		
III, n=5 (10.87%)	1409.11	0.031
IV, n=41 (89.13%)	7658.99	
ECOG PS		
< 2, n=31 (67.39%)	4652.13	0.025
≥ 2, n=15 (32.61%)	22459.61	
Smoking		
Smoker, n=26 (56.52%)	6488.23	0.94
Former smoker, n=20 (43.48%)	6155.56	
Number of metastases		
≤ 2, n=22 (47.82%)	4563.83	0.05
> 2, n=24 (52.17%)	12973.33	
Liver metastases		
No, n=23 (50.0%)	3355.91	0.0002
Yes, n=23 (50.0%)	24759.83	
Bone metastases		
No, n=18 (39.13%)	3265.055	0.17
Yes, n=28 (60.87%)	3355.91	
Lymph node metastases		
No, n=10 (21.74%)	4563.83	0.12
Yes, n=36 (78.26%)	7658.99	
Treatment		
Chemotherapy, n=33 (71.74%)	6130.59	0.36
Chemotherapy plus Immunotherapy, n=13 (28.26%)	10676.99	

Abbreviations: GE: genomic equivalents; SD: standard deviation.

In addition, 20 healthy controls were included. Sample collection was performed before therapy onset (n=46), 3 weeks after initiation of therapy (n=40; 2 patients died and in 4 patients sample collection was not possible) and at the time of progression disease (n=25; 4 patients not progressed, 10 patients died and in 7 patients sample collection was not possible) (Figure 3.1).

Median PFS and OS were 174 (range 4-483) and 229 (range 4-748) days, respectively.

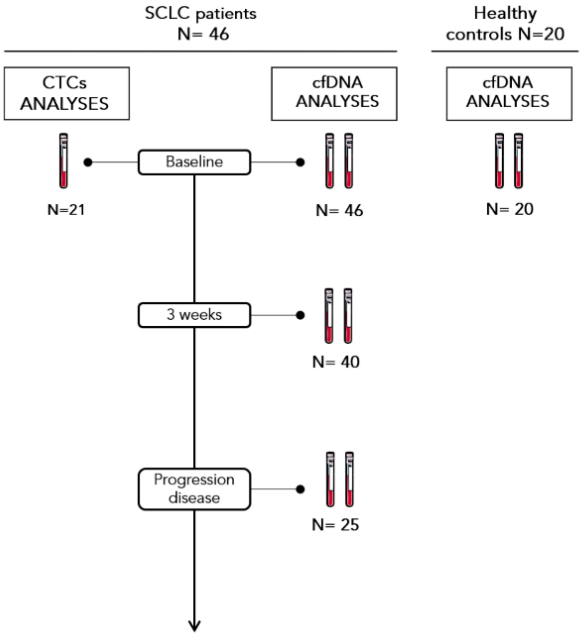

Figure 3.1. Study sampling points and different cohorts included in the study.

3.2 CfDNA levels are specifically increased in SCLC patients

To determine the better method to quantify the total cfDNA in patients with SCLC, we compared the Qubit 4 Fluorometer (Thermo Fisher Scientific, Waltham, MA, USA) versus qPCR method by analysing the *hTERT* single-copy gene (Thermo Fisher Scientific, Waltham, MA, USA). A good correlation between both approaches at different times of the therapy (baseline, 3 weeks and progression disease) was found (R^2 =0.959) (Figure 3.2).

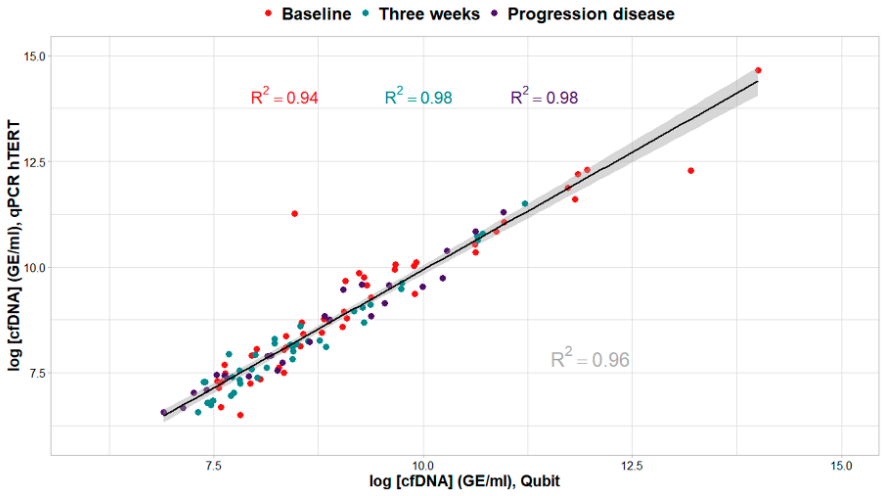

Figure 3.2. Scatter plot representing correlation between cfDNA levels using Qubit method and qPCR assay at different times of therapy (baseline, 3 weeks and progression disease) using Pearson's correlation method. A good correlation between was found (R^2 =0.959). Abbreviations: GE, genomic equivalents.

In addition, 20 healthy controls were included to compare their cfDNA levels with our patient cohort using both approaches. Total cfDNA levels in healthy controls were statistically lower than in our SCLC cohort (Wilcoxon test p= $1.2x10^{-08}$ and p=$1.5x10^{-11}$, using Qubit assay and qPCR assay, respectively) (Figure 3.3A-B).

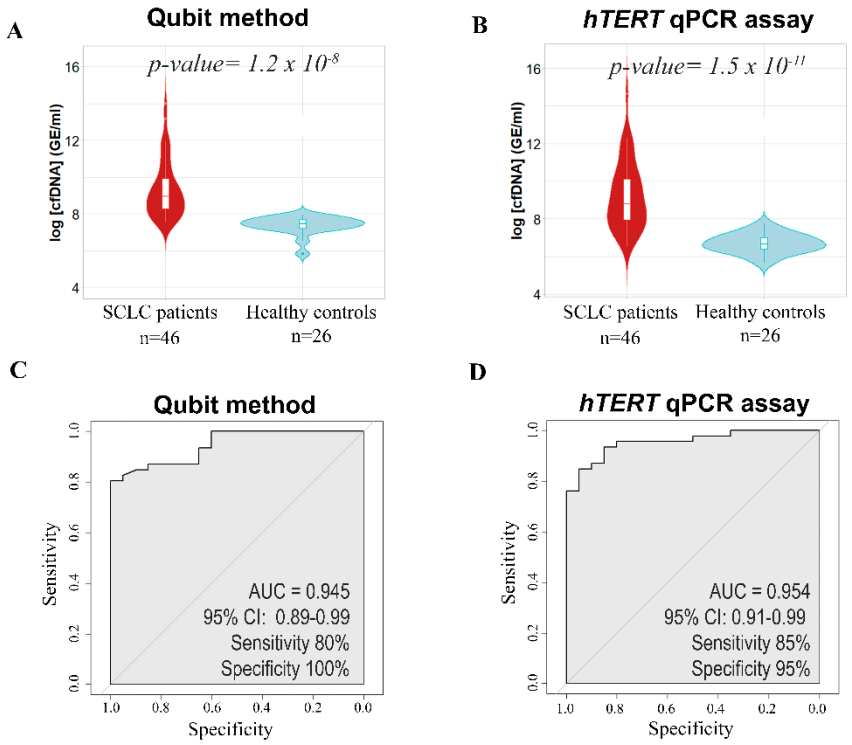

Figure 3.3. CfDNA levels using two different approaches. (A-C) Total cfDNA levels in healthy controls and patients with SCLC. Statistical analysis between both groups was performed by the Mann–Whitney–Wilcoxon U-Test. (B-D) ROC curves for qPCR assay (B) and Qubit method (D) show high sensitivity and specificity. Abbreviations: GE, genomic equivalents; AUC, area under the curve; CI, confidence interval.

Our qPCR assay showed an excellent AUC= 0.954 (specificity 95% and sensibility 85%) (Figure 3.3B). Thus, we chose the qPCR assay by analyzing the *hTERT* single-copy gene (Thermo Fisher Scientific, Waltham, MA, USA) as the standard method to quantify total cfDNA levels. These results evidenced that cfDNA levels were increased because of the malignant disease in SCLC patients showing the clear association between cfDNA levels and the high disease burden that characterized SCLC disease and reinforced their interest as a potential biomarker to follow-up the disease evolution.

3.3 Clinical interest of total cfDNA analysis before therapy

Next, total cfDNA was quantified by qPCR assay at different time points in our patient cohort with the goal to evaluate its potential as a monitoring tool (Table 3.2).

Table 3.2. Statistics of cfDNA levels at baseline, at 3 weeks after the onset of therapy and at disease progression.

	Sample size	Mean (GE/mL)	Median (GE/mL)	Standard deviation	Range (GE/mL)
Baseline	46	81174.03	6488.23	342126.8	660.7-2320370.4
Three weeks post-treatment	40	9034.88	2912.55	18500.36	709-98040
Progression disease	25	11595.13	3747.6	18398.2	705.1-80440.3

Abbreviations: GE, genomic equivalents.

At baseline, cfDNA levels were significantly higher in patients with stage IV cancer, poor performance status, an elevated number of sites of metastasis and presence of liver metastases (p-value ≤ 0.05) (Table 3.1). There was no statistically significant association with respect to age, sex, smoking status, presence of bone metastasis, presence of lymph node metastases and the treatment used.

In addition, the possible role of cfDNA as a prognostic biomarker before therapy in SCLC was investigated. Thus, the cfDNA levels were log-transformed and the patients were dichotomized into high and low cfDNA level groups based on ROC analysis (Table 3.3). The thresholds of baseline log cfDNA levels were chosen at 7.650 (~2100.65 GE/mL plasma) and 8.077 (~3219.56 GE/mL plasma) for PFS and OS analyses, respectively.

Table 3.3. Receiver operating characteristic curves analysis to determine the value of cfDNA levels to discriminate progression or death.

Parameters	AUC	Threshold	Sensitivity	Specificity
PFS				
Log cfDNA at baseline	0.834	7.650	0.854	0.800
Log cfDNA at 3 weeks	0.754	7.879	0.629	1.000
OS				
Log cfDNA at baseline	0.783	8.077	0.789	0.750
Log cfDNA at 3 weeks	0.707	7.879	0.625	0.750
Log cfDNA at progression disease	0.606	8.495	0.545	1.000

Abbreviations: AUC, area under the curve.

We found that patients with high levels of total cfDNA at baseline presented shorter PFS (log rank *p*=0.0005, hazard ratio, 5.06; 95% CI 1.89–13.6) and OS (log rank *p*=0.002, hazard ratio, 3.32; 95% CI 1.50-7.37) than those with low levels of total cfDNA (Figure 3.4A-B; Figure 3.5). The median PFS of patients in the low baseline cfDNA group was 350 days versus 156 days in the high baseline cfDNA group, whereas the median OS was 426 and 210 days in the two respective groups (low vs high baseline total cfDNA levels).

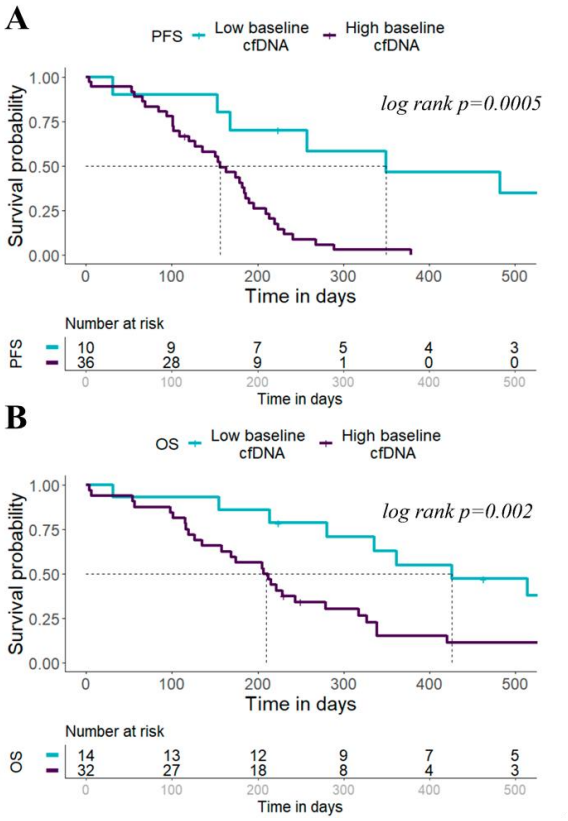

Figure 3.4. cfDNA levels as a prognostic biomarker at baseline. (A-B) Kaplan-Meier survival analysis of cfDNA levels at baseline for PFS (A) and OS (B).

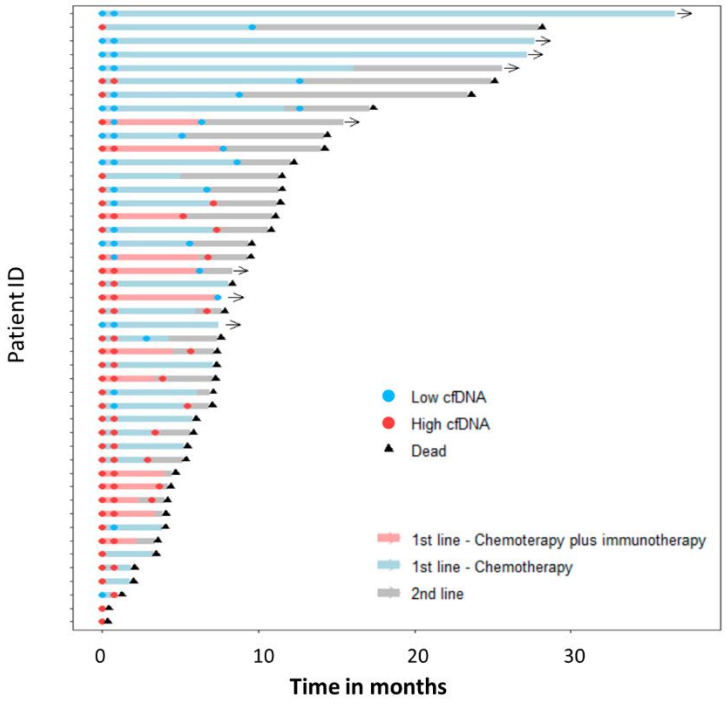

Figure 3.5. Clinical course of all patients included in the study. Swimmers' plot showing each patient therapy and the different times of sample collection. The total length of each bar indicates the duration of survival from the diagnoses. Alive patients are represented with the black arrowhead.

3.4 Longitudinal analysis of total cfDNA during therapy

To determine whether cfDNA levels can be employed to monitor patients' evolution during therapy, we quantified longitudinal cfDNA levels at 3 weeks after initiation of treatment (n=40) and at progression disease (n=25). We found that levels of total cfDNA were significantly higher before therapy than at 3 weeks after therapy onset (Wilcoxon test *p*-value =0.002; Figure 3.6), suggesting clearance of ctDNA after therapy start which impact

on cfDNA levels. However, no significant differences between cfDNA levels at baseline and at progression disease were found (Figure 3.6).

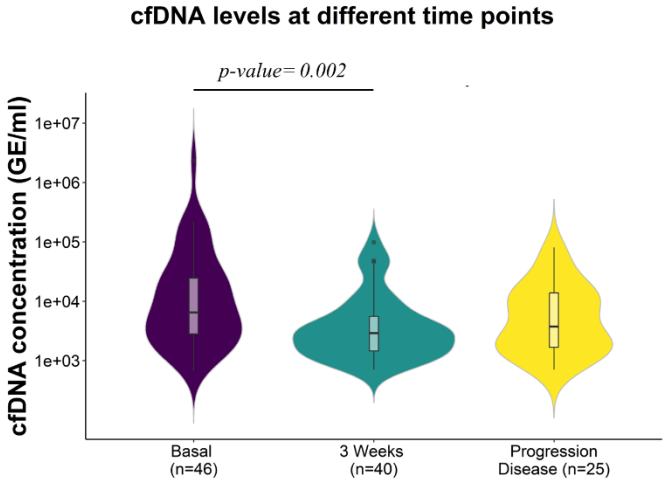

Figure 3.6. CfDNA levels in SCLC patients at different time-points (baseline, 3 weeks after treatment onset and at progression disease). Total cfDNA levels at baseline were significantly higher than at 3 weeks after the therapy onset (Wilcoxon test *p*-value =0.002). Abbreviations: GE, genomic equivalents.

Again, to analyse the possible prognostic role of cfDNA monitoring during therapy, cfDNA levels were also log-transformed and the patients were dichotomized into high and low cfDNA level groups based on ROC analysis (Table 3.3) in each sample time. The threshold of three weeks post-treatment log cfDNA levels was chosen at 7.879 (~2641.23 GE/mL plasma) both for PFS and OS analyses. Thus, the possible prognostic role of monitoring cfDNA levels at 3 weeks after initiation of treatment was investigated. cfDNA levels were defined as high or low depending on the threshold obtained with ROC curves analyses described above. Patients with low cfDNA levels at 3 weeks showed a shorter PFS (log rank p <0.0005, hazard ratio, 3.5; 95% CI 1.69-

7.23) and OS (log rank p <0.0005 hazard ratio, 3.67; 95% CI 1.72-7.82) (Figure 3.7A-B) than the patients with high cfDNA levels.

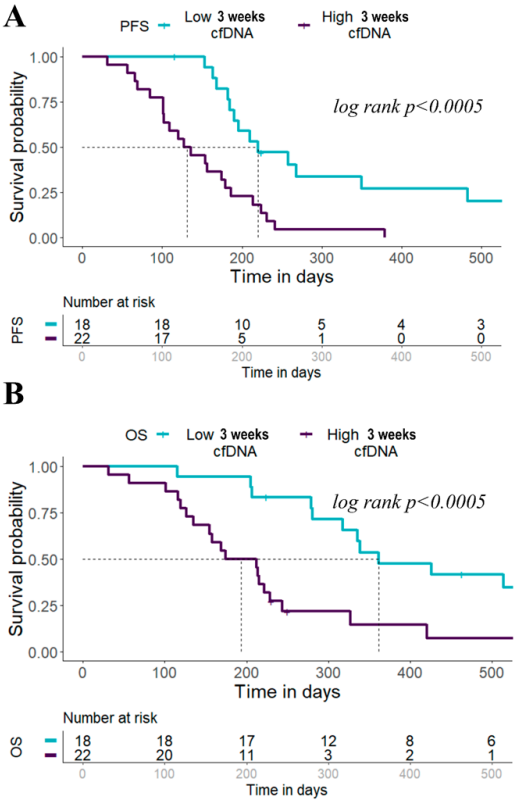

Figure 3.7. cfDNA levels as a prognostic biomarker during treatment. Kaplan-Meier survival analysis of cfDNA levels at 3 weeks for PFS (A) and OS (B).

Finally, cfDNA quantification at the time of progression disease was performed in 25 SCLC patients. Our results reported that patients with high cfDNA levels at this time point survive fewer days than patients with low cfDNA levels (log rank p <0.001, hazard ratio, 5.73; 95% CI 1.93-17.0; 177

days in the high cfDNA levels group versus 74.5 days in the low cfDNA levels group) (Figure 3.8).

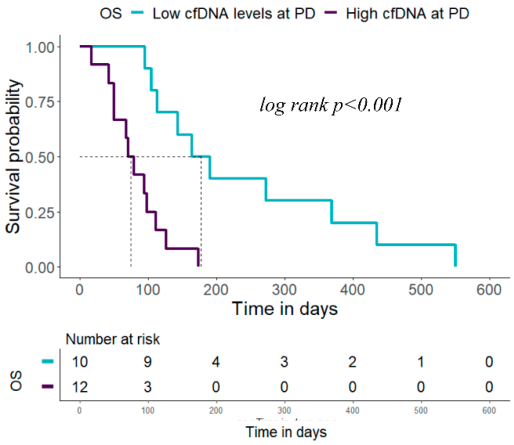

Figure 3.8. Kaplan-Meier survival analysis of cfDNA levels at progression disease for OS.

3.5 Circulating tumour cells analyses and prognostic value

CTCs analyses were performed in 21 patients with SCLC before starting the treatment. We found that 85.71% of patients (18 of 21 patients) presented at least 1 CTC with a median of 26 CTCs (range 0 – 4796) (Figure 3.9).

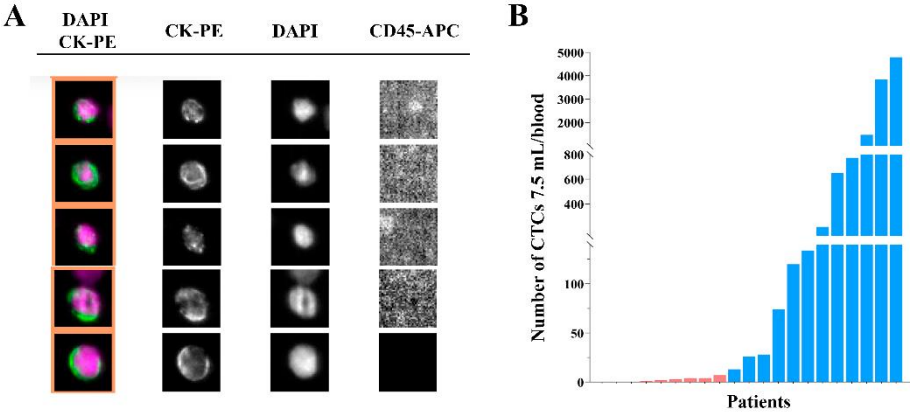

Figure 3.9. CTCs detected in SCLC patient using CellSearch® system. (A) Representative images of CTCs detected in our cohort using the CellSearch® system. (B) Number of CTCs detected in each patient. Patients with presence of <10 CTCs are represented in red columns.

Different cut-offs were analysed to determine the possible prognostic value of CTCs (Table 3.4). Thus, we found that the presence of ≥150 CTCs/7.5mL of blood was significantly associated with shorter PFS rates (log rank p =0.02) in our cohort (Figure 3.10). We also found CTC clusters (≥2 CTCs or CTC with white blood cells) in all patients with >10 CTCs/7.5mL of blood, however no additional prognostic value was found.

Table 3.4. Analysis to determine the prognostic value of CTCs to discriminate progression or death.

CellSearch® CTC count	n (%)	PFS			OS		
		Median (days)	HR (95%CI)	*p*-value	Median (days)	HR (95%CI)	*p*-value
0	3 (14.3)	-	-	-	-	-	-
≥1	18 (85.7)	179	7.2 (0.9-56.3)	0.066	236	4.98 (0.6-38.1)	0.09
≥2	17 (80.9)	179	3.9 (0.9-17.6)	0.078	229	3.2 (0.7-14.2)	0.079
≥5	13 (61.9)	185	1.6 (0.6-4.4)	0.4	244	1.6 (0.6-4.5)	0.348
≥10	12 (57.1)	179	1.7 (0.7-4.5)	0.3	236	1.6 (0.6-4.4)	0.2
≥50	9 (42.9)	163	1.8 (0.7-4.7)	0.11	229	1.7 (0.6-4.7)	0.3
≥100	8 (38.1)	171	1.6 (0.6-4.3)	0.2	254	1.5 (0.5-4.2)	0.5
≥150	6 (28.6)	158	2.5 (0.8-7.9)	0.028	217	2.3 (0.8-7.1)	0.067
≥500	5 (23.8)	163	2.8 (0.8-9.7)	0.10	229	2.4 (0.7-7.9)	0.2
≥1000	3 (14.3)	154	4.6 (0.9-23)	0.036	205	2.1 (0.5-9.4)	0.2

CellSearch® CTC levels: CTC, median (range), 26 (0-4,796); mean ± SE, 579.2 ± 284.5. Abbreviations: CI, confidence interval, HR, hazard ratio.

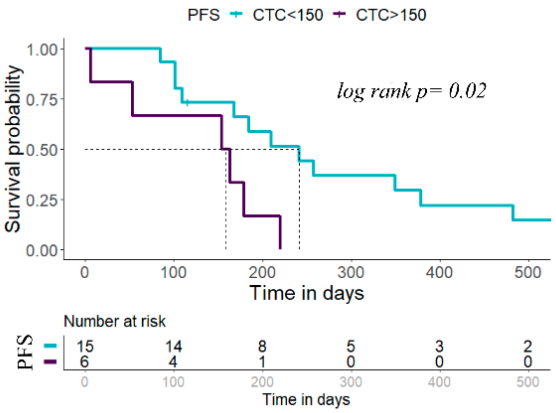

Figure 3.10. Kaplan-Meier survival analysis of CTCs levels at baseline for PFS. The presence of ≥150 CTCs/7.5mL of blood was significantly associated with shorter PFS rates.

In another hand, CTCs number at baseline was significantly higher in patients with extensive disease (stage IV; Figure 3.11E) and with poor ECOG PS (Figure 3.11F). Also, the presence of CTCs and high cfDNA levels were significantly associated (Figure 3.11K), indicating that both markers are reflecting the tumour burden.

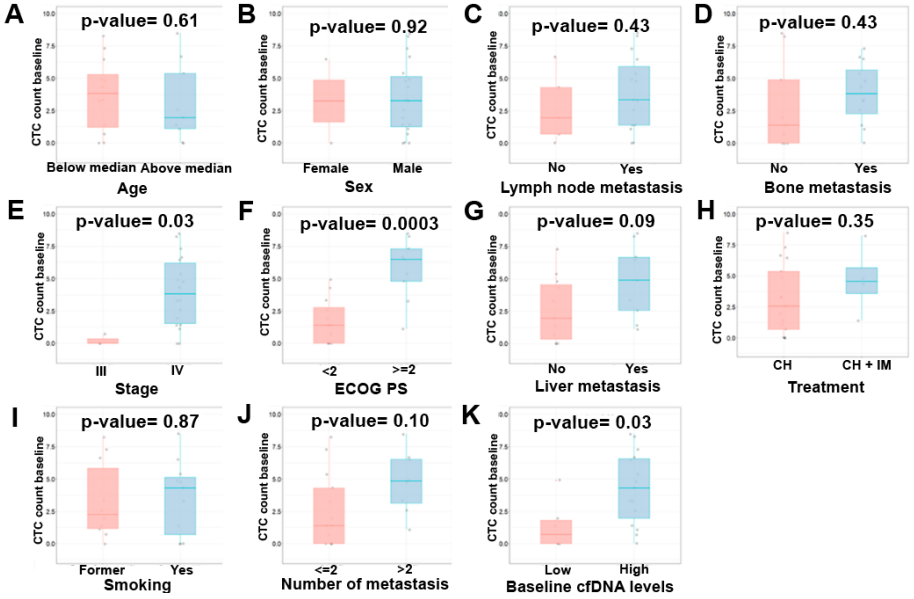

Figure 3.11. CTCs and association with clinical characteristics. The number of CTCs detected in our cohort were significantly associated with the stage of patients and a poor performance status. Also, high cfDNA levels and the presence of CTCs at baseline were significantly associated. Abbreviations: CH, chemotherapy; CH + IM, chemotherapy plus immunotherapy.

3.6 Multivariate analyses and prognostic model for PFS and OS

Univariate and multivariate Cox regression analyses of PFS and OS were performed considering various clinical and demographic variables (ECOG PS, sex, age, stage, number of metastases, presence of liver metastasis and smoking status) (Table 3.5). Multivariate regression analyses confirmed the value of the cfDNA levels at baseline as an early independent predictor biomarker for PFS and OS (hazard ratio, 46.0; 95% CI, 3.16-672; *p*-value =0.005 and hazard ratio, 32.4; 95% CI, 3.05-344; *p*-value =0.004, respectively).

Table 3.5. Univariate and multivariate Cox regression analyses of cfDNA levels, CTC counts and clinical parameters.

Variable	Univariate		Multivariate	
	***p*-value**	**HR (95% CI)**	***p*-value**	**HR (95% CI)**
PFS				
Baseline log cfDNA (high vs. low cfDNA)	0.001	5.06 (1.89-13.6)	0.005	46.0 (3.16-672)
Baseline CTC count, CellSearch® (≥150 vs. <150)	0.028	3.47 (1.14-10.6)		
ECOG (≥2 vs. <2)	<0.001	3.57 (1.72-7.40)	0.04	17.9 (1.11-289)
Sex (male vs. female)	0.2	1.76 (0.74-4.22)		
Age (continue)	0.5	1.01 (0.97-1.05)		
Stage (IV vs. III)	0.07	3.00 (0.91-9.91)		
Number of metastasis (>2 vs. ≤2)	0.1	1.70 (0.90-3.19)		
Liver metastasis (yes vs. no)	0.08	1.74 (0.93-3.23)		
Smoking (smoker vs. former smoker)	0.8	0.92 (0.49-1.70)		
3 weeks log cfDNA (high vs. low cfDNA)*	<0.0001	3.50 (1.69-7.23)	0.004	3.49 (1.50-8.12)
OS				
Baseline log cfDNA (high vs. low cfDNA)	0.003	3.32 (1.50-7.37)	0.004	32.4 (3.05-344)
Baseline CTC count, CellSearch® (≥150 vs. <150)	0.07	2.71 (0.93-7.88)		
ECOG (≥2 vs. <2)	<0.001	4.54 (2.13-9.68)		
Sex (male vs. female)	0.2	1.80 (0.75-4.36)		
Age (continue)	0.5	1.01 (0.97-1.06)		
Stage (IV vs. III)	0.08	2.86 (0.86-9.47)		
Number of metastasis (>2 vs. ≤2)	0.5	1.23 (0.65-2.33)		
Liver metastasis (yes vs. no)	0.3	1.45 (0.77-2.76)		
Smoking (smoker vs. former smoker)	0.5	0.82 (0.43-1.55)		
3 weeks log cfDNA (high vs. low cfDNA)*	<0.001	3.67 (1.72-7.82)	0.002	4.35 (1.68-11.3)
PD log cfDNA (high vs. low cfDNA)*	<0.001	15.2 (3.28-70.7)	0.001	19.5 (3.30-115)

*Multivariate Cox regression model including sex, age, Eastern Cooperative Oncology Group Performance Score, stage, number of metastases, presence of liver metastasis and smoking status. The levels of cfDNA were determined as low (<cut-off) or high (≥cut-

off) based on the cut-off obtained from the ROC curve analyses. Abbreviations; HR, hazard ratio; CI, confidence interval.

Regarding the cfDNA at 3 weeks, multivariate regression analyses also confirm its independence as a prognostic biomarker of PFS and OS (hazard ratio, 3.49.0; 95% CI, 1.50-8.12; *p*-value =0.004 and hazard ratio, 4.35; 95% CI, 1.68-11.3; *p*-value =0.002, respectively) (Table 3.5). In contrast, multivariate analysis in CTCs did not show value as an independent predictive biomarker of PFS and OS.

Next, an independent prognostic model for both PFS and OS was developed. Three variables were retained in the final prognostic model: cfDNA levels (high vs. low levels), ECOG PS (<2 vs. ≥2) and sex (male vs. female). The detailed results of the multivariate analyses are shown in Figure 3.12.

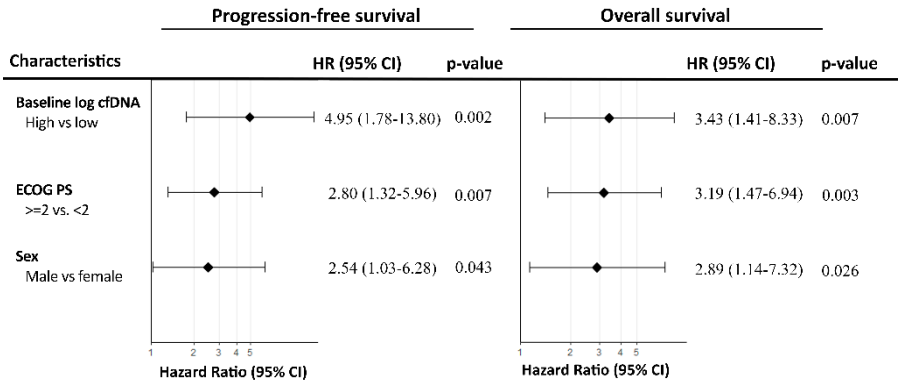

Figure 3.12. Final multivariate Cox regression prognostic model for (A) PFS and (B) OS. Abbreviations: HR, hazard ratio; CI, confidence interval.

Subsequently, we segregated patients into three risk categories: patients with all adverse prognostic factors were classified in the poor-risk category (high cfDNA levels, ECOG PS≥2 and male sex), patients with two adverse

prognostic factors were classified in the intermediate-risk category, and patients with one or no adverse prognostic factor were classified in the favorable-risk category. The Kaplan–Meier curves representing the three risk categories and median PFS and OS are presented in Figure 3.13. Median PFS ranged from 124 to 289 days based on the number of adverse prognostic factors present before therapy. Median OS ranged from 115 to 514 days.

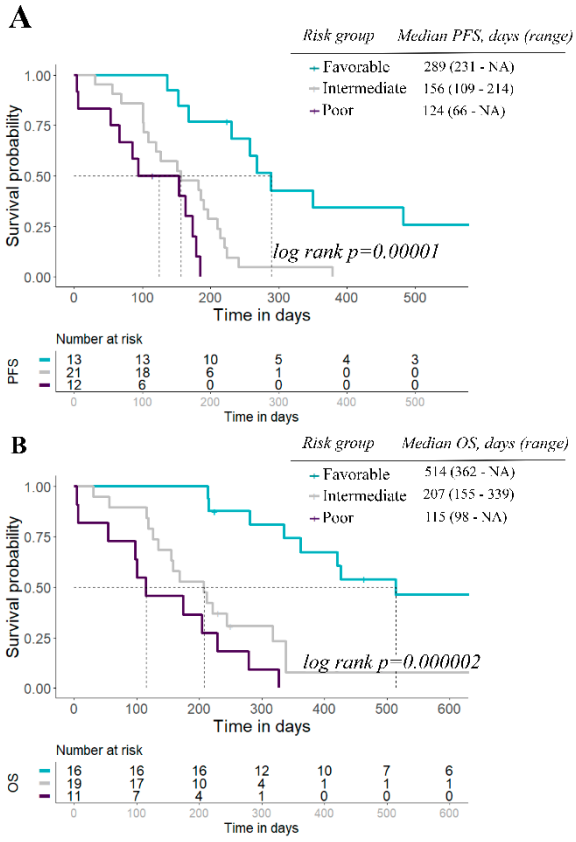

Figure 3.13. Kaplan-Meier survival analysis according to risk-group for PFS (A) and OS (B). Abbreviations: NA, not applicable.

Our prognostic model indicates an increased risk of 5-times to present disease recurrence (HR= 5.37, 95% CI, 2.32-12,4; *p*-value =$3x10^{-5}$) and 6-

times the risk of death (HR= 6.02, 95% CI, 2.66-13.6; *p*-value =$3x10^{-6}$) in the unfavorable category (intermediate and poor groups) than in the favorable group (Table 3.6).

Table 3.6. PFS and OS probabilities estimated according two risk groups.

Risk Groups	***PFS***			***OS***		
	HR	95% CI	*p*-value	HR	95% CI	*p*-value
Favourable	1	(Ref.)	-	1	(Ref.)	-
Intermediate-poor	5.37	2.32-12.4	< 0.001	6.02	2.66-13.6	< 0.001

Abbreviations: HR, hazard ratio; CI, confidence interval.

4. DISCUSSION

Precision medicine has the objective of optimizing the selection of the best therapy for each patient. In this context, liquid biopsy has born as a promising and minimally invasive tool for this due to its ability to provide a total image of primary and metastatic tumours at different times across therapy (344). Recently, the management of SCLC has changed and new therapies, such as immunotherapy, have been investigated and approved for clinical use (3,345,346). Nevertheless, the necessity to find a prognostic biomarker for helping to select the therapy prescribed and to monitor the evolution of the disease during the treatment, remains a challenge in SCLC patients. In this study, we report for the first time the possibility to employ the cfDNA and its quantification as a prognostic biomarker in SCLC prior to starting therapy and at different time points. Our analyses allowed us to identify a group of low-risk patients characterized by low cfDNA levels at baseline who probably will benefit from both: chemotherapy in monotherapy or the combination of

immunotherapy and chemotherapy. The study of another common circulating biomarker, CTCs, also provided us information for the prognostic of patients before starting therapy, although the results were less clear. We found a significant association between presence of a high number of CTCs (≥150 CTCs) and worse PFS.

Total cfDNA refers to a heterogeneous and complex DNA fraction free released in body fluids by any cell type (not only tumoral) through several cell death mechanisms such as secretion, apoptosis and necrosis (138,150). Of note, the source of cfDNA is an intriguing question in cancer. According to previous studies, the fraction of ctDNA varies from 0.1–89% of cfDNA but it increases it accordance with the tumour burden. Therefore, although cfDNA content is not tumour specific, it can be assumed that total cfDNA in cancer patients originates from tumour cells, cells in the tumour microenvironment or from cells involved in the antitumour response (137). Therefore, cfDNA can be uses as a surrogate of ctDNA, but always taking into account that they are different entities that can provide us different information. In line with our results, it's well reported that cancer patients present higher cfDNA levels than healthy controls (347,348), but few studies have investigated the possible prognostic and predictive value of total cfDNA quantification in patients with SCLC. In contrast, the ctDNA, the tumour-derived fraction of this cfDNA, has been reported as a prognostic and predictive biomarker in several works (349–353). Almodovar et al. reported that changes in the mutant allele frequencies on ctDNA were associated with response to treatment and relapse. Twenty-seven patients with SCLC were analysed by next-generation sequencing (NGS) custom panel, however, the lack of driver mutations known in SCLC, limited the number of genes analysed (349). In another work, Devarakonda et

al. analysed 564 patients using a larger NGS panel, including 73 genes, and, according to previous results, *RB1* and *TP53* were the most frequent mutant, however, no prognostic or predictive value was reported in this study (354).

In this way, total cfDNA quantification allows to detect the total DNA released from normal and also tumour cells into the blood. Thus, despite the few known driver mutations found in SCLC, cfDNA quantification allows to quantify the total levels before treatment and monitor the changes during therapy. Recently, our group demonstrated the feasibility to quantify cfDNA levels in NSCLC patients and its association with patients' outcomes (261), suggesting its possible utility in SCLC.

Thus, in the present work, we quantified total cfDNA levels using two different technologies, a fluorometric assay, Qubit and a more specific one, the qPCR assay analysing the *hTERT* gene. CfDNA quantification by both technologies showed good concordance. Furthermore, the concordance of cfDNA levels at any time point of therapy using both methods also showed a good concordance. Therefore, both methods could be used to robustly measure the cfDNA content. However, to complete our study we chose the qPCR assay, which is a high sensitive and specific assay for cfDNA quantification in SCLC patients, and was previously employed in studies focused on NSCLC (261,270,273,288).

Regarding the clinical meaning of cfDNA content, we found that high levels were significantly associated with shorter PFS and OS before therapy onset, being a robust independent prognostic biomarker in newly diagnosed SCLC patients. Also, cfDNA levels at baseline were higher in patients with stage IV that could be a consequence of a more aggressive disease. This can

be partially explained by an increase of ctDNA levels released from the tumour cells to the bloodstream, increasing the total cfDNA fraction. Moreover, analyses showed that cfDNA levels at 3 weeks are associated with patients' outcomes, being those patients with high values at 3 weeks, the ones with the worst prognosis. In addition, high cfDNA levels at the time of disease recurrence were associated with a higher risk of death. Of note, multivariate analyses showed the independence of cfDNA levels at 3 weeks and at progression disease as a prognostic biomarker. These results suggest that cfDNA monitoring could provide valuable information for the management of SCLC as our group previously reported in NSCLC (261). Thus, in clinical practice, in those SCLC patients with high levels of cfDNA at the time of disease recurrence, the selection of a more aggressive therapy or the intensification of clinical visits would be considered.

Besides cfDNA levels, we investigated the prognostic value of additional biomarkers such as CTCs and clinical characteristics. CTCs were analysed in a cohort of 21 SCLC patients using the CellSearch® system. According to the literature (3), a detection rate of 85.71% was found in our study. Moreover, the CTC count at baseline determined using the CellSearch® system was significantly associated with PFS and OS (334,337,338,355,356). For example, Naito et al. reported that the presence of ≥8 CTCs/7.5mL of blood was associated with worse OS (334), however, another study employed 50 CTCs as cut-off for PFS and OS (338). In fact, a consensus regarding the optimal cut-off of CTCs and the prognostic value remains a challenge (3). In this work, we found a discrete association between the presence of ≥150 CTCs and a shorter PFS, however multivariate analyses did not show independent value for the CTC count. Interestingly, high cfDNA levels and the presence

of CTCs at baseline were significantly associated, reporting the clear association between both circulating biomarkers and disease burden. CTCs release in the bloodstream is related to the intravasation process of potentially metastatic cancer cells. Nevertheless, cfDNA is released by any cell type including tumoral and normal cells, however, how cfDNA release relates to tumour biology is currently unknown. In another hand, we evaluate several factors that could influence the patients' outcomes. Thus, we proposed a simple model to segregate patients into three categories based on risk of progression and death (considering the cfDNA levels, ECOG PS and sex of patients). We found that patients with one or less adverse prognostic factors were classified in the favourable-risk category and present a longer PFS and OS. Regarding the clinical relevance of these results, some limitations in our design should be considered. First, the sample size of our CTC cohort was relatively small and CTC monitoring during therapy could provide more valuable information. Second, our patient cohort are not homogenous regarding treatment regimen, 71.74% SCLC patients were treated with while 28.26% SCLC patients were treated with chemo-immunotherapy. In addition, a validation study of our prognostic model in a larger independent cohort is needed.

In conclusion, we describe an important potential role of cfDNA levels as a prognostic biomarker in newly diagnosed SCLC patients and also as a tool that could provide useful information about disease evolution. Finally, a prognostic model based on cfDNA levels, and some clinical characteristics (ECOG PS and sex) would allow us to stratify patients and detect those who could particularly benefit from the treatment.

CHAPTER IV

Circulating proteins as predictive biomarkers for immunotherapy in metastatic NSCLC patients.

Circulating proteins as predictive biomarkers for immunotherapy in metastatic non-small cell lung cancer patients

Patricia Mondelo-Macía[1,2,3], Jorge García-González[4,5], Luis León-Mateos[2,3,4,5,6], Alicia Abalo[1], Susana Bravo[7], María del Pilar Chantada Vazquez[7], Laura Muinelo-Romay[1,3,6], Rafael López-López[1,2,3,4,5,6,9], Roberto Díaz-Peña[3,8] and Ana B Dávila-Ibáñez[6,9].

[1] Liquid Biopsy Analysis Unit, Translational Medical Oncology (Oncomet), Health Research Institute of Santiago (IDIS), Santiago de Compostela, Spain.

[2] Universidade de Santiago de Compostela (USC), Santiago de Compostela, Spain.

[3] Galician Precision Oncology Research Group (ONCOGAL), Medicine and Dentistry School, Universidade de Santiago de Compostela (USC), Santiago de Compostela, Spain.

[4] Department of Medical Oncology, Complexo Hospitalario Universitario de Santiago de Compostela (SERGAS), Santiago de Compostela, Spain.

[5] Translational Medical Oncology (Oncomet), Health Research Institute of Santiago (IDIS), Santiago de Compostela, Spain.

[6] CIBERONC, Centro de Investigación Biomédica en Red Cáncer, Madrid, Spain

[7] Proteomic Unit, Instituto de Investigaciones Sanitarias-IDIS, Complejo Hospitalario Universitario de Santiago de Compostela (CHUS), Santiago de Compostela, Spain

[8] Fundación Pública Galega de Medicina Xenómica, SERGAS; Grupo de Medicina Xenomica-USC, Health Research Institute of Santiago (IDIS), Santiago de Compostela, Spain.

[9] Roche-Chus Joint Unit, Translational Medical Oncology Group, Oncomet, Health Research Institute of Santiago de Compostela (IDIS), Santiago de Compostela, Spain

Circulating proteins as predictive biomarkers for immunotherapy in metastatic non-small cell lung cancer patients

ABSTRACT

Immunotherapy has improved survival rates in cancer patients, but identifying those who will respond to treatment remains a challenge. Biomarkers such as PD-L1 expression, tumour mutational burden, and microsatellite instability have been studied, but their limitations have led researchers to explore other options. Recent advances in proteomic technologies have enabled the identification and quantification of nearly all expressed proteins in a single experiment. Integration of mass spectrometry with other high-throughput technologies has paved the way for comprehensive and systematic analysis of the plasma proteome in cancer, facilitating early diagnosis and personalized treatment. However, despite its potential, the use of mass spectrometry-based proteomics for plasma analysis in cancer research is still limited, with few studies utilizing this methodology. In this context, the objective of our study was to investigate the predictive and prognostic value of plasma proteome analysis using the SWATH-MS (Sequential Window Acquisition of All Theoretical Mass Spectra) strategy in newly diagnosed NSCLC patients who received pembrolizumab therapy. SWATH-MS technology is a method for data-independent acquisition (DIA) mass spectrometry, allowing comprehensive and unbiased analysis of complex proteomes with high sensitivity and reproducibility. For this purpose, 64 newly diagnosed advanced NSCLC patients treated with pembrolizumab

therapy were enrolled and blood samples were collected from all patients before and during therapy. In total 171 blood samples were collected and analysed employing SWATH-MS strategy. Next, we compared the plasma protein expression of metastatic NSCLC patients prior to receiving pembrolizumab treatment and divided the cohort into two groups based on immunotherapy response. The results identified 324 differentially expressed proteins between responder and non-responder patients. Later, we developed a predictive model and found a combination of seven proteins, including ATG9A, DCDC2, HPS5, FIL1L, LZTL1, PGTA, and SPTN2, with stronger predictive value than PD-L1 expression alone. Additionally, survival analyses showed that low levels of ATG9A, DCDC2, and HPS5 were associated with longer PFS and OS, while low levels of SPTN2 were associated with worse OS. These analyses shed light on the correlation between the response to immunotherapy in patients with NSCLC and our 7 proteins.

Keywords: NSCLC, immunotherapy, predictive biomarkers, circulating proteins.

1. INTRODUCTION

Immunotherapy is one of the most promising cancer treatments due to its differential mechanism of action, long-lasting effects, and ability to improve overall survival in a percentage of patients. (357). The ICI agents, the most thoroughly investigated class of immunotherapy, target PD1, PD-L1 or CTLA-4, being its objective stimulate the immune response of patients against cancer (358). In recent years, immunotherapy has reported an improvement survival rates in comparison with chemotherapy in NSCLC patients (51,359). Pembrolizumab, is one of the most employed ICIs in advanced NSCLC patients. For years, the selection of patients who received these drugs was based on the PD-L1 expression on tumour tissue. Nevertheless, posterior studies reported that pembrolizumab in combination with chemotherapy, showed a significant improvement in survival results, independently of the PD-L1 expression (55,56), showing the lack of value of PD-L1 expression in tumour tissue to predict the response to this therapy.

Therefore, despite ICI therapies have improved patients' outcomes in comparison with chemotherapy, the clinical use of immunotherapy experiences several challenges related to both efficacy and safety. Regarding efficacy, a large group of patients do not respond to ICI treatment (primary resistance), where even in large phase III studies of ICIs combined with chemotherapy, overall response rates are 47–63% at best (55,56,360). Regarding safety, adverse reactions to ICI treatment (265,361), as well as an accelerated progression, denominated hyperprogression, have been reported (362).

In this context, the management of NSCLC with ICIs requires the identification of new and robust biomarkers to select patients who will benefit

from immunotherapy. Liquid biopsy could allow to discover new biomarkers that could help clinicians to select patients who will benefit from ICIs treatment (363). Numerous studies focus on potential biomarkers in blood such as CTCs, ctDNA, cfDNA, exosomes, miRNA or proteins among others, due to the several advantages that present liquid biopsy compared with tumour tissue. Next-generation sequencing allows the analysis of genomes and opens the door to find new alterations associated with response to therapies and discover new possible therapy targets. However, typically the causes of cancer disease are multifactorial and different approaches, including the analysis of proteomes, are required for a more comprehensive understanding. Plasma circulating proteins are an alternative biomarker that can provide information about the physical condition and status of patients. In oncology, several single serum or plasma proteins are used for diagnosis and monitoring of cancer, such as cancer antigen 125 (CA-125) in ovarian cancer and the prostate-specific antigen (PSA) in prostate cancer among others (364). However, nowadays the use of these single proteins should always be interpreted in conjunction with other diagnostic tests and clinical findings. Large analyses of circulating proteins could provide a wealth of information about oncogenic processes, and to explore their usefulness as tumour biomarkers in response to different treatments, including immunotherapy in lung cancer (365).

In the last decades, proteomic technologies have advanced in terms of instrumentation improvements, sample preparation and computational analyses, allowing us to identify and quantify nearly all expressed proteins in a single experiment (366). An emerging strategy named SWATH–MS (sequential window acquisition of all theoretical fragment-ion spectra–mass spectrometry) is a specific variant of data-independent acquisition (DIA)

method that combines deep proteome coverage capabilities and allow to identify and quantify circulating proteins with consistency and accuracy (367).

In the present study, we hypothesized that plasma proteins can serve as a prognostic and predictive biomarker in NSCLC patients under first-line immunotherapy. We performed a differential proteomic quantitative analysis based on SWATH–MS technology to analyse the proteome in blood samples collected from patients with advanced NSCLC prior to the start therapy and during the treatment. Finally, we reported a proteomic signature of 7 proteins that could predict the response to immunotherapy in advanced NSCLC patients before starting therapy, as well as at 6 and 12 weeks after starting immunotherapy.

2. MATERIAL AND METHODS

2.1 Patients and blood sample collection

In total, 64 newly diagnosed advanced NSCLC patients treated with pembrolizumab therapy at the Department of Medical Oncology of Complexo Hospitalario Universitario de Santiago de Compostela, were included in the present study. A first cohort (Discovery cohort) included a total of 48 patients with newly diagnosed advanced NSCLC. A posterior validation cohort enrolled 16 new diagnosed advanced NSCLC patients. The study was performed in accordance with the Declaration of Helsinki (as revised in 2013) and all individuals signed informed consent forms approved by Santiago de Compostela and Lugo Ethics Committee (Ref: 2017/538) prior to enrolling in the study and they could withdraw their consent at any time. Blood samples of 64 patients were collected before the therapy onset. In addition, 107

longitudinal blood samples were collected at 6 weeks (n=46) and 12 weeks (n=36) after starting the therapy and at time of progression disease (n=25).

Best response to pembrolizumab treatment was based on RECIST1.1, according to the following criteria: Complete response (CR), partial response (PR), stable disease (SDi) or progressive disease (PD). Responders were defined as the proportion of patients with CR, PR, or SDi.

2.2 Blood sample processing

Ten mL of peripheral blood were obtained by direct venipuncture in CellSave tubes (Menarini, Silicon Biosystems, Bologna, Italy) and processed within 96 hours after blood collection for the discovery cohort. In the case of the validation cohort, peripheral blood was obtained in EDTA tubes and processed within 4 hours. In both cases, plasma and cellular components were separated by centrifugation at 1,600 g for 10 minutes at room temperature. A second centrifugation was performed at 5,500 g for 10 minutes at room temperature to remove any remaining cellular debris. Plasma samples were aliquoted for storage at -80 ºC until use.

2.3 Plasma preparation for mass spectrometry (MS) analysis

Plasma abundant proteins depletion

Plasma samples were fractionated prior proteolytic digestion to enrich the spectral library employed in SWATH-MS quantification. For this purpose, aliquots of each sample (30 µl) were depleted with dithiothreitol (DTT). Fresh DTT (500 mM) was mixed with the 30 µl of human plasma samples and vortex briefly (368,369). Then, samples were incubated until observe a viscous white precipitate that persisted for 60 minutes, and they were centrifugated at 18,840 g for 20 minutes. Supernatants were transferred to a clean tube.

Isolation and proteins digestion

To make global protein identification, an equal amount of protein from all samples were loaded on a 10% SDS-PAGE gel. The run was stopped as soon as the front had penetrated 3 mm into the resolving gel (370,371). The protein band was detected by Sypro-Ruby fluorescent staining (Lonza, Switzerland), excised, and processed for in-gel manual tryptic digestion, as described elsewhere (20). Proteins were reduced with DTT 10mM in Ambic 40mM and alkylated with 55 mM iodoacetamide in 50 mM ammonium bicarbonate. Then, the gel pieces were rinsed with 50 mM ammonium bicarbonate in 50% methanol dehydrated by addition of acetonitrile and dried in a SpeedVac. Modified porcine was added to the dry gel pieces at a final concentration of 20 ng/µl in 20mM ammonium bicarbonate, incubating them at 37 °C for 16 hours. Peptides were extracted by carrying out three 20 minutes incubations in 40 µL of 60% acetonitrile dissolved in 0.5% HCOOH. The resulting peptide extracts were pooled, concentrated in a SpeedVac, and stored at −20 °C.

2.4 Protein quantification by SWATH-MS (Sequential Window Acquisition of all Theoretical Mass Spectra)

Creation of the spectral library - Data-dependent acquisition (DDA)

To construct the MS/MS spectral libraries, the peptide solutions from the discovery cohort were analysed by a shotgun data-dependent acquisition (DDA) approach by micro-liquid chromatography-MS/MS. To get a good representation of the peptides and proteins present in all samples, pooled vials of samples from each group (basal n=48, 6 weeks n=35, 12 weeks n=30 and progression disease, n=21) were prepared using equal mixtures of the original samples for the spectral library building. Four µL (1 µg/µL) of the pool was

separated using Reverse Phase Chromatography. Gradient was created using a micro liquid chromatography system (micro-LC) Ekspert nLC425 (Eksigent Technologies nanoLC 400, Sciex, CA, USA) coupled to high-speed Triple TOF 6600 mass spectrometer (Sciex, CA, USA) with a micro flow source. The chosen analytical column was a silica-based reversed phase column Chrom XP C18 150 × 0.30 mm, 3 mm particle size and 120 Å pore size (Eksigent, Sciex, CA, USA). The trap column was a YMC-TRIART C18 (YMC Technologies, Teknokroma) with a 3 mm particle size and 120 Å pore size, switched on-line with the analytical column. The loading pump delivered a solution of 0.1% formic acid in water at 10 µl/min. The micro-pump generated a flow-rate of 5 µl/min and was operated under gradient elution conditions. Water and acetonitrile, both containing 0.1% formic acid, were used as solvents A and B, respectively. The gradient run consisted of 5% to 95% B for 30 min, 5 min at 90% B and finally 5 min at 5% B for column equilibration, for a total run time of 40 min.

When the peptides eluted, they were directly ionized and injected into a hybrid quadrupole-TOF mass spectrometer Triple TOF 6600 (Sciex, CA, USA) operated with a Data dependent acquisition (DDA) system in positive ion mode. A Micro source (Sciex, CA, USA) was used for the interface between micro-LC and MS, with an application of 2600 V voltage. The acquisition mode consisted of a 250 ms survey MS scan from 400 to 1250 m/z followed by an MS/MS scan from 100 to 1500 m/z (25 ms acquisition time) of the top 65 precursor ions from the survey scan, for a total cycle time of 2.8 seconds. The fragmented precursors were then added to a dynamic exclusion list for 15 seconds; any singly charged ions were excluded from the MS/MS analysis. The instrument was automatically calibrated every 4 hours using

external calibrant tryptic peptides from PepCalMix solution (AB SCIEX, Framingham, MA, United States).

The peptide and protein identifications were performed using Protein Pilot software (version 5.0.2, Sciex, CA, USA) searched against a Human specific Uniprot database (https://www.uniprot.org/), specifying iodoacetamide as Cys alkylation and Trypsin as enzyme used in digestion. The software uses the algorithm Paragon™ for database search and Progroup™ for data grouping. The false discovery rate (FDR) was set to 1% for both peptides and proteins, using a non-lineal fitting method (372). The MS/MS spectra of the identified peptides were then used to generate the spectral library for SWATH peak extraction using the plug-in MS/MS^{ALL} with SWATH Acquisition MicroApp (version 2.0, Sciex) for PeakView Software (version 2.2, Sciex, CA, USA). Peptides with a confidence score above 99% (as obtained from Protein Pilot database search) were included in the spectral library.

In addition, a spectral online library called, Human Pan-Human library, which contained 12,046 proteins (https://db.systemsbiology.net/sbeams/cgi/PeptideAtlas/GetDIALibs), was also employed in order to improve and expand the coverage of the identified NSCLC cancer plasma proteome in our library. The sum of the two libraries constitutes our final library, denominated NSClibrary.

Relative quantification by SWATH acquisition - DIA

SWATH-MS acquisition was performed on a TripleTOF® 6600 LC-MS/MS system (AB Sciex, CA, USA). Samples were analysed using a DIA method (n=171 samples). Each sample (4 µL) was analysed using the LC-MS

equipment and LC gradient described above for building the spectral library but instead using the SWATH-MS acquisition method. The method consisted of repeating a cycle that is composed of the acquisition of 100 TOF MS/MS scans (400 to 1500 m/z, high sensitivity mode, 50 ms acquisition time) of overlapping sequential precursor isolation windows of variable width (1 m/z overlap) covering the 400 to 1250 m/z mass range with a previous TOF MS scan (400 to 1500 m/z, 50 ms acquisition time) for each cycle. Total cycle time was 6.3 seconds. For the sample set, the width of the 100 variable windows was optimized according to the ion density found in the DDA runs using a SWATH variable window calculator worksheet from Sciex. SWATH quantification was attempted for all proteins in the ion library that were identified by ProteinPilot with an FDR below 1%.

The DIA raw data were firstly converted into mzML format filtered by SWATH Acquisition MicroApp (version 2.0) then analyzed by PeakView (version 2.2), against our spectral NSCLibrary. PeakView computed an FDR and a score for each assigned peptide according to the chromatographic and spectra components; only peptides with an FDR below 1% were used for protein quantitation. The retention time (RT) adjustment were performed using the own peptides of the proteins presents in the library from the peptides that were selected for each protein. Them the RT of all peptides were realigned in each run according to the iRT peptides spiked of the selected peptides in each sample and eluted along the whole time axis. The extracted ion chromatograms were then generated for each selected fragment ion; the peak areas for the peptides were obtained by summing the peak areas from the corresponding fragment ions. Protein quantitation was calculated by adding the peak areas of the corresponding peptides Up to ten peptides per protein

and seven fragments per peptide were selected, based on signal intensity; any shared and modified peptides were excluded from the processing. Five-minute windows and 30 ppm widths were used to extract the ion chromatograms. Them this integrated peak areas (processed. mrkvw files from PeakView) were directly exported to the MarkerView 1.3.1 software (AB Sciex, CA, USA) for relative quantitative analysis (373–376). The export data will generate three files containing quantitative information about individual ions, the summed intensity of different ions for a particular peptide and the summed intensity of different peptides for a particular protein.

2.5 Quality control and statistical analysis

Next, a quality control was performed. Proteins with over 30% missing values in the sample set were filtered out. Next, missing values of the remaining proteins were imputed using the RandomForest R package (377,378) and protein values were normalized by quantile normalization.

Finally, statistical analyses were performed. Continues data were compared using t test for independent samples and categorical variables were compared using the Fisher's exact test. Swimmer plot was provided to visualize every patient's therapy response and the time of survival from the diagnoses. Kaplan-Meier method was used to plot the survival curves applying the log rank test. Student's t test was applied to identify differentially expressed proteins (DEPs), with a p-value <0.05 and p-value <0.01. To identify the functions and relevant pathways of the DEPs, we performed gene ontology (GO) using Metascape (379). The Kyoto Encyclopedia of Genes and Genomes (KEGG) pathway of each group was generated and visualize with proteomaps, using a web tool based on the t-test difference values without

log2 transformation (380). A final predictive model to separate responder group to non-responder group was developed. Comparisons of Cox proportional hazard regression models were made using the AIC technique (341), with a smaller AIC value indicating the better model. A stepwise backward elimination procedure was performed to minimize the AIC. ROC curves were computed based on protein levels, representing the AUC values, and computing the CI at 95% confidence levels. ROC curves were also constructed to evaluate the thresholds of baseline proteins levels for survival analyses. All statistical analyses were performed using GraphPad Prism version 8.0, IBM® SPSS® statistics version 25.0 and R version 4.1.1. The following R packages were used: survival (277), survminer, ggplot2 (342), pROC (276), gtsummary (343), swimplot, RandomForest, MASS and stats.

3. RESULTS

3.1 Patient characteristics

In total, 64 newly diagnosed NSCLC patients undergoing first-line pembrolizumab treatment in monotherapy (n=40) or in combination with chemotherapy (n=24) were included in the study (Figure 4.1, Table 4.1). Patients were enrolled in two different sub-cohorts: a discovery cohort with 48 NSCLC patients and a validation cohort with 16 NSCLC patients. The validation cohort was included to evaluate a possible impact of the blood collection tubes.

In global terms, the mean age was 64.7 years (range: 45–80), most of patients were males (75%), current or former smokers (87.5%) and had

tumours with adenocarcinoma histology (81.25%) (Table 4.1). The ECOG PS of <1 accounted for 17.2% of patients.

Table 4.1. Patients' demographics and clinical characteristics at baseline.

Clinical Characteristics	Discovery cohort (n=48)			Validation cohort (n=16)		
	R (n=30) N (%)	**NR (n=18) N (%)**	***p*-value**	**R (n=10) N (%)**	**NR (n=6) N (%)**	***p*-value**
Mean age ± SD, range	64.3 ± 8.2, 50-80	61.9 ± 9.5, 45-78	NS	71.5 ± 5.4, 60-77	63.2 ± 7.6, 51-74	NS
Sex						
Female	6 (20.0)	5 (27.8)	NS	1 (9.1)	4 (66.7)	**0.03**
Male	24 (80.0)	13 (72.2)		9 (90.9)	2 (33.3)	
Smoking						
Smoker / Former smoker	25 (83.3)	16 (88.9)	NS	9 (90)	6 (100)	
Never	5 (16.7)	2 (11.1)		1 (10)	0 (0.0)	NS
ECOG PS						
0	8 (26.7)	1 (5.6)		1 (10)	0 (0.0)	
1	21 (70.0)	13 (72.2)	NS	10 (90)	4 (66.7)	NS
2	1 (3.3)	4 (22.2)		0 (0.0)	2 (33.3)	
Histology						
Adenocarcinoma	26 (86.7)	16 (88.9)		6 (60)	4 (66.6)	
Squamous cell carcinoma	3 (10.0)	2 (11.1)	NS	4 (40)	1 (16.7)	NS
Others	1 (3.3)	0 (0.0)		0 (0.0)	1 (16.7)	
Number of metastatic sites						
≤ 2	25 (83.3)	7 (38.9)	**<0.01**	7 (70)	4 (66.6)	NS
> 2	5 (16.7)	11 (61.1)		3 (30)	2 (33.3)	
Pembrolizumab treatment						
Monotherapy	17 (56.7)	15 (83.3)	NS	5 (50)	3 (50.0)	NS
Plus chemotherapy	13 (43.3)	3 (16.7)		5 (50)	3 (50.0)	
PFS (median days)	19.3 months	2.3 months	**<0.001**	10 months	2.7 months	**<0.001**
OS (median days)	35.7 months	3.4 months	**<0.001**	NA	3.9 months	**<0.001**

Abbreviations: NR, non-responders; R, responders; SD: standard deviation.

Regarding the clinical characteristics of R and NR patients it's important to mention that 61.1% of NR had more than two metastatic sites *versus* 16.7% for the R group (Fisher test; *p*-value< 0.01). In addition, the R group showed

significant better PFS (19.27 *versus* 2.3 months, respectively) and OS (35.7 *versus* 3.4 months, respectively) than NR (Table 4.1).

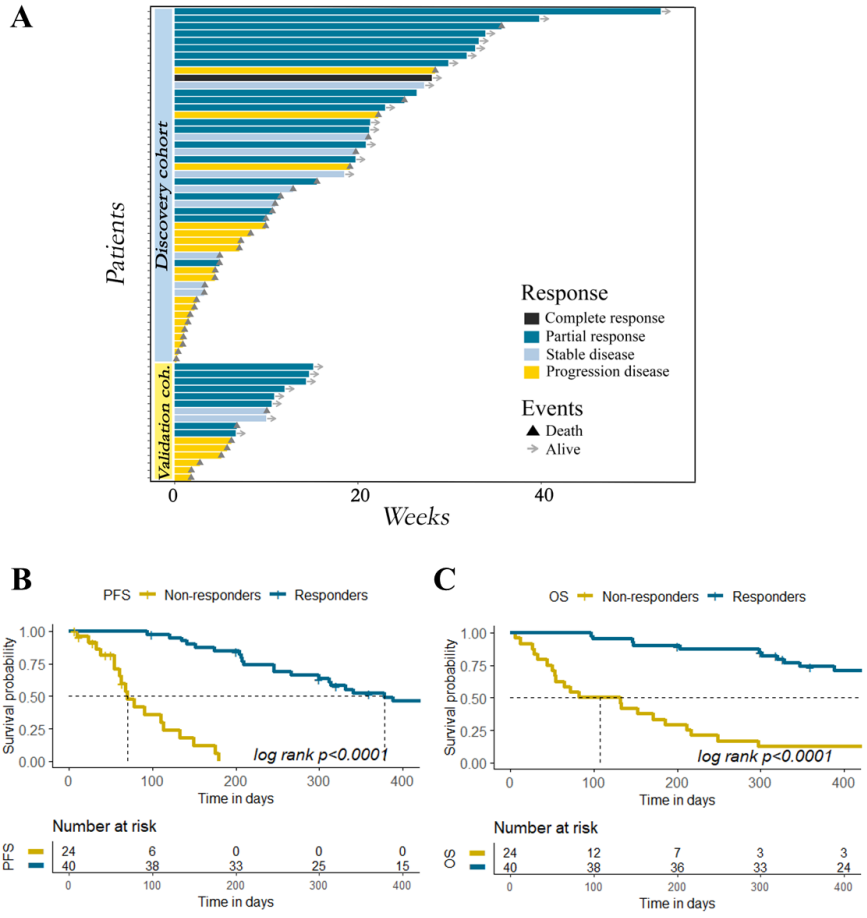

Figure 4.1. (A) Swimmers' plot on patients showing the response of therapy. The total length of each bar indicates the duration of survival from the diagnoses. (B-C) Kaplan-Meier plots show highly significant differences between responders and non-responders to pembrolizumab treatment in PFS (B) and OS (C).

In the validation cohort, the analysed samples were taken from 16 patients with advanced NSCLC undergoing first-line pembrolizumab

treatment in monotherapy (n=8) or in combination with chemotherapy (n=8) (Table 4.1). 62.5% of patients were classified as R (including stable disease (n=2) and partial response (n=8)) and 37.5% of patients were denominated NR (progressive disease; n=6). The validation cohort presented similar characteristics than the discovery cohort, except sex distribution (Table 4.1). Similar to the previous cohort, R and NR presented significant differences in the PFS and OS rates.

3.2 Global proteomic quantitative analysis of NSCLC blood samples

One hundred seventy-one samples from 64 NSCLC patients were analysed using high-resolution mass spectrometry (Figure 4.2) to identify as many proteins as possible into the plasma samples. First, to obtain quantitative protein information from SWATH-MS, we generated an extensive spectral, based on pooled samples and the online Human Pan-Human library. Thus, our final spectral library, called NSCLibrary, contained 7,115 unique proteins. Next, we analysed each separated sample against our spectral NSCLibrary and we extracted quantitative data from the discovery cohort, a set of 18 non-responder and 30 responder patients. An average of 6,483 proteins/sample using a minimum of ten peptides/protein and a 1% false discovery rate (FDR) on the peptide and protein level were found. Next, after sample normalization by quantile method and sample filtering, we quantified a total of 6,364 unique proteins, of which 2,418 had observations in all samples. In a second step, 37 plasma samples from 16 NSCLC patients corresponding to validation cohort, were also analysed using the same protocol, obtained an average of 6,325 proteins/sample.

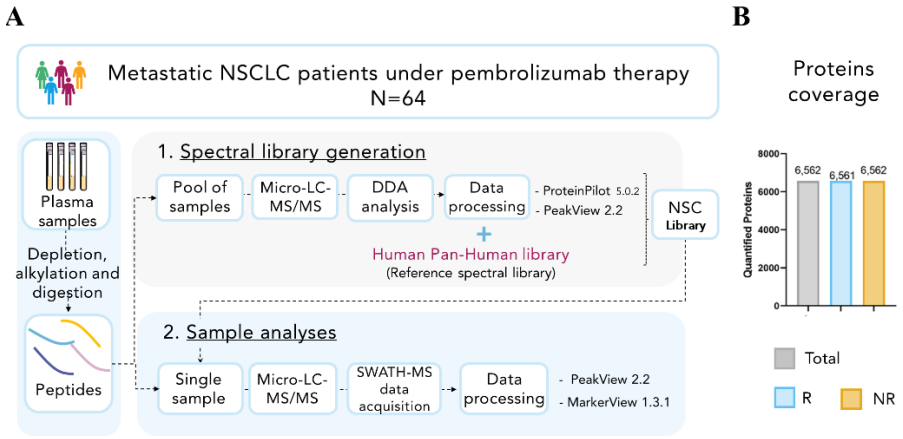

Figure 4.2 Proteomic of NSCLC response to pembrolizumab treatment. (A) The proteomic workflow involved plasma extraction from blood samples of 48 NSCLC patients undergoing pembrolizumab Then, 30 µl of plasma samples were employed for proteins extraction. The proteins were trypsin-digested to obtained peptides (fractionation). A pool of total peptides samples was employed to generate a spectral library using a DDA method. Finally, pooled peptides of each sample were analysed using a SWATH-MS method employing the previous spectral library and the Human Pan-Human Library. (B) Total number of proteins quantified in each group of patients.

3.3 Plasma proteome in NSCLC patients is associated with immunotherapy response

Aiming to identify a protein signature associated with response to immunotherapy, we compared the plasma protein expression profile of 30 R and 18 NR from the first cohort of 48 NSCLC patients. Importantly, there were no differences in the proteins' coverage between R and NR group (Figure 4.2B). We applied Student's t tests with a nominal *p*-value cut-off of 0.05 (*p*-value <0.05) and we identified 324 DEPs. Of them, 172 proteins appeared upregulated while 152 were downregulated in R *versus* NR (Figure 4.3A-B).

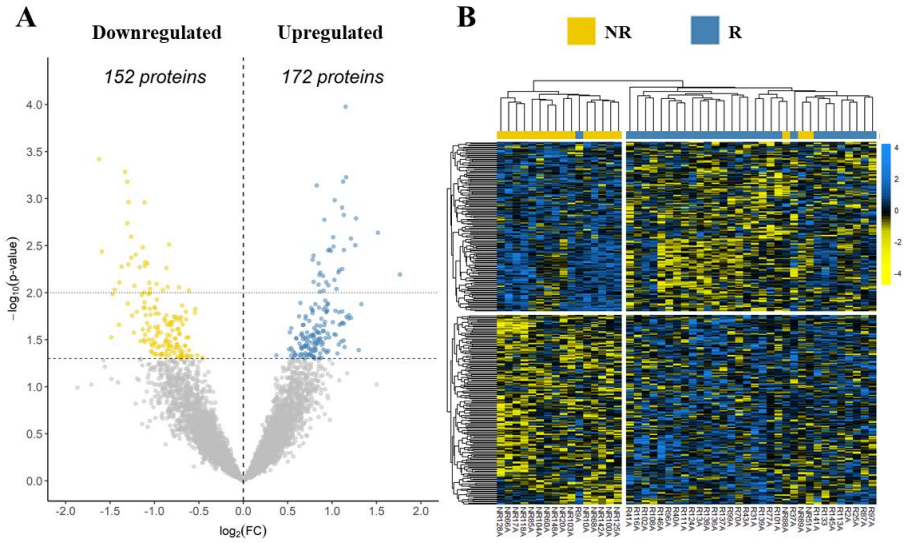

Figure 4.3. (A) Volcano plot of differentially expressed proteins at baseline. Upregulated proteins are represented in blue while downregulated proteins are represented in yellow. **(B)** Heatmap of 324 differentially expressed proteins at baseline (*p*-value <0.05), that discriminate between R and NR patients to pembrolizumab therapy.

We conducted functional enrichment analyses with the 324 DEPs found between R (172 proteins) and NR (152 proteins) to identify the biological functions and relevant pathways involved in the sensitivity to pembrolizumab therapy. Global analyses not reported clear results about the GO process involved with the 324 DEPs in conjunction (Figure 4.4).

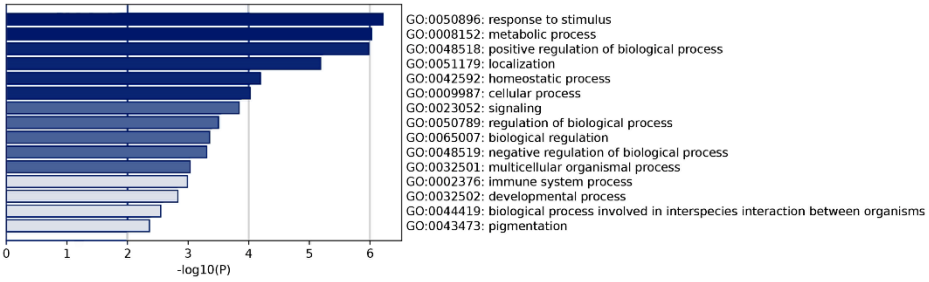

Figure 4.4. Bar graph for viewing of the top 15 enriched GO process involved the 324 DEPs. A colour scale represents statistical significance.

Briefly, GO pathways comparing both groups reported that the 172 proteins more present in the R group were associated with different processes such as metabolic and cellular processes or immune system process, in contrast with the pathways obtained in NR group. Of note, the immune system process (GO:0002376) was enriched exclusively in the R group. (Figure 4.5).

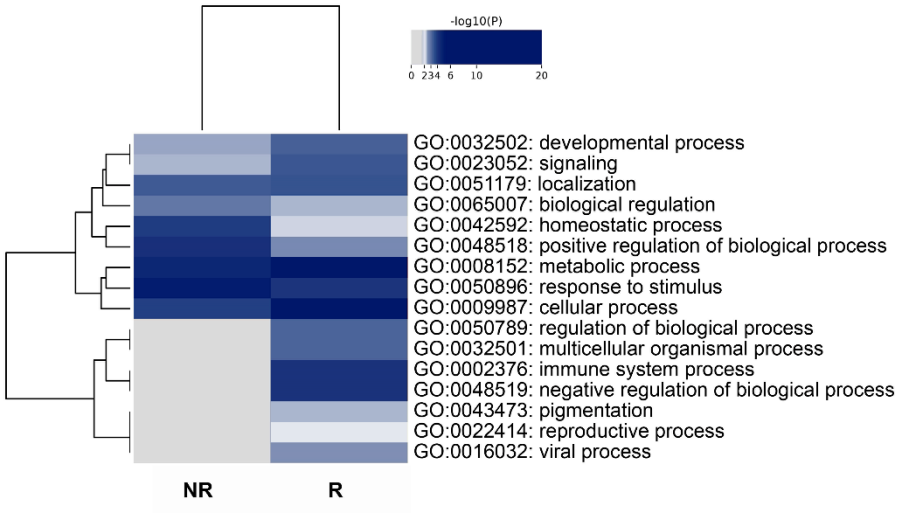

Figure 4.5. Heatmap showing the top enrichment clusters, one row per group, using a colour scale to represent statistical significance. Gray colour indicates a lack of significance.

In addition, proteomaps clustering the differentially expressed proteins according to their Genes and Genomes KEGG pathway annotations (Figure 4.6), reported discrete differences between both groups. Despite the results should be taken with caution, R group seem to be characterized by higher levels of metabolic proteins than NR.

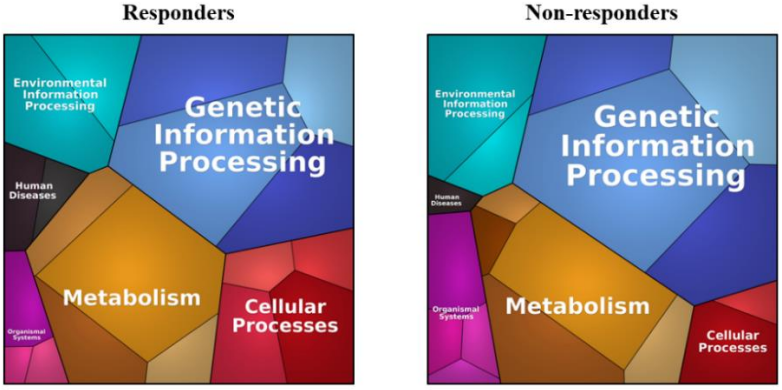

Figure 4.6. Proteomaps that showed the functional differences between R (left) and NR (right) to immunotherapy. Each polygon corresponds to a single KEGG pathway, and its size correlates with the ratio between both groups.

3.4 Identification and development of a model that enables the prediction of response to pembrolizumab.

To develop a model that allows us to predict immunotherapy response we selected the DEPs (n=66) with a tight *p*-value (*p*-value <0.01) between R and NR patients. Thirty-six of these proteins were more expressed in the R group, while 30 were more expressed in the NR group, performing a good discrimination between both groups (Figure 4.7).

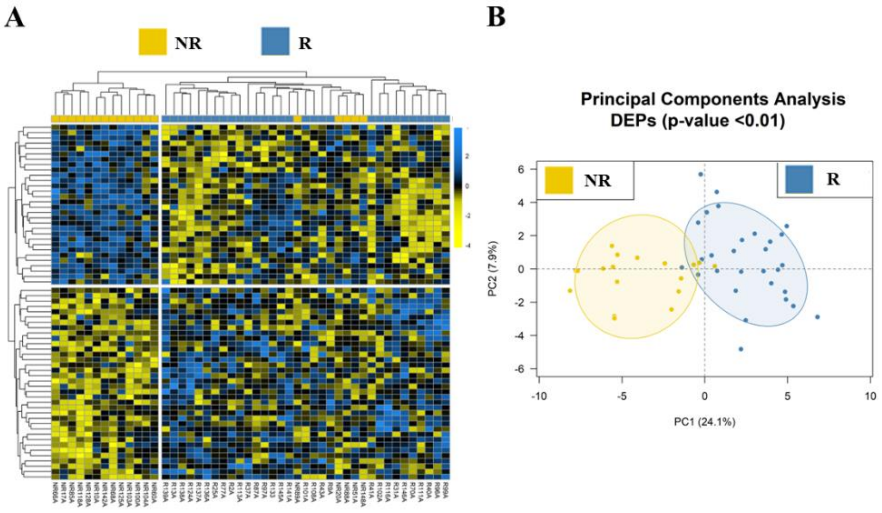

Figure 4.7. (A) Heat-map of differentially expressed proteins at baseline. (B) PCA analysis showing the separation of samples from responders (blue) and non-responders (yellow) to pembrolizumab therapy according the 66 DEPs found by LC-MS/MS analysis.

Then, we aimed to create a proteome signature that could accurately distinguish between these patient groups with a minimal number of proteins using stepwise forward variable selection method based on AIC. Thus, a predictive model composed of 7 proteins was selected to effectively discriminate R and NR. Of these 7 selected proteins, 5 of them were more expressed in NR group and 2 of them were more expressed in the R group. The characteristics of the selected proteins are specified in table 4.2.

Table 4.2. Characteristics of the 7 proteins that allow us to predict immunotherapy response in advanced NSCLC patients.

Protein and Uniprot reference	Name	Gene	Up or Down
SPTN2_O15020	Spectrin beta chain, non-erythrocytic 2	SPTBN2	Up
PGTA_Q92696	Geranylgeranyl transferase type-2 subunit alpha	RABGGTA	Up
FIL1L_Q4L180	Filamin A-interacting protein 1-like	FILIP1L	Down
ATG9A_Q7Z3C6	Autophagy-related protein 9A	ATG9A	Down
LZTL1_Q9NQ48	Leucine zipper transcription factor-like protein 1	LZTL1	Down
HPS5_Q9UPZ3	BLOC-2 complex member HPS5	HPS5	Down
DCDC2_Q9UHG0	Doublecortin domain-containing protein 2	DCDC2	Down

Single proteins showed a good discriminatory power to distinguish responders to non-responders (AUC= 0.72-0.78). In addition, in ROC analyses their combination showed a high AUC (AUC= 1). (Figure 4.8), in contrast with the results obtained with the PD-L1 expression on tumour tissue (AUC= 0.638). PD-L1 expression showed a lower predictive value than our proteins and their combination (Figure 4.8C).

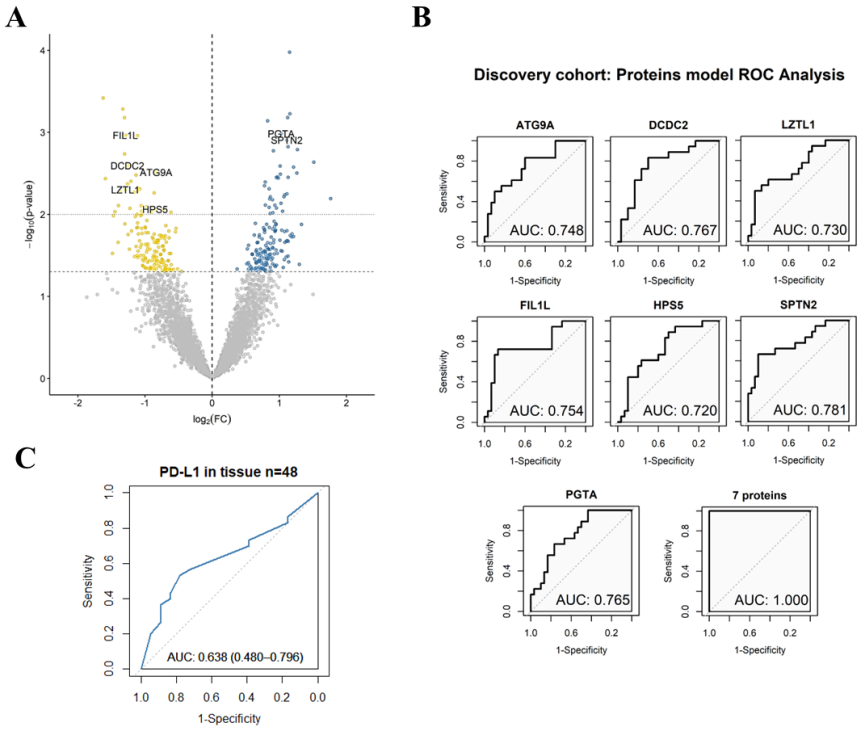

Figure 4.8. (A) Volcano plot showing the 7 proteins of our predictive model. (B) ROCs curves of each protein and the combination in the discovery cohort. (C) ROC curve analyses of the PD-L1 expression on tumour tissue. Abbreviations: AUC, area under the curve; FC, foldchange.

Next, an internal validation was performed using an additional cohort of 16 NSCLC patients (Table 4.1), from whom blood samples were collected in EDTA tubes instead CellSave tubes but analysed with the same methodology than the discovery cohort. The protein levels of our proteomic signature were analysed between R (n=10) and NR (n=6). No significant differences were found between both groups, likely due to the small size of the cohort. Nevertheless, ROC analyses were conducted to combine the 7 proteins of the model, which showed a perfect discrimination rate (AUC=1) in the validation cohort (Figure 4.9).

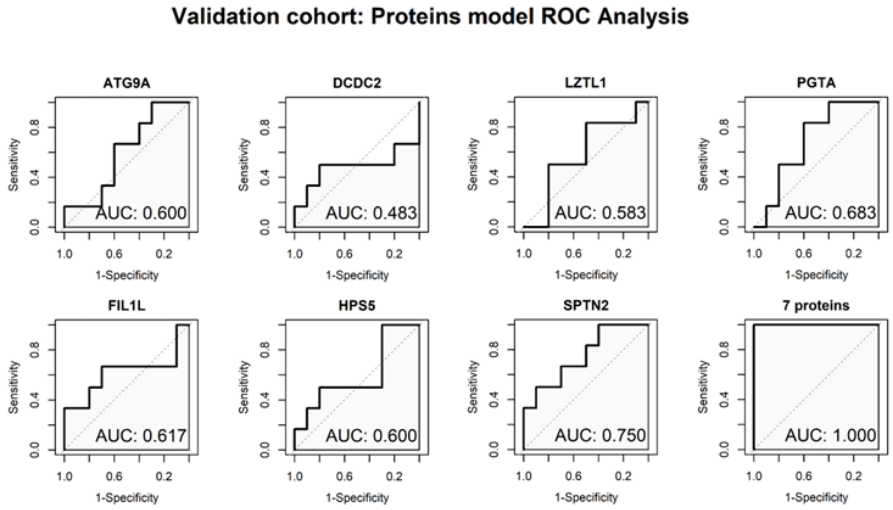

Figure 4.9. ROC curves of each protein and the combination in the validation cohort.

3.5 The proteome signature was associated with progression free survival and overall survival in NSCLC patients.

To explore the prognostic significance of the 7 selected proteins, we investigated their expression levels in association with PFS and OS in our global cohort. Kaplan-Meier curve analysis showed that low levels of ATG9A and high levels of SPTN2 were significantly associated with longer PFS (log-rank $p < 0.001$ and log rank $p = 0.017$ for ATG9A and SPTN2, respectively) in NSCLC patients. Additionally, low levels of HPS5 showed a trend towards being associated with longer PFS (log-rank $p = 0.054$) and were significantly associated with longer OS (log-rank $p < 0.001$). Low expression levels of DCDC2 were also significantly associated with longer OS in our global cohort (log-rank $p < 0.01$) (Figure 4.10). No association with the patients' survival was found for the proteins PGTA, FIL1L, and LZTL1.

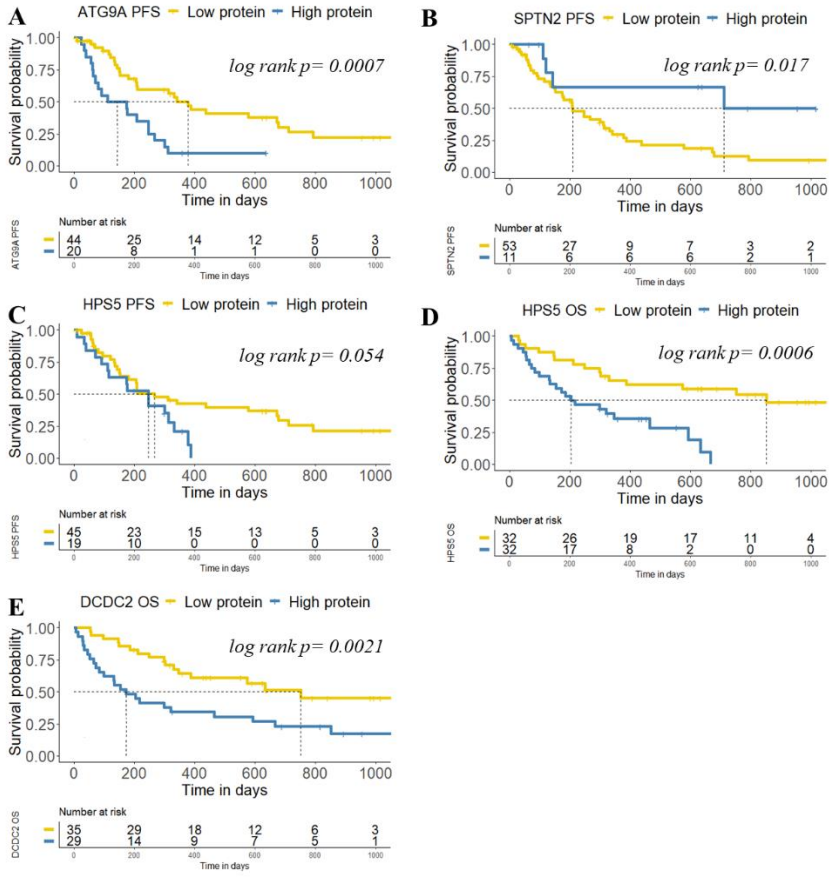

Figure 4.10. Kaplan-Meier survival analysis of ATG9A, SPTN2, HPS5 and DCDC2 proteins levels at baseline. Kaplan-Meier plots of PFS (A-C) and OS (D-E) showed significant associations between proteins levels before start therapy and prognosis in metastatic NSCLC under immunotherapy regimens.

3.6 Dynamics of the Proteome Signature during pembrolizumab therapy

Next, 107 plasma samples collected at different time points were analysed to investigate whether our protein model undergoes changes during immunotherapy treatment. A total of 46 samples were analysed at 6 weeks, 36

at 12 weeks, and 25 at the time of disease progression. The results obtained showed that proteins levels did not show significant changes during different time points of the immunotherapy regimen, neither in the overall cohort nor when separated by response groups (Figure 4.11).

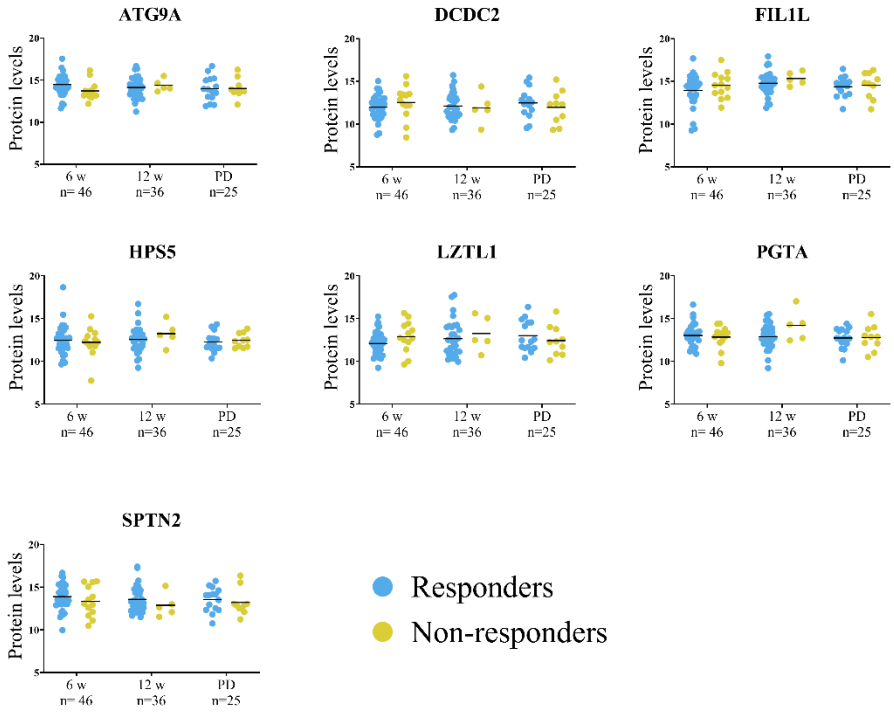

Figure 4.11. Protein levels ATG9A, DCDC2, FIL1L, HPS5, LZTL1, PGTA and SPTN2 were measured at different time points during the immunotherapy regimen. Abbreviations: PD, progression of disease.

ROC curves analyses at 6 weeks and at 12 weeks were also performed. In all time points, our model allows us to predict therapy response with an AUC >0.70. Importantly, at 12 weeks after start therapy, a good discriminatory rate was found (AUC=0.935) (Figure 4.12), suggesting the

potential value of the model to determine the response to immunotherapy also during the treatment.

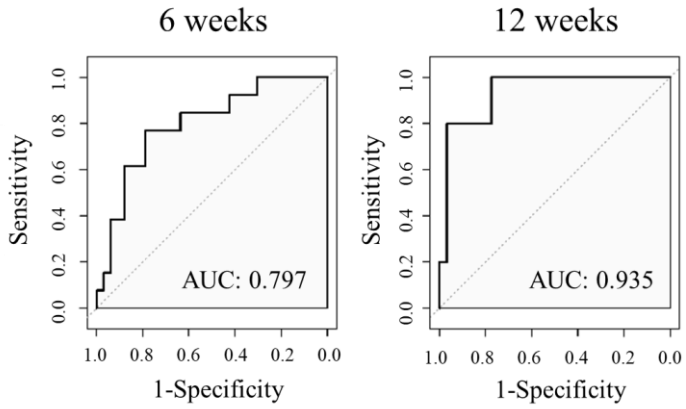

Figure 4.12. ROC analyses with the protein model at different time points during the immunotherapy regimen (at 6 weeks and at 12 weeks after start therapy).

4. DISCUSSION

Immunotherapy, in particular ICIs, have improved survival rates in cancer patients, including those with NSCLC. However, it remains unclear how to select those patients who will respond to this therapy. PD-L1 expression on tumour tissue has been reported as a possible biomarker, but some patients without PD-L1 expression also respond to ICIs (381,382). TMB, which refers to the number of somatic mutations in tumours, has recently emerged as another possible biomarker in the immunotherapy field. Nevertheless, there are several challenges for clinical implementation of TMB, especially in standardizing detection methods and appropriate thresholds by tumour type (383,384). MSI, usually based on immunohistochemistry analyses for four mismatch repair proteins, may represent a novel biomarker to select patients who will benefit from ICIs

therapy in several cancer types (70); however, this alteration is scarcely present in lung cancer (385). The search for new predictive and prognostic biomarkers for ICI therapies will improve patient selection. Proteomics, the study of the entire set of proteins expressed in a cell, tissue, or individual, has become an important field in molecular sciences, as it provides valuable information on the identity, expression levels, and modification of proteins (386). In this work, we hypothesized that plasma proteome analyses could have predictive and prognostic value in newly diagnosed NSCLC patients who started pembrolizumab therapy. We employed SWATH-MS, a new technology that allows detection of tens of thousands of peptides in a single injection and enables identification and quantification of circulating proteins. Previously, several studies in breast (387), bladder (388), and endometrial cancer patients (389), among others, have shown the potential of this emerging technology.

Importantly, our study apport a dataset that might serve the scientific community as a resource of clinical proteomic data in lung cancer samples, previously reported in melanoma (390) and ovarian cancer (391,392).

More importantly, the analyses had allowed us to identify 324 DEPs between R and NR, showing the potential value of proteomic analysis to identify differences between both groups. Previously our group has employed the methodology here described to study the red blood cells population proteome in breast cancer patients (393). A similar study focuses on breast cancer reported that this approach was useful to determine DEPs in serum samples associated with the response to neoadjuvant chemotherapy. The authors of this study described three proteins specially correlated with resistance to this therapy (387). Some other studies focused on melanoma

patients, also reported the potential of proteomic technologies to identify DEPs and predict therapy response in tissue (390) and plasma samples (365).

Regarding the enrichment analyses of biological functions and pathways, and even though the results should be interpreted with caution, we observed a high degree of variability in GO processes among the 324 DEPs between R and NR groups, indicating the significant heterogeneity present in the plasma samples. These samples can reflect both individual characteristics and tumour features, as well as the tumour microenvironment (394). Next, comparing both groups, we found that the process involved in immune system was enriched exclusively in R, as expected given the known role of the immune system in response to ICI therapies. More analyses should be performed to confirm these results. In KEGG pathways, R appear to have higher levels of metabolic proteins than NR patients, but caution should be exercised when interpreting the results due to the lack of statistical significance. Nevertheless, our findings are consistent with those of Harel et al. (390) in their study of melanoma patients. Their research aimed to investigate why most cancer patients do not respond to immunotherapy by profiling the proteome of tumour tissue samples from advanced melanoma patients undergoing either TIL-based or anti-PD1 immunotherapy. They found 414 DEPs and 636 DEPs between responder and non-responder patients in the TIL and anti-PD1 immunotherapy cohort, respectively. Pathway analyses revealed that responders had higher oxidative phosphorylation and lipid metabolism, which increases melanoma immunogenicity and sensitivity to T cell-mediated killing. These findings suggest that the metabolic state of melanoma may play a role in the response to immunotherapy and could lead to improved therapeutic responses in the future. A similar process may be occurring in our NSCLC patients.

Next, a predictive model to identify proteins that can be associated with the response to immunotherapy treatment was developed, showing that the combination of 7 proteins can predict the response to immunotherapy with high sensitivity and specificity, in a discovery cohort and, in addition, in a validation cohort. Regarding the proteins, five of them were more expressed in NR than R group: ATG9A, DCDC2, HPS5, FIL1L and LZTL1. The ATG9A protein is a transmembrane protein that plays an important role in the formation and regulation of autophagosomes, which are cellular structures involved in the process of autophagy. This protein is localized on the membranes of the endoplasmic reticulum and Golgi (395). A recent study characterizes novel functions of ATG9A as component of a TNF-induced cell death checkpoint (396). DCDC2 is a protein expressed in the brain that has been linked to the development of cognitive skills such as reading and language processing. DCDC2 has been found to be localized to the cilia of neurons in the developing brain, where is involved in the control of ciliogenesis and ciliary length (397,398). In addition, DCDC2 seems to play a role in the inhibition of canonical Wnt signaling pathway (399). HPS5 is a protein that plays a crucial role in the biogenesis and function of lysosome-related organelle and may be involved in the regulation of general functions of integrins (400). On the other side FIL1L is a protein that acts as a regulator of the antiangiogenic activity on endothelial cells. The overexpression in endothelial cells leads to inhibition of cell proliferation and migration and increase in apoptosis (401). In oncology field, FIL1L has been previously reported as a protein downregulated in ovarian cancer (402). LZTL1 regulates ciliary localization of the BBSome complex (403) and may have tumour suppressor function in several primary cancer types (404).

In another hand, PGTA and SPTN2, showed higher levels in R than NR group in our study. Both proteins have been less explored. Regarding PGTA it is believed to play a role as catalytic protein (405). In contrast, SPTN2 probably plays an important role in neuronal membrane skeleton.

To our knowledge, this is the first time that these proteins have been associated with immunotherapy response in NSCLC patients.

Importantly, our proteomic signature (considering the combination of the 7 proteins or the use of single proteins) showed a stronger value to predict immunotherapy response than the actual biomarker, the PD-L1 expression in tumour tissue. Hence, the proposed model could be useful to select which patients can be treated with immunotherapy, and in which patients, an alternative therapy should be considered. In addition, survival analyses showed that low levels of ATG9A, DCDC2, and HPS5 were associated with longer PFS or OS rates, while low levels of SPTN2 were significantly associated with worse OS.

In another hand, longitudinal samples were analysed in the global cohort to investigate the value of the predictive model during immunotherapy. Although no significant differences were found between the R and NR groups during therapy, ROC analyses at 6 and 12 weeks showed a good discriminatory rate between the two groups. The determination at 6 weeks could assist clinicians in detecting an early response to therapy in NSCLC patients or in cases where sample extraction was not possible at baseline. Interestingly, at 12 weeks a higher AUC was found with our model, which could help clinicians determine treatment response in cases where patients experience pseudoprogressions through imaging techniques (406), suggesting

the possibility to use in a complementary manner both approaches during ICIs therapies. However, it's important to note that larger studies should be conducted to provide a more detailed and conclusive interpretation.

Finally, some limitations should be considered in the present study. First, a validation cohort with more patients should be employed to confirm the predictive value of our model and their utility during immunotherapy. Next, to implement a technology based on quantifying the 7 protein levels into clinical routine, a simpler approach such as an ELISA assay would be more appropriate. Thus, an analytical validation employing an ELISA assay should be performed.

In summary, the results derived from Chapter IV of this thesis confirmed that circulating proteins can be used as predictive and prognostic biomarkers in patients with metastatic NSCLC and allow us to detect a proteomic signature of 7 proteins (ATG9A, HPS5, DCDC2, PGTA, FIL1L, LZTL1, and SPTN2) which enables the selection of those patients who will benefit from anti-PD1 immunotherapy.

OVERALL DISCUSSION

OVERALL DISCUSSION

The term “Cancer” englobes more than 200 different types of disease which are characterised by uncontrolled growth and spread of abnormal cells. Nowadays, cancer remains to be a top cause of mortality worldwide, second only to cardiovascular diseases (407). In Spain, it is estimated that 112,000 deaths in 2020 were due to solid tumours. Unfortunately, and despite numerous advances in early cancer diagnosis, new therapies and better patients’ management, the future numbers are not expected to be better. By 2040, it is estimated more than 159,000 deaths in Spain and 16.1 million deaths worldwide (an increment of 39% regarding the 6.3 million deaths in 2020 worldwide) (408). In the last few years, numerous social campaigns around the world have highlighted the importance of cancer research, as critical in the fight against this devastating disease. A better understanding of the disease and the mechanisms behind its progression can lead to improved early detection and higher survival rates. In addition, improving the quality of life for those who have already been diagnosed with cancer, by finding ways to manage the side effects of treatments and refining therapy selection is an important challenge.

In recent years, precision medicine is becoming increasingly important in the fight against cancer, having the potential to lead to better diagnoses, improve therapies selection, and ultimately, higher survival rates. Precision medicine is an evolving field that combines the latest advancements in genetic research and technology to create targeted and personalised treatment plans for each patient. The goal is to provide the most effective and least toxic

treatments, while reducing the risk of side effects as it has the potential to revolutionise the way that patients are diagnosed and treated (409). In this context, as we extensively described in the present manuscript, **liquid biopsy** provides a non-invasive way to obtain information about genetic makeup and the specific molecular alterations characterizing the tumours. This information can then be used to create a personalised treatment plan for each patient as well as monitoring the disease in a non-invasive way. By combining the principles of precision medicine with the latest advancements in liquid biopsy technology, professionals can work towards providing the most effective and least toxic treatments for each patient. As a matter of fact, in the last 20 years, there have been numerous research works exploring the potential of liquid biopsy to reach precision medicine. Figure 25 shows the increasing number of publications published per year, in PubMed, containing the terms "precision medicine" and "liquid biopsy".

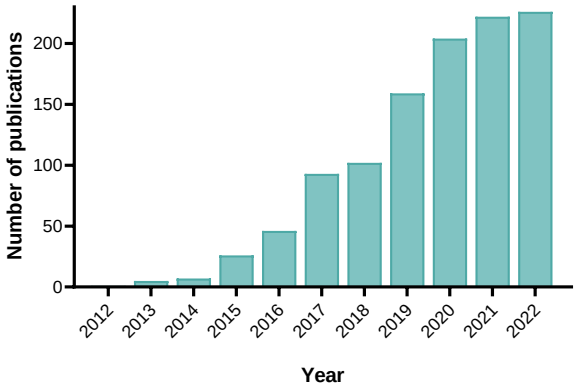

Figure 25. Number of publications per year containing the terms "precision medicine" and "liquid biopsy" in PubMed between 2012 and 2022.

In 2018, a blood test named CancerSEEK highlighted the importance of using liquid biopsy samples in cancer screening (410). Indeed, the test showed potential value to early detection of eight common cancer types through assessment of the levels of circulating proteins and mutations in cfDNA. In agreement, numerous studies have reported in the last years the potential value of different liquid biopsy components to guide treatment decisions, monitor disease progression, detect minimal residual disease and predict recurrence (411).

The present thesis focuses on advanced lung cancer patients, the leading cause of death among solid tumours worldwide. The value of different liquid biopsy components (ctDNA, CTCs, total cfDNA and circulating proteins) to improve the management of these patients was further investigated. Overall, 250 lung cancer patients were enrolled in the current thesis. Figure 26 showed the 250 patients subdivided according to lung cancer type, and treatment regimen.

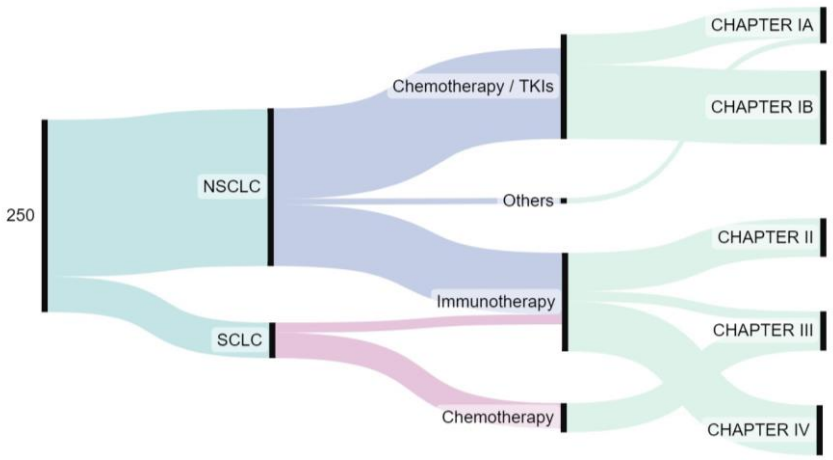

Figure 26. Sankey diagram showing the total lung cancer patients included in the present thesis, subdivided by lung cancer type, stage and therapy.

NSCLC serves as a prime example of the move towards precision medicine in cancer treatment. Fortunately, nowadays there are numerous options and treatments available for the management of NSCLC patients. Although some blood-based technologies have been already approved by the FDA to guide the therapy selection (see Introduction section, point 2), the prioritization of the most helpful for each case is not always clear. In the present thesis, one of the first objectives was to investigate and select the more accurate liquid biopsy-based technology to choose those patients that will benefit from EGFR and MET inhibitors. Despite ctDNA can be found in a variety of fluids, including urine, peritoneal fluid or cerebrospinal fluids (CSF) (412–414), plasma remains the preferred source (415). Thus, two different platforms to analyse specific mutations in ctDNA derived from blood samples were studied (CHAPTER I).

In CHAPTER I.A, advanced NSCLC patients were analysed by Idylla™ technology, a qPCR-based method, to detect *EGFR* mutations in plasma samples. In contrast, a ddPCR-based method was employed in CHAPTER I.B to detect *MET* amplification.

It is well known that the sensibility of a qPCR method such as Idylla™ technology, is lower than other technologies such as ddPCR or some NGS approaches (154). Nevertheless, we hypothesised that, in some cases, a qPCR determination can be useful and present the advantage to be more rapid and simple than other approaches. Results obtained in the first chapter of this thesis showed a good overall concordance with NGS method (93.3%) or BEAMing technology (88.9%) in our cohort of metastatic cancer patients, demonstrating its utility to have a fast and accurate results to genotype the tumour despite the lowest sensitivity. Therefore, our results demonstrate that

Idylla™ technology represents an alternative to the classic qPCR or ddPCR to determine the EGFR status in NSCLC patients, always considering its limitation for detecting ctDNA presence in tumours low cfDNA shedders, since cases below 0.5% of VAFs were found as false negatives in our study. Thus, the EGFR characterization on cfDNA in patients with low tumour burden (146) or metastasis located only in brain, which release lower DNA amount, should be attempted with a high-sensitive technology such as the ddPCR. Also, in cases where the input of cfDNA is low the preference should be the most sensitive technology. Our results incise on the importance of standardising the method for the ctDNA genotyping and pointed out to the use of the qPCR assay as a first *EGFR* screen to avoid costs and long result-times. In addition, thanks to the simple workflow that Idylla™ technology offers, it can be easily implemented into clinical routine.

In CHAPTER I.B, blood samples of NSCLC patients were analysed in order to detect *MET* amplification, an alteration associated with acquired resistance to EGFR inhibitors (416). In this case, due to the detection of CNA needs higher sensitivity and sensibility than a qPCR method, a ddPCR blood-based test was developed. High detection rate of *MET* amplification was found in patients with high cfDNA levels suggesting that those patients who present high tumour burden and, in addition, who received several lines of TKIs are likely to present *MET* amplification, so they are good candidates to make the MET assessment in cfDNA looking for therapy alternatives. Importantly the ddPCR assay employed in the present thesis can represents a transversal clinical tool as it can be applied in different tumour types.

Thus, in the first chapter of this thesis (CHAPTER I.A and I.B), we showed the utility of two different blood-based technologies to detect ctDNA

alterations: a qPCR method to detect *EGFR* mutations and ddPCR to detect *MET* amplification. These minimally invasive determinations can help to make important therapeutic decisions. Idylla™ assay could be employed as a first screen in metastatic NSCLC patients to select who will benefit from TKI based therapies and to monitor tumour evolution. In the case of *MET* amplification, ddPCR method represents the most sensitive strategy to identify this resistance mechanism against the activity of EGFR inhibitors in patients who have undergone several lines of treatment. In both cases, blood-based technologies allow to detect clinically relevant alterations in non-invasive samples and provide a more complete image of the disease, since information from metastatic locations is also evaluated with both strategies.

However, although qPCR and ddPCR methods allowed us to detect specific mutations in ctDNA of blood samples, one limitation of these techniques is the requirement of previous information about the tumour and the mutations characterising this tumour. For this reason, PCR-based techniques to interrogate ctDNA are commonly employed to select targeted therapies or detect mutations associated with resistance in clinical context where these mutations are clearly defined. Thus, the lack of clear driver genes or a high genetic heterogeneity make more difficult the clinical translation of the ctDNA assessment in some tumours, including for example SCLC. To face this limitation, in the present thesis we wanted to explore the possible clinical interest of quantifying total cfDNA levels in advanced lung cancer patients as a simpler and cost-effective analysis than ctDNA determination. CfDNA is released into the bloodstream through apoptosis or necrosis (among other mechanisms; see Introduction section, point 2 to expand the information) of both normal and tumour cells. cfDNA from normal cells is found in plasma at

low levels (347). In contrast, tumour cell turnover is higher than that of normal tissue, therefore, cancer patients tend to have higher total amounts of cfDNA than healthy patients (347).

In CHAPTER II and CHAPTER III, the total cfDNA levels in advanced NSCLC and SCLC patients were quantified using a qPCR-based method. As result, we validated a simple blood-based qPCR tool that allowed us to quantify total cfDNA levels with high sensitivity and specificity and discriminated cancer patients from healthy controls. Interestingly, some studies similar to our approach, reported a good discrimination between melanoma patients (stage III and IV) and healthy controls based on cfDNA levels quantification by Qubit method (AUC=0.72) (417). Similar results were also obtained among bladder cancer patients and healthy controls (418) interrogating cfDNA content. In concordance with bibliography, results derived from this thesis reported that total cfDNA levels (based on the detection of *hTERT* gene) from lung cancer patients (both advanced NSCLC and SCLC patients) were higher than cfDNA levels in a control population cohort, showing a good discriminatory power (AUC=0.88) (Figure 27). Moreover, in SCLC patients cfDNA levels were higher than in NSCLC patients, in concordance with the aggressiveness that characterized this lung cancer type.

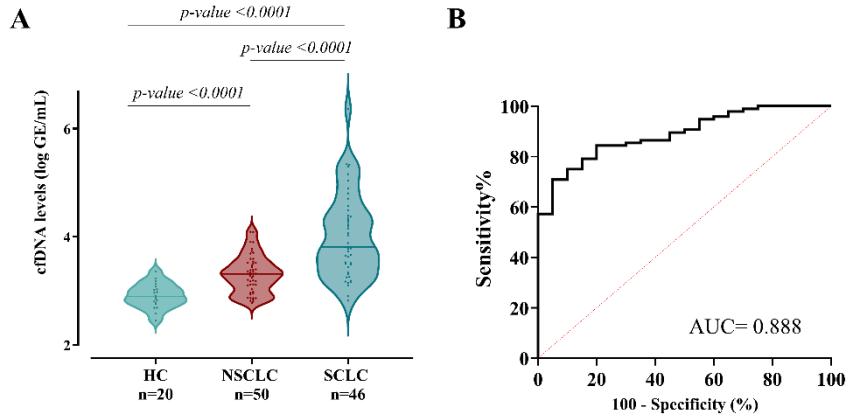

Figure 27. Total cfDNA levels in lung cancer patients and healthy controls. (A) Boxplot of cfDNA levels in NSCLC, SCLC, and healthy controls (Mann-Whitney test). (B) ROC showing the discriminatory value of cfDNA levels to discriminate against lung cancer patients versus healthy controls (AUC=0.8885).

In both lung cancer types high cfDNA levels before therapy onset were determined as a negative prognostic factor in terms of PFS and OS in NSCLC patients treated with immunotherapy and in SCLC patients treated with immunotherapy or immunotherapy in combination with chemotherapy. According to our results, several studies have reported high cfDNA levels as a negative prognostic factor in other cancer types such as melanoma (417,419), colorectal (420), prostate (421) and bladder cancer (418), confirming the interest of quantify total cfDNA levels independently of the value of the ctDNA assessment.

In addition, we reported that cfDNA dynamics provides predictive and prognostic information in both NSCLC patients under immunotherapy treatment and SCLC under immunotherapy or chemotherapy regimen. In the first case, we described a prognostic and predictive value of cfDNA levels 12 weeks after therapy onset. In SCLC, cfDNA levels analysed 3 weeks after the

therapy administration had a prognostic role. The early results obtained in SCLC patients could suggest that due to the aggressiveness of this subtype, molecular changes can be detected earlier than in NSCLC. Results derived from this thesis are in accordance with a recent study, where quantitative changes in cfDNA values between baseline and time of radiological evaluation correlated with responses to therapy and relapse of disease in treatment-naïve patients with advanced NSCLC undergoing TKIs- and immunotherapy-based treatments (422). Another study showed the potential utility of quantifying cfDNA levels at 4 weeks. Indeed, elevated cfDNA levels at 4 weeks were reported as a negative prognostic factor for OS in metastatic castration-resistant prostate cancer treated with androgen receptor pathway inhibitor (421).

Together with cfDNA, CTCs constitute the main liquid biopsy biomarkers employed in the oncology field. CTCs can be shed from primary tumour tissue or different metastatic localizations, travel into the blood to future metastatic sites and represent a good option to capture the tumour heterogeneity in metastatic lung cancer patients (423). Moreover, several studies have shown that CTC numbers may serve as useful predictive markers of recurrence and survival in patients with solid tumours, including NSCLC (333,424). However, the widespread adoption of CTCs in routine clinical practice will require strong evidence of their analytic validity, clinical validity, and most importantly, their clinical utility (425,426). In NSCLC, the number of CTCs detected in the blood is usually low, around 1-10 cells. Some studies suggest that this low number can be due to CTCs in NSCLC may be under an EMT (427), therefore, finding a good platform that enables detection of all types of CTCs remains to be a challenge.

Taking this context in mind, in CHAPTER I.B and CHAPTER II, two different platforms were compared to investigate the best CTC isolation method in NSCLC patients: Parsortix system (Angle, Germany), a size-based method and, CellSearch® system (Menarini, Bologna, Italy) an EpCAM-dependent method (Figure 28). In concordance with bibliography, results derived from these chapters do not allow to define which platform is the best, since we obtained a high heterogeneity of the CTCs count determined with both technologies among patients. In another hand, different assays to detect the expression of MET and PD-L1 expression in CTCs were developed in both systems.

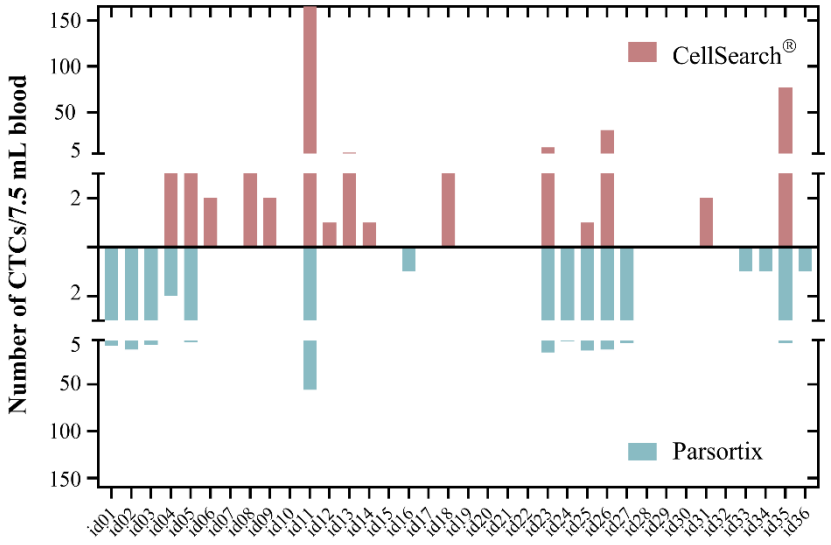

Figure 28. CTCs detected in 36 NSCLC patients employing two different isolation methods.

In addition, in CHAPTER III, we employed the CellSearch® system to detect CTCs in SCLC patients. Comparing the NSCLC cohort (from Chapter I.B and Chapter II) and SCLC cohort, we observed that in SCLC the number of CTCs detected was significantly higher than in NSCLC patients, closely

related to the higher stage and poorer prognosis of this tumour type (Figure 29). Indeed, in NSCLC 63.3% of patients did not present CTCs while in SCLC only 14.3% of patients did not present any CTCs.

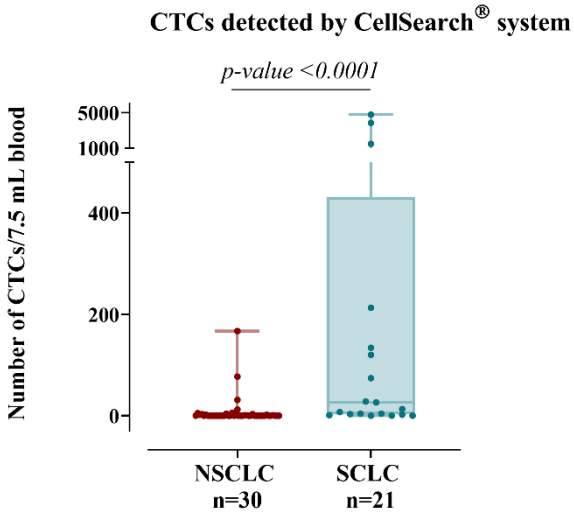

Figure 29. CTCs detected in NSCLC and SCLC cohorts using the CellSearch® system. SCLC patients presented statistically higher number of CTCs than NSCLC patients (*p*-value <0.001; Mann-Whitney test).

Survival analyses were performed in both subtypes to predict the prognostic role of CTCs in NSCLC under immunotherapy (n=30) and in SCLC under chemotherapy (n=21). Comparing both cohorts, very different cut-offs (≥1 CTCs in NSCLC patients and ≥150 CTCs in SCLC) at baseline were employed, due again to the higher aggressiveness that characterized to SCLC. The presence of CTCs has been associated with worse PFS and OS in NSCLC under immunotherapy regimens (n=30) and multivariate analyses showed their independence value. In contrast, in SCLC the prognostic role of CTCs was less clear. A discrete association between high CTCs levels and PFS was found but multivariate analyses did not show their independent value.

The results derived from these chapters suggest that epithelial CTCs play a more important role in advanced NSCLC patients in contrast with SCLC. A possible explanation could be related to the EMT. It's important to keep in mind that both in NSCLC and SCLC cohort, we detected CTCs with an epithelial phenotype. However, some CTCs could be not detected due to a more mesenchymal phenotype, correlated in some studies with poor clinical outcomes (428). In our cohort of SCLC patients, the faint prognostic impact found suggests than in this cancer type, mesenchymal CTCs could have a principal role in tumour evolution.

In another hand, in CHAPTER II and CHAPTER III, we evaluated the prognostic role of combining CTCs, cfDNA levels and clinical characteristics. We can conclude that the combination of CTCs and cfDNA in NSCLC or cfDNA and clinical variables in SCLC, represents a powerful tool for cancer management, offering valuable information for treatment decision-making and predicting patient outcomes in lung cancer patients, previously described in breast cancer (429) and bladder cancer (430) among others. Multimodality approaches, incorporating several components as those employed in the present thesis, seem to be the correct direction to reach a personalised medicine.

Last but not least, in CHAPTER IV, we characterize other liquid biopsy components, circulating proteins, showing their potential utility to select who patients will benefit from immunotherapy and which regimen is the most appropriated. Several benefits of using circulating proteins over CTCs and cfDNA have been proposed in the field of cancer research. Firstly, circulating proteins are typically easier to measure, makes them a more accessible and cost-effective biomarker for clinical use (431). In addition, circulating

proteins can provide information about the microenvironment surrounding the tumour, such as the immune response and inflammatory state, which may have important implications for treatment response and patient outcomes (387,432,433).

In our study we made a deep characterization of the plasma proteome of NSCLC patients receiving immunotherapy. The results obtained confirmed that circulating proteins can be useful as predictive and prognostic biomarkers in metastatic NSCLC patients and allowed us to identify a proteomic signature with promising value to select who patients will benefit most from immunotherapy regimens. Finally, a proteomic model consisting of 7 proteins was developed, which enables the prediction of immunotherapy response before the start of therapy and at 6 and 12 weeks after starting pembrolizumab therapy.

To sum up, metastatic lung cancer is a complex and heterogeneous disease that requires a multidisciplinary approach for its diagnosis and management. Omics, including genomics, and proteomics are powerful tools for identifying biomarkers and therapeutic targets in cancer. Furthermore, liquid biopsy, which involves the analysis of CTCs, cfDNA and molecules in the blood, has emerged as a non-invasive and highly sensitive tool for the detection of cancer and monitoring treatment response, where each component provides unique information about the tumour and its microenvironment. The combination of these liquid biopsy markers with omics technologies and importantly, with clinical data, such as patient history and imaging, offers a powerful approach for understanding the complexity of metastatic lung cancer and developing personalized treatment strategies.

Based on the results of this thesis, we can conclude that the use of different liquid biopsy components along with clinical characteristics can help identify the most suitable therapy for each lung cancer patient, leading to precision medicine. Given the differences between individuals and the heterogeneity of lung cancer, liquid biopsy components, alone or in combination, can provide a comprehensive analysis of the cancer disease, leading to improved patient outcomes. A single blood sample is a powerful tool that enables us to gain a better understanding of lung cancer and anticipate cancer evasion mechanisms, thereby improving survival times in patients with metastatic lung cancer. Nevertheless, some limitations should be considered. Firstly, larger cohort studies should be conducted to validate the results obtained in the present thesis, particularly in the cohorts where CTC populations were analysed. Secondly, alternative markers in Parsortix assays should be considered to detect mesenchymal CTC populations to draw more conclusive results about CTC phenotype. Additionally, other clinical parameters, such as a more comprehensive quantification of image analyses in patient cohorts, could provide informative data.

Finally, it is important to emphasize that our results have enabled us to standardize and validate analysis strategies that currently serve as a genuinely useful diagnostic tool in the clinical practice of our hospital. Additionally, we have identified a new predictive signature using a poorly explored technology that opens the door to new studies in this area. These discovery holds great promise for future research in advanced lung cancer, as it opens up avenues for larger-scale validation studies and provides a cornerstone towards the ultimate goal of precision medicine. Ongoing studies are being conducted to validate the biomarkers found, with the aim of improving survival rates for

those affected by this disease and paving the way for more effective, personalized treatments. We remain optimistic about the potential of this work and look forward to the advancements it will bring in the fight against lung cancer.

As a conclusion of this thesis project, we have demonstrated that the analysis of different liquid biopsy components can predict therapy response and improve patients' outcomes in both NSCLC and SCLC, underscoring the importance of including this approach in the standard clinical practice.

CONCLUSIONS

CONCLUSIONS

Overall, results obtained in our work provided relevant information to standardize new protocols to study different circulating biomarkers and demonstrated their potential to help clinicians in therapy decision making and the follow-up of lung cancer patients. The main conclusions drawn from the current PhD thesis research are summarized below.

1. Idylla™ ctEGFR Mutation Assay showed a good concordance with the ddPCR or BEAMing assays in advanced NSCLC patients with VAFs > 0.5%. These results support the use of this qPCR-based assay as a screen tool to detect *EGFR* mutations and guide treatment with TKIs.

2. We established specific and non-invasive assays to monitor *MET* status in cfDNA/CTCs and demonstrated its utility as a biomarker for monitoring the appearance of resistance to anti-EGFR therapy in advanced NSCLC patients.

3. Two efficient strategies (EpCAM dependent and independent) to monitor PD-L1 expression on CTCs from patients with advanced NSCLC were developed, however the detection of CTCs PD-L1^{+}, lacked predictive and prognostic significance.

4. Both baseline CTCs, and cfDNA levels, analysed independently, showed prognostic value in metastatic NSCLC patients receiving pembrolizumab

therapy. In addition, combined analysis of CTCs and cfDNA improved the capacity to predict progression-free survival (PFS) rates.

5. The presence of high cfDNA levels in newly diagnosed SCLC patients was associated with a poor evolution of the disease in terms of PFS and overall survival (OS) rates.

6. We identified a model based on cfDNA levels, ECOG PS and the patients' sex that has value in identifying SCLC patients who particularly benefit from the treatment.

7. Extensive characterization of plasma circulating proteins in metastatic NSCLC patients allowed us to identify a novel protein signature (including ATG9A, DCDC2, HPS5, FIL1L, LZTL1, PGTA, and SPTN2) associated with the response to immunotherapy.

REFERENCES

REFERENCES

1. Mondelo-Macía P, Castro-Santos P, Castillo-García A, Muinelo-Romay L, Diaz-Peña R. Circulating Free DNA and Its Emerging Role in Autoimmune Diseases. J Pers Med. 2021 Feb;11(2).
2. Mondelo-Macía P, Rodríguez-Ces AM, Suárez-Cunqueiro MM, Romay LM. Methods for the Detection of Circulating Biomarkers in Cancer Patients. Adv Exp Med Biol. 2022;1379:525–52.
3. Mondelo-Macía P, García-González J, León-Mateos L, Castillo-García A, López-López R, Muinelo-Romay L, et al. Current status and future perspectives of liquid biopsy in small cell lung cancer. Biomedicines. 2021;9(1):1–22.
4. Sung H, Ferlay J, Siegel RL, Laversanne M, Soerjomataram I, Jemal A, et al. Global Cancer Statistics 2020: GLOBOCAN Estimates of Incidence and Mortality Worldwide for 36 Cancers in 185 Countries. CA Cancer J Clin. 2021;71(3):209–49.
5. Kocher F, Hilbe W, Seeber A, Pircher A, Schmid T, Greil R, et al. Longitudinal analysis of 2293 NSCLC patients: a comprehensive study from the TYROL registry. Lung Cancer. 2015 Feb;87(2):193–200.
6. Tobacco Smoking and Cancer of the Lung: Statement of the [British] Medical Research Council. CA Cancer J Clin. 1958 Mar 1;8(2):66–8.
7. Wynder EL. Tobacco as a cause of lung cancer: some reflections. Am J Epidemiol. 1997 Nov;146(9):687–94.
8. Thun M, Peto R, Boreham J, Lopez AD. Stages of the cigarette epidemic on entering its second century. Tob Control. 2012 Mar;21(2):96–101.
9. Ng M, Freeman MK, Fleming TD, Robinson M, Dwyer-Lindgren L, Thomson B, et al. Smoking prevalence and cigarette consumption in 187 countries, 1980-2012. JAMA. 2014 Jan;311(2):183–92.
10. Sun S, Schiller JH, Gazdar AF. Lung cancer in never smokers - A different disease. Nat Rev Cancer. 2007;7(10):778–90.
11. Subramanian J, Govindan R. Molecular genetics of lung cancer in people who have never smoked. Lancet Oncol. 2008;9(7):676–82.
12. Corrales L, Rosell R, Cardona AF, Martín C, Zatarain-Barrón ZL, Arrieta O. Lung cancer in never smokers: The role of different risk factors other than tobacco smoking. Crit Rev Oncol Hematol. 2020;148.

13. Malhotra J, Malvezzi M, Negri E, La Vecchia C, Boffetta P. Risk factors for lung cancer worldwide. Eur Respir J. 2016;48(3):889–902.

14. Turner MC, Andersen ZJ, Baccarelli A, Diver WR, Gapstur SM, Pope CA 3rd, et al. Outdoor air pollution and cancer: An overview of the current evidence and public health recommendations. CA Cancer J Clin. 2020 Aug;

15. Mucci LA, Hjelmborg JB, Harris JR, Czene K, Havelick DJ, Scheike T, et al. Familial Risk and Heritability of Cancer Among Twins in Nordic Countries. JAMA. 2016 Jan;315(1):68–76.

16. Travis WD, Brambilla E, Nicholson AG, Yatabe Y, Austin JHM, Beasley MB, et al. The 2015 World Health Organization Classification of Lung Tumors: Impact of Genetic, Clinical and Radiologic Advances since the 2004 Classification. J Thorac Oncol. 2015;10(9):1243–60.

17. Thai AA, Solomon BJ, Sequist L V., Gainor JF, Heist RS. Lung cancer. Lancet. 2021;398(10299):535–54.

18. Huang R, Wei Y, Hung RJ, Liu G, Su L, Zhang R, et al. Associated Links Among Smoking, Chronic Obstructive Pulmonary Disease, and Small Cell Lung Cancer: A Pooled Analysis in the International Lung Cancer Consortium. EBioMedicine. 2015 Nov;2(11):1677–85.

19. Yu L, Lai Q, Gou L, Feng J, Yang J. Opportunities and obstacles of targeted therapy and immunotherapy in small cell lung cancer. J Drug Target. 2020;0(0):000.

20. Edition S, Edge SB, Byrd DR. AJCC cancer staging manual. AJCC cancer staging Man. 2017;

21. Detterbeck FC, Boffa DJ, Kim AW, Tanoue LT. The Eighth Edition Lung Cancer Stage Classification. Chest. 2017;151(1):193–203.

22. Van Meerbeeck JP, Fennell DA, De Ruysscher DKM. Small-cell lung cancer. Lancet. 2011;378(9804):1741–55.

23. Micke P, Faldum A, Metz T, Beeh KM, Bittinger F, Hengstler JG, et al. Staging small cell lung cancer: Veterans Administration Lung Study Group versus International Association for the Study of Lung Cancer - What limits limited disease? Lung Cancer. 2002 Sep;37(3):271–6.

24. Howlader N, Noone AM, Krapcho M, Miller D, Brest A, Yu M, Ruhl J, Tatalovich Z, Mariotto A, Lewis DR, Chen HS, Feuer EJ CK. SEER Cancer Statistics Review, 1975-2016, National Cancer Institute. Natl Cancer Institute. 2018;

25. Planchard D, Popat S, Kerr K, Novello S, Smit EF, Faivre-Finn C, et al. Metastatic non-small cell lung cancer: ESMO Clinical Practice Guidelines for

diagnosis, treatment and follow-up. Ann Oncol. 2018;29(Supplement 4):iv192–237.

26. Wang M, Herbst RS, Boshoff C. Toward personalized treatment approaches for non-small-cell lung cancer. Nat Med. 2021;27(8):1345–56.

27. Herbst RS, Morgensztern D, Boshoff C. The biology and management of non-small cell lung cancer. Nature. 2018;553(7689):446–54.

28. Howlader N, Forjaz G, Mooradian MJ, Meza R, Kong CY, Cronin KA, et al. The Effect of Advances in Lung-Cancer Treatment on Population Mortality. N Engl J Med. 2020;383(7):640–9.

29. Allemani C, Matsuda T, Di Carlo V, Harewood R, Matz M, Nikšić M, et al. Global surveillance of trends in cancer survival 2000–14 (CONCORD-3): analysis of individual records for 37 513 025 patients diagnosed with one of 18 cancers from 322 population-based registries in 71 countries. Lancet. 2018;391(10125):1023–75.

30. Mok TS, Wu Y-L, Thongprasert S, Yang C-H, Chu D-T, Saijo N, et al. Gefitinib or carboplatin-paclitaxel in pulmonary adenocarcinoma. N Engl J Med. 2009 Sep;361(10):947–57.

31. Zhou C, Wu YL, Chen G, Feng J, Liu X-Q, Wang C, et al. Final overall survival results from a randomised, phase III study of erlotinib versus chemotherapy as first-line treatment of EGFR mutation-positive advanced non-small-cell lung cancer (OPTIMAL, CTONG-0802). Ann Oncol Off J Eur Soc Med Oncol. 2015 Sep;26(9):1877–83.

32. Rosell R, Carcereny E, Gervais R, Vergnenegre A, Massuti B, Felip E, et al. Erlotinib versus standard chemotherapy as first-line treatment for European patients with advanced EGFR mutation-positive non-small-cell lung cancer (EURTAC): a multicentre, open-label, randomised phase 3 trial. Lancet Oncol. 2012 Mar;13(3):239–46.

33. Wu Y-L, Zhou C, Liam C-K, Wu G, Liu X, Zhong Z, et al. First-line erlotinib versus gemcitabine/cisplatin in patients with advanced EGFR mutation-positive non-small-cell lung cancer: analyses from the phase III, randomized, open-label, ENSURE study. Ann Oncol Off J Eur Soc Med Oncol. 2015 Sep;26(9):1883–9.

34. Yang JJ, Zhou Q, Yan HH, Zhang XC, Chen HJ, Tu HY, et al. A phase III randomised controlled trial of erlotinib vs gefitinib in advanced non-small cell lung cancer with EGFR mutations. Br J Cancer. 2017 Feb;116(5):568–74.

35. Sequist L V, Yang JC-H, Yamamoto N, O'Byrne K, Hirsh V, Mok T, et al. Phase III study of afatinib or cisplatin plus pemetrexed in patients with metastatic lung adenocarcinoma with EGFR mutations. J Clin Oncol Off J Am Soc Clin Oncol. 2013 Sep;31(27):3327–34.

36. Rotow J, Bivona TG. Understanding and targeting resistance mechanisms in NSCLC. Nat Rev Cancer. 2017;17(11):637–58.

37. Yun CH, Mengwasser KE, Toms A V., Woo MS, Greulich H, Wong KK, et al. The T790M mutation in EGFR kinase causes drug resistance by increasing the affinity for ATP. Proc Natl Acad Sci U S A. 2008;105(6):2070–5.

38. Cortot AB, Jänne PA. Molecular mechanisms of resistance in epidermal growth factor receptor-mutant lung adenocarcinomas. Eur Respir Rev an Off J Eur Respir Soc. 2014 Sep;23(133):356–66.

39. Schmid S, Li JJN, Leighl NB. Mechanisms of osimertinib resistance and emerging treatment options. Lung Cancer. 2020 Sep;147:123–9.

40. Offin M, Chan JM, Tenet M, Rizvi HA, Shen R, Riely GJ, et al. Concurrent RB1 and TP53 Alterations Define a Subset of EGFR-Mutant Lung Cancers at risk for Histologic Transformation and Inferior Clinical Outcomes. J Thorac Oncol Off Publ Int Assoc Study Lung Cancer. 2019 Oct;14(10):1784–93.

41. Yu HA, Arcila ME, Rekhtman N, Sima CS, Zakowski MF, Pao W, et al. Analysis of tumor specimens at the time of acquired resistance to EGFR-TKI therapy in 155 patients with EGFR-mutant lung cancers. Clin cancer Res an Off J Am Assoc Cancer Res. 2013 Apr;19(8):2240–7.

42. Lee J-K, Lee J, Kim S, Kim S, Youk J, Park S, et al. Clonal History and Genetic Predictors of Transformation Into Small-Cell Carcinomas From Lung Adenocarcinomas. J Clin Oncol Off J Am Soc Clin Oncol. 2017 Sep;35(26):3065–74.

43. Boumahdi S, de Sauvage FJ. The great escape: tumour cell plasticity in resistance to targeted therapy. Nat Rev Drug Discov. 2020;19(1):39–56.

44. Beatty GL, Gladney WL. Immune escape mechanisms as a guide for cancer immunotherapy. Clin cancer Res an Off J Am Assoc Cancer Res. 2015 Feb;21(4):687–92.

45. Havel JJ, Chowell D, Chan TA. The evolving landscape of biomarkers for checkpoint inhibitor immunotherapy. Nat Rev Cancer. 2019 Mar;19(3):133–50.

46. Morad G, Helmink BA, Sharma P, Wargo JA. Hallmarks of response, resistance, and toxicity to immune checkpoint blockade. Cell. 2021 Oct;184(21):5309–37.

47. Garon EB, Rizvi NA, Hui R, Leighl N, Balmanoukian AS, Eder JP, et al. Pembrolizumab for the treatment of non-small-cell lung cancer. N Engl J Med. 2015 May;372(21):2018–28.

48. Vokes EE, Ready N, Felip E, Horn L, Burgio MA, Antonia SJ, et al. Nivolumab versus docetaxel in previously treated advanced non-small-cell lung cancer (CheckMate 017 and CheckMate 057): 3-year update and outcomes in patients

with liver metastases. Ann Oncol Off J Eur Soc Med Oncol. 2018 Apr;29(4):959–65.

49. Rittmeyer A, Barlesi F, Waterkamp D, Park K, Ciardiello F, von Pawel J, et al. Atezolizumab versus docetaxel in patients with previously treated non-small-cell lung cancer (OAK): a phase 3, open-label, multicentre randomised controlled trial. Lancet. 2017;389(10066):255–65.

50. Herbst RSR, Baas P, Kim D-WD, Felip E, Pérez-Gracia JL, Han J-Y, et al. Pembrolizumab versus docetaxel for previously treated, PD-L1-positive, advanced non-small-cell lung cancer (KEYNOTE-010): a randomised controlled trial. Lancet. 2016 Apr;387(10027):1540–50.

51. Reck M, Rodríguez-Abreu D, Robinson AG, Hui R, Csőszi T, Fülöp A, et al. Pembrolizumab versus Chemotherapy for PD-L1–Positive Non–Small-Cell Lung Cancer. N Engl J Med. 2016 Nov 10;375(19):1823–33.

52. Brahmer J, Reckamp KL, Baas P, Crinò L, Eberhardt WEE, Poddubskaya E, et al. Nivolumab versus Docetaxel in Advanced Squamous-Cell Non-Small-Cell Lung Cancer. N Engl J Med. 2015 Jul 9;373(2):123–35.

53. Borghaei H, Paz-Ares L, Horn L, Spigel DR, Steins M, Ready NE, et al. Nivolumab versus Docetaxel in Advanced Nonsquamous Non-Small-Cell Lung Cancer. N Engl J Med. 2015 Oct 22;373(17):1627–39.

54. Carbone DP, Reck M, Paz-Ares L, Creelan B, Horn L, Steins M, et al. First-Line Nivolumab in Stage IV or Recurrent Non–Small-Cell Lung Cancer. N Engl J Med. 2017 Jun;376(25):2415–26.

55. Gandhi L, Rodríguez-Abreu D, Gadgeel S, Esteban E, Felip E, De Angelis F, et al. Pembrolizumab plus Chemotherapy in Metastatic Non–Small-Cell Lung Cancer. N Engl J Med. 2018 May 31;378(22):2078–92.

56. Paz-Ares L, Luft A, Vicente D, Tafreshi A, Gümüş M, Mazières J, et al. Pembrolizumab plus Chemotherapy for Squamous Non–Small-Cell Lung Cancer. N Engl J Med. 2018 Nov 22;379(21):2040–51.

57. Schiller JH, Harrington D, Belani CP, Langer C, Sandler A, Krook J, et al. Comparison of four chemotherapy regimens for advanced non-small-cell lung cancer. N Engl J Med. 2002 Jan;346(2):92–8.

58. Sandler A, Gray R, Perry MC, Brahmer J, Schiller JH, Dowlati A, et al. Paclitaxel-carboplatin alone or with bevacizumab for non-small-cell lung cancer. N Engl J Med. 2006 Dec;355(24):2542–50.

59. Paz-Ares LG, de Marinis F, Dediu M, Thomas M, Pujol J-L, Bidoli P, et al. PARAMOUNT: Final overall survival results of the phase III study of maintenance pemetrexed versus placebo immediately after induction treatment

with pemetrexed plus cisplatin for advanced nonsquamous non-small-cell lung cancer. J Clin Oncol Off J Am Soc Clin Oncol. 2013 Aug;31(23):2895–902.

60. Formenti SC, Demaria S. Combining radiotherapy and cancer immunotherapy: a paradigm shift. J Natl Cancer Inst. 2013 Feb;105(4):256–65.

61. Marchetti A, Felicioni L, Malatesta S, Grazia Sciarrotta M, Guetti L, Chella A, et al. Clinical features and outcome of patients with non-small-cell lung cancer harboring BRAF mutations. J Clin Oncol Off J Am Soc Clin Oncol. 2011 Sep;29(26):3574–9.

62. Cardarella S, Ogino A, Nishino M, Butaney M, Shen J, Lydon C, et al. Clinical, pathologic, and biologic features associated with BRAF mutations in non-small cell lung cancer. Clin cancer Res an Off J Am Assoc Cancer Res. 2013 Aug;19(16):4532–40.

63. Awad MM, Oxnard GR, Jackman DM, Savukoski DO, Hall D, Shivdasani P, et al. MET Exon 14 Mutations in Non-Small-Cell Lung Cancer Are Associated With Advanced Age and Stage-Dependent MET Genomic Amplification and c-Met Overexpression. J Clin Oncol Off J Am Soc Clin Oncol. 2016 Mar;34(7):721–30.

64. Kalemkerian GP, Narula N, Kennedy EB, Biermann WA, Donington J, Leighl NB, et al. Molecular Testing Guideline for the Selection of Patients With Lung Cancer for Treatment With Targeted Tyrosine Kinase Inhibitors: American Society of Clinical Oncology Endorsement of the College of American Pathologists/International Association for the. J Clin Oncol Off J Am Soc Clin Oncol. 2018 Mar;36(9):911–9.

65. Lindeman NI, Cagle PT, Aisner DL, Arcila ME, Beasley MB, Bernicker EH, et al. Updated Molecular Testing Guideline for the Selection of Lung Cancer Patients for Treatment With Targeted Tyrosine Kinase Inhibitors: Guideline From the College of American Pathologists, the International Association for the Study of Lung Cancer, and the. Arch Pathol Lab Med. 2018 Mar;142(3):321–46.

66. Gibney GT, Weiner LM, Atkins MB. Predictive biomarkers for checkpoint inhibitor-based immunotherapy. Vol. 17, The Lancet Oncology. 2016. p. e542–51.

67. Schoenfeld AJ, Rizvi H, Bandlamudi C, Sauter JL, Travis WD, Rekhtman N, et al. Clinical and molecular correlates of PD-L1 expression in patients with lung adenocarcinomas. Ann Oncol Off J Eur Soc Med Oncol. 2020 May;31(5):599–608.

68. Lantuejoul S, Sound-Tsao M, Cooper WA, Girard N, Hirsch FR, Roden AC, et al. PD-L1 Testing for Lung Cancer in 2019: Perspective From the IASLC

Pathology Committee. J Thorac Oncol Off Publ Int Assoc Study Lung Cancer. 2020 Apr;15(4):499–519.

69. Overman MJ, McDermott R, Leach JL, Lonardi S, Lenz H-J, Morse MA, et al. Nivolumab in patients with metastatic DNA mismatch repair-deficient or microsatellite instability-high colorectal cancer (CheckMate 142): an open-label, multicentre, phase 2 study. Lancet Oncol. 2017 Sep;18(9):1182–91.

70. Luchini C, Bibeau F, Ligtenberg MJL, Singh N, Nottegar A, Bosse T, et al. ESMO recommendations on microsatellite instability testing for immunotherapy in cancer, and its relationship with PD-1/PD-L1 expression and tumour mutational burden: a systematic review-based approach. Ann Oncol. 2019 Aug;30(8):1232–43.

71. Grunnet M, Sorensen JB. Carcinoembryonic antigen (CEA) as tumor marker in lung cancer. Lung Cancer. 2012 May;76(2):138–43.

72. Eisenhauer EA, Therasse P, Bogaerts J, Schwartz LH, Sargent D, Ford R, et al. New response evaluation criteria in solid tumours: revised RECIST guideline (version 1.1). Eur J Cancer. 2009 Jan;45(2):228–47.

73. Rizvi NA, Hellmann MD, Snyder A, Kvistborg P, Makarov V, Havel JJ, et al. Cancer immunology. Mutational landscape determines sensitivity to PD-1 blockade in non-small cell lung cancer. Science. 2015 Apr;348(6230):124–8.

74. Cristescu R, Aurora-Garg D, Albright A, Xu L, Liu XQ, Loboda A, et al. Tumor mutational burden predicts the efficacy of pembrolizumab monotherapy: a pan-tumor retrospective analysis of participants with advanced solid tumors. J Immunother cancer. 2022 Jan;10(1).

75. Shirasawa M, Yoshida T, Shimoda Y, Takayanagi D, Shiraishi K, Kubo T, et al. Differential Immune-Related Microenvironment Determines Programmed Cell Death Protein-1/Programmed Death-Ligand 1 Blockade Efficacy in Patients With Advanced NSCLC. J Thorac Oncol Off Publ Int Assoc Study Lung Cancer. 2021 Dec;16(12):2078–90.

76. Jiang T, Bai Y, Zhou F, Li W, Gao G, Su C, et al. Clinical value of neutrophil-to-lymphocyte ratio in patients with non-small-cell lung cancer treated with PD-1/PD-L1 inhibitors. Lung Cancer. 2019 Apr 1;130:76–83.

77. Pan Y, Fu Y, Zeng Y, Liu X, Peng Y, Hu C, et al. The key to immunotherapy: how to choose better therapeutic biomarkers for patients with non-small cell lung cancer. Biomark Res. 2022 Mar;10(1):9.

78. Mezquita L, Auclin E, Ferrara R, Charrier M, Remon J, Planchard D, et al. Association of the Lung Immune Prognostic Index With Immune Checkpoint Inhibitor Outcomes in Patients With Advanced Non-Small Cell Lung Cancer. JAMA Oncol. 2018 Mar;4(3):351–7.

79. Govindan R, Page N, Morgensztern D, Read W, Tierney R, Vlahiotis A, et al. Changing epidemiology of small-cell lung cancer in the United States over the last 30 years: Analysis of the surveillance, epidemiologic, and end results database. J Clin Oncol. 2006 Oct 1;24(28):4539–44.

80. Dingemans AC, Früh M, Ardizzoni A, Besse B, Hendriks LE, Lantuejoul S, et al. Small-cell lung cancer : ESMO Clinical Practice Guidelines for diagnosis, Ann Oncol. 2021;32(7):839–53.

81. George J, Lim JS, Jang SJ, Cun Y, Ozretić L, Kong G, et al. Comprehensive genomic profiles of small cell lung cancer. Nature. 2015 Aug;524(7563):47–53.

82. Peifer M, Fernández-Cuesta L, Sos ML, George J, Seidel D, Kasper LH, et al. Integrative genome analyses identify key somatic driver mutations of small-cell lung cancer. Nat Genet. 2012 Oct;44(10):1104–10.

83. Rudin CM, Durinck S, Stawiski EW, Poirier JT, Modrusan Z, Shames DS, et al. Comprehensive genomic analysis identifies SOX2 as a frequently amplified gene in small-cell lung cancer. Nat Genet. 2012 Oct;44(10):1111–6.

84. Iwakawa R, Kohno T, Totoki Y, Shibata T, Tsuchihara K, Mimaki S, et al. Expression and clinical significance of genes frequently mutated in small cell lung cancers defined by whole exome/RNA sequencing. Carcinogenesis. 2015 Jun;36(6):616–21.

85. Rudin CM, Poirier JT, Byers LA, Dive C, Dowlati A, George J, et al. Molecular subtypes of small cell lung cancer: a synthesis of human and mouse model data. Nat Rev Cancer. 2019 May;19(5):289–97.

86. Hanna N, Bunn PAJ, Langer C, Einhorn L, Guthrie TJ, Beck T, et al. Randomized phase III trial comparing irinotecan/cisplatin with etoposide/cisplatin in patients with previously untreated extensive-stage disease small-cell lung cancer. J Clin Oncol Off J Am Soc Clin Oncol. 2006 May;24(13):2038–43.

87. Lee J, Maeng CH, Song J-U. The Role of Prophylactic Cranial Irradiation in Patients With Extensive-Stage Small Cell Lung Cancer: A Systematic Review and Meta-Analysis. Vol. 14, Journal of thoracic oncology : official publication of the International Association for the Study of Lung Cancer. United States; 2019. p. e60–1.

88. Turrisi AT, Kim K, Blum R, Sause WT, Livingston RB, Komaki R, et al. Twice-daily compared with once-daily thoracic radiotherapy in limited small-cell lung cancer treated concurrently with cisplatin and etoposide. N Engl J Med. 1999 Jan 28 [cited 2020 Oct 12];340(4):265–71.

89. Faivre-Finn C, Snee M, Ashcroft L, Appel W, Barlesi F, Bhatnagar A, et al. Concurrent once-daily versus twice-daily chemoradiotherapy in patients with

limited-stage small-cell lung cancer (CONVERT): an open-label, phase 3, randomised, superiority trial. Lancet Oncol. 2017 Aug 1;18(8):1116–25.

90. Rossi A, Di Maio M, Chiodini P, Rudd RM, Okamoto H, Skarlos DV, et al. Carboplatin- or cisplatin-based chemotherapy in first-line treatment of small-cell lung cancer: the COCIS meta-analysis of individual patient data. J Clin Oncol Off J Am Soc Clin Oncol. 2012 May;30(14):1692–8.

91. Dómine M, Moran T, Isla D, Martí JL, Sullivan I, Provencio M, et al. SEOM clinical guidelines for the treatment of small-cell lung cancer (SCLC) (2019). Clin Transl Oncol. 2020 Feb 1;22(2):245–55.

92. Esposito G, Palumbo G, Carillio G, Manzo A, Montanino A, Sforza V, et al. Immunotherapy in Small Cell Lung Cancer. Cancers (Basel). 2020 Sep 4;12(9):2522.

93. Facchinetti F, Di Maio M, Tiseo M. Adding PD-1/PD-L1 inhibitors to chemotherapy for the first-line treatment of extensive stage small cell lung cancer (Sclc): A meta-analysis of randomized trials. Vol. 12, Cancers. MDPI AG; 2020. p. 1–18.

94. Horn L, Mansfield AS, Szczęsna A, Havel L, Krzakowski M, Hochmair MJ, et al. First-Line Atezolizumab plus Chemotherapy in Extensive-Stage Small-Cell Lung Cancer. N Engl J Med. 2018 Dec;379(23):2220–9.

95. Paz-Ares L, Dvorkin M, Chen Y, Reinmuth N, Hotta K, Trukhin D, et al. Durvalumab plus platinum–etoposide versus platinum–etoposide in first-line treatment of extensive-stage small-cell lung cancer (CASPIAN): a randomised, controlled, open-label, phase 3 trial. Lancet. 2019 Nov 23;394(10212):1929–39.

96. Rudin CM, Awad MM, Navarro A, Gottfried M, Peters S, Csőszi T, et al. Pembrolizumab or Placebo Plus Etoposide and Platinum as First-Line Therapy for Extensive-Stage Small-Cell Lung Cancer: Randomized, Double-Blind, Phase III KEYNOTE-604 Study. J Clin Oncol. 2020 Jul 20;38(21):2369–79.

97. Früh M, Panje CM, Reck M, Blackhall F, Califano R, Cappuzzo F, et al. Choice of second-line systemic therapy in stage IV small cell lung cancer (SCLC) – A decision-making analysis amongst European lung cancer experts. Lung Cancer. 2020 Aug 1;146:6–11.

98. Trigo J, Subbiah V, Besse B, Moreno V, López R, Sala MA, et al. Lurbinectedin as second-line treatment for patients with small-cell lung cancer: a single-arm, open-label, phase 2 basket trial. Lancet Oncol. 2020 May;21(5):645–54.

99. Antonia SJ, López-Martin JA, Bendell J, Ott PA, Taylor M, Eder JP, et al. Nivolumab alone and nivolumab plus ipilimumab in recurrent small-cell lung cancer (CheckMate 032): a multicentre, open-label, phase 1/2 trial. Lancet Oncol. 2016 Jul 1;17(7):883–95.

100. Chung HC, Lopez-Martin JA, Kao SC-H, Miller WH, Ros W, Gao B, et al. Phase 2 study of pembrolizumab in advanced small-cell lung cancer (SCLC): KEYNOTE-158. J Clin Oncol. 2018 May 20;36(15_suppl):8506–8506.

101. Reck M, Vicente D, Ciuleanu T, Gettinger S, Peters S, Horn L, et al. Efficacy and safety of nivolumab (nivo) monotherapy versus chemotherapy (chemo) in recurrent small cell lung cancer (SCLC): Results from CheckMate 331. Ann Oncol. 2018 Dec;29:x43.

102. Byers LA, Rudin CM. Small cell lung cancer: where do we go from here? Cancer. 2015 Mar;121(5):664–72.

103. Kalemkerian GP. Advances in pharmacotherapy of small cell lung cancer. Expert Opin Pharmacother. 2014 Nov;15(16):2385–96.

104. Hirsch FR, Scagliotti G V, Mulshine JL, Kwon R, Curran WJJ, Wu Y-L, et al. Lung cancer: current therapies and new targeted treatments. Lancet (London, England). 2017 Jan;389(10066):299–311.

105. Camidge DR, Doebele RC, Kerr KM. Comparing and contrasting predictive biomarkers for immunotherapy and targeted therapy of NSCLC. Nat Rev Clin Oncol. 2019 Jun;16(6):341–55.

106. Owonikoko TK, Niu H, Nackaerts K, Csoszi T, Ostoros G, Mark Z, et al. Randomized Phase II Study of Paclitaxel plus Alisertib versus Paclitaxel plus Placebo as Second-Line Therapy for SCLC: Primary and Correlative Biomarker Analyses. J Thorac Oncol Off Publ Int Assoc Study Lung Cancer. 2020 Feb;15(2):274–87.

107. Pietanza MC, Waqar SN, Krug LM, Dowlati A, Hann CL, Chiappori A, et al. Randomized, double-blind, phase II study of temozolomide in combination with either veliparib or placebo in patients with relapsed-sensitive or refractory small-cell lung cancer. J Clin Oncol. 2018 Aug 10;36(23):2386–94.

108. Sidaway P. SLFN11: a new synthetic lethal target? Vol. 15, Nature Reviews Clinical Oncology. Nature Publishing Group; 2018. p. 533.

109. Rudin CM, Pietanza MC, Bauer TM, Ready N, Morgensztern D, Glisson BS, et al. Rovalpituzumab tesirine, a DLL3-targeted antibody-drug conjugate, in recurrent small-cell lung cancer: a first-in-human, first-in-class, open-label, phase 1 study. Lancet Oncol. 2017 Jan 1;18(1):42–51.

110. Melichar B, Adenis A, Lockhart AC, Bennouna J, Dees EC, Kayaleh O, et al. Safety and activity of alisertib, an investigational aurora kinase A inhibitor, in patients with breast cancer, small-cell lung cancer, non-small-cell lung cancer, head and neck squamous-cell carcinoma, and gastro-oesophageal adenocarcinoma: a five-arm p. Lancet Oncol. 2015 Apr;16(4):395–405.

111. Drpa G, Sutic M, Baranasic J, Jakopovic M, Samarzija M, Kukulj S, et al. Neutrophil-to-lymphocyte ratio can predict outcome in extensive-stage small cell lung cancer. Radiol Oncol. 2020 Sep;54(4):437–46.

112. Alix-Panabières C, Pantel K. Clinical applications of circulating tumor cells and circulating tumor DNA as liquid biopsy. Cancer Discov. 2016 May 1;6(5):479–91.

113. Crowley E, Di Nicolantonio F, Loupakis F, Bardelli A. Liquid biopsy: Monitoring cancer-genetics in the blood. Nat Rev Clin Oncol. 2013;10(8):472–84.

114. Bardelli A, Pantel K. Liquid Biopsies, What We Do Not Know (Yet). Cancer Cell. 2017;31(2):172–9.

115. Mann J, Reeves HL, Feldstein AE. Liquid biopsy for liver diseases. Gut. 2018;1–9.

116. Rezaei M, Winter M, Zander-Fox D, Whitehead C, Liebelt J, Warkiani ME, et al. A Reappraisal of Circulating Fetal Cell Noninvasive Prenatal Testing. Trends Biotechnol. 2019;37(6):632–44.

117. Wang Y, Springer S, Mulvey CL, Silliman N, Schaefer J, Sausen M, et al. Detection of somatic mutations and HPV in the saliva and plasma of patients with head and neck squamous cell carcinomas. Sci Transl Med. 2015;7(293):1–16.

118. Chen CK, Liao J, Li MS, Khoo BL. Urine biopsy technologies: Cancer and beyond. Theranostics. 2020;10(17):7872–88.

119. Heidrich I, Ačkar L, Mossahebi Mohammadi P, Pantel K. Liquid biopsies: Potential and challenges. Int J Cancer. 2020;(May):1–18.

120. Bradley SH, Barclay ME. "Liquid biopsy" for cancer screening. Vol. 372, BMJ (Clinical research ed.). England; 2021. p. m4933.

121. Chouaid C, Dujon C, Do P, Monnet I, Madroszyk A, Le Caer H, et al. Feasibility and clinical impact of re-biopsy in advanced non small-cell lung cancer: a prospective multicenter study in a real-world setting (GFPC study 12-01). Lung Cancer. 2014 Nov;86(2):170–3.

122. Vanderlaan PA, Yamaguchi N, Folch E, Boucher DH, Kent MS, Gangadharan SP, et al. Success and failure rates of tumor genotyping techniques in routine pathological samples with non-small-cell lung cancer. Lung Cancer. 2014 Apr;84(1):39–44.

123. Ganesh K, Massagué J. Targeting metastatic cancer. Nat Med. 2021;27(1):34–44.

124. Hudson TJ, Anderson W, Aretz A, Barker AD, Bell C, Bernabé RR, et al. International network of cancer genome projects. Nature. 2010;464(7291):993–8.

125. Campbell PJ, Getz G, Korbel JO, Stuart JM, Jennings JL, Stein LD, et al. Pan-cancer analysis of whole genomes. Nature. 2020;578(7793):82–93.

126. Ignatiadis M, Sledge GW, Jeffrey SS. Liquid biopsy enters the clinic — implementation issues and future challenges. Nat Rev Clin Oncol. 2021 May 20;18(5):297–312.

127. McGranahan N, Swanton C. Clonal Heterogeneity and Tumor Evolution: Past, Present, and the Future. Cell. 2017;168(4):613–28.

128. De Rubis G, Rajeev Krishnan S, Bebawy M. Liquid Biopsies in Cancer Diagnosis, Monitoring, and Prognosis. Trends Pharmacol Sci. 2019;40(3):172–86.

129. Mandel P, Metais P. Les acides nucléiques du plasma sanguin chez l'homme. C R Seances Soc Biol Fil. 1948 Feb;142(3–4):241–3.

130. Tan EM, Schur PH, Carr RI, Kunkel HG. Deoxybonucleic acid (DNA) and antibodies to DNA in the serum of patients with systemic lupus erythematosus. J Clin Invest. 1966;45(11):1732–40.

131. Leon SA, Ehrlich GE, Shapiro B, Labbate VA. Free DNA in the serum of rheumatoid arthritis patients. J Rheumatol. 1977;4(2):139–43.

132. Vasioukhin V, Anker P, Maurice P, Lyautey J, Lederrey C, Stroun M. Point mutations of the N-ras gene in the blood plasma DNA of patients with myelodysplastic syndrome or acute myelogenous leukaemia. Br J Haematol. 1994 Apr;86(4):774–9.

133. Sorenson GD, Pribish DM, Valone FH, Memoli VA, Bzik DJ, Yao SL. Soluble normal and mutated DNA sequences from single-copy genes in human blood. Cancer Epidemiol biomarkers Prev a Publ Am Assoc Cancer Res cosponsored by Am Soc Prev Oncol. 1994;3(1):67–71.

134. Rolfo C, Cardona AF, Cristofanilli M, Paz-Ares L, Diaz Mochon JJ, Duran I, et al. Challenges and opportunities of cfDNA analysis implementation in clinical practice: Perspective of the International Society of Liquid Biopsy (ISLB). Crit Rev Oncol Hematol. 2020;151(April):102978.

135. Szilágyi M, Pös O, Márton É, Buglyó G, Soltész B, Keserű J, et al. Circulating cell-free nucleic acids: Main characteristics and clinical application. Int J Mol Sci. 2020;21(18):1–20.

136. Pös O, Biró O, Szemes T, Nagy B. Circulating cell-free nucleic acids : characteristics and applications. 2018;937–45.

137. Kustanovich A, Schwartz R, Peretz T, Grinshpun A. Life and death of circulating cell-free DNA. Cancer Biol Ther. 2019;20(8):1057–67.

138. Aucamp J, Bronkhorst AJ, Badenhorst CPS, Pretorius PJ. The diverse origins of circulating cell-free DNA in the human body: a critical re-evaluation of the literature. Biol Rev. 2018;93(3):1649–83.

139. Thierry AR, El Messaoudi S, Gahan PB, Anker P, Stroun M. Origins, structures, and functions of circulating DNA in oncology. Cancer Metastasis Rev. 2016;35(3):347–76.

140. Fernando MR, Jiang C, Krzyzanowski GD, Ryan WL. New evidence that a large proportion of human blood plasma cell-free DNA is localized in exosomes. PLoS One. 2017;12(8):e0183915.

141. Duvvuri B, Lood C. Cell-free DNA as a biomarker in autoimmune rheumatic diseases. Front Immunol. 2019;10(MAR):1–21.

142. Guo H, Xie M, Zhou C, Zheng M. The relevance of pyroptosis in the pathogenesis of liver diseases. Life Sci. 2019 Apr;223:69–73.

143. Fang Y, Tian S, Pan Y, Li W, Wang Q, Tang Y, et al. Pyroptosis: A new frontier in cancer. Biomed Pharmacother. 2020 Jan;121:109595.

144. Celec P, Vlková B, Lauková L, Bábíčková J, Boor P. Cell-free DNA: the role in pathophysiology and as a biomarker in kidney diseases. Expert Rev Mol Med. 2018;20:1–14.

145. Teo YV, Capri M, Morsiani C, Pizza G, Faria AMC, Franceschi C, et al. Cell-free DNA as a biomarker of aging. Aging Cell. 2019;18(1):1–14.

146. Hummel EM, Hessas E, Müller S, Beiter T, Fisch M, Eibl A, et al. Cell-free DNA release under psychosocial and physical stress conditions. Transl Psychiatry. 2018.

147. Vittori LN, Tarozzi A, Latessa PM. Circulating cell-free DNA in physical activities. Methods Mol Biol. 2019;1909:183–97.

148. García Moreira V, De La Cera Martínez T, Gago González E, Prieto García B, Alvarez Menéndez F V. Increase in and clearance of cell-free plasma DNA in hemodialysis quantified by real-time PCR. Clin Chem Lab Med. 2006;44(12):1410–5.

149. Bettegowda C, Sausen M, Leary RJ, Kinde I, Wang Y, Agrawal N, et al. Detection of circulating tumor DNA in early- and late-stage human malignancies. Sci Transl Med. 2014 Feb;6(224):224ra24.

150. Keller L, Belloum Y, Wikman H, Pantel K. Clinical relevance of blood-based ctDNA analysis: mutation detection and beyond. Br J Cancer. 2020;(November 2019).

151. Diehl F, Schmidt K, Choti MA, Romans K, Goodman S, Li M, et al. Circulating mutant DNA to assess tumor dynamics. Nat Med. 2008 Sep;14(9):985–90.

152. Vidal J, Muinelo L, Dalmases A, Jones F, Edelstein D, Iglesias M, et al. Plasma ctDNA RAS mutation analysis for the diagnosis and treatment monitoring of metastatic colorectal cancer patients. Ann Oncol. 2017;28(6):1325–32.

153. Kilgour E, Rothwell DG, Brady G, Dive C. Liquid Biopsy-Based Biomarkers of Treatment Response and Resistance. Cancer Cell. 2020;37(4):485–95.

154. Elazezy M, Joosse SA. Techniques of using circulating tumor DNA as a liquid biopsy component in cancer management. Comput Struct Biotechnol J. 2018;16:370–8.

155. Kwapisz D. The first liquid biopsy test approved. Is it a new era of mutation testing for non-small cell lung cancer? Ann Transl Med. 2017 Feb;5(3):46.

156. Thress KS, Brant R, Carr TH, Dearden S, Jenkins S, Brown H, et al. EGFR mutation detection in ctDNA from NSCLC patient plasma: A cross-platform comparison of leading technologies to support the clinical development of AZD9291. Lung Cancer. 2015 Dec;90(3):509–15.

157. Bando H, Kagawa Y, Kato T, Akagi K, Denda T, Nishina T, et al. A multicentre, prospective study of plasma circulating tumour DNA test for detecting RAS mutation in patients with metastatic colorectal cancer. Br J Cancer. 2019 May;120(10):982–6.

158. García-Foncillas J, Tabernero J, Élez E, Aranda E, Benavides M, Camps C, et al. Prospective multicenter real-world RAS mutation comparison between OncoBEAM-based liquid biopsy and tissue analysis in metastatic colorectal cancer. Br J Cancer. 2018 Dec;119(12):1464–70.

159. Ou C-Y, Vu T, Grunwald JT, Toledano M, Zimak J, Toosky M, et al. An ultrasensitive test for profiling circulating tumor DNA using integrated comprehensive droplet digital detection. Lab Chip. 2019 Mar;19(6):993–1005.

160. Chen M, Zhao H. Next-generation sequencing in liquid biopsy: cancer screening and early detection. Hum Genomics. 2019 Aug;13(1):34.

161. Malapelle U, Sirera R, Jantus-Lewintre E, Reclusa P, Calabuig-Fariñas S, Blasco A, et al. Profile of the Roche cobas® EGFR mutation test v2 for non-small cell lung cancer. Expert Rev Mol Diagn. 2017 Mar;17(3):209–15.

162. Lamb YN, Dhillon S. Epi proColon(®) 2.0 CE: A Blood-Based Screening Test for Colorectal Cancer. Mol Diagn Ther. 2017 Apr;21(2):225–32.

163. André F, Ciruelos E, Rubovszky G, Campone M, Loibl S, Rugo HS, et al. Alpelisib for PIK3CA-Mutated, Hormone Receptor-Positive Advanced Breast Cancer. N Engl J Med. 2019 May;380(20):1929–40.

164. Laufer-Geva S, Rozenblum AB, Twito T, Grinberg R, Dvir A, Soussan-Gutman L, et al. The Clinical Impact of Comprehensive Genomic Testing of Circulating Cell-Free DNA in Advanced Lung Cancer. J Thorac Oncol. 2018;13(11):1705–16.

165. Woodhouse R, Li M, Hughes J, Delfosse D, Skoletsky J, Ma P, et al. Clinical and analytical validation of FoundationOne Liquid CDx, a novel 324-Gene cfDNA-based comprehensive genomic profiling assay for cancers of solid tumor origin. PLoS One. 2020;15(9):e0237802.

166. Le DT, Durham JN, Smith KN, Wang H, Bartlett BR, Aulakh LK, et al. Mismatch repair deficiency predicts response of solid tumors to PD-1 blockade. Science. 2017 Jul;357(6349):409–13.

167. Ashworth TR. A case of cancer in which cells similar to those in the tumours were seen in the blood after death. Aust Med J. 1869;14:146.

168. Perez FM, Yonemoto RH. The enigma of circulating malignant cells. Calif Med. 1962;97:166–9.

169. Alexander RF, Spriggs AI. The differential diagnosis of tumour cells in circulating blood. J Clin Pathol. 1960;13:414–24.

170. ROBERTS S, WATNE A, McGRATH R, McGREW E, COLE WH. Technique and results of isolation of cancer cells from the circulating blood. AMA Arch Surg. 1958 Mar;76(3):334–46.

171. Bidard F-C, Peeters DJ, Fehm T, Nolé F, Gisbert-Criado R, Mavroudis D, et al. Clinical validity of circulating tumour cells in patients with metastatic breast cancer: a pooled analysis of individual patient data. Lancet Oncol. 2014 Apr;15(4):406–14.

172. Bao-Caamano A, Rodriguez-Casanova A, Diaz-Lagares A. Epigenetics of Circulating Tumor Cells in Breast Cancer. Adv Exp Med Biol. 2020;1220:117–34.

173. Pantel K, Hille C, Scher HI. Circulating Tumor Cells in Prostate Cancer: From Discovery to Clinical Utility. Clin Chem. 2019 Jan;65(1):87–99.

174. Lindsay CR, Blackhall FH, Carmel A, Fernandez-Gutierrez F, Gazzaniga P, Groen HJM, et al. EPAC-lung: pooled analysis of circulating tumour cells in advanced non-small cell lung cancer. Eur J Cancer. 2019;117(December 2018):60–8.

175. Cohen SJ, Punt CJA, Iannotti N, Saidman BH, Sabbath KD, Gabrail NY, et al. Relationship of circulating tumor cells to tumor response, progression-free survival, and overall survival in patients with metastatic colorectal cancer. J Clin Oncol Off J Am Soc Clin Oncol. 2008 Jul;26(19):3213–21.

176. Hamilton G, Rath B. Mesenchymal-epithelial transition and circulating tumor cells in small cell lung cancer. Adv Exp Med Biol. 2017;994:229–45.

177. Allan AL, Vantyghem SA, Tuck AB, Chambers AF, Chin-Yee IH, Keeney M. Detection and quantification of circulating tumor cells in mouse models of human breast cancer using immunomagnetic enrichment and multiparameter flow cytometry. Cytometry A. 2005 May;65(1):4–14.

178. Baccelli I, Schneeweiss A, Riethdorf S, Stenzinger A, Schillert A, Vogel V, et al. Identification of a population of blood circulating tumor cells from breast cancer patients that initiates metastasis in a xenograft assay. Nat Biotechnol. 2013 Jun;31(6):539–44.

179. Pantel K, Speicher MR. The biology of circulating tumor cells. Oncogene. 2016;35(10):1216–24.

180. Genna A, Vanwynsberghe AM, Villard A V, Pottier C, Ancel J, Polette M, et al. EMT-Associated Heterogeneity in Circulating Tumor Cells: Sticky Friends on the Road to Metastasis. Cancers (Basel). 2020 Jun;12(6).

181. Mariscal J, Alonso-Nocelo M, Muinelo-Romay L, Barbazan J, Vieito M, Abalo A, et al. Molecular Profiling of Circulating Tumour Cells Identifies Notch1 as a Principal Regulator in Advanced Non-Small Cell Lung Cancer. Sci Rep. 2016 Nov;6:37820.

182. Abreu M, Cabezas-Sainz P, Alonso-Alconada L, Ferreirós A, Mondelo-Macía P, Lago-Lestón RM, et al. Circulating Tumor Cells Characterization Revealed TIMP1 as a Potential Therapeutic Target in Ovarian Cancer. Cells. 2020 May;9(5).

183. Habli Z, Alchamaa W, Saab R, Kadara H, Khraiche ML. Circulating tumor cell detection technologies and clinical utility: Challenges and opportunities. Cancers (Basel). 2020;12(7):1–30.

184. Alix-Panabières C, Pantel K. Circulating tumor cells: Liquid biopsy of cancer. Clin Chem. 2013;59(1):110–8.

185. Riethdorf S, O'Flaherty L, Hille C, Pantel K. Clinical applications of the CellSearch platform in cancer patients. Adv Drug Deliv Rev. 2018;125:102–21.

186. Rushton AJ, Nteliopoulos G, Shaw JA, Coombes RC. A Review of Circulating Tumour Cell Enrichment Technologies. Cancers (Basel). 2021 Feb 26;13(5).

187. Grover PK, Cummins AG, Price TJ, Roberts-Thomson IC, Hardingham JE. Circulating tumour cells: the evolving concept and the inadequacy of their enrichment by EpCAM-based methodology for basic and clinical cancer research. Ann Oncol Off J Eur Soc Med Oncol. 2014 Aug;25(8):1506–16.

188. Kowalik A, Kowalewska M, Góźdź S. Current approaches for avoiding the limitations of circulating tumor cells detection methods-implications for

diagnosis and treatment of patients with solid tumors. Transl Res. 2017;185:58-84.e15.

189. Liu Z, Fusi A, Klopocki E, Schmittel A, Tinhofer I, Nonnenmacher A, et al. Negative enrichment by immunomagnetic nanobeads for unbiased characterization of circulating tumor cells from peripheral blood of cancer patients. J Transl Med. 2011 May 19;9:70.

190. Szczerba BM, Castro-Giner F, Vetter M, Krol I, Gkountela S, Landin J, et al. Neutrophils escort circulating tumour cells to enable cell cycle progression. Nature. 2019;566(7745):553–7.

191. Vona G, Sabile A, Louha M, Sitruk V, Romana S, Schütze K, et al. Isolation by size of epithelial tumor cells : a new method for the immunomorphological and molecular characterization of circulatingtumor cells. Am J Pathol. 2000 Jan;156(1):57–63.

192. Hao S-J, Wan Y, Xia Y-Q, Zou X, Zheng S-Y. Size-based separation methods of circulating tumor cells. Adv Drug Deliv Rev. 2018 Feb;125:3–20.

193. Farace F, Massard C, Vimond N, Drusch F, Jacques N, Billiot F, et al. A direct comparison of CellSearch and ISET for circulating tumour-cell detection in patients with metastatic carcinomas. Br J Cancer. 2011 Sep 6;105(6):847–53.

194. Miller MC, Robinson PS, Wagner C, O'Shannessy DJ. The Parsortix™ Cell Separation System-A versatile liquid biopsy platform. Cytometry A. 2018;93(12):1234–9.

195. Hou HW, Warkiani ME, Khoo BL, Li ZR, Soo RA, Tan DS-W, et al. Isolation and retrieval of circulating tumor cells using centrifugal forces. Sci Rep. 2013;3:1259.

196. Gascoyne PRC, Shim S. Isolation of circulating tumor cells by dielectrophoresis. Cancers (Basel). 2014 Mar 12;6(1):545–79.

197. Nagrath S, Sequist L V., Maheswaran S, Bell DW, Irimia D, Ulkus L, et al. Isolation of rare circulating tumour cells in cancer patients by microchip technology. Nature. 2007;450(7173):1235–9.

198. Dizdar L, Fluegen G, van Dalum G, Honisch E, Neves RP, Niederacher D, et al. Detection of circulating tumor cells in colorectal cancer patients using the GILUPI CellCollector: results from a prospective, single-center study. Mol Oncol. 2019;13(7):1548–58.

199. Fischer JC, Niederacher D, Topp SA, Honisch E, Schumacher S, Schmitz N, et al. Diagnostic leukapheresis enables reliable detection of circulating tumor cells of nonmetastatic cancer patients. Proc Natl Acad Sci U S A. 2013 Oct 8;110(41):16580–5.

200. Valihrach L, Androvic P, Kubista M. Platforms for Single-Cell Collection and Analysis. Int J Mol Sci. 2018 Mar;19(3).

201. Lawson DA, Kessenbrock K, Davis RT, Pervolarakis N, Werb Z. Tumour heterogeneity and metastasis at single-cell resolution. Nat Cell Biol. 2018 Dec;20(12):1349–60.

202. Cortés-Hernández LE, Eslami-S Z, Pantel K, Alix-Panabières C. Molecular and Functional Characterization of Circulating Tumor Cells: From Discovery to Clinical Application. Clin Chem. 2019 Dec 6;66(1):97–104.

203. Allard WJ, Matera J, Miller MC, Repollet M, Connelly MC, Rao C, et al. Tumor cells circulate in the peripheral blood of all major carcinomas but not in healthy subjects or patients with nonmalignant diseases. Clin Cancer Res. 2004;10(20):6897–904.

204. Maheswaran S, Sequist L V., Nagrath S, Ulkus L, Brannigan B, Collura C V., et al. Detection of Mutations in EGFR in Circulating Lung-Cancer Cells. N Engl J Med. 2008 Jul 24;359(4):366–77.

205. Siravegna G, Marsoni S, Siena S, Bardelli A. Integrating liquid biopsies into the management of cancer. Nat Rev Clin Oncol. 2017;14(9):531–48.

206. Hayes DF, Cristofanilli M, Budd GT, Ellis MJ, Stopeck A, Miller MC, et al. Circulating tumor cells at each follow-up time point during therapy of metastatic breast cancer patients predict progression-free and overall survival. Clin cancer Res an Off J Am Assoc Cancer Res. 2006 Jul;12(14 Pt 1):4218–24.

207. de Bono JS, Scher HI, Montgomery RB, Parker C, Miller MC, Tissing H, et al. Circulating tumor cells predict survival benefit from treatment in metastatic castration-resistant prostate cancer. Clin cancer Res an Off J Am Assoc Cancer Res. 2008 Oct;14(19):6302–9.

208. Cohen EN, Jayachandran G, Moore RG, Cristofanilli M, Lang JE, Khoury JD, et al. A Multi-Center Clinical Study to Harvest and Characterize Circulating Tumor Cells from Patients with Metastatic Breast Cancer Using the Parsortix(®) PC1 System. Cancers (Basel). 2022 Oct;14(21).

209. Pasini L, Ulivi P. Extracellular vesicles in non-small-cell lung cancer: Functional role and involvement in resistance to targeted treatment and immunotherapy. Vol. 12, Cancers. MDPI AG; 2020. p. 40.

210. Zhang H-G, Grizzle WE. Exosomes and cancer: a newly described pathway of immune suppression. Clin cancer Res an Off J Am Assoc Cancer Res. 2011 Mar;17(5):959–64.

211. Logozzi M, De Milito A, Lugini L, Borghi M, Calabrò L, Spada M, et al. High levels of exosomes expressing CD63 and caveolin-1 in plasma of melanoma patients. PLoS One. 2009;4(4):e5219.

212. Pasini L, Ulivi P. Liquid Biopsy for the Detection of Resistance Mechanisms in NSCLC: Comparison of Different Blood Biomarkers. J Clin Med. 2019 Jul 9;8(7):998.

213. Nilsson RJA, Balaj L, Hulleman E, van Rijn S, Pegtel DM, Walraven M, et al. Blood platelets contain tumor-derived RNA biomarkers. Blood. 2011 Sep;118(13):3680–3.

214. Luo C-L, Xu Z-G, Chen H, Ji J, Wang Y-H, Hu W, et al. LncRNAs and EGFRvIII sequestered in TEPs enable blood-based NSCLC diagnosis. Cancer Manag Res. 2018;10:1449–59.

215. Best MG, Vancura A, Wurdinger T. Platelet RNA as a circulating biomarker trove for cancer diagnostics. J Thromb Haemost. 2017 Jul;15(7):1295–306.

216. Velez G, Nguyen H V, Chemudupati T, Ludwig CA, Toral M, Reddy S, et al. Liquid biopsy proteomics of uveal melanoma reveals biomarkers associated with metastatic risk. Vol. 20, Molecular cancer. 2021. p. 39.

217. Mondelo-Macía P, Lago-Lestón RM, Rodríguez-Casanova A, Abalo A, Díaz-Lagares Á, García-González J, et al. Rapid Idylla mutational testing to detect EGFR mutations in plasma samples and to monitor therapy in advanced non-small cell lung cancer patients. Pathology. England; 2023.

218. Singal G, Miller PG, Agarwala V, Li G, Kaushik G, Backenroth D, et al. Association of Patient Characteristics and Tumor Genomics With Clinical Outcomes Among Patients With Non-Small Cell Lung Cancer Using a Clinicogenomic Database. Jama. 2019;321(14):1391–9.

219. Kang Q, Henry NL, Paoletti C, Jiang H, Vats P, Chinnaiyan AM, et al. Comparative analysis of circulating tumor DNA stability In K(3)EDTA, Streck, and CellSave blood collection tubes. Clin Biochem. 2016 Dec;49(18):1354–60.

220. Garcia J, Wozny A-S, Geiguer F, Delherme A, Barthelemy D, Merle P, et al. Profiling of circulating tumor DNA in plasma of non-small cell lung cancer patients, monitoring of epidermal growth factor receptor p.T790M mutated allelic fraction using beads, emulsion, amplification, and magnetics companion assay and evaluation in fut. Cancer Med. 2019 Jul;8(8):3685–97.

221. Zulato E, Tosello V, Nardo G, Bonanno L, Del Bianco P, Indraccolo S. Implementation of Next Generation Sequencing-Based Liquid Biopsy for Clinical Molecular Diagnostics in Non-Small Cell Lung Cancer (NSCLC) Patients. Diagnostics (Basel, Switzerland). 2021 Aug;11(8).

222. Oliveros JC. Venny. An interactive tool for comparing lists with Venn's diagram.

223. Delgado-Garciá M, Weynand B, Gómez-Izquierdo L, Hernández MJ, Blanco ÁM, Varela M, et al. Clinical performance evaluation of the Idylla™ EGFR

Mutation Test on formalin-fixed paraffin-embedded tissue of non-small cell lung cancer. BMC Cancer. 2020;20(1):1–10.

224. Momeni-Boroujeni A, Salazar P, Zheng T, Mensah N, Rijo I, Dogan S, et al. Rapid EGFR Mutation Detection Using the Idylla Platform: Single-Institution Experience of 1200 Cases Analyzed by an In-House Developed Pipeline and Comparison with Concurrent Next-Generation Sequencing Results. J Mol Diagnostics. 2021 Mar;23(3):310–22.

225. Gilson P, Saurel C, Salleron J, Husson M, Demange J, Merlin JL, et al. Evaluation of the Idylla ctEGFR mutation assay to detect EGFR mutations in plasma from patients with non-small cell lung cancers. Sci Rep. 2021;11(1):1–11.

226. Janku F, Huang HJ, Claes B, Falchook GS, Fu S, Hong D, et al. BRAF Mutation testing in cell-free DNA from the plasma of patients with advanced cancers using a rapid, automated molecular diagnostics system. Mol Cancer Ther. 2016;15(6):1397–404.

227. Vivancos A, Aranda E, Benavides M, Élez E, Gómez-España MA, Toledano M, et al. Comparison of the Clinical Sensitivity of the Idylla Platform and the OncoBEAM RAS CRC Assay for KRAS Mutation Detection in Liquid Biopsy Samples. Sci Rep. 2019;9(1):1–8.

228. Finall A, Davies G, Jones T, Emlyn G, Huey P, Mullard A. Integration of rapid PCR testing as an adjunct to NGS in diagnostic pathology services within the UK: evidence from a case series of non-squamous, non-small cell lung cancer (NSCLC) patients with follow-up. J Clin Pathol. 2022 Jan;

229. Heeke S, Hofman V, Benzaquen J, Otto J, Tanga V, Zahaf K, et al. Detection of EGFR Mutations From Plasma of NSCLC Patients Using an Automatic Cartridge-Based PCR System. Front Pharmacol. 2021;12(April):1–5.

230. Mondelo-Macía P, Rodríguez-López C, Valiña L, Aguín S, León-Mateos L, García-González J, et al. Detection of MET Alterations Using Cell Free DNA and Circulating Tumor Cells from Cancer Patients. Cells. 2020 Feb;9(2).

231. Maroun CR, Rowlands T. The Met receptor tyrosine kinase: A key player in oncogenesis and drug resistance. Pharmacol Ther. 2014;142(3):316–38.

232. Mo H-N, Liu P. Targeting MET in cancer therapy. Chronic Dis Transl Med. 2017;3(3):148–53.

233. Trusolino L, Bertotti A, Comoglio PM. MET signalling: Principles and functions in development, organ regeneration and cancer. Nat Rev Mol Cell Biol. 2010;11(12):834–48.

234. Drilon A, Cappuzzo F, Ou SHI, Camidge DR. Targeting MET in Lung Cancer: Will Expectations Finally Be MET? Vol. 12, Journal of Thoracic Oncology. 2017. p. 15–26.

235. Tovar EA, Graveel CR. MET in human cancer: germline and somatic mutations. Ann Transl Med. 2017 May;5(10):205–205.

236. Bardelli A, Corso S, Bertotti A, Hobor S, Valtorta E, Siravegna G, et al. Amplification of the MET receptor drives resistance to anti-EGFR therapies in colorectal cancer. Cancer Discov. 2013;3(6):658–73.

237. Duplaquet L, Kherrouche Z, Baldacci S, Jamme P, Cortot AB, Copin M-C, et al. The multiple paths towards MET receptor addiction in cancer. Oncogene. 2018 Jun 19;37(24):3200–15.

238. Kwak EL, Ahronian LG, Siravegna G, Mussolin B, Godfrey JT, Clark JW, et al. Molecular heterogeneity and receptor coamplification drive resistance to targeted therapy in MET-Amplified esophagogastric cancer. Cancer Discov. 2015;5(12):1271–81.

239. Kwak Y, Kim S, Park C, Paek SH, Lee S, Park S. C-MET overexpression and amplification in gliomas. 2015;8(11):14932–8.

240. Jia L, Yang X, Tian W, Guo S, Huang W, Zhao W. Increased Expression of c-Met is Associated with Chemotherapy-Resistant Breast Cancer and Poor Clinical Outcome. Med Sci Monit. 2018 Nov 16;24:8239–49.

241. Li Y, Li W, He Q, Xu Y, Ren X, Tang X, et al. Prognostic value of MET protein overexpression and gene amplification in locoregionally advanced nasopharyngeal carcinoma. Oncotarget. 2015;6(15).

242. Zhang Y, Du Z, Zhang M. Biomarker development in MET-targeted therapy. Oncotarget. 2016;7(24).

243. De Bacco F, Luraghi P, Medico E, Reato G, Girolami F, Perera T, et al. Induction of MET by ionizing radiation and its role in radioresistance and invasive growth of cancer. J Natl Cancer Inst. 2011;103(8):645–61.

244. Lee M, Jain P, Wang F, Ma PC, Borczuk A, Halmos B. MET alterations and their impact on the future of non-small cell lung cancer (NSCLC) targeted therapies. Expert Opin Ther Targets. 2021;25(4):249–68.

245. Parikh PK, Ghate MD. Recent advances in the discovery of small molecule c-Met Kinase inhibitors. Eur J Med Chem. 2018 Jan 1;143:1103–38.

246. Ilie M, Hofman V, Long E, Bordone O, Selva E, Washetine K, et al. Current challenges for detection of circulating tumor cells and cell-free circulating nucleic acids, and their characterization in non-small cell lung carcinoma patients. What is the best blood substrate for personalized medicine? Ann Transl Med. 2014 Nov;2(11):107.

247. Park S, Choi Y La, Sung CO, An J, Seo J, Ahn MJ, et al. High MET copy number and MET overexpression: Poor outcome in non-small cell lung cancer patients. Histol Histopathol. 2012;27(2):197–207.

248. Cappuzzo F, Marchetti A, Skokan M, Rossi E, Gajapathy S, Felicioni L, et al. Increased MET gene copy number negatively affects survival of surgically resected non-small-cell lung cancer patients. J Clin Oncol. 2009;27(10):1667–74.

249. Kitz J, Lowes LE, Goodale D, Allan AL. Circulating Tumor Cell Analysis in Preclinical Mouse Models of Metastasis. Diagnostics (Basel, Switzerland). 2018 Apr;8(2).

250. Alunni-Fabbroni M, Sandri MT. Circulating tumour cells in clinical practice: Methods of detection and possible characterization. Methods. 2010. p. 289–97.

251. Marrinucci D, Bethel K, Bruce RH, Curry DN, Hsieh B, Humphrey M, et al. Case study of the morphologic variation of circulating tumor cells. Hum Pathol. 2007;38(3):514–9.

252. Zhang T, Boominathan R, Foulk B, Rao C, Kemeny G, Strickler JH, et al. Development of a Novel c-MET-Based CTC Detection Platform. Mol Cancer Res. 2016;14(6):539–47.

253. Ilie M, Szafer-glusman E, Hofman V, Long-mira E. Expression of MET in circulating tumor cells correlates with expression in tumor tissue from advanced-stage lung cancer patients. 2017;8(16):26112–21.

254. Zhang Y, Tang ET, Du Z. Detection of MET gene copy number in cancer samples using the droplet digital PCR method. PLoS One. 2016;11(1):1–8.

255. Ikeda S, Schwaederle M, Mohindra M, Fontes Jardim DL, Kurzrock R. MET alterations detected in blood-derived circulating tumor DNA correlate with bone metastases and poor prognosis. J Hematol Oncol. 2018;11(1):76.

256. Wang Q, Yang S, Wang K, Sun SY. MET inhibitors for targeted therapy of EGFR TKI-resistant lung cancer. Vol. 12, Journal of Hematology and Oncology. 2019.

257. Shi P, Oh YT, Zhang G, Yao W, Yue P, Li Y, et al. Met gene amplification and protein hyperactivation is a mechanism of resistance to both first and third generation EGFR inhibitors in lung cancer treatment. Cancer Lett. 2016;380(2):494–504.

258. Kang J, Chen HJ, Wang Z, Liu J, Li B, Zhang T, et al. Osimertinib and Cabozantinib Combinatorial Therapy in an EGFR-Mutant Lung Adenocarcinoma Patient with Multiple MET Secondary-Site Mutations after Resistance to Crizotinib. J Thorac Oncol. 2018;13(4):e49–53.

259. Deng L, Kiedrowski LA, Ravera E, Cheng H, Halmos B. Response to Dual Crizotinib and Osimertinib Treatment in a Lung Cancer Patient with MET Amplification Detected by Liquid Biopsy Who Acquired Secondary Resistance to EGFR Tyrosine Kinase Inhibition. Vol. 13, Journal of Thoracic Oncology. 2018. p. e169–72.

260. Zhu VW, Schrock AB, Ali SM, Ou SHI. Differential response to a combination of fulldose osimertinib and crizotinib in a patient with EGFR-mutant non-small cell lung cancer and emergent MET amplification. Lung Cancer Targets Ther. 2019;10:21–6.

261. Mondelo-Macía P, García-González J, León-Mateos L, Anido U, Aguín S, Abdulkader I, et al. Clinical potential of circulating free DNA and circulating tumour cells in patients with metastatic non-small-cell lung cancer treated with pembrolizumab. Mol Oncol. 2021;15(11):2923–40.

262. Siegel RL, Miller KD, Jemal A. Cancer statistics, 2019. CA Cancer J Clin. 2019 Jan 8;69(1):7–34.

263. Pardoll DM. The blockade of immune checkpoints in cancer immunotherapy. Nat Rev Cancer. 2012 Apr;12(4):252–64.

264. Blons H, Garinet S, Laurent-Puig P, Oudart J-B. Molecular markers and prediction of response to immunotherapy in non-small cell lung cancer, an update. J Thorac Dis. 2019 Jan;11(Suppl 1):S25–36.

265. Rossi S, Castello A, Toschi L, Lopci E. Immunotherapy in non-small-cell lung cancer: potential predictors of response and new strategies to assess activity. Immunotherapy. 2018 Jul 1;10(9):797–805.

266. Tellez-Gabriel M, Heymann MF, Heymann D. Circulating tumor cells as a tool for assessing tumor heterogeneity. Theranostics. 2019;9(16):4580–94.

267. Russano M, Napolitano A, Ribelli G, Iuliani M, Simonetti S, Citarella F, et al. Liquid biopsy and tumor heterogeneity in metastatic solid tumors: the potentiality of blood samples. J Exp Clin Cancer Res. 2020;39(1):120.

268. Brozos-Vázquez EM, Díaz-Peña R, García-González J, León-Mateos L, Mondelo-Macía P, Peña-Chilet M, et al. Immunotherapy in nonsmall-cell lung cancer: current status and future prospects for liquid biopsy. Cancer Immunology, Immunotherapy 2020.

269. de Wit S, Rossi E, Weber S, Tamminga M, Manicone M, Swennenhuis JF, et al. Single tube liquid biopsy for advanced non-small cell lung cancer. Int J cancer. 2019 Jun;144(12):3127–37.

270. Alama, Coco, Genova, Rossi, Fontana, Tagliamento, et al. Prognostic Relevance of Circulating Tumor Cells and Circulating Cell-Free DNA Association in

Metastatic Non-Small Cell Lung Cancer Treated with Nivolumab. J Clin Med. 2019 Jul 10;8(7):1011.

271. Giroux Leprieur E, Herbretau G, Dumenil C, Julie C, Giraud V, Labrune S, et al. Circulating tumor DNA evaluated by Next-Generation Sequencing is predictive of tumor response and prolonged clinical benefit with nivolumab in advanced non-small cell lung cancer. Oncoimmunology. 2018 May 4;7(5):e1424675.

272. Zhou X, Li C, Zhang Z, Li DY, Du J, Ding P, et al. Kinetics of plasma cfDNA predicts clinical response in non-small cell lung cancer patients. Sci Rep. 2021 Apr;11(1):7633.

273. Sirera R, Bremnes RM, Cabrera A, Jantus-Lewintre E, Sanmartín E, Blasco A, et al. Circulating DNA is a useful prognostic factor in patients with advanced non-small cell lung cancer. J Thorac Oncol Off Publ Int Assoc Study Lung Cancer. 2011 Feb;6(2):286–90.

274. Mazel M, Jacot W, Pantel K, Bartkowiak K, Topart D, Cayrefourcq L, et al. Frequent expression of PD-L1 on circulating breast cancer cells. Mol Oncol. 2015;9(9):1773–82.

275. Scheel AH, Baenfer G, Baretton G, Dietel M, Diezko R, Henkel T, et al. Interlaboratory concordance of PD-L1 immunohistochemistry for non-small-cell lung cancer. Histopathology. 2018 Feb 1;72(3):449–59.

276. Robin X, Turck N, Hainard A, Tiberti N, Lisacek F, Sanchez J-C, et al. pROC: an open-source package for R and S+ to analyze and compare ROC curves. BMC Bioinformatics. 2011 Dec 17;12(1):77.

277. Therneau TM, Grambsch PM. Modeling Survival Data: Extending the Cox Model. New York: Springer; 2000.

278. Hellmann MD, Ciuleanu T-E, Pluzanski A, Lee JS, Otterson GA, Audigier-Valette C, et al. Nivolumab plus Ipilimumab in Lung Cancer with a High Tumor Mutational Burden. N Engl J Med. 2018;378(22):2093–104.

279. Hellmann MD, Paz-Ares L, Bernabe Caro R, Zurawski B, Kim S-W, Carcereny Costa E, et al. Nivolumab plus Ipilimumab in Advanced Non–Small-Cell Lung Cancer. N Engl J Med. 2019 Nov;381(21):2020–31.

280. Gandara DR, Paul SM, Kowanetz M, Schleifman E, Zou W, Li Y, et al. Blood-based tumor mutational burden as a predictor of clinical benefit in non-small-cell lung cancer patients treated with atezolizumab. Nat Med. 2018 Sep 6;24(9):1441–8.

281. Fenizia F, Pasquale R, Roma C, Bergantino F, Iannaccone A, Normanno N. Measuring tumor mutation burden in non-small cell lung cancer: Tissue versus liquid biopsy. Transl Lung Cancer Res. 2018;7(6):668–77.

282. Chen YT, Seeruttun SR, Wu XY, Wang ZX. Maximum Somatic Allele Frequency in Combination With Blood-Based Tumor Mutational Burden to Predict the Efficacy of Atezolizumab in Advanced Non-small Cell Lung Cancer: A Pooled Analysis of the Randomized POPLAR and OAK Studies. Front Oncol. 2019;9(December):1–9.

283. Wood MA, Weeder BR, David JK, Nellore A, Thompson RF. Burden of tumor mutations, neoepitopes, and other variants are weak predictors of cancer immunotherapy response and overall survival. Genome Med. 2020 Dec;12(1):33.

284. Tissot C, Toffart A-C, Villar S, Souquet P-J, Merle P, Moro-Sibilot D, et al. Circulating free DNA concentration is an independent prognostic biomarker in lung cancer. Eur Respir J. 2015 Dec 1;46(6):1773–80.

285. Ai B, Liu H, Huang Y, Peng P. Circulating cell-free DNA as a prognostic and predictive biomarker in non-small cell lung cancer. Oncotarget. 2016 Jul 12;7(28):44583–95.

286. Cargnin S, Canonico PL, Genazzani AA, Terrazzino S. Quantitative Analysis of Circulating Cell-Free DNA for Correlation with Lung Cancer Survival: A Systematic Review and Meta-Analysis. J Thorac Oncol. 2017 Jan 1;12(1):43–53.

287. Trigg RM, Martinson LJ, Parpart-Li S, Shaw JA. Factors that influence quality and yield of circulating-free DNA: A systematic review of the methodology literature. Heliyon. 2018 Jul;4(7):e00699.

288. Paci M, Maramotti S, Bellesia E, Formisano D, Albertazzi L, Ricchetti T, et al. Circulating plasma DNA as diagnostic biomarker in non-small cell lung cancer. Lung Cancer. 2009 Apr;64(1):92–7.

289. Pavan A, Boscolo Bragadin A, Calvetti L, Ferro A, Zulato E, Attili I, et al. Role of next generation sequencing-based liquid biopsy in advanced non-small cell lung cancer patients treated with immune checkpoint inhibitors: impact of STK11, KRAS and TP53 mutations and co-mutations on outcome. Transl Lung Cancer Res. 2021 Jan;10(1):202–20.

290. Guibert N, Jones G, Beeler JF, Plagnol V, Morris C, Mourlanette J, et al. Targeted sequencing of plasma cell-free DNA to predict response to PD1 inhibitors in advanced non-small cell lung cancer. Lung Cancer. 2019 Nov 1 [cited 2020 Mar 23];137:1–6.

291. Khagi Y, Goodman AM, Daniels GA, Patel SP, Sacco AG, Randall JM, et al. Hypermutated circulating tumor DNA: Correlation with response to checkpoint inhibitor–based immunotherapy. Clin Cancer Res. 2017 Oct;23(19):5729–36.

292. Bratman S V, Yang SYC, Iafolla MAJ, Liu Z, Hansen AR, Bedard PL, et al. Personalized circulating tumor DNA analysis as a predictive biomarker in solid tumor patients treated with pembrolizumab. Nat Cancer. 2020;1(9):873–81.

293. Ricciuti B, Jones G, Severgnini M, Alessi J V, Recondo G, Lawrence M, et al. Early plasma circulating tumor DNA (ctDNA) changes predict response to first-line pembrolizumab-based therapy in non-small cell lung cancer (NSCLC). J Immunother cancer. 2021 Mar;9(3).

294. Cabel L, Riva F, Servois V, Livartowski A, Daniel C, Rampanou A, et al. Circulating tumor DNA changes for early monitoring of anti-PD1 immunotherapy: A proof-of-concept study. Ann Oncol. 2017 Aug 1;28(8):1996–2001.

295. Goldberg SB, Narayan A, Kole AJ, Decker RH, Teysir J, Carriero NJ, et al. Early assessment of lung cancer immunotherapy response via circulating tumor DNA. Clin Cancer Res. 2018;24(8):1872–80.

296. Cheng C, Omura-Minamisawa M, Kang Y, Hara T, Koike I, Inoue T. Quantification of circulating cell-free DNA in the plasma of cancer patients during radiation therapy. Cancer Sci. 2009 Feb;100(2):303–9.

297. Gautschi O, Bigosch C, Huegli B, Jermann M, Marx A, Chassé E, et al. Circulating deoxyribonucleic Acid as prognostic marker in non-small-cell lung cancer patients undergoing chemotherapy. J Clin Oncol Off J Am Soc Clin Oncol. 2004 Oct;22(20):4157–64.

298. Sozzi G, Conte D, Leon M, Ciricione R, Roz L, Ratcliffe C, et al. Quantification of free circulating DNA as a diagnostic marker in lung cancer. J Clin Oncol Off J Am Soc Clin Oncol. 2003 Nov;21(21):3902–8.

299. Meddeb R, Dache ZAA, Thezenas S, Otandault A, Tanos R, Pastor B, et al. Quantifying circulating cell-free DNA in humans. Sci Rep. 2019;9(1):1–16.

300. Brodbeck K, Schick S, Bayer B, Anslinger K, Krüger K, Mayer Z, et al. Biological variability of cell-free DNA in healthy females at rest within a short time course. Int J Legal Med. 2020 May;134(3):911–9.

301. Janning M, Kobus F, Babayan A, Wikman H, Velthaus JL, Bergmann S, et al. Determination of PD-L1 expression in circulating tumor cells of NSCLC patients and correlation with response to PD-1/PD-L1 inhibitors. Cancers (Basel). 2019;11(6):835.

302. Kurokawa M, Ise N, Omi K, Goishi K, Higashiyama S. Cisplatin influences acquisition of resistance to molecular-targeted agents through epithelial-mesenchymal transition-like changes. Cancer Sci. 2013 Jul;104(7):904–11.

303. Jakobsen KR, Demuth C, Sorensen BS, Nielsen AL. The role of epithelial to mesenchymal transition in resistance to epidermal growth factor receptor

tyrosine kinase inhibitors in non-small cell lung cancer. Transl Lung Cancer Res. 2016 Apr;5(2):172–82.

304. Fukuda K, Takeuchi S, Arai S, Katayama R, Nanjo S, Tanimoto A, et al. Epithelial-to-mesenchymal transition is a mechanism of ALK inhibitor resistance in lung cancer independent of ALK mutation status. Cancer Res. 2019 Apr;79(7):1658–70.

305. Zhu X, Chen L, Liu L, Niu X. EMT-Mediated Acquired EGFR-TKI Resistance in NSCLC: Mechanisms and Strategies. Vol. 9, Frontiers in Oncology. Frontiers Media S.A.; 2019. p. 1044.

306. Chudziak J, Burt DJ, Mohan S, Rothwell DG, Mesquita B, Antonello J, et al. Clinical evaluation of a novel microfluidic device for epitope-independent enrichment of circulating tumour cells in patients with small cell lung cancer. Analyst. 2016 Jan;141(2):669–78.

307. Ilié M, Szafer-Glusman E, Hofman V, Chamorey E, Lalvée S, Selva E, et al. Detection of PD-L1 in circulating tumor cells and white blood cells from patients with advanced non-small-cell lung cancer. Ann Oncol. 2018;29(1):193–9.

308. Guibert N, Delaunay M, Lusque A, Boubekeur N, Rouquette I, Clermont E, et al. PD-L1 expression in circulating tumor cells of advanced non-small cell lung cancer patients treated with nivolumab. Lung Cancer. 2018;120(March):108–12.

309. Boffa DJ, Graf RP, Salazar MC, Hoag J, Lu D, Krupa R, et al. Cellular Expression of PD-L1 in the Peripheral Blood of Lung Cancer Patients is Associated with Worse Survival. Cancer Epidemiol Biomarkers Prev. 2017 Jul 1;26(7):1139–45.

310. Nicolazzo C, Raimondi C, Mancini M, Caponnetto S, Gradilone A, Gandini O, et al. Monitoring PD-L1 positive circulating tumor cells in non-small cell lung cancer patients treated with the PD-1 inhibitor Nivolumab. Sci Rep. 2016;6:31726.

311. Dhar M, Wong J, Che J, Matsumoto M, Grogan T, Elashoff D, et al. Evaluation of PD-L1 expression on vortex-isolated circulating tumor cells in metastatic lung cancer. Sci Rep. 2018;8(1):2592.

312. Cheng Y, Wang T, Lv X, Li R, Yuan L, Shen J, et al. Detection of PD-L1 Expression and Its Clinical Significance in Circulating Tumor Cells from Patients with Non-Small-Cell Lung Cancer. Cancer Manag Res. 2020 Mar 19;Volume 12:2069–78.

313. Koh Y, Yagi S, Akamatsu H, Kanai K, Hayata A, Tokudome N, et al. Heterogeneous Expression of Programmed Death Receptor-ligand 1 on Circulating Tumor Cells in Patients With Lung Cancer. Clin Lung Cancer. 2019;20(4):270–7.

314. Guibert N, Pradines A, Mazieres J, Favre G. Current and future applications of liquid biopsy in nonsmall cell lung cancer from early to advanced stages. Eur Respir Rev. 2020;29(155).

315. Jacot W, Mazel M, Mollevi C, Pouderoux S, D'Hondt V, Cayrefourcq L, et al. Clinical Correlations of Programmed Cell Death Ligand 1 Status in Liquid and Standard Biopsies in Breast Cancer. Clin Chem. 2020 Aug;66(8):1093–101.

316. Haragan A, Field JK, Davies MPA, Escriu C, Gruver A, Gosney JR. Heterogeneity of PD-L1 expression in non-small cell lung cancer: Implications for specimen sampling in predicting treatment response. Lung Cancer. 2019 Aug;134:79–84.

317. Alidousty C, Duerbaum N, Wagener-Ryczek S, Baar T, Martelotto LG, Heydt C, et al. Prevalence and potential biological role of TERT amplifications in ALK translocated adenocarcinoma of the lung. Histopathology. 2021 Mar;78(4):578–85.

318. Barthel FP, Wei W, Tang M, Martinez-Ledesma E, Hu X, Amin SB, et al. Systematic analysis of telomere length and somatic alterations in 31 cancer types. Nat Genet. 2017 Mar;49(3):349–57.

319. Mondelo-Macía P, García-González J, Abalo A, Mosquera-Presedo M, Aguín S, Mateos M, et al. Plasma cell-free DNA and circulating tumor cells as prognostic biomarkers in small cell lung cancer patients. Transl Lung Cancer Res. 2022;11(10):1995–2009.

320. Rudin CM, Brambilla E, Faivre-Finn C, Sage J. Small-cell lung cancer. Nat Rev Dis Prim. 2021 Dec 14;7(1):3.

321. Gazdar AF, Bunn PA, Minna JD. Small-cell lung cancer: What we know, what we need to know and the path forward. Nat Rev Cancer. 2017;17(12):725–37.

322. Dumoulin DW, Dingemans AMC, Aerts JGJV, Remon J, de Ruysscher DKM, Hendriks LEL. Immunotherapy in small cell lung cancer: One step at a time: A narrative review. Transl Lung Cancer Res. 2021;10(6):2970–87.

323. Kalemkerian GP, Loo BW, Akerley W, Attia A, Bassetti M, Boumber Y, et al. NCCN guidelines® insights: Small cell lung cancer, version 2.2018 featured updates to the NCCN guidelines. JNCCN J Natl Compr Cancer Netw. 2018;16(10):1171–82.

324. Ortega-Franco A, Ackermann C, Paz-Ares L, Califano R. First-line immune checkpoint inhibitors for extensive stage small-cell lung cancer: clinical developments and future directions. ESMO Open. 2021;6(1):100003.

325. Blackhall F, Frese KK, Simpson K, Kilgour E, Brady G, Dive C. Will liquid biopsies improve outcomes for patients with small-cell lung cancer? Lancet Oncol. 2018 Sep 1;19(9):e470–81.

326. Herath S, Sadeghi Rad H, Radfar P, Ladwa R, Warkiani M, O'Byrne K, et al. The Role of Circulating Biomarkers in Lung Cancer. Front Oncol. 2021;11:801269.

327. Cheng ML, Pectasides E, Hanna GJ, Parsons HA, Choudhury AD, Oxnard GR. Circulating tumor DNA in advanced solid tumors: Clinical relevance and future directions. CA Cancer J Clin. 2021;71(2):176–90.

328. García-Pardo M, Makarem M, Li JJN, Kelly D, Leighl NB. Integrating circulating-free DNA (cfDNA) analysis into clinical practice: opportunities and challenges. Br J Cancer. 2022 Mar;

329. Mathios D, Johansen JS, Cristiano S, Medina JE, Phallen J, Larsen KR, et al. Detection and characterization of lung cancer using cell-free DNA fragmentomes. Nat Commun. 2021 Aug;12(1):5060.

330. Romero A, Nadal E, Serna R, Insa A, Campelo MRG, Benito C, et al. OA20.02 Pre-Treatment Levels of ctDNA for Long-Term Survival Prediction in Stage IIIA NSCLC Treated With Neoadjuvant Chemo-Immunotherapy. J Thorac Oncol. 2021;16(10):S883–4.

331. Moding EJ, Liu Y, Nabet BY, Chabon JJ, Chaudhuri AA, Hui AB, et al. Circulating tumor DNA dynamics predict benefit from consolidation immunotherapy in locally advanced non-small-cell lung cancer. Nat Cancer. 2020;1:176–183.

332. Cheng ML, Lau CJ, Milan MSD, Supplee JG, Riess JW, Bradbury PA, et al. Plasma ctDNA Response Is an Early Marker of Treatment Effect in Advanced NSCLC. JCO Precis Oncol. 2021;5.

333. Cristofanilli M, Budd GT, Ellis MJ, Stopeck A, Matera J, Miller MC, et al. Circulating tumor cells, disease progression, and survival in metastatic breast cancer. N Engl J Med. 2004;351(8):781–91.

334. Naito T, Tanaka F, Ono A, Yoneda K, Takahashi T, Murakami H, et al. Prognostic impact of circulating tumor cells in patients with small cell lung cancer. J Thorac Oncol. 2012;7(3):512–9.

335. Igawa S, Gohda K, Fukui T, Ryuge S, Otani S, Masago A, et al. Circulating tumor cells as a prognostic factor in patients with small cell lung cancer. Oncol Lett. 2014 May;7(5):1469–73.

336. Cheng Y, Liu XQ, Fan Y, Liu YP, Liu Y, Liu Y, et al. Circulating tumor cell counts/change for outcome prediction in patients with extensive-stage small-cell lung cancer. Futur Oncol. 2016;12(6):789–99.

337. Salgia R, Weaver RW, McCleod M, Stille JR, Yan SB, Roberson S, et al. Prognostic and predictive value of circulating tumor cells and CXCR4 expression as biomarkers for a CXCR4 peptide antagonist in combination with

carboplatin-etoposide in small cell lung cancer: exploratory analysis of a phase II study. Invest New Drugs. 2017;35(3):334–44.

338. Aggarwal C, Wang X, Ranganathan A, Torigian D, Troxel A, Evans T, et al. Circulating tumor cells as a predictive biomarker in patients with small cell lung cancer undergoing chemotherapy. Lung Cancer. 2017 Oct;112:118–25.

339. Radfar P, Aboulkheyr Es H, Salomon R, Kulasinghe A, Ramalingam N, Sarafraz-Yazdi E, et al. Single-cell analysis of circulating tumour cells: enabling technologies and clinical applications. Trends Biotechnol. 2022 Mar;

340. van Dessel LF, Beije N, Helmijr JCA, Vitale SR, Kraan J, Look MP, et al. Application of circulating tumor DNA in prospective clinical oncology trials - standardization of preanalytical conditions. Mol Oncol. 2017 Mar;11(3):295–304.

341. Akaike H. A New Look at the Statistical Model Identification. In 1974. p. 215–22.

342. Hadley W. Ggplot2: Elegrant graphics for data analysis. Springer; 2016.

343. Sjoberg, Daniel D, Whiting K, Curry M, Lavery, Jessica A, Larmarange J. Reproducible Summary Tables with the gtsummary Package. R J. 2021;13(1):570.

344. Oliveira KCS, Ramos IB, Silva JMC, Barra WF, Riggins GJ, Palande V, et al. Current Perspectives on Circulating Tumor DNA, Precision Medicine, and Personalized Clinical Management of Cancer. Mol Cancer Res. 2020 Apr;18(4):517–28.

345. Schwendenwein A, Megyesfalvi Z, Barany N, Valko Z, Bugyik E, Lang C, et al. Molecular profiles of small cell lung cancer subtypes: therapeutic implications. Mol Ther - Oncolytics. 2021;20(March):470–83.

346. Yang S, Zhang Z, Wang Q. Emerging therapies for small cell lung cancer. J Hematol Oncol. 2019 May;12(1):47.

347. Leon SA, Shapiro B, Sklaroff DM, Yaros MJ. Free DNA in the serum of cancer patients and the effect of therapy. Cancer Res. 1977 Mar;37(3):646–50.

348. van der Drift MA, Hol BEA, Klaassen CHW, Prinsen CFM, van Aarssen YAWG, Donders R, et al. Circulating DNA is a non-invasive prognostic factor for survival in non-small cell lung cancer. Lung Cancer. 2010 May;68(2):283–7.

349. Almodovar K, Iams WT, Meador CB, Zhao Z, York S, Horn L, et al. Longitudinal cell-free DNA analysis in patients with small cell lung cancer reveals dynamic insights into treatment efficacy and disease relapse. 2018;13(1):112–23.

350. Nong J, Gong Y, Guan Y, Yi X, Yi Y, Chang L, et al. Circulating tumor DNA analysis depicts subclonal architecture and genomic evolution of small cell lung cancer. Nat Commun. 2018;9(1):1–8.

351. Du M, Thompson J, Fisher H, Zhang P, Huang CC, Wang L. Genomic alterations of plasma cell-free DNAs in small cell lung cancer and their clinical relevance. Lung Cancer]. 2018;120(April):113–21.

352. Mohan S, Foy V, Ayub M, Leong HS, Schofield P, Sahoo S, et al. Profiling of Circulating Free DNA Using Targeted and Genome-wide Sequencing in Patients with SCLC. J Thorac Oncol. 2020;15(2):216–30.

353. Iams WT, Kopparapu PR, Yan Y, Muterspaugh A, Zhao Z, Chen H, et al. Blood-Based Surveillance Monitoring of Circulating Tumor DNA From Patients With SCLC Detects Disease Relapse and Predicts Death in Patients With Limited-Stage Disease. JTO Clin Res Reports. 2020;1(2):100024.

354. Devarakonda S, Sankararaman S, Herzog BH, Gold KA, Owonikoko TK, Li BT, et al. Circulating Tumor DNA Profiling in Small Cell Lung Cancer Identifies Potentially Targetable Alterations. 2019;25(20):6119–26.

355. Hou JM, Greystoke A, Lancashire L, Cummings J, Ward T, Board R, et al. Evaluation of circulating tumor cells and serological cell death biomarkers in small cell lung cancer patients undergoing chemotherapy. Am J Pathol. 2009;175(2):808–16.

356. Hou JM, Krebs MG, Lancashire L, Sloane R, Backen A, Swain RK, et al. Clinical significance and molecular characteristics of circulating tumor cells and circulating tumor microemboli in patients with small-cell lung cancer. J Clin Oncol. 2012;30(5):525–32.

357. Riley RS, June CH, Langer R, Mitchell MJ. Delivery technologies for cancer immunotherapy. Nat Rev Drug Discov. 2019;18(3):175–96.

358. Bagchi S, Yuan R, Engleman EG. Immune Checkpoint Inhibitors for the Treatment of Cancer: Clinical Impact and Mechanisms of Response and Resistance. Annu Rev Pathol Mech Dis. 2021 Jan 24;16(1):223–49.

359. Spigel D, de Marinis F, Giaccone G, Reinmuth N, Vergnenegre A, Barrios CH, et al. IMpower110: Interim overall survival (OS) analysis of a phase III study of atezolizumab (atezo) vs platinum-based chemotherapy (chemo) as first-line (1L) treatment (tx) in PD-L1-selected NSCLC. Ann Oncol. 2019 Oct;30:v915.

360. Socinski MA, Jotte RM, Cappuzzo F, Orlandi F, Stroyakovskiy D, Nogami N, et al. Atezolizumab for First-Line Treatment of Metastatic Nonsquamous NSCLC. N Engl J Med. 2018;378(24).

361. Kennedy LB, Salama AKS. A review of cancer immunotherapy toxicity. CA Cancer J Clin. 2020;70(2):86–104.

362. Shen P, Han L, Ba X, Qin K, Tu S. Hyperprogressive Disease in Cancers Treated With Immune Checkpoint Inhibitors. Front Pharmacol. 2021;12(July):1–13.

363. Hofman P, Heeke S, Alix-Panabières C, Pantel K. Liquid biopsy in the era of immuno-oncology: Is it ready for prime-time use for cancer patients? Ann Oncol. 2019;30(9):1448–59.

364. Janse van Rensburg HJ, Spiliopoulou P, Siu LL. Circulating Biomarkers for Therapeutic Monitoring of Anti-cancer Agents. Oncologist. 2022 May 6;27(5):352–62.

365. Babačić H, Lehtiö J, Pico De Coaña Y, Pernemalm M, Eriksson H. In-depth plasma proteomics reveals increase in circulating PD-1 during anti-PD-1 immunotherapy in patients with metastatic cutaneous melanoma. J Immunother Cancer. 2020;8(1).

366. Altelaar AFM, Munoz J, Heck AJR. Next-generation proteomics: towards an integrative view of proteome dynamics. Nat Rev Genet. 2013 Jan 4;14(1):35–48.

367. Ludwig C, Gillet L, Rosenberger G, Amon S, Collins BC, Aebersold R. Data-independent acquisition-based SWATH - MS for quantitative proteomics: a tutorial . Mol Syst Biol. 2018;14(8):1–23.

368. de Jesus JR, da Silva Fernandes R, de Souza Pessôa G, Raimundo IM, Arruda MAZ. Depleting high-abundant and enriching low-abundant proteins in human serum: An evaluation of sample preparation methods using magnetic nanoparticle, chemical depletion and immunoaffinity techniques. Talanta. 2017;170(March):199–209.

369. Fernández C, Santos HM, Ruíz-Romero C, Blanco FJ, Capelo-Martínez JL. A comparison of depletion versus equalization for reducing high-abundance proteins in human serum. Electrophoresis. 2011;32(21):2966–74.

370. Bonzon-Kulichenko E, Pérez-Hernández D, Núñez E, Martínez-Acedo P, Navarro P, Trevisan-Herraz M, et al. A robust method for quantitative high-throughput analysis of proteomes by 18O labeling. Mol Cell Proteomics. 2011;10(1):1–14.

371. Perez-Hernandez D, Gutiérrez-Vázquez C, Jorge I, López-Martín S, Ursa A, Sánchez-Madrid F, et al. The intracellular interactome of tetraspanin-enriched microdomains reveals their function as sorting machineries toward exosomes. J Biol Chem. 2013;288(17):11649–61.

372. Shilov I V., Seymourt SL, Patel AA, Loboda A, Tang WH, Keating SP, et al. The paragon algorithm, a next generation search engine that uses sequence temperature values sequence temperature values and feature probabilities to identify peptides from tandem mass spectra. Mol Cell Proteomics. 2007;6(9):1638–55.

373. Luo Y, Mok TS, Lin X, Zhang W, Cui Y, Guo J, et al. SWATH-based proteomics identified carbonic anhydrase 2 as a potential diagnosis biomarker for nasopharyngeal carcinoma. Sci Rep. 2017;7(January):1–11.

374. Meyer JG, Schilling B. Clinical applications of quantitative proteomics using targeted and untargeted data-independent acquisition techniques. Expert Rev Proteomics. 2017 May 4;14(5):419–29.

375. Ortea I, Ruiz-Sánchez I, Cañete R, Caballero-Villarraso J, Cañete MD. Identification of candidate serum biomarkers of childhood-onset growth hormone deficiency using SWATH-MS and feature selection. J Proteomics. 2018;175(2017):105–13.

376. Tan HT, Chung MCM. Label-Free Quantitative Phosphoproteomics Reveals Regulation of Vasodilator-Stimulated Phosphoprotein upon Stathmin-1 Silencing in a Pair of Isogenic Colorectal Cancer Cell Lines. Proteomics. 2018;18(8):1–13.

377. McGurk KA, Dagliati A, Chiasserini D, Lee D, Plant D, Baricevic-Jones I, et al. The use of missing values in proteomic data-independent acquisition mass spectrometry to enable disease activity discrimination. Bioinformatics. 2020 Apr;36(7):2217–23.

378. Jin L, Bi Y, Hu C, Qu J, Shen S, Wang X, et al. A comparative study of evaluating missing value imputation methods in label-free proteomics. Sci Rep. 2021 Jan;11(1):1760.

379. Zhou Y, Zhou B, Pache L, Chang M, Khodabakhshi AH, Tanaseichuk O, et al. Metascape provides a biologist-oriented resource for the analysis of systems-level datasets. Nat Commun. 2019 Apr 3;10(1):1523.

380. Liebermeister W, Noor E, Flamholz A, Davidi D, Bernhardt J, Milo R. Visual account of protein investment in cellular functions. Proc Natl Acad Sci. 2014 Jun 10;111(23):8488–93.

381. Davis AA, Patel VG. The role of PD-L1 expression as a predictive biomarker: an analysis of all US Food and Drug Administration (FDA) approvals of immune checkpoint inhibitors. J Immunother Cancer. 2019 Dec 26;7(1):278.

382. Banchereau R, Leng N, Zill O, Sokol E, Liu G, Pavlick D, et al. Molecular determinants of response to PD-L1 blockade across tumor types. Nat Commun. 2021 Dec 25;12(1):3969.

383. Jardim DL, Goodman A, de Melo Gagliato D, Kurzrock R. The Challenges of Tumor Mutational Burden as an Immunotherapy Biomarker. Cancer Cell. 2021 Feb;39(2):154–73.

384. Chan TA, Yarchoan M, Jaffee E, Swanton C, Quezada SA, Stenzinger A, et al. Development of tumor mutation burden as an immunotherapy biomarker: utility for the oncology clinic. Ann Oncol. 2019 Jan;30(1):44–56.

385. Yanagawa N, Yamada N, Sugimoto R, Osakabe M, Uesugi N, Shiono S, et al. The Frequency of DNA Mismatch Repair Deficiency Is Very Low in Surgically Resected Lung Carcinoma. Front Oncol. 2021 Oct 6;11.

386. Kwon YW, Jo H-S, Bae S, Seo Y, Song P, Song M, et al. Application of Proteomics in Cancer: Recent Trends and Approaches for Biomarkers Discovery. Front Med. 2021 Sep 22;8.

387. Chantada-Vázquez M del P, Conde-Amboage M, Graña-López L, Vázquez-Estévez S, Bravo SB, Núñez C. Circulating Proteins Associated with Response and Resistance to Neoadjuvant Chemotherapy in HER2-Positive Breast Cancer. Cancers (Basel). 2022 Feb 21;14(4):1087.

388. Gómez BB, López-Cortés R, Casas-Nebra FJ, Vázquez-Estévez S, Pérez-Fentes D, Chantada-Vázquez M del P, et al. Detection of Circulating Serum Protein Biomarkers of Non-Muscle Invasive Bladder Cancer after Protein Corona-Silver Nanoparticles Analysis by SWATH-MS. Nanomaterials. 2021 Sep 13;11(9):2384.

389. Janacova L, Faktor J, Capkova L, Paralova V, Pospisilova A, Podhorec J, et al. SWATH-MS Analysis of FFPE Tissues Identifies Stathmin as a Potential Marker of Endometrial Cancer in Patients Exposed to Tamoxifen. J Proteome Res. 2020 Jul 2;19(7):2617–30.

390. Harel M, Ortenberg R, Varanasi SK, Mangalhara KC, Mardamshina M, Markovits E, et al. Proteomics of Melanoma Response to Immunotherapy Reveals Mitochondrial Dependence. Cell. 2019;179(1):236-250.e18.

391. Coscia F, Lengyel E, Duraiswamy J, Ashcroft B, Bassani-Sternberg M, Wierer M, et al. Multi-level Proteomics Identifies CT45 as a Chemosensitivity Mediator and Immunotherapy Target in Ovarian Cancer. Cell. 2018;175(1):159-170.e16.

392. Yu KH, Levine DA, Zhang H, Chan DW, Zhang Z, Snyder M. Predicting ovarian cancer patients' clinical response to platinum-based chemotherapy by their tumor proteomic signatures. J Proteome Res. 2016;15(8):2455–65.

393. Pereira-Veiga T, Bravo S, Gómez-Tato A, Yáñez-Gómez C, Abuín C, Varela V, et al. Red Blood Cells Protein Profile Is Modified in Breast Cancer Patients. Mol Cell Proteomics. 2022 Dec;21(12):100435.

394. Hanash SM, Pitteri SJ, Faca VM. Mining the plasma proteome for cancer biomarkers. Nature. 2008 Apr 2;452(7187):571–9.

395. Maeda S, Yamamoto H, Kinch LN, Garza CM, Takahashi S, Otomo C, et al. Structure, lipid scrambling activity and role in autophagosome formation of ATG9A. Nat Struct Mol Biol. 2020 Dec 26;27(12):1194–201.

396. Huyghe J, Priem D, Van Hove L, Gilbert B, Fritsch J, Uchiyama Y, et al. ATG9A prevents TNF cytotoxicity by an unconventional lysosomal targeting pathway. Science (80-). 2022 Dec 16;378(6625):1201–7.

397. Girard M, Bizet AA, Lachaux A, Gonzales E, Filhol E, Collardeau-Frachon S, et al. DCDC2 Mutations Cause Neonatal Sclerosing Cholangitis. Hum Mutat. 2016 Oct;37(10):1025–9.

398. Grati M, Chakchouk I, Ma Q, Bensaid M, Desmidt A, Turki N, et al. A missense mutation in DCDC2 causes human recessive deafness DFNB66, likely by interfering with sensory hair cell and supporting cell cilia length regulation. Hum Mol Genet. 2015 May 1;24(9):2482–91.

399. Schueler M, Braun DA, Chandrasekar G, Gee HY, Klasson TD, Halbritter J, et al. DCDC2 mutations cause a renal-hepatic ciliopathy by disrupting Wnt signaling. Am J Hum Genet. 2015 Jan 8;96(1):81–92.

400. Huizing M, Hess R, Dorward H, Claassen DA, Helip-Wooley A, Kleta R, et al. Cellular, Molecular and Clinical Characterization of Patients with Hermansky-Pudlak Syndrome Type 5. Traffic. 2004 Sep;5(9):711–22.

401. Kwon M, Hanna E, Lorang D, He M, Quick JS, Adem A, et al. Functional Characterization of Filamin A Interacting Protein 1–Like, a Novel Candidate for Antivascular Cancer Therapy. Cancer Res. 2008 Sep 15;68(18):7332–41.

402. Mok SC, Wong K-K, Chan RKW, Lau CC, Tsao S-W, Knapp RC, et al. Molecular Cloning of Differentially Expressed Genes in Human Epithelial Ovarian Cancer. Gynecol Oncol. 1994 Feb;52(2):247–52.

403. Seo S, Zhang Q, Bugge K, Breslow DK, Searby CC, Nachury M V., et al. A Novel Protein LZTFL1 Regulates Ciliary Trafficking of the BBSome and Smoothened. Barsh GS, editor. PLoS Genet. 2011 Nov 3;7(11):e1002358.

404. Wei Q, Zhou W, Wang W, Gao B, Wang L, Cao J, et al. Tumor-Suppressive Functions of Leucine Zipper Transcription Factor–Like 1. Cancer Res. 2010 Apr 1;70(7):2942–50.

405. Farnsworth CC, Seabra MC, Ericsson LH, Gelb MH, Glomset JA. Rab geranylgeranyl transferase catalyzes the geranylgeranylation of adjacent cysteines in the small GTPases Rab1A, Rab3A, and Rab5A. Proc Natl Acad Sci. 1994 Dec 6;91(25):11963–7.

406. Jia W, Gao Q, Han A, Zhu H, Yu J. The potential mechanism, recognition and clinical significance of tumor pseudoprogression after immunotherapy. Cancer Biol Med. 2019 Nov;16(4):655–70.

407. Society AC. Global Cancer Facts & Figures 4th Edition. Vol. 29, Atlanta: American Cancer Society. 2018. 138–144 p.

408. Sociedad Española de Oncología Médica (SEOM). Las cifras del cáncer en España 2023. 2023.

409. König IR, Fuchs O, Hansen G, von Mutius E, Kopp M V. What is precision medicine? Eur Respir J. 2017 Oct;50(4).

410. Cohen JD, Li L, Wang Y, Thoburn C, Afsari B, Danilova L, et al. Detection and localization of surgically resectable cancers with a multi-analyte blood test. Science. 2018 Feb;359(6378):926–30.

411. Alix-Panabières C, Pantel K. Liquid biopsy: From discovery to clinical application. Cancer Discov. 2021;11(4):858–73.

412. Reckamp KL, Melnikova VO, Karlovich C, Sequist L V, Camidge DR, Wakelee H, et al. A Highly Sensitive and Quantitative Test Platform for Detection of NSCLC EGFR Mutations in Urine and Plasma. J Thorac Oncol Off Publ Int Assoc Study Lung Cancer. 2016 Oct;11(10):1690–700.

413. Villatoro S, Mayo-de-Las-Casas C, Jordana-Ariza N, Viteri-Ramírez S, Garzón-Ibañez M, Moya-Horno I, et al. Prospective detection of mutations in cerebrospinal fluid, pleural effusion, and ascites of advanced cancer patients to guide treatment decisions. Mol Oncol. 2019 Dec;13(12):2633–45.

414. Zheng M-M, Li Y-S, Tu H-Y, Jiang B-Y, Yang J-J, Zhou Q, et al. Genotyping of Cerebrospinal Fluid Associated With Osimertinib Response and Resistance for Leptomeningeal Metastases in EGFR-Mutated NSCLC. J Thorac Oncol Off Publ Int Assoc Study Lung Cancer. 2021 Feb;16(2):250–8.

415. Merker JD, Oxnard GR, Compton C, Diehn M, Hurley P, Lazar AJ, et al. Circulating Tumor DNA Analysis in Patients With Cancer: American Society of Clinical Oncology and College of American Pathologists Joint Review. J Clin Oncol Off J Am Soc Clin Oncol. 2018 Jun;36(16):1631–41.

416. Engelman JA, Zejnullahu K, Mitsudomi T, Song Y, Hyland C, Joon OP, et al. MET amplification leads to gefitinib resistance in lung cancer by activating ERBB3 signaling. Science (80-). 2007;316(5827):1039–43.

417. Váraljai R, Elouali S, Lueong SS, Wistuba-Hamprecht K, Seremet T, Siveke JT, et al. The predictive and prognostic significance of cell-free DNA concentration in melanoma. J Eur Acad Dermatol Venereol. 2021 Feb;35(2):387–95.

418. Papadimitriou M-A, Levis P, Kotronopoulos G, Stravodimos K, Avgeris M, Scorilas A. Preoperative Cell-Free DNA (cfDNA) in Muscle-Invasive Bladder Cancer Treatment Outcome. Clin Chem. 2023 Feb;

419. Valpione S, Gremel G, Mundra P, Middlehurst P, Galvani E, Girotti MR, et al. Plasma total cell-free DNA (cfDNA) is a surrogate biomarker for tumour burden

and a prognostic biomarker for survival in metastatic melanoma patients. Eur J Cancer. 2018 Jan;88:1–9.

420. Hamfjord J, Guren TK, Dajani O, Johansen JS, Glimelius B, Sorbye H, et al. Total circulating cell-free DNA as a prognostic biomarker in metastatic colorectal cancer before first-line oxaliplatin-based chemotherapy. Ann Oncol Off J Eur Soc Med Oncol. 2019 Jul;30(7):1088–95.

421. Fettke H, Kwan EM, Bukczynska P, Ng N, Nguyen-Dumont T, Southey MC, et al. Prognostic Impact of Total Plasma Cell-free DNA Concentration in Androgen Receptor Pathway Inhibitor-treated Metastatic Castration-resistant Prostate Cancer. Eur Urol Focus. 2021 Nov;7(6):1287–91.

422. Gristina V, Barraco N, La Mantia M, Castellana L, Insalaco L, Bono M, et al. Clinical Potential of Circulating Cell-Free DNA (cfDNA) for Longitudinally Monitoring Clinical Outcomes in the First-Line Setting of Non-Small-Cell Lung Cancer (NSCLC): A Real-World Prospective Study. Cancers (Basel). 2022 Dec;14(23).

423. Keller L, Pantel K. Unravelling tumour heterogeneity by single-cell profiling of circulating tumour cells. Nat Rev Cancer. 2019 Oct;19(10):553–67.

424. Krebs MG, Sloane R, Priest L, Lancashire L, Hou J-M, Greystoke A, et al. Evaluation and prognostic significance of circulating tumor cells in patients with non-small-cell lung cancer. J Clin Oncol Off J Am Soc Clin Oncol. 2011 Apr;29(12):1556–63.

425. Alix-Panabières C, Schwarzenbach H, Pantel K. Circulating tumor cells and circulating tumor DNA. Annu Rev Med. 2012;63:199–215.

426. Mego M, De Giorgi U, Dawood S, Wang X, Valero V, Andreopoulou E, et al. Characterization of metastatic breast cancer patients with nondetectable circulating tumor cells. Int J cancer. 2011 Jul;129(2):417–23.

427. Shi Z-M, Wang L, Shen H, Jiang C-F, Ge X, Li D-M, et al. Downregulation of miR-218 contributes to epithelial-mesenchymal transition and tumor metastasis in lung cancer by targeting Slug/ZEB2 signaling. Oncogene. 2017 May;36(18):2577–88.

428. Pantazaka E, Vardas V, Roumeliotou A, Kakavogiannis S, Kallergi G. Clinical Relevance of Mesenchymal- and Stem-Associated Phenotypes in Circulating Tumor Cells Isolated from Lung Cancer Patients. Cancers (Basel). 2021 Apr;13(9).

429. Bortolini Silveira A, Bidard F-C, Tanguy M-L, Girard E, Trédan O, Dubot C, et al. Multimodal liquid biopsy for early monitoring and outcome prediction of chemotherapy in metastatic breast cancer. NPJ breast cancer. 2021 Sep;7(1):115.

430. Ruiz-Bañobre J, Molina-Díaz A, Fernández-Calvo O, Fernández-Núñez N, Medina-Colmenero A, Santomé L, et al. Rethinking prognostic factors in locally advanced or metastatic urothelial carcinoma in the immune checkpoint blockade era: a multicenter retrospective study. ESMO Open. 2021;6(2):100090.

431. Papachristos A, Sivolapenko GB. Pharmacogenomics, Pharmacokinetics and Circulating Proteins as Biomarkers for Bevacizumab Treatment Optimization in Patients with Cancer: A Review. J Pers Med. 2020 Aug 4;10(3).

432. Veyssière H, Bidet Y, Penault-Llorca F, Radosevic-Robin N, Durando X. Circulating proteins as predictive and prognostic biomarkers in breast cancer. Clin Proteomics. 2022 Dec 11;19(1):25.

433. Christensen TD, Maag E, Larsen O, Feltoft CL, Nielsen KR, Jensen LH, et al. Development and validation of circulating protein signatures as diagnostic biomarkers for biliary tract cancer. JHEP Reports. 2023 Mar;5(3):100648.

ANNEX 1

INDEX FIGURES AND TABLES

ANNEX 1: Index figures and tables

1. FIGURES INDEX

Resumen *in extenso*

Resumo *in extenso*

Figura 7. Principais compoñentes da biopsia líquida estudados ao longo da presente tese.

Figura 8. Resumo gráfico do traballo realizado no CHAPTER IA. Abreviaturas: NSCLC, do inglés *non-small cell lung cancer*, cancro de pulmón non microcítico; ctDNA, do inglés *circulating tumour DNA*, ADN tumoral circulante; qPCR, PCR cuantitativa.

Figura 9. Resumo gráfico do traballo realizado no CHAPTER IB. Abreviaturas: ddPCR, do inglés *digital droplet PCR*, PCR dixital; NSCLC, do inglés *non-small cell lung cancer*, cancro de pulmón non microcítico; ctDNA, do inglés *circulating tumour DNA*, ADN tumoral circulante; CTCs, do inglés *circulating tumour cells*, células tumorales circulantes; CN, do inglés *copy number*, número de copias.

Figura 10. Resumo gráfico do traballo realizado no CHAPTER II. Abreviaturas: NSCLC, do inglés *non-small cell lung cancer*, cancro de pulmón non microcítico; cfDNA, do inglés *circulanting free DNA*, ADN libre circulante; CTCs, do inglés *circulating tumour cells*, células tumorales circulantes; qPCR, PCR cuantitativa.

Figura 11. Resumo gráfico do traballo realizado no CHAPTER III. Abreviaturas: SCLC, do inglés *small cell lung cancer*, cancro de pulmón microcítico; cfDNA, do inglés *circulanting free DNA*, ADN libre circulante; CTCs, do inglés *circulating tumour cells*, células tumorales circulantes; qPCR, PCR cuantitativa; ECOG PS, do inglés *Eastern Cooperative Oncology Group Performance Status.*

Figura 12. Resumo gráfico do traballo realizado no CHAPTER IV. Abreviaturas: NSCLC, do inglés *non-small cell lung cancer*, cancro de pulmón non microcítico.

Introduction

Figure 13. Distribution of cases and deaths for the top 3 most common cancers in 2020. Source: GLOBOCAN 2020.

Figure 14. Definitions for T, N and M components in lung cancer tumours.

CHAPTER I.A

that present Del.ex19 or L858R mutation in tissue sample and blood sample using Idylla™ solution. Abbreviations: MUT: mutated; WT: wild type.

Figure 1.3. Comparison among BEAMing, AVENIO and IdyllaTM technologies. (A) Concordance between BEAMing and Idylla™ assay in cfDNA samples (n=18). (B) Concordance between NGS and Idylla™ assay in cfDNA samples (n=15). (C) Variant allele frequencies (VAF) detected by BEAMIing or NGS panel versus Idylla™ ΔCq. Red symbols represent discordant samples detected by BEAMing or NGS (n=3), green symbols represent concordant samples detected by both technologies. Abbreviations: MUT: mutated; WT: wild type; VAF, variant allele frequency.

Figure 1.4. Monitoring *EGFR* status in NSCLC patients using the ctEGFR Idylla™ mutation assay. Swimmer' plot on monitored patients (n=10).

Figure 1.5. Evolution of cfDNA levels and EGFR L861Q mutations in patient ID13 during Gefitinib treatment. The L86Q1 mutation appeared at progression disease, which confirmed by image analyses. Abbreviations: SDi: stable disease; PD: progression disease.

Figure 1.6. Evolution of cfDNA levels and *EGFR* L858R mutation in patient ID19 (A) and patient ID11 (B) during different TKIs treatment. Abbreviations: PD: progression disease; SDi: stable disease.

CHAPTER I.B

Figure 1.7. Signalling pathway of c-MET and HGF.

Figure 1.8. Study design for *MET* status assessment in cancer patients. CN: copy number; CCLE: cancer cell line encyclopedia.

Figure 1.9. *MET* CN analysis. (A) Scatterplot representing correlation between *MET* CN in cancer cell lines determined by ddPCR versus SNP array (n = 8) using Pearson's correlation. (B) Reproducibility of the *MET* CN determination by ddPCR. We represented some examples (3 cancer cell lines). Abbreviations: CN, copy number.

Figure 1.10. (A) *MET* CN analysis. Plasma *MET* CN detected in healthy controls (n= 49), non-metastatic patients (n=34) and metastatic patients (n= 140). Differences were analysed using the Mann-Whitney-Wilcoxon U-Test. (B) Correlation between cfDNA levels and plasma *MET* CN in metastatic cancer patients (n= 140) using Pearson's correlation. Abbreviations: CN, copy number.

Figure 1.11. Plasma MET CN values in the different metastatic cancers included in the study. Abbreviations: CN, copy number.

Figure 1.12. Comparison of MET CN status in tissue and cfDNA. (A) Distribution of MET CN measured by ddPCR and FISH (the point larger indicates the discordant value, whereas the horizontal and vertical dotted lines indicate cut-off points of ddPCR and FISH, respectively). (B) Representative example of a negative case for MET amplification obtained in a NSCLC patient by FISH. (C) Representative example of a positive case for MET amplification obtained in a NSCLC patient by FISH. Abbreviations: CN, copy number.

Figure 1.13. Evaluation of the enrichment capacity of CellSearch® and Parsortix systems, using healthy blood spiked with cancer cell lines. (A) Percentage of spiked tumor cancer cells captured using CellSearch® and Parsortix systems. *p*-value $<5x10^{-3}$, in all comparisons between CellSearch® and Parsortix System in each cell line using paired student t test. (B) Correlation between EPCaM mRNA expression levels measured by Affymetrix microarrays and RNA-seq. LNCaP, NCI-N87, SNU-5, and AU565 express EpCAM while Hs746T and C32 express low levels or do not express EpCAM respectively. (C) Immunofluorescence characterization of EpCAM in our cancer cell lines. Scale bar represents 100 µm.

Figure 1.14. Detection of c-MET expression using tumour cancer cells with the CellSearch® and Parsortix systems (Figure A and B, respectively). Representative images of c-MET expression scored on score 0 (cell line LNCaP), 1 (cell line AU565), 2 (cell line Hs746T) and 3 (cell line SNU-5).

CHAPTER II

Figure 2.6. *hTERT* cfDNA changes from baseline to 12 weeks. (A) *hTERT* cfDNA concentrations for the two cfDNA patterns (increase/decrease at 12 weeks) and showing the response to therapy. (B) Percentage of patients and median PFS for each cfDNA pattern. (C) Proportion of patients with high and low levels baseline, 6 and 12 weeks. *p*-value was calculated by Fisher's exact test. (D) Kaplan-Meier plot of progression-free survival of the favourable/unfavourable changes at 12 weeks*. Abbreviations: CR/PR, complete response/partial response SDi/PD, stable disease/progression disease.

Figure 2.7. Immunofluorescence characterization of PD-L1 in cancer cell lines. We used three lung cancer cell lines with different grade of PD-L1 expression (NCI-H460, medium-high expression, NCI-H322, low-medium expression and A549, no expression). Scale bar represents 100 µm.

Figure 2.8. (A-B) Detection of PD-L1 expression after spiking cancer cells lines in healthy blood and analyse them with the CellSearch® and Parsortix systems, respectively and representative images of different grades of PD-L1 expression. NCI-H460 stimulated with IFN-γ shown high expression, NCI-H460 medium expression, NCI-H322, low-medium expression and A549, no expression.

Figure 2.9. (A) Representative images of CTCs detected with the CellSearch® system in patients with NSCLC. Samples were subjected to immunostaining with DAPI, CD45 (APC), CKs (FLU) and PD-L1 (PE). (B) Representative images of CTCs detected with the Parsortix system in patients with NSCLC. Samples were subjected to immunostaining with DAPI, CD45 (AF647), CKs (AF488) and PD-L1 (PE).

Figure 2.10. Correlation of PD-L1 positivity between tumour tissues (by tumour proportion scores) and CTCs with the CellSearch® (A) and Parsortix systems (B).

Figure 2.11. Correlation of PD-L1 positivity between tumour tissues (by tumour proportion scores) and CTCs with the CellSearch® (A) and Parsortix systems (B).

Figure 2.12. Kaplan–Meier survival analysis of CTCs at baseline. Kaplan–Meier plots of PFS (A) and OS (B). (C) Comparison of the response to pembrolizumab based on CTC detection using CellSearch®. *p*-value was calculated by Fisher's exact test.

Figure 2.13. CTCs and *hTERT* cfDNA levels correlate with the prognosis of patients with NSCLC treated with pembrolizumab and the response of therapy. (A) Kaplan-Meier survival plot of progression-free survival based on the combination of cfDNA and CTC levels at baseline. (B) Kaplan-Meier survival plot of overall survival based on the combination of cfDNA and CTC levels at baseline. (C) Objective response rate in patients with low cfDNA levels and undetectable CTCs (n=12) versus patients with high cfDNA levels and undetectable CTCs or low cfDNA levels and detectable CTCs or high cfDNA levels and detectable CTCs (n=18).

CHAPTER III

Figure 3.1. Study sampling points and different cohorts included in the study.

Figure 3.2. Scatter plot representing correlation between cfDNA levels using Qubit method and qPCR assay at different times of therapy (baseline, 3 weeks and progression disease) using Pearson's correlation method. A good correlation between was found (R^2 =0.959). Abbreviations: GE, genomic equivalents.

Figure 3.3. CfDNA levels using two different approaches. (A-C) Total cfDNA levels in healthy controls and patients with SCLC. Statistical analysis between both groups was performed by the Mann–Whitney–Wilcoxon U-Test. (B-D) ROC curves for qPCR assay (B) and Qubit method (D) show high sensitivity and specificity. Abbreviations: GE, genomic equivalents; AUC, area under the curve; CI, confidence interval.

Figure 3.4. cfDNA levels as a prognostic biomarker at baseline. (A-B) Kaplan-Meier survival analysis of cfDNA levels at baseline for PFS (A) and OS (B).

Figure 3.5. Clinical course of all patients included in the study. Swimmers' plot showing each patient therapy and the different times of sample collection. The total length of each bar indicates the duration of survival from the diagnoses.

Figure 3.6. CfDNA levels in SCLC patients at different time-points (baseline, 3 weeks after treatment onset and at progression disease). Total cfDNA levels at baseline were significantly higher than at 3 weeks after the therapy onset (Wilcoxon test p= 0.002). Abbreviations: GE, genomic equivalents.

Figure 3.7. cfDNA levels as a prognostic biomarker during treatment. Kaplan-Meier survival analysis of cfDNA levels at 3 weeks for PFS (A) and OS (B).

Figure 3.8. Kaplan-Meier survival analysis of cfDNA levels at progression disease for OS.

Figure 3.9. CTCs detected in SCLC patient using CellSearch® system. (A) Representative images of CTCs detected in our cohort using the CellSearch® system. (B) Number of CTCs detected in each patient. Patients with presence of <10 CTCs are represented in red columns.

Figure 3.10. Kaplan-Meier survival analysis of CTCS levels at baseline for PFS. The presence of ≥150 CTCs/7.5mL of blood was significantly associated with shorter PFS rates.

Figure 3.11. CTCs and association with clinical characteristics. The number of CTCs detected in our cohort were significantly associated with the stage of patients and a poor performed status. Also, high cfDNA levels and the presence of CTCs at baseline were significantly associated. Abbreviations: CH, chemotherapy; CH + IM, chemotherapy plus immunotherapy.

Figure 3.12. Final multivariate Cox regression prognostic model for (A) PFS and (B) OS. Abbreviations: HR, hazard ratio; CI, confidence interval.

Figure 3.13. Kaplan-Meier survival analysis according to risk-group PFS (A) and OS (B). Abbreviations: NA, not applicable.

CHAPTER IV

Figure 4.1. (A) Swimmers' plot on patients showing the response of therapy. The total length of each bar indicates the duration of survival from the diagnoses. (B-C) Kaplan-Meier plots show highly significant differences between responders and non-responders to pembrolizumab treatment in PFS (B) OS (C).

Figure 4.2. Proteomic of NSCLC response to pembrolizumab treatment. (A) The proteomic workflow involved plasma extraction from blood samples of 48 NSCLC patients undergoing pembrolizumab Then, 30 µl of plasma samples therapy. were employed to proteins extraction. The proteins were trypsin-digested to obtained peptides (fractionation). A pool of total peptides samples was employed to generate a spectral library using a DDA method. Finally, pooled peptides of each sample were analysed using a SWATH-MS method employing the previous spectral library and the Human Pan-Human Library. (B) Total number of proteins quantified in each group of patients.

Figure 4.3. (A) Volcano plot of differentially expressed proteins at baseline. Upregulated proteins are in blue and downregulated proteins are in yellow. (B) Heatmap of 324 differentially expressed proteins at baseline (p-value <0.05), that discriminate between responder and non-responder patients to pembrolizumab therapy.

Figure 4.4. Bar graph for viewing of the top 15 enriched GO process involved the 324 DEPs. A colour scale represents statistical significance.

Figure 4.5. Heatmap showing the top enrichment clusters, one row per group, using a colour scale to represent statistical significance. Gray colour indicates a lack of significance.

Figure 4.6. Proteomaps that showed the functional differences between responders (left) and non-responders (right) to immunotherapy. Each polygon corresponds to a single KEGG pathway, and its size correlates with the ratio between both groups.

Figure 4.7. (A) Volcano plot and heat map of differentially expressed proteins at baseline. (B) PCA analysis showing the separation of samples from responders (blue) and non-responders (yellow) to pembrolizumab therapy according the 66 DEPs found by LC-MS/MS analysis.

Figure 4.8. (A) Volcano plot showing the 7 proteins of our predictive model. (B) ROC curves of each protein and the combination in the discovery cohort. (C) ROC curve

analyses of the PD-L1 expression on tumour tissue. Abbreviations: AUC, area under the curve; FC, foldchange.

Figure 4.9. ROC curves of each protein and the combination in the validation cohort.

Figure 4.10. Kaplan-Meier survival analysis of ATG9A, SPTN2, HPS5 and DCDC2 proteins levels at baseline. Kaplan-Meier plots of progression-free survival (A-C) and overall survival (D-E) showed significant associations between proteins levels before start therapy and prognosis in metastatic NSCLC under immunotherapy regimens.

Figure 4.11. Protein levels of our protein models were measured at different time points during the immunotherapy regimen. Abbreviations: PD, progression of disease.

Figure 4.11. ROC analyses with the protein model at different time points during the immunotherapy regimen (at 6 weeks and at 12 weeks after start therapy).

Overall discussion

Figure 25. Number of publications per year containing the terms "precision medicine" and "liquid biopsy" in PubMed between 2012 and 2022.

Figure 26. Sankey diagram showing the total lung cancer patients included in the present thesis, subdivided by lung cancer type, stage and therapy.

Figure 27. Total cfDNA levels in lung cancer patients and healthy controls. (A) Boxplot of cfDNA levels in NSCLC, SCLC and healthy controls (Mann-Whitney test). (B) ROC showing the discriminatory value of cfDNA levels to discriminate against lung cancer patients versus healthy controls (AUC=0.8885).

Figure 28. CTCs detected in 36 NSCLC patients employing two different isolation methods.

Figure 29. CTCs detected in NSCLC and SCLC cohorts using the CellSearch® system. SCLC patients presented statistically higher number of CTCs than NSCLC patients (p-value <0.001; Mann-Whitney test).

2. TABLES INDEX

Introduction

CHAPTER I.A

CHAPTER I.B

CHAPTER II

CHAPTER III

CHAPTER IV

ANNEX 2

LIST OF PUBLICATIONS

ANNEX 2: List of publications and patents

1. LIST OF PUBLICATIONS PRESENTED IN THIS THESIS

1.1 Reviews and book chapters

a. Current status and future perspectives of liquid biopsy in small cell lung cancer.

Patricia Mondelo-Macía, Jorge García-González, Luis León-Mateos, Adrián Castillo-García, Rafael López-López, Laura Muinelo-Romay, Roberto Díaz-Peña.

Biomedicines. 2021;9(1):1–22.

ISSN 2227-9059

MDPI, 07/01/2021

Full-text available: https://doi.org/10.3390/biomedicines9010048

Journal Citation Reports (JCR) category rank (2020)**:** Q1 (62/295) Biochemistry & Molecular Biology

Journal Impact factor (2020) – 6.081

Contribution to this work: I, Patricia Mondelo, has been involved in bibliography review, writing original draft and review all manuscript. Particularly, I have writing "Introduction", "Liquid biopsy as a Clinical Tool in SCLC", and "Conclusion" and I have revised all the manuscript.

b. Circulating Free DNA and Its Emerging Role in Autoimmune Diseases.

Patricia Mondelo-Macía, Patricia Castro-Santos, Adrián Castillo-García, Laura Muinelo-Romay, Roberto Díaz-Peña.

J Pers Med. 2021 Feb;11(2).

ISSN 2075-4426

MDPI, 20/02/2021

Full-text available: https://doi.org/10.3390/jpm11020151

Journal Citation Reports (JCR) category rank (2020): Q1 (15/107) Health care sciences & services

Journal Impact factor (2020) – 4.945

Contribution to this work: I, Patricia Mondelo, in bibliography review, writing original draft and review all manuscript. Particularly, I have writing "Introduction", "Circulating free DNA characteristics and Clinical Interest", part of "Circulating Free DNA in other autoimmune disorders", "Conclusion" and I have revised all the manuscript.

c. Methods for the Detection of Circulating Biomarkers in Cancer Patients – *Chapter book*

Patricia Mondelo-Macía, Ana María Rodríguez-Ces, María de las Mercedes Suárez-Cunqueiro, Laura Muinelo-Romay.

Adv Exp Med Biol. 2022;1379:525–52.

ISBN 978-3-031-04038-2

Springer Nature, 28/06/2022

Full-text available: https://doi.org/10.1007/978-3-031-04039-9_21

Journal Citation Reports (JCR) category rank: Q2 (33/94) Biology

Journal Impact factor (2021) – 3.650

Contribution to this work: I, Patricia Mondelo, in bibliography review, writing original draft, visualizations and review all manuscript. Particularly, I have writing "Strategies for CTCs Isolation and Characterization", "Strategies for cfDNA/ctDNA Characterization", part of "Alternative Circulating Biomarkers", "Conclusions" and I have revised all the manuscript.

1.2 Research Articles and correspondences

a. Rapid Idylla™ mutational testing to detect EGFR mutations in plasma samples and to monitor therapy in advanced NSCLC patients - *Correspondence.*

Patricia Mondelo-Macía, Ramón Manuel Lago-Lestón, Aitor Rodríguez-Casanova, Alicia Abalo, Ángel Díaz-Lagares, Jorge García-González, Luis León-Mateos, Roberto Díaz-Peña*, Laura Muinelo-Romay*.

* Corresponding.

Pathology. 2023; S0031-3025(23)00081-8.

ISSN 0031-3025 – EISSN 1465-3931

Elservier Ltd, 15/03/2023

Full-text available: https://doi.org/10.1016/j.pathol.2023.01.004

Journal Citation Reports (JCR) category rank (2021): Q1 (19/77): Pathology

Journal Impact factor (2021) – 5.335

Contribution to this work: I, Patricia Mondelo, has been involved in the Conceptualization, Methodology, Investigation, Writing – original draft, Writing – review & editing and Visualization. Particularly, I have performed Idylla™ system set up, blood samples processing, Idylla™ assays, statistical analyses, and manuscript writing.

b. Detection of MET Alterations Using Cell Free DNA and Circulating Tumor Cells from Cancer Patients - *Article Research.*

Patricia Mondelo-Macía[#], Carmela Rodríguez-López[#], Laura Valiña, Santiago Aguín, Luis León-Mateos, Jorge García-González, Alicia Abalo, Óscar Rapado-González, Mercedes Suárez-Cunqueiro, Angel Díaz-Lagares, Teresa Curiel, Silvia Calabuig-Fariñas, Aitor Azkárate, Antònia Obrador-Hevia, Ihab Abdulkader, Laura Muinelo-Romay[*], Roberto Diaz-Peña[*] and Rafael López-López.

* Corresponding. / [#] These authors have contributed equally to this work

Cells. 2020; 9(2):522

ISSN 2073-4409

MDPI, 21/02/2020

Full-text available: https://doi.org/10.3390/cells9020522

Journal Citation Reports (JCR) category rank (2020)**:** Q2 (53/195): Cell biology

Journal Impact factor (2020) – 6.600

Contribution to this work:

I, Patricia Mondelo, has been involved in the Methodology, Validation, Formal Analyses, Investigation, Writing – original draft and Visualization. Particularly, I have performed cell culture, spiked experiments, immunofluorescence, blood samples processing, nuclei acid extraction, ddPCR assays, Parsortix and CellSearch® assays, statistical analyses, and manuscript writing.

c. Clinical Potential of Circulating Free DNA and Circulating Tumour Cells in Patients with Metastatic Non-Small-Cell Lung Cancer treated with Pembrolizumab - *Article Research.*

Patricia Mondelo-Macía, Jorge García-González, Luis León-Mateos, Urbano Anido, Santiago Aguín, Ihab Abdulkader, María Sánchez-Ares, Alicia Abalo, Aitor Rodríguez-Casanova, Ángel Díaz-Lagares, Ramón Manuel Lago-Lestón, Laura Muinelo-Romay, Rafael López-López and Roberto Díaz-Peña*.

* Corresponding.

Molecular Oncology. 2021; 15 (11) p. 2923–2940.

ISSN 1878-0261

FebsPress, 31/08/2021

Full-text available: https://doi.org/10.3390/cells9020522

Journal Citation Reports (JCR) category rank (2021): Q1 (51/245): Oncology

Journal Impact factor (2021) – 7.449

Contribution to this work:

I, Patricia Mondelo, has been involved in the Conceptualization, Methodology, Investigation, Data curation, Software, Writing – original draft and Analysis of data. Particularly, I have performed cell culture, spiked experiments, immunofluorescence, blood samples processing, nuclei acid extraction, qPCR assays, Parsortix and CellSearch® assays, statistical analyses and manuscript writing.

d. Plasma cell-free DNA and CTCs as prognostic biomarkers in small cell lung cancer patients - *Article Research.*

Patricia Mondelo-Macía, Jorge García-González, Alicia Abalo, Manuel Mosquera-Presedo, Santiago Aguín, María Mateos, Rafael López-López, Luis León-Mateos*, Laura Muinelo-Romay*, and Roberto Díaz-Peña*.

* Corresponding.

Translational Lung Cancer Research. 2022; (10):1995-2009.

ISSN 2218-6751; EISSN 2226-4477

AME Publishing Company, 31/08/2022

Full-text available: https://doi.org/10.21037/tlcr-22-273

Journal Citation Reports (JCR) category rank (2021): Q2 (105/245): Oncology

Journal Impact factor (2021) – 4.726

Contribution to this work:

I, Patricia Mondelo, has been involved in the Conceptualization and design, Methodology, Investigation, Data analysis and Interpretations, Writing – original draft. Particularly, I have performed data curation, blood samples processing, nuclei acid extraction, qPCR assays, CellSearch® assays, statistical analyses and manuscript writing.

1.3 Patents derived from this thesis

Patent: *MAPRI: In vitro method for predicting cancer patient response to PD-1 and/or PD-L1 inhibitors.*

Inventors: Ana Belén Dávila Ibáñez, Rafael López López, Roberto Díaz Peña, Susana Bravo López, Patricia Mondelo-Macía, Laura Muinelo Romay, Luis Ángel León Mateos y Jorge José García González.

EP No*. 23 382 377.2.*

ANNEX 3

ETHICAL CONSIDERATIONS and ATTACHED PERMISSIONS

ANNEX *3*: Ethical considerations and attached permissions

1. IMAGES USE

Unless clarified, all the images presented in this thesis have been produced by the author. In the case of images reused or adapted from other manuscripts, permission has been granted by the publishers, and the legal use has been clarified at the bottom of the corresponding figures.

In addition, the free resource Flaticon.com and Servier Medical Art (smart.servier.com) by Servier (licensed under a Creative Commons Attribution 3.0 Unported License) were employed.

2. HUMAN CELL CULTURE

All cancer lines used in this work were acquired from commercially available resources (American Tissue Culture Collection, ATCC) and cultured in the conditions recommended by the manufacturers and only used for the research purposes specifically described in this thesis.

3. PATIENT'S SAMPLES

Blood samples were collected in accordance with the guidelines and protocols approved by the Institutional Ethical Committees, Galician Clinical Research Ethics Committee, SERGAS: code approval: 2017/538. All individuals signed informed consent forms and could withdraw their consent at any time. The study was performed in accordance with the Declaration of Helsinki.

4. ATTACHED PERMISIONS

a. Favourable report (Clinical research ethics committee of Galicia, CEIC).

XUNTA DE GALICIA
CONSELLERÍA DE SANIDADE
Secretaría Xeral Técnica

Secretaría Técnica
Comité Autonómico de Ética da Investigación de Galicia
Secretaría Xeral. Consellería de Sanidade
Edificio Administrativo San Lázaro
15703 SANTIAGO DE COMPOSTELA
Tel: 881546425. Correo-e: ceic@sergas.es

galicia

DICTAMEN DEL COMITÉ DE ÉTICA DE LA INVESTIGACIÓN DE SANTIAGO-LUGO

Guillermo José Prada Ramallal, Secretario del Comité de Ética de la Investigación de Santiago-Lugo,

CERTIFICA:

Que este Comité evaluó en su reunión del día 21 de diciembre de 2017 el estudio:

Título: Identificación de marcadores de diagnóstico, pronóstico y seguimiento mediante el análisis de Biopsia Líquida en pacientes con cáncer
Promotor: Rafael López López
Tipo de estudio: Outros
Versión: Versión 1 de 31 de Octubre de 2017
Código del Promotor:
Código de Registro: 2017/538

Y, tomando en consideración las siguientes cuestiones:

- La pertinencia del estudio, teniendo en cuenta el conocimiento disponible, así como los requisitos legales aplicables, y en particular la Ley 14/2007, de investigación biomédica, el Real Decreto 1716/2011, de 18 de noviembre, por el que se establecen los requisitos básicos de autorización y funcionamiento de los biobancos con fines de investigación biomédica y del tratamiento de las muestras biológicas de origen humana, y se regula el funcionamiento y organización del Registro Nacional de Biobancos para investigación biomédica, la ORDEN SAS/3470/2009, de 16 de diciembre, por la que se publican las Directrices sobre estudios Postautorización de Tipo Observacional para medicamentos de uso humano, y la Circular nº 07/2004, de investigaciones clínicas con productos sanitarios.
- La idoneidad del protocolo en relación con los objetivos del estudio, justificación de los riesgos y molestias previsibles para el sujeto, así como los beneficios esperados.
- Los principios éticos da Declaración de Helsinki vigente.
- Los Procedimientos Normalizados de Trabajo del Comité.

Emite un dictamen **FAVORABLE** para la realización del estudio **por el/la investigador/a del centro:**

Centros	Investigadores Principales
C.H. Universitario de Santiago	Rafael López López, Laura Muinelo Romay, Roberto Díaz Peña

En Santiago de Compostela, a 28 de diciembre 2017.

El Secretario del Comité Territorial de Ética de la Investigación de Santiago Lugo,

guillermo.jose.prada.ramallal@sergas.es
2017.12.29 13:33:30 +02'00'

Guillermo José Prada Ramallal

XUNTA DE GALICIA
CONSELLERÍA DE SANIDADE
Secretaría Xeral Técnica

Secretaría Técnica
Comité Autonómico de Ética da Investigación de Galicia
Secretaría Xeral. Consellería de Sanidade
Edificio Administrativo San Lázaro
15703 SANTIAGO DE COMPOSTELA
Tel: 881546425. Correo-e: celc@sergas.es

galicia

Guillermo José Prada Ramallal, Secretario del Comité de Ética de la Investigación de Santiago-Lugo,

HACE CONSTAR QUE:

1.- El Comité Territorial de Ética de la Investigación de Santiago-Lugo cumple tanto en su composición como en sus PNTs los requisitos legales vigentes (RD 1090/2015 de ensayos clínicos, y la Ley 14/2007 de Investigación Biomédica).

2.- La composición actual del Comité Territorial de Ética de la Investigación de Santiago-Lugo es:

- **Juan Manuel Vázquez Lago (Presidente).** Médico especialista en Medicina Preventiva y Salud Pública. Área de Gestión Integrada de Santiago.
- **Pilar Rodríguez Ledo (Vicepresidenta).** Médico especialista en Medicina Familiar y Comunitaria. Área de Gestión Integrada de Lugo.
- **Guillermo José Prada Ramallal (Secretario).** Médico especialista en Farmacología Clínica. Área de Gestión Integrada de Santiago. Fundación Ramón Domínguez.
- **Lorenzo Armenteros del Olmo (Vicesecretario).** Médico especialista en Medicina Familiar y Comunitaria. Área de Gestión Integrada de Lugo.
- **Francisco Campos Pérez.** Biólogo. Instituto de Investigación Sanitaria de Santiago de Compostela.
- **Rosana Castelo Domínguez.** Farmacéutica de Atención Primaria. Área de Gestión Integrada de Santiago.
- **Ricardo García Martínez.** Licenciado en Derecho. Área de Gestión Integrada de Lugo.
- **Jaime Gulín Dávila.** Farmacéutico especialista en Farmacia Hospitalaria. Área de Gestión Integrada de Lugo.
- **Victor Herrán Carreira.** Paciente. ADIL-Asociación de Diabéticos Lucense.
- **María Jesús Lamas Díaz.** Farmacéutica especialista en Farmacia Hospitalaria. Área de Gestión Integrada de Santiago.
- **Carlos Rodríguez Moreno.** Médico especialista en Farmacología Clínica. Área de Gestión Integrada de Santiago.
- **Rafael Carlos Vidal Pérez.** Médico especialista en Cardiología. Área de Gestión Integrada de Lugo.
- **María Jesús Wandosell Picatoste.** Enfermera. Área de Gestión Integrada de Santiago.

Para que conste donde proceda, y a petición del promotor/investigador, en Santiago de Compostela, a 28 de diciembre de 2017.

El Secretario del Comité Territorial de Ética de la Investigación de Santiago Lugo,

guillermo.jose.prada.ramallal@sergas.es
2017.12.29 13:33:34 +02'00'

Liquid biopsy and targeted therapies have revolutionised the oncology field, particularly in lung cancer. However, more research is required to integrate these techniques into clinical practice and improve survival rates. This thesis investigates the value of different blood biomarkers to improve the management of advanced lung cancer patients through the analysis of circulating free DNA (cfDNA), circulating tumour cells (CTCs), and circulating proteins. New protocols were established and validated to characterize clinically relevant alterations in CTCs and cfDNA and their prognostic and predictive value was demonstrated. Of note, a proteomic signature with value to predict immunotherapy response was identified. Our results contribute to achieve precision medicine through liquid biopsy in advanced lung cancer.